Theses and Dissertations

December 2013

An Experimental Investigation Characterizing the Tribological Performance of Natural and Synthetic Biolubricants Composed of Carboxylic Acids for Energy Conservation and Sustainability

Carlton Jonathan Reeves
University of Wisconsin-Milwaukee

Follow this and additional works at: https://dc.uwm.edu/etd

Part of the Chemistry Commons, Mathematics Commons, and the Mechanical Engineering Commons

www.manaraa.com

AN EXPERIMENTAL INVESTIGATION CHARACTERIZING THE

TRIBOLOGICAL PERFORMANCE OF NATURAL AND SYNTHETIC

BIOLUBRICANTS COMPOSED OF CARBOXYLIC ACIDS FOR ENERGY

CONSERVATION AND SUSTAINABILITY

By

Carlton Jonathan Reeves

A Dissertation Submitted in

Partial Fulfillment of the

Requirements for the Degree of

Doctor of Philosophy

in Engineering

at

The University of Wisconsin-Milwaukee

December 2013

ABSTRACT

AN EXPERIMENTAL INVESTIGATION CHARACTERIZING THE

TRIBOLOGICAL PERFORMANCE OF NATURAL AND SYNTHETIC

BIOLUBRICANTS COMPOSED OF CARBOXYLIC ACIDS FOR ENERGY

CONSERVATION AND SUSTAINABILITY

By

Carlton Jonathan Reeves

The University of Wisconsin-Milwaukee, 2013

Under the Supervision of Professors Tien-Chien Jen and Michael R. Lovell

Over the last several decades the lubrication industry has been striving to bring bio-based lubricants known as biolubricants to prominence. The reasons for the increased environmental initiatives are due to depletion of oil reserves, increases in oil price, stringent government regulations on petroleum-based oils, and most importantly, concerns for protecting the environment. With an estimated, 50% of all lubricants entering the environment and much of these being composed of toxic mineral oils, biolubricants have begun to witness a resurgence. This experimental investigation seeks to develop a new class of ecofriendly biolubricants that are less toxic to the environment, derived from renewable resources, and provide feasible and economical alternatives to traditional petroleum-based lubricants. Advantages of biolubricants include their higher

lubricity, lower volatility, higher shear stability, higher viscosity index, higher load carrying capacity, and superior detergency and dispersancy when compared to petroleum-based lubricants.

This work highlights the evolution of biolubricants derived from natural oils and fats to green lamellar solid additives to a new class of "greener" functional fluids known as room temperature ionic liquids (RTILs). The attraction to biolubricants began with natural oils due to their low friction and wear characteristics owing to fatty acid monolayers that enable high lubricity. Despite these accolades, natural oils suffer from thermal-oxidative instability and high pour points. To improve upon the tribological properties, natural oils were combined with solid powders additives. Currently, RTIL lubricants derived from bio-based feedstock represent a more promising potential solution to many of the problems associated with previous biolubricants. In a final study the RTILs where shown to benefit from the use of solid powder additives to further improve upon their tribological performance.

In this experimental investigation, friction and wear tests were carried out using a pin-on-disk tribometer under ambient and high temperature conditions to evaluate the tribological performance of the various natural and synthetic biolubricants. A thermogravimetric analysis (TGA) was conducted to study the thermal response of the lubricants in a high temperature oxygen-free environment. Scanning electron microscopy and surface profilometry studies were performed to assess the surface roughness.

These experiments investigated the performance of natural oils as neat bio-based lubricants to understanding the effects that long chain fatty acids have on the tribological

performance of natural oils. The experiments revealed that natural oils with low unsaturation numbers due to high concentrations of oleic acid demonstrated to have the superior friction and wear properties as well as high thermal-oxidative stability. Extensive testing of multiple natural oils with various particulate additives composed of a variety of types, sizes, and shapes revealed that natural oils benefit tremendously from nanometer-sized spherical shaped particles. However, this is not without its complexities as surface roughness, sphericity, particle size, and capillary effects all influenced the use and performance of particulate additives.

In an effort to refine the natural oils composed of particulate additives, RTILs were chosen because of their ability to lubricate in boundary lubrication due to their inherent polar molecules; their ability to be tuned for specific applications; and most notably their lack of vapor pressure providing new opportunities for liquid lubricants. Investigations into the ionic liquid lubricants revealed that longer alkyl chains on the cations with aromatic carboxylate anions exhibited the most lubricity as neat lubricants i.e. lubricants with negligible additives. Again, these lubricants were subjected to particulate additivation and it was revealed that smaller nanometer sized particles independent of the particle type provided the greatest benefit to lowering friction and minimizing wear. The performance of the ionic liquids improved with the particulate additives and it was further verified that phosphonium and imidazolium cations combined with food grade carboxylate anions such as saccharinate, salicylate, or benzoate formed biolubricants that maintained superior tribological properties as well as maintained a high degree of thermal-oxidative stability. This experimental investigation has illuminated the

iv

potential of RTIL biolubricants to satisfy the growing environmental, health, economic, and performance concerns of modern lubricants. The mechanisms governing the chemical compositions, improved tribological performance, and thermal response of the lubricants are extensively discussed along with their viability as sustainable and renewable biolubricants.

DEDICATION

This is dedicated to my parents, Thomas and Lydia Reeves, who spent their life dedicated

to their children and my little sister Marlena, may you find your path.

TABLE OF CONTENTS

LIST OF FIGURES

Chapter 3

Chapter 4

Chapter 6

xv

Chapter 7

xviii

LIST OF TABLES

xxiii

ACKNOWLEDGEMENTS

I would like use this opportunity to thank all those people who have helped me along this journey. First and foremost, I would like to express my sincere gratitude towards Dr. Michael Lovell and Dr. Tien-Chien Jen for their guidance, support, and mentoring as we collectively explored new areas in the field of tribology. Without their support, I would not have been able to pursue my degree or have made it as far I have today. Their ability to provide constructive criticism and challenge me to think through my research problems has made me a better engineer. I am forever grateful for their willingness to provide me opportunities to disseminate my research findings at national and international conferences thus allowing me to gain the feedback necessary for me to improve upon my research goals. These experiences interacting with the broader scientific community has allowed me to develop my professional career while gaining a wider perspective about the value of my research and the implications associated with poor tribological practices.

A special thank you goes to Dr. Pradeep Menezes for his willingness to work with me each and every day through this journey. He was always there to discuss my ideas, develop new research goals, proofread my writings, work with me in lab, and refine my presentations. He literally taught me all that I know about acquiring reliable experimental data and showed me how to use all of the scientific equipment that I used throughout my research. He was always enthusiast and constructive when reviewing the experimental

results and he challenged me to reach my full potential as a scientist and as an individual. He has become more than a mentor, Dr. Menezes has truly become a dear friend.

I would like to thank the members of my thesis committee Dr. Illya Avdeev, Dr. Pradeep Menezes, Dr. Junhong Chen, and Dr. Dexuan Xie for their time, support, and guidance. I would also like to thank the administrative members of the Department of Mechanical Engineering who have helped and supported me since my arrival at the University of Wisconsin-Milwaukee. You have made navigating the complexities of graduate school manageable and for that I am grateful.

I would like to thank Dr. Mark Dietz and Dr. Sarah Garvey for their collaboration with the investigations in the ionic liquids; this was truly serendipitous. Without your openness to explore new uses for ionic liquids, we would never have realized the tribological potential of such a substance. I am truly grateful for all the time you spend synthesizing the ionic liquids and performing the thermogravimetic analysis. Your assistance and our collaborative efforts have truly made an impact.

I would like to thank my previous advisor Dr. C. Fred Higgs III for his guidance throughout my collegiate career. You have been a wonderful mentor since undergrad and I am truly thankful for you pushing me to pursue my Ph.D. Your wisdom and advice are tools I continue to use daily and share with others. I would also like to thank my previous

advisor Dr. Emmanuel Wornyoh, through our experiences, I have learned that through hard work, resilience, and dedication all problems can be solved.

I would like to thank all of my previous laboratory colleagues and friends at the Green Lubrication & Tribology Laboratory, the Thermal Machining Laboratory, and the Tribology and Energy Diagnostics Lab at the University of Wisconsin-Milwaukee; the Particle Flow & Tribology Lab at Carnegie Mellon University; and The Energy and Tribology Laboratory at Columbia University for their motivating and inspiring discussions, scholarly input, and support as many of the members of these research labs pursued their doctoral degrees along with me. It was nice to have a sounding board and a group of friends that understood the rigors of graduate school and a research project in the field of tribology.

I would like to thank Dr. Steven Hardcastle for letting me use the scanning electron microscope in the Advanced Analysis Facility and Dr. Ben Church for letting me use the scanning electron microscope in the Department of Materials Science and Engineering. I enjoyed getting to know both individuals throughout my time at UWM.

I would like to thank the College of Engineering machine shop for accommodating my needs when I needed to manufacture the test specimen. Your hands on insight were valuable in the design process and I enjoyed working with you.

I would like to thank the India Institute of Science, Bangalore, India for their help in performing the 3D optical surface profilometry as well as the ultra-high magnification of the boron nitride particles.

Finally, I would like to thank my parents, Thomas and Lydia Reeves, who spent their life dedicated to their children in hopes that we would pursue our intellectual curiosity, strive after our inner potential, and give back to our community. Thank you for nurturing my love for science and engineering. Your continuous love and support made it possible for me to get through undergrad, graduate school, and now my Ph.D. I can never thank you enough for everything you have done for me and everything you continue to do for me. You are truly my inspiration and possibly the best parents a child could have. To my sibling, Rachel, Angie, Greg, and Marlena, thank you for tolerating my insatiable curiosity to learn, discover, and explore. I think you all knew I would pursue an engineering degree since we were children. Thank you for your support, you were always willing to listen to my trials and tribulations.

To all those people who have supported, encouraged, and inspired me over the years thank you. This work is for you.

Chapter 1 Introduction

1.1 Fundamentals of Lubrication

A lubricant is a substance introduced between two moving surfaces to reduce friction, minimize wear, distribute heat, remove contaminants, and improve efficiency. The importance of lubricants and sustainable lubrication systems cannot be fully appreciated until understanding the implications of not using an appropriate lubricant or a lubricant at all. In 1979, it was estimated that over $200 billion was spent in North America on machine maintenance [1]. Within the $200 billion, approximately one-third ($66.7 billion) could have been avoided with the use of adequate lubricants. More recently, estimates claim that the amount of energy wasted due to insufficient knowledge applied to the science of friction, lubrication, and wear resulted in roughly 0.4% of the gross domestic product (GDP) being wasted [2]. In the United States, this means that over $60.36 billion of the $15.08 trillion GDP was wasted due to energy loss [3]. When considering the many applications that utilize lubricants such as internal combustion engines, turbines, hydraulic systems, compressors, vehicle and industrial gearboxes, and journal and thrust bearings, it becomes easy to understand the importance that lubricants play in the compliance, effectiveness, and operation of many of these applications.

Within the lubrication market there are a vast number of applications which require specifically formulated lubricants that have given rise to the upwards of 10,000 different lubricants that satisfy more than 90% of all lubricant applications worldwide [2]. Figure 1.1 dissects the global lubrication market as of 2004, which consumed roughly

37.4 million tons of lubricant [2]. This figure illustrates how automotive and industrial lubricants are the most prevalent. Industrial lubricants amount to 32% and were composed of 12% hydraulic oils, 10% other industrial oils, 5% metalworking fluids, 3% greases, and 2% industrial gear oils [4, 5]. The 10% of other industrial oils within the industrial lubricants section consist of a wide range of lubricants such as air and gas compressor oils, bearing and circulating system oils, refrigerator compressor oils, and steam and gas turbine oils. In the automotive lubricants section, the most commonly used liquid lubricants were engine oils (petrol and diesel engine oils), automatic transmission fluids, gearbox fluids, brake fluids, and hydraulic fluids.
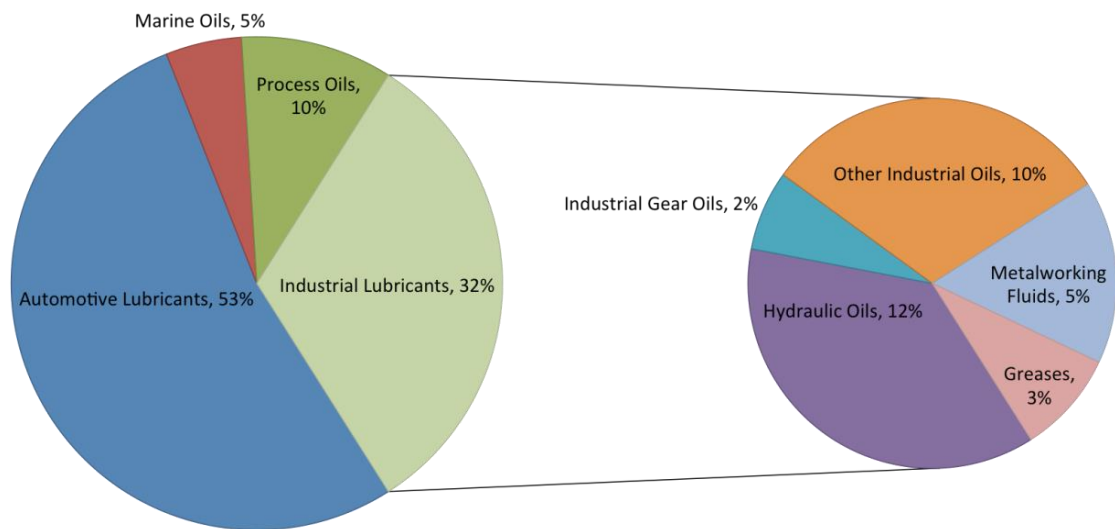
Figure 1.1: 2004 Worldwide lubrication consumption [2]

Lubricants originally consisted of natural oils and fats derived from plant and animal-based raw materials which date back to 1400 B.C. The modern lubrication market developed after the first oil well was drilled in 1959 in Titusville, PA. Since then, lubricants have evolved from mineral oils to petrochemically modified synthetic oils arriving in the 1960s, to today's bio-based lubricants harvested from raw materials derived from the oleo-chemical industry. Recently, bio-based lubricants have begun to seek prominence for their environmental-friendliness and superior tribological properties. The current trend in the lubrication industry is to develop more bio-based lubricants due to estimates indicating that nearly 50% of all lubricants sold worldwide pollute the environment, through spillage, evaporation, and total loss applications [6]. An example of lubrication pollution is that of the diesel engine particulate emissions, where approximately one third of the engine oil vaporizes thus polluting the atmosphere. The large quantity of lubricant loss into the environment is the reason behind the development of environmentally friendly lubricants. Although the lubrication market is shifting to become more environmentally responsible by reducing the use of petroleum-based lubricants due to concerns of protecting the environment, depletion of oil reserves, and increases in oil price, mineral oil remains to be the largest constituent and the foundation to most lubricants [6].

Lubricants generally consist of about 90% base oils, less than 10% additives, and minute portions of other components. The exact formulation of a lubricant is typically linked to the specific application or intended use designated by the lubricant manufacture. Lubricants vary dramatically due to the wide functionality of a lubricant to dissolve or

transport foreign particles, carrying away contaminants and debris, prevent corrosion or rust, seal clearances, dissipate heat and minimize friction and wear of components. In general, there are three categories of lubricants: liquid, solid, and gaseous. For the purpose of providing relevant background information, the focus will be on lubrication fundamentals pertaining to liquid and solid lubricants.

1.1.1 Types of Lubricants

Liquid lubricants may be characterized in a variety of methods and the most common method is by the type of base oil used. Notable base oil types are lanolin (wool grease, a natural water repellant), water, mineral oils (derived from crude oil), natural oils (derived from plants and animals), and synthetic oils (consisting of oleo-chemical compounds synthesized from compounds other than crude oil) [7]. Liquid lubricants are often viscous fluids that require circulatory pumping systems or rotary mechanical systems such as bearings or gears to distribute the fluid through the various machine elements. The primary function of a liquid lubricant is to control friction, wear, and surface damage over the intended life of a system. Secondary functions of liquid lubricants are to prevent corrosion and remove heat, dirt, and wear debris. In some instances, liquid lubricants are used to transfer either force or energy as in hydraulic systems.

Solid or dry lubricants are generally powders or semi-solids in the form of a grease or solid-liquid suspension. Some of the commonly known powder lubricant materials are graphite (C), molybdenum disulphide (MoS_2), tungsten disulphide (WS_2), and titanium dioxide (TiO_2) [8-14]. Solid lubricants offer lubrication at temperatures (up

to 350°C) that are higher than many liquid oil-based lubricants. Solid lubricants such as Teflon or PTFE (Polytetrafluoroethylene) are typically used as a coating layer to provide a non-stick surface [15]. Solid-liquid suspensions consist of solid lubricants mixed into a liquid fluid such as water or oil to form a colloidal suspension. These slurry, two-phase, or compound lubricants are often utilized in metalworking processes such as forging and extrusion. Solid lubricants can also be used in a less viscous approach where they are applied as suspension in a carrier fluid such as vegetable oil [6, 16, 17].

Greases are complex semi-solid lubricants consisting of liquid-base oils mixed with various thickening agents derived from soaps or other organic or inorganic substances [18]. Greases can also include a multitude of additives such as powder lubricants and their consistency closely resembles that of a paste [19]. They range in multiple viscosities and are available in semi-solid (synonymous with semi-liquid) form to solid form known as block greases. Greases are often processed in special grease-making facilities, as they require special equipment for their production.

1.1.2 Lubrication Regimes

Lubricants are used to reduce the frictional force between surfaces, known as a tribological system. A tribological system (or tribosystem), consists of four components as described in Fig. 1.2: (1) a contacting surface; (2) an opposing contacting surface; (3) the contacting interface along with the lubricant medium in the interface; and (4) the environment and all external properties [2, 20, 21]. Tribosystems can consist of numerous components and systems. For example, a plain bearing is a tribosystem. In this example,

the material pair is the shaft and bearing shell, with the lubricant located in the annuls gap. Other examples of material pairs that form tribosystems are in combustion engines such as the piston rings and cylinder wall and the camshaft lobes and tappets [7]. In metalworking, the tool and the work piece also constitute as a material pair forming a tribosystem.
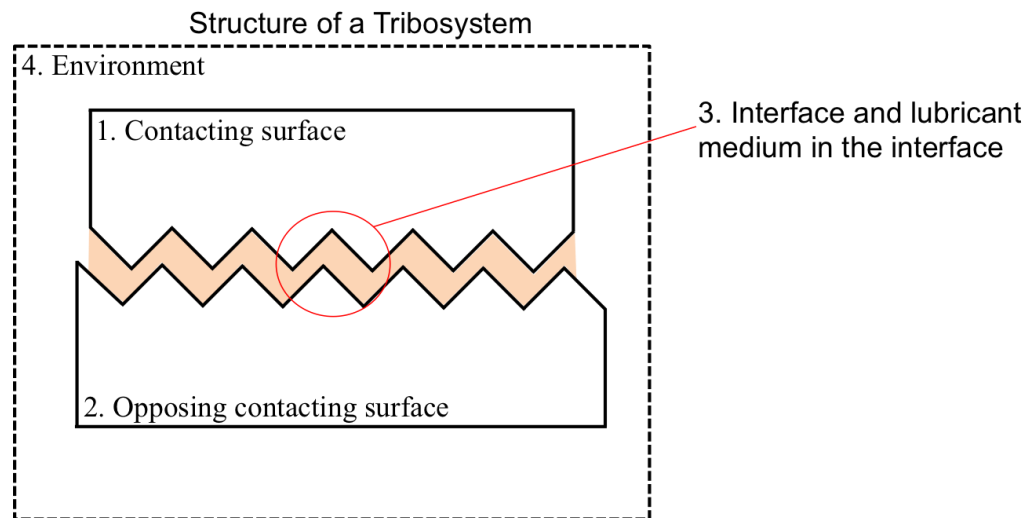
Figure 1.2: Structure of a tribosystem: (1) contacting surface; (2) opposing contacting surface; (3) interface and lubricant medium in the interface; and (4) environment

A lubricant functions by introducing a medium with a lower shear strength than the opposing surfaces. In some lubricated tribosystems, the lubricant may not completely prevent asperity contact between the surfaces. However, the lubricant will reduce the number of asperity contacts and it may also reduce the shear strength of the junctions formed during asperity contact. In other cases, the lubricant completely separates the surfaces and no asperity contacts are formed at all. Lubrication regimes are normally

associated with dominant lubrication mechanisms involved in the mechanical system as illustrated in the Stribeck curve as shown in Fig. 1.3 [2] for liquid lubrication. The three main lubrication regimes can be referred to as boundary lubrication, mixed/elastohydrodynamic lubrication, and hydrodynamic lubrication, with new definitions of these lubrication regimes presented in this experimental study.

(1) Boundary friction (h → 0)
(2) Mixed film friction (h ≅ R)
(3) Elastohydrodynamic lubrication (h > R)
(4) Hydrodynamic lubrication (h >> R)
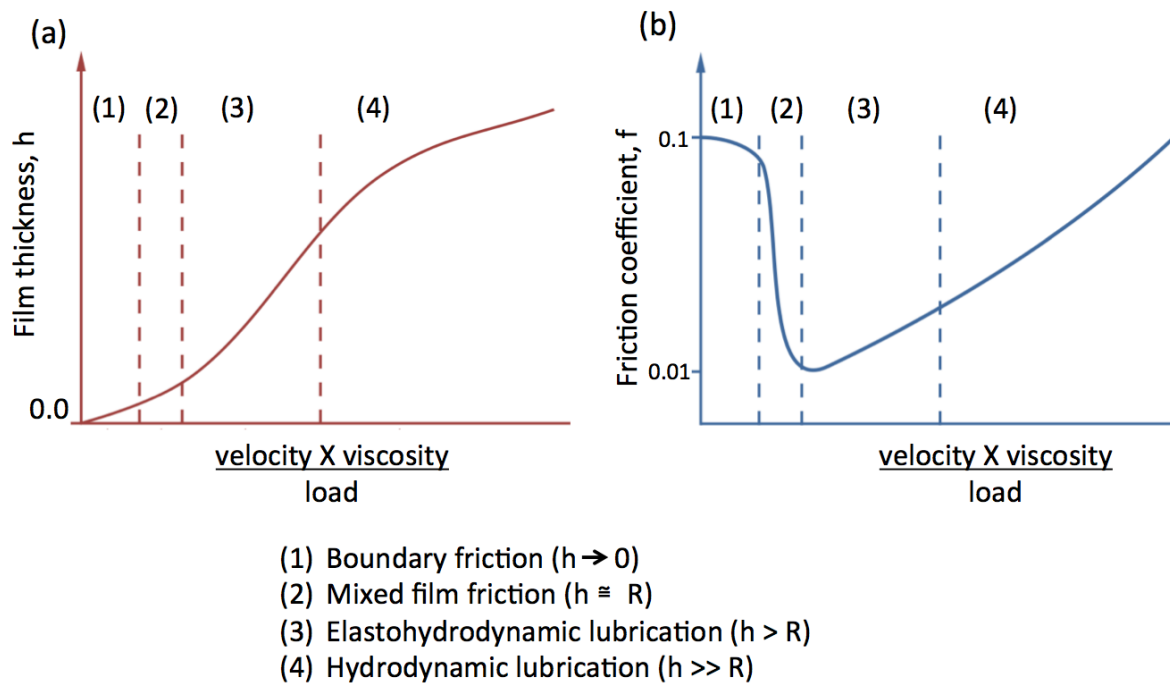
Figure 1.3: Demarcation of lubrication regimes: (A) film thickness vs. Hersey's number; (B) coefficient of friction vs. Hersey's number (i.e. Stribeck curve)

1.1.2.1 Boundary Lubrication

Boundary lubrication or boundary friction is the lubrication regime with the most asperity contact between the surfaces occurring due the presence of a thin fluid film

graphically depicted in Fig. 1.3(a) and illustrated in Fig. 1.4. Boundary lubrication is a complex process and is controlled by additives in the oil that form a thin molecular layer (monolayer) of fluid film through physical adsorption, chemisorption, and tribochemical reactions on the contacting surfaces [22]. One of the more common boundary lubrication additives are fatty acids which adhere to the metallic surfaces and form a tightly packed monolayer [23, 24]. This monolayer helps to reduce the asperity contacts that lead to high values of friction and wear. The development of a monolayer film is vital in boundary lubrication because in many practical applications thick, long-lasting, lubricant films cannot be sustained between opposing surfaces and thus these monolayer films help to reduce the amount of surface interaction [25].
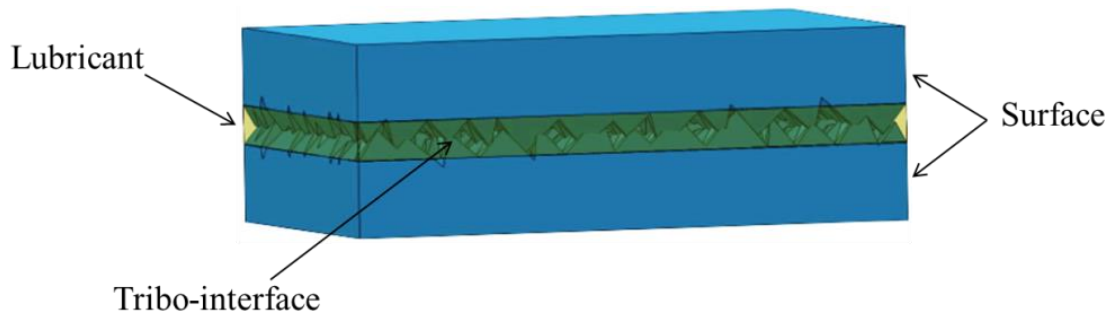
Figure 1.4: Boundary lubrication at the interface of a tribosystem; full contact of the asperities and lubrication occurs through surface interactions

1.1.2.2 Mixed/Elastohydrodynamic Lubrication

Mixed film lubrication is the combination of full film hydrodynamic lubrication and boundary lubrication. In this lubrication regime, the surfaces are transitioning away from boundary lubrication into hydrodynamic lubrication where there may be frequent asperity contacts, but at least a portion of the bearing surface remains supported partially

by a hydrodynamic film [22] as shown in Fig. 1.5. In mixed lubrication, the effects of monolayers formed by physical absorption, chemisorption, and chemical reaction remain critical to prevent unwanted adhesion during the asperity contacts [2].
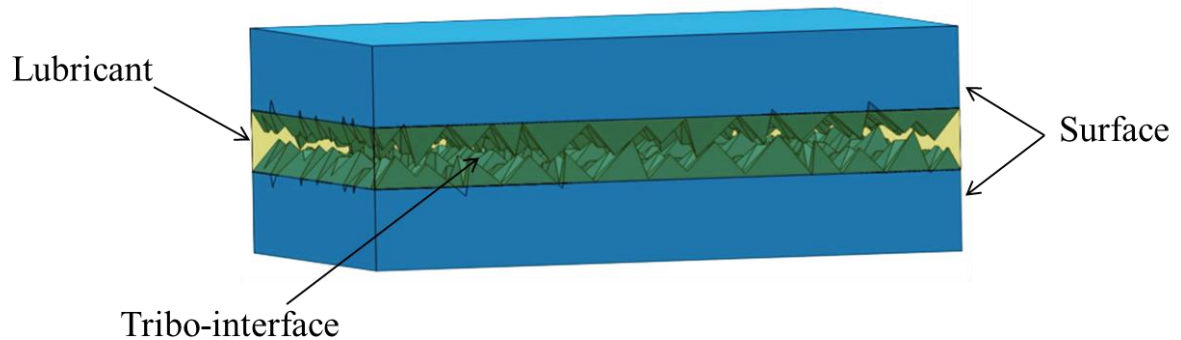
Figure 1.5: Mixed lubrication/elastohydrodynamic lubrication at the interface of a tribosystem partial asperity; contact where fluid film is on the order of the surface roughness

Elastohydrodynamic (EHD) lubrication is a subset of hydrodynamic (HD) lubrication in which the elastic deformation of the contacting solids plays a significant role in the HD lubrication process. The film thickness in EHD lubrication is thinner (typically 0.5-5μm) than that in HD lubrication and the load is still primarily supported by the EHD film [22]. In this transitional region, there is less asperity contact than that of mixed lubrication with more of the contacting surfaces being supported by the hydrodynamic fluid film.

1.1.2.3 Hydrodynamic Lubrication

Hydrodynamic lubrication also known as fluid-film or thick-film lubrication involves two non-parallel surfaces in relative motion with a layer of fluid pulled in between the surfaces to develop adequate hydrodynamic pressure to support the load of the opposing surfaces and prevent asperity contact [2]. In this lubrication regime, the surfaces are no longer in contact as illustrated in Fig. 1.6 and the fluid has established itself in significant form to create a thick-film.
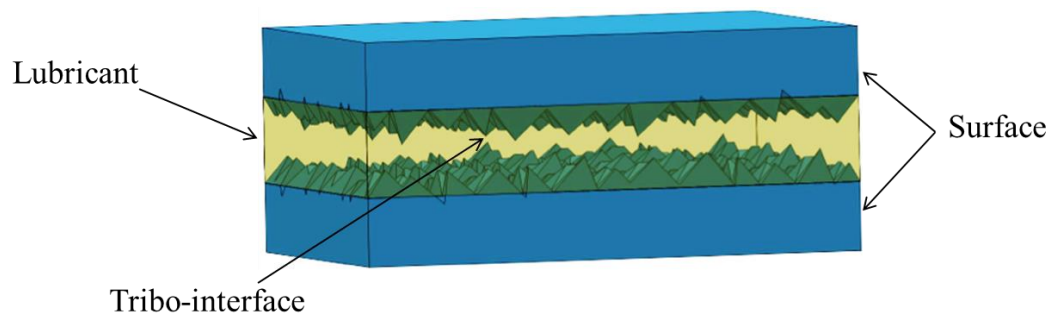
Figure 1.6: Hydrodynamic lubrication at the interface of a tribosystem; full separation of the two surfaces by the lubricant occur

1.1.2.4 Stribeck Curve

The Stribeck curve shown in Fig. 1.3(b), is a plot of the coefficient of friction against a nondimensional number known as Hersey's number (also referred to as the Stribeck number). Hersey's number was instrumental in demarcation of the aforementioned lubrication regimes [22]. Hersey's number is given by ($\eta v/p$), where 'η' is the lubricant viscosity, 'v' is sliding velocity, and 'p' is load per unit width. The values of the coefficient of friction that are depicted in the original Stribeck curve remain constant when Hersey's number approaches zero in the boundary lubrication regime.

Experimental work done by Fischer et al. [26] led to the modification of the Stribeck curve. They showed that the coefficient of friction does not remain constant in the boundary lubrication regime, but reduces as the value of Hersey's number increases. The slope of this curve is determined by the efficiency of the boundary lubricant. At low values of Heresy's number the thickness of the lubricant film, h develops much less than the surface roughness, R. In boundary lubrication (illustrated in Fig. 1.4) thin monolayers develop causing the film thickness to approach zero, resulting in significant asperity contact and high friction. An increase in sliding speed or a decrease in load at constant viscosity can cause the film thickness to steadily increase therefore shifting the lubrication regime from boundary lubrication into mixed or elastohydrodynamic lubrication. This transition results in lower coefficient of friction values and thicker hydrodynamic fluid films. In the mixed lubrication regime the fluid film thickness can be on the same order of magnitude as the surface roughness ($h \cong R$) and in the elastohydrodynamic lubrication regime the fluid film thickness can be greater than the surface roughness ($h > R$). As the sliding speed continues to increase or the load decreases with a constant viscosity, this allows progress through the elastohydrodynamic regime allowing a full uninterrupted fluid film to develop that is significantly thicker than the surface roughness ($h \gg R$). When the fluid film is much greater than the surface roughness then the hydrodynamic lubrication regime dominates. In this lubrication regime, internal friction in the lubricating film adds to external friction causing the coefficient of friction to increase as shown in Fig. 1.4. Other methods have been proposed to quantify the various lubrication regimes. The Hamrock and Dowson model

provided a formula for calculation of minimum film thickness in lubricated contacts [27-30]. The fluid film thickness parameter, λ decides the lubrication regime with boundary lubrication characterized by a value of λ less than 1; mixed or elastohydrodynamic lubrication described as $1 \leq \lambda \leq 3$; and hydrodynamic lubrication characterized by a value of λ greater than 3 [7, 22, 25, 31-34]. The fluid film thickness parameter, λ given in Eq. 1.1(a), is the ratio of fluid film thickness, h and the composite surface roughness, σ.

$$\lambda = \frac{h}{\sigma}$$ Eq. 1.1(a)

$$\sigma = \sqrt{\sigma_1^2 + \sigma_2^2}$$ Eq. 1.1(b)

In Eq. 1.1(a), the composite surface roughness is given in Eq. 1.1(b) where and σ_1 and σ_2 are RMS roughness of the two mating surfaces. The calculation of minimum film thickness for metals and polymers are presented in various publications throughout the literature [35-39].

1.1.3 Rheology of Liquid Lubricants

The characteristics of lubricants and their properties involve understanding the rheology of liquid lubricants. Many of the important characteristics of a lubricant include viscosity, consistency, flow properties, thermal stability, oxidative properties, and physiochemical properties. Viscosity of a fluid may be defined as its resistance to flow. Different oils exhibit different viscosities. Lubricant viscosity changes with temperature, load, shear rate, and pressure. Viscosity is important in the selection process of oils, because many oils have similar characteristics, but their viscosities differ. Viscosity directly relates to a lubricant's film strength and ability to keep moving parts separated.

The importance of proper viscosity selection is vital for the success of many lubrication systems. If an application operates at high speeds, low loads, and low temperatures, then it is generally accepted to use a low viscosity lubricant. Conversely, if an application operates at low speeds, high loads, and high temperatures then higher viscous lubricants should be utilized [2]. Ultimately, when choosing a lubricant based on viscosity, it is important that the lubricant is viscous enough to adequately provide a continuous fluid film in the contacting interface, but not too viscous as to create fluid friction due to viscous shearing. Viscous shearing is the phenomena that occurs when the oil is too thick for a given application and the shear planes or layers of the fluid begin to drag over one another causing increased fluid friction also known as churning.

Lubricants have three important thermal properties: specific heat, thermal conductivity, and thermal diffusivity. These parameters are important in evaluating the thermal effects during lubrication, such as the operating temperature of the surfaces and the cooling properties of the oil. The temperature characteristics are important in the selection process of a lubricant for a specific application. Other important thermal properties of a lubricant are pour point, cloud point, flash point, fire point, volatility and evaporation, oxidation and thermal stability, as well as surface tension. The pour point of a liquid is the lowest temperature at which it becomes semi-solid and loses its flow characteristics. This property is important in the lubrication of any system exposed to low temperature, such as automotive engines, construction machines, military devices, and space applications, because it provides a lower bound for the operating temperature specification. The cloud point of a fluid is the temperature at which dissolved solids such

as paraffin waxes are no longer soluble and begin to precipitate as a second phase giving the fluid a cloudy appearance during heating. The cloud point has a practical application in capillary or wick fed lubrication systems in which the forming wax could potential obstruct the oil flow. The only thermal properties, which define the fire hazard of a lubricant, are the flash and fire points. These properties are extremely important for safe application and use of a lubricant. The flash point of a lubricant is the temperature at which its vapor will flash ignite. The fire point of oil is the temperature at which enough vapor is produced to sustain burning after ignition. The fire point is always higher than the flash point. In general, the flash point and fire point of oils increases with increasing molecular weight. For a typical lubricating oil, the flash point is about 210°C whereas the fire point is about 230°C [40]. In many extended use or variable temperature applications the loss of lubricant due to evaporation can be substantial. In particular, at elevated temperatures, oils may become more viscous and eventually dry out due to evaporation. The measure of evaporation losses defines the volatility of a lubricant.

Oxidation stability is the resistance of a lubricant to molecular decomposition or reaction at elevated temperatures in an oxygen-enriched environment. Oxidation typically occurs in ambient environments where the air is composed of about 21% oxygen. Lubricating oils rapidly oxidize when exposed to air at elevated temperatures, resulting in a strong impact on the useful life of an oil. Oxidation of oils is a complex process that includes thermally activated and physicochemical reactions that depend on the level of oil refinement, temperature, presence of metal catalysts, and operating conditions. Different compounds react at different temperatures and under different conditions [41, 42]. A

lubricant that oxidizes rapidly requires more frequent maintenance or replacement resulting in higher operating costs. All substances when heated above a certain temperature will naturally start to decompose, even if no oxygen is present. In this context, thermal stability is the resistance of a lubricant to molecular decomposition or reaction at elevated temperatures in the absence of oxygen. For example, when mineral oil is heated it degrades to methane, ethane and ethylene. Similarly, natural oils that are composed of fatty acids and esters have significant thermal instability due to the present of double bonds in the unsaturated fatty acids. The presence of the double bonds in natural oils affects the thermal stability and causes the oil to breakdown at various temperatures into organic compounds, which adversely affect the functionality of the oil. Thermal stability of oils can often be improved through multiple types of refining processes such as epoxidation, metathesis, acylation, estolide formation, transesterification, and selective hydrogenation [43-56].

Surface tension is a property of a liquid that allows it to resist an external force. Many lubricants show varying degrees of wettability and spreadability on surfaces. The wettability and spreadability characteristics of a lubricant are dependent on surface tension, which is especially sensitive to physicochemical changes. Depending on the degree of oxidation or the amount of additives present in a lubricant, the oils can have different wetting and spreading properties. Surface and interfacial tension are related to the free energy of the surface and the attraction between the surface molecules, thus influencing the wetting and spreading characteristics. Surface tension refers to the free energy at a gas-liquid interface, while interfacial tension refers to interface between two

immiscible liquids. A liquid with a high surface tension resulting in less physical spreading across the surface thus acting as a poor lubricant. On the contrary a liquid with a small contact angle, having a low surface tension, and thus spreading easily across the surface acting as a good lubricant. The temperature range over which a lubricant can be used is of extreme importance because at high temperatures, oils can decompose or degrade, while at low temperatures oils may become solid or freeze. Oils can decompose by thermal and oxidative degradation. The decomposition of oil can cause a secondary effect where damage to the sensitive lubricated equipment may occur. A prime example of secondary damage is corrosion caused by the acidity of oxidized oils.

1.1.4 Lubricant Additives

Base oils (vegetable oils, mineral oils, and synthetic oils) cannot always satisfy the demands of a high performance lubricant by themselves [6]. For this reason, additives are mixed with base fluids to improve upon the lubricant's ability to reduce friction and wear, increase viscosity, improve viscosity index, resist corrosion and oxidation, increase component and lubricant lifetime, and minimize contamination [25]. Additives are synthetic chemical substances mixed with base oils to improve various characteristics of lubricants so the oils can placate the higher demand placed on them and satisfy specification requirements. Additives often improve existing properties, suppress undesirable properties, and introduce new properties to the base oils. One of the most important properties that additives enhance is a lubricant's ability to form protective films, which is especially important in boundary lubrication conditions. The use of additives has

a large influence on the performance of lubricants that make it possible to fulfill the increasing complex demands placed on lubricants. Nevertheless, there are some properties that cannot be influenced by additives, such as volatility, air release properties, thermal stability, thermal conductivity, compressibility, and boiling point. Many of these properties require chemical modifications through various refinement processes. When blending additives with base oils, it is important to have a well-balanced and optimized composition to improve the performance of the lubricant. This usually requires the formulation of high performance base oils that are derived from highly refined oils and then mixed with additives to further enhance the lubricant's properties. Lubricant additives are usually organic or organometallic chemicals that are added to oils to improve the lubricating capacity and durability of the oil. Specific purposes of lubricant additives are to [1, 2]:

    (1) enhance the wear and friction characteristics,

    (2) improve the oxidation resistance,

    (3) minimize corrosion,

    (4) control of contamination by reaction products, wear particles, and other debris,

    (5) reduce excessive decrease of lubricant viscosity at high temperatures,

    (6) decrease the pour point, and

    (7) inhibit the generation of foam.

Many of the most common additive bundles used in lubricant formulations are antiwear additives, extreme pressure additives, oxidation inhibitors, corrosion inhibitors, detergents and dispersants, viscosity improvers, pour point depressants, and foam

inhibitors. In some instances other additives like dyes and odor improvers are also added to the oils.

Additives, which improve wear and friction properties, are the most important additives used in lubricant formulations and will be a critical part to the presented experimental investigation. In machinery, when two surfaces engage in metal-to-metal contact and begin to move relative to each other, hydrodynamic lubrication does not occur at the onset or in the case of severe stress, hence, the lubricating system runs in the boundary or mixed lubrication regime. In this case, wear and friction improvers are necessary in any metalworking fluid, engine oil, hydraulic fluid or lubricating grease to prevent welding of the moving parts, reduce wear, and lower friction. Wear and friction improvers consist of chemical additives that can be divided into three groups: adsorption or boundary additives; antiwear (AW) additives; and extreme pressure (EP) additives. 'Boundary' additives are friction and wear modifiers such as fatty acids that are added to oil to minimize the asperity contact. The term 'antiwear' commonly refers to wear reduction at moderate loads and temperatures whereas the term 'extreme pressure' refers to high loads and temperatures. All of these additives control the lubricating performance of the oil, making their usage very important. If oil lacks its lubricating ability, excessive wear and friction will result, causing damage to the moving parts with usually an increase in energy consumption. Of particular importance in the current investigation are the role of boundary additives and extreme pressure additives for their ability to influence the tribological performance of lubricants.

Another important additive type is adsorption or boundary additives, also known as "friction modifiers", that control the adsorption type of lubrication and are often used to prevent stick-slip phenomena [57]. Adsorption additives are vital in boundary lubrication. The additives most commonly used in industry are fatty acids, esters, and amines of the fatty acids. These types of additives generally consist of a polar carboxyl group (-OH) at one end of the molecule that reacts with the contacting surfaces through an adsorption (adherence) mechanism to form a surface film as illustrated through the intermolecular contact depicted in Figure 1.7. The molecules attach to the charged surface by the polar carboxyl group to form a layer of molecules, which maintains load support that minimizes asperity contact as well as reduces friction and wear by having low interfacial shear stress [40]. The low shear stress is a result of the weak bonding or repulsion between opposing alkyl groups of the fatty acid molecules. The surface films or monolayers produced are only effective in boundary lubrication at relatively low temperatures and low loads.
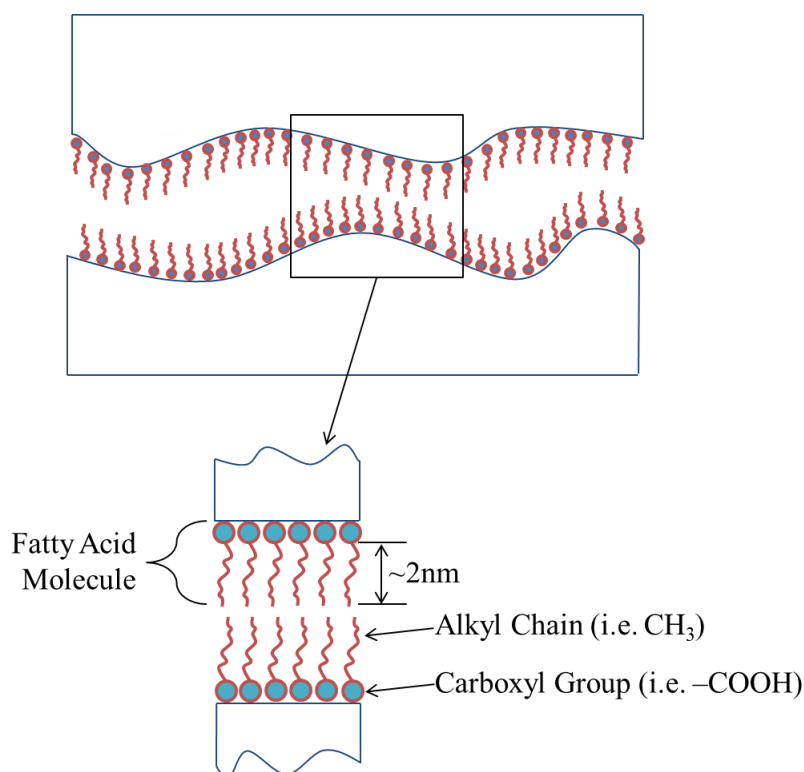
Figure 1.7: Intermolecular contact and load support of adsorbed fatty acid molecules on a surface forming a monolayer

The important characteristic of these additives is their molecular structure consisting of an unbranched chain of carbon atoms with sufficient length to ensure a stable and durable film that allows for the formation of close packed monolayers. In natural oils, these molecules are generally unsaturated fatty acids have chain lengths of 18 or 16 carbon atoms consisting of oleic, linoleic, stearic, and palmitic acids [6]. In some specialized lubricants, unique additives are utilized which combine adsorption or boundary properties with corrosion protection or some other property for a specific application [57]. Depending on the type of additive used, adsorption additives are highly sensitive to the effects of temperature and can lose their effectiveness at temperatures

between 80°C and 150°C. With increased temperature, these additives can reach a critical temperature threshold where the energy input to the surface is high enough to cause the additive to desorb rendering it inept. This critical temperature can be controlled by changing the additive's concentration, where a higher concentration results in a higher critical temperature. However, there is a downside to using a higher concentration as it also causes the lubricant to be more expensive, thus for specific applications it is important to compare lubricant performance with cost.

1.2 Tribology of Solid Lubricants

Over the last seven decades, extreme operating conditions encountered in many industrial and engineering applications - particularly those within the aerospace industry - have driven the evolution of more advanced commercial lubricants. While many long standing lubrication techniques utilize liquid or grease-type lubricants, new tribological applications have developed over the last seventy years that have led to the development of lubricants derived from solid materials and coatings with self-lubricating properties. Many tribological applications require two surfaces to slide over one another in relative motion, resulting in friction and wear, such as in cutting and forming operations, gears, bearings, and engine parts. Increasingly, more of these applications are operating in extreme environments (such as high vacuum, microgravity, high/low temperatures, extreme pressure, space radiation, and corrosive gas environments) that are beyond the tolerable and usable domain of liquid and grease-based lubricants. This has propelled the development of dry/solid lubricants that are nonvolatile and can withstand such extreme

environmental conditions. In this section, a review of the state of solid lubrication and the utilization of solid lubricants as powder transfer films, thin film coatings, and colloidal mixtures, are presented from the field of tribology as they will be discussed and utilized extensively in the experimental investigations.

1.2.1 Advantages and Disadvantages

Solid lubricants offer many advantages over liquid lubricants in applications (see Table 1.1) involving high vacuum, high temperature, cryogenic temperature, radiation, extreme dust, or corrosive environments [8, 58-60]. In extreme pressure applications (i.e., high to ultrahigh vacuum conditions—a vacuum of ~10^{-2} Pa or higher or a gas density of ~10^{-12} molecules/cm^3 or lower) liquid lubricants can vaporize [8]. For example, in space, a liquid lubricant would vaporize, thus contaminating the device it is lubricating and potentially damaging it. This example could occur in the case of an optical or electronic equipment application. On the contrary, if a solid lubricant were used this problem would no longer exist. In high temperature applications extending beyond 523 K, liquid lubricants often vaporize or decompose, limiting their use as a lubricant. In contrast, when compared to liquid lubricants, solid lubricants at these temperatures can maintain relatively low coefficients of friction. Liquid lubricants can also solidify or become highly viscous and may not be effective at cryogenic temperatures. For this reason, solid lubricants are used when operating at temperatures as low as 0 K. In radiation environments, liquid lubricants tend to decompose at 10^6 rads (radiation dose absorbed of 10^4 J/kg), whereas solid lubricants demonstrate better radiation resistance and relatively

low friction. In extreme dust areas, dust particles would ordinarily adhere to liquid lubricants, forming a grinding paste. This paste can cause abrasive wear and damage surfaces and sensitive equipment. In such a case, hard solid lubricants, such as diamond-like carbon and boron nitride films are preferred. In aerospace applications (e.g. weight-limited spacecraft and rovers) where weight limits are critical, solid lubrication is advantageous. Solid lubricants weigh substantially less than liquid lubricants and their use eliminates the need for recirculatory oil systems with pumps and heat exchangers [8, 58]. Moreover, the limited use of liquid lubricants and their replacement by solid lubricants would reduce spacecraft weight and therefore, have a dramatic impact on mission extent and spacecraft maneuverability. Under intermittent loading conditions or in corrosive environments, liquid lubricants can become contaminated, lose their lubricity, and lead to seizure of components. Changes in critical service and environmental conditions such as loading, time, contamination, pressure, temperature, and radiation, also affect liquid lubricant efficiency. When equipment is stored or is idle for extended periods, solid lubricants provide permanent satisfactory lubrication by maintaining their physicochemical attributes unlike liquid lubricants.

Table 1.1: Advantages and Disadvantages of Solid Lubricants [61]

Advantages	Disadvantages
• Are highly stable in high-temperature, cryogenic temperature, vacuum, and high-pressure environments • Have high heat dissipation with high thermally conductive lubricants, such as diamond films • Have high resistance to deterioration in high-radiation environments • Have high resistance to abrasion in high-dust environments • Have high resistance to deterioration in reactive environments • Are more effective than fluid lubricants at intermittent loading, high loads, and high speeds • Enable equipment to be lighter and simpler because lubrication distribution systems and seals are not required • Offer a distinct advantage in locations where access for servicing is difficult • Can provide translucent or transparent coatings, such as diamond and diamond-like carbon films, where desirable	• Have higher coefficients of friction and wear than for hydrodynamic lubrication • Have poor heat dissipation with low thermally conductive lubricants, such as polymer-based films • Have poor self-healing properties so that a broken solid film tends to shorten the useful life of the lubricant (however, a solid film, such as a carbon nanotube film, may be readily reapplied to extend the useful life.) • May have undesirable color, such as with graphite and carbon nanotubes

Some of the disadvantages of solid lubricants are their higher coefficient of friction and wear rates when used in hydrodynamic lubrication processes. Many solid lubricants maintain poor heat dissipation with low thermal conductivity when compared to liquid lubricants. For this reason, applications that require heat dissipation generally resort to liquid lubricants that can be pumped or circulated to remove heat. In cases where a solid lubricant is used and minimal heat generation is required, alternative techniques

must be implemented to dissipate the heat. Additionally, solid lubricants have poor self-healing properties in the sense that a broken solid film or the inability to establish a transfer layer can cause a decrease in the useful life of particular mechanical components.

1.2.2 Properties of Solid Lubricants

One method of quantifying lubricants is through their physiochemical properties. This method classifies them based on their chemistry, crystal structure, and lubricity. Table 1.2 presents the most widely used and most recently developed lubricants by their subclasses as well as providing their coefficient of friction range. The ranges in the coefficient of friction are due to the fact that friction is a system dependent property that is dependent upon test environment, operating conditions, and surface geometrical configuration. Ambient conditions such as temperature and humidity as well as the type of counter face materials and surface texture also affect the friction coefficient of a given solid lubricant. Moreover, even the physical nature (i.e., powder, thin film, bulk, composite, and crystalline or amorphous state), deposition method, and/or application method of the solid lubricant can cause variations in the friction and wear properties.

Table 1.2: Solid Materials with Self-Lubricating Capabilities [7]

Classification	Key Examples	Typical Range of Friction Coefficient
Lamellar Solids	MoS_2	0.002–0.25
	WS_2	0.01–0.2
	hBN	0.150–0.7
	Graphite	0.07–0.5
	Graphite fluoride	0.05–0.15
	H_3BO_3	0.02–0.2
	GaSe, GaS, SnSe	0.15–0.25
Soft Metals	Ag	0.2–0.35
	Pb	0.15–0.2
	Au	0.2–0.3
	In	0.15–0.25
	Sn	0.2
Mixed Oxides	$CuO–Re_2O_7$	0.3–0.1
	$CuO–MoO_3$	0.35–0.2
	$PbO–B2O_3$	0.2–0.1
	$CoO–MoO_3$	0.47–0.2
	$Cs_2O–MoO_3$	0.18
	$NiO–MoO_3$	0.3–0.2
	$Cs_2O–SiO_2$	0.1
Single Oxides	B_2O_3	0.15–0.6
	Re_2O_7	0.2
	MoO_3	0.2
	TiO_2 (sub-stoichiometric)	0.1
	ZnO	0.1–0.6
Halides and Sulfates or Alkaline Earth Metals	$CaF2, BaF_2, SrF_2$	0.2–0.4
	$CaSO_4, BaSO_4, SrSO_4$	0.15–0.2
Carbon-Based Solids	Diamond	0.02–1

	Diamond-like carbon	0.003–0.5
	Glassy carbon	0.15
	Hollow carbon nanotubes	—
	Fullerenes	0.15
	Carbon-carbon and carbon-graphite-based composites	0.05–0.3
Organic Materials/Polymers	Zinc stearite	0.1–0.2
	Waxes	0.2–0.4
	Soaps	0.15–0.25
	PTFE	0.04–0.15
Bulk or thick-film (>50μm) composites	Metal-, polymer-, and ceramic-matrix composites consisting of graphite, WS$_2$, MoS$_2$, Ag, CaF$_2$, and BaF$_2$	0.05-0.04
Thin-film (<50 μm) composites	Electroplated Ni and Cr films consisting of PTFE, graphite, diamond, B$_4$C, etc., particles as lubricants	0.1–0.5
		0.05–0.15
	Nanocomposite or multilayer coatings consisting of MoS$_2$, Ti, DLC, etc.	

Lamellar or layered solid lubricants are some of the most widely used class of lubricants by engineers. A significant amount of research and development has been performed to understand the tribological characteristics of these lubricants as well as determining the optimal lubricant for specific applications. A few examples of lamellar lubricants are graphite, molybdenum disulfide (MoS$_2$), hexagonal boron nitride (hBN), gallium selenium (GaSe) and boric acid (H$_3$BO$_3$). These lamellar solid powders all have similar molecular structures composed of layers of atoms bonded together with covalent

bonds. These layers are held together by the weak van der Waals force and maintain different distances between the layers for different molecules. Figures 1.8 and 1.9 show a schematic representation of the layered crystal structure of GaSe and H_3BO_3 molecules respectively.
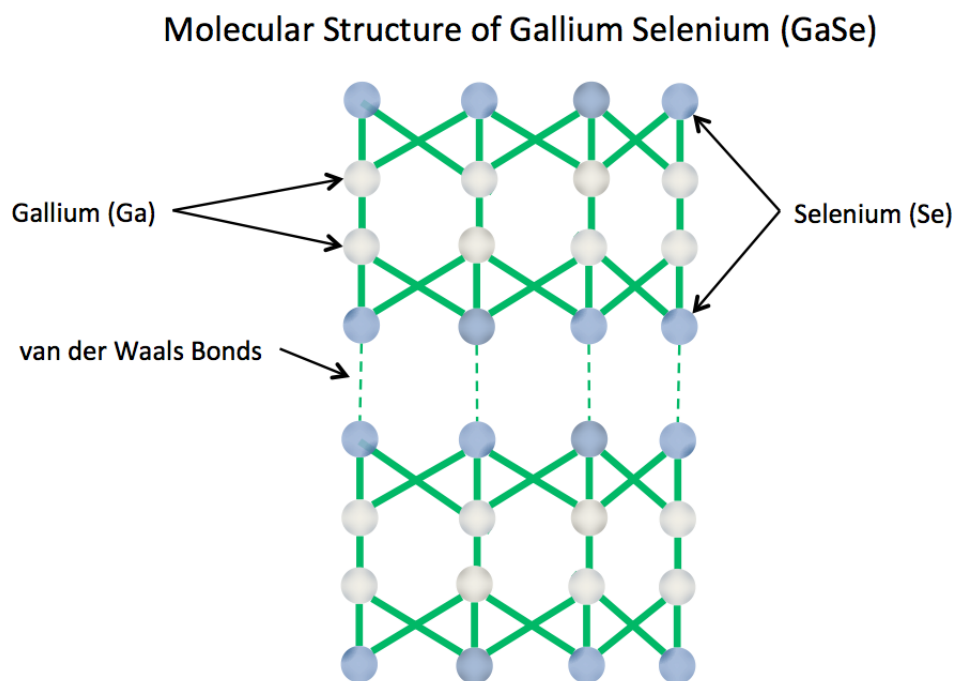
Figure 1.8: Illustration of the layered crystal molecular structure of Gallium Selenium (GaSe) a Monochalcogenide

Molecular Structure of Boron Acid (H₃BO₃)
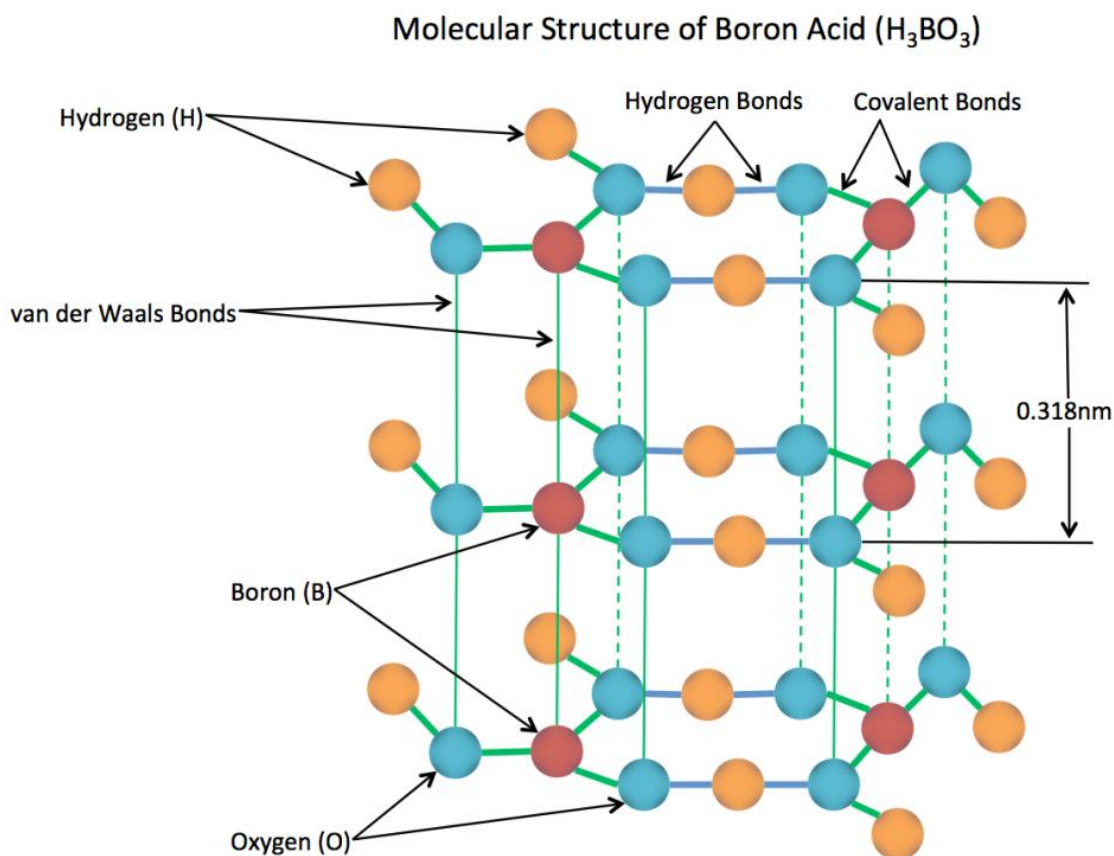
Figure 1.9: Illustration of the layered crystal molecular structure of boric acid (H_3BO_3)

Some of the more widely used solid lubricants are derived from natural minerals, extracted from deposits found in the earth such as MoS_2, graphite, and boric acid. Other solid lubricants are synthetic, for example WS_2, hBN, fluorinated graphite, and transition metals diselenides (consist of two selenide molecules) and ditellurides (consist of two telluride molecules). The use of diselenides and ditellurides as solid lubricants is significantly less common than the use of graphite and MoS_2. As with many lamellar lubricants, transition metal dichalcogenides gain their lubricity from their layered crystal

structure caused by the low intra-layer shear resistance due to the weak van der Waals force. Furthermore, not a single lubricant, including solid lubricants, can provide both low and consistent friction coefficients over a wide variety of test conditions, temperatures, environments, and deposition methods. Therefore, it is customary for lubrication engineers to optimize a lubricant for a specific application with a defined set of operational and environmental conditions.

Due to the sensitivity of each lubricant to its environment, many techniques have been developed to optimize a particular lubricant for a specific application. In extreme environments consisting of vacuum or high/low temperatures MoS_2, WS_2, and hBN are preferred as solid lubricants [62, 63]. Graphite and H_3BO_3 are superior lubricants in moist air environments, however, they are poor lubricants in dry or vacuum environments. As a modification, tribologists have learned that if graphite is fluorinated through a process of electrolysis in a solution of hydrogen fluoride, this creates graphite fluoride. Graphite fluoride has larger spacing between the carbon-carbon layers in graphite resulting in easier shear and hence better lubricity in dry environments. Among the lamellar solids, MoS_2 and WS_2 have some of the best overall load-carrying capacities when used as thin films. Most lamellar solids have good wetting capability and chemical affinity for ferrous surfaces [64]. On a rough or porous sliding surface, MoS_2 and WS_2 accumulate in the valleys between asperities, thus providing a smoother surface finish. When applied properly, these solid lubricants can withstand extreme contact pressures without being squeezed out of the load-bearing surfaces. WS_2 is preferred over MoS_2 when applications involve relatively higher temperatures [14]. However, WS_2 is a synthetic lubricant and

therefore it is more expensive than MoS_2, which is derived from a natural mineral known as molybdenite. Selenides of molybdenum (Mo), tungsten (W), and niobium (Nb) can provide even higher temperature capabilities than their sulfide counterparts, and have demonstrated greater electrical conductivity, however, they too are expensive and hence they are used less frequently [7].

1.2.2.1 Transition-Metal Dichalcogenides

Transition-metal dichalcogenides such as MoS_2 shown in Fig. 1.10 are among the lowest-friction materials known for their use in dry, vacuum, and cryogenic environments. They comprise of MX_2 structure, where M is a transition metal consisting of molybdenum (Mo), tungsten (W), niobium (Nb), or tantalum (Ta) and X_2 refers to a chalogenide consisting on two atoms from Group 16 in the periodic table, most notably consisting of sulfur (S), selenium (Se), or tellurium (Te). MoS_2 and WS_2 are among the most widely used transition-metal dichalcogenides. Dichalcogenides are chemically stable and resist attack by most acids with the exception of aqua regia (also known as nitro-hydrochloric acid), hydrochloric acid (HCL), sulfuric acid (H_2SO_4), and nitric acid (HNO_3). At room temperature in ultrahigh vacuum, these solid lubricants can provide the lowest coefficient of friction values ranging from 0.002 to 0.2. Their shortcomings occur in the presence of moisture environments, which has a detrimental effect on their lubricity [65, 66]. Oxidation of MoS_2 begins when temperatures reach about 648 K and at approximately 773 K, rapid oxidation occurs resulting in MoO_3 and SO as byproducts. The thermal-oxidative stability of WS_2 is better than that of MoS_2 and thus it is used in

higher temperature application.

Molecular Structure of Molybdenum Disulfide(MoS$_2$)
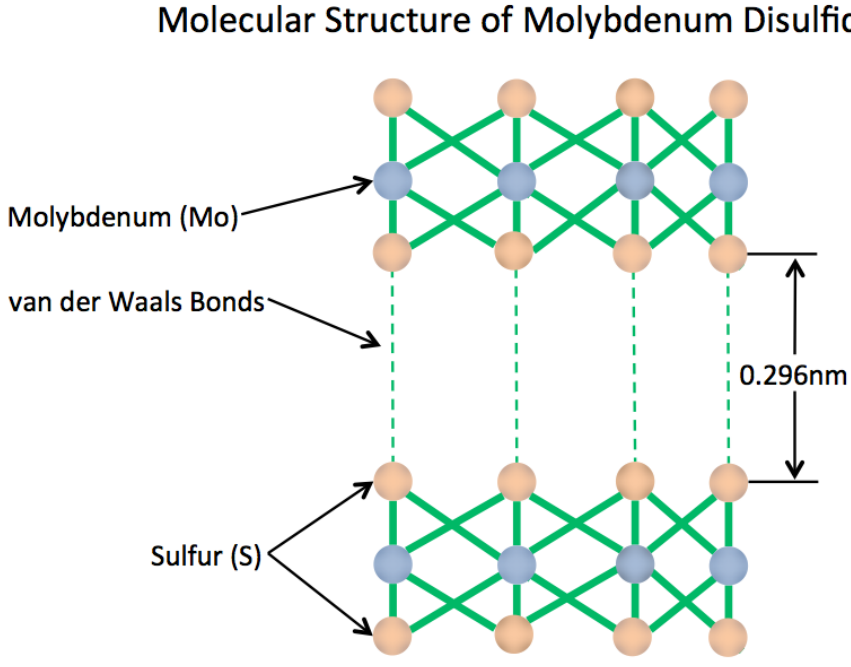
Figure 1.10: Illustration of the layered crystal molecular structure of molybdenum disulfide (MoS$_2$) a dichalcogenide

1.2.2.2 Graphite

Another lamellar solid that offers superior friction reduction and wear resistance properties is graphite. Graphite occurs naturally from deposits in the earth and can be synthesized by heating petroleum coke to temperatures of 2973 K beyond that of graphitization, which converts carbon to graphite. Graphite has been used in many industrial applications due to its good lubricity, abundance, low cost, and resistance to both acids and bases. Graphite can be used as a lubricant in a variety of forms such as a

powder, bulk, thin film, colloidal dispersion, solid, and composite forms to combat friction and wear. In some applications, it is used as a dispersant in water, solvents, oils, and greases to achieve better lubricity under extreme application conditions such as lubrication of molds and dies in metal forming; flange on rails; and railcar wheels. Graphite has even found uses as a self-lubricating filler in various metal, ceramic, and polymer matrix composites used in various engines, aircraft components, and seal applications [67-69]. Graphite is one of the softest materials with a relatively poor thermal conductivity but a good electrical conductor. The structure of graphite is sheet-like crystals where carbon atoms are strongly bonded in a plane to form a layer and the layers are weakly held together by van der Waals forces. The layered crystal molecular structure of graphite is shown in Fig. 1.11. In dry air, inert atmospheres, or vacuum, the lubricity of graphite degrades quickly, causing it to be removed from the contacting surfaces. In contrast, the tribological properties of graphite are superior in moist or humid environments. Research has shown that the lubricity of graphite is not solely due to its layered crystal structure, but depends strongly on the quantity of water vapor in the environment. Graphite requires a small amount of condensable vapor to allow the atomic layers to slide with ease thus improving its lubricity. The thermal-oxidative stability of graphite allows it to lubricate in open-air environments where the temperature is below 773 K, however the friction does tend to increase as the temperature rises. Beyond this temperature threshold, graphite begins to rapidly oxidize and lose its lubricity. In vacuum environments, the trends are reversed for graphite. For example, it has an initially higher coefficient of friction of 0.4 at lower temperatures in vacuum, however when the

temperature increases, the coefficient of friction decreases. At a maximum temperature of 1573 K, the coefficient of friction decreases to about 0.2 and beyond this temperature, graphite begins decompose and lose its lubricity.

Molecular Structure of Graphite (C)
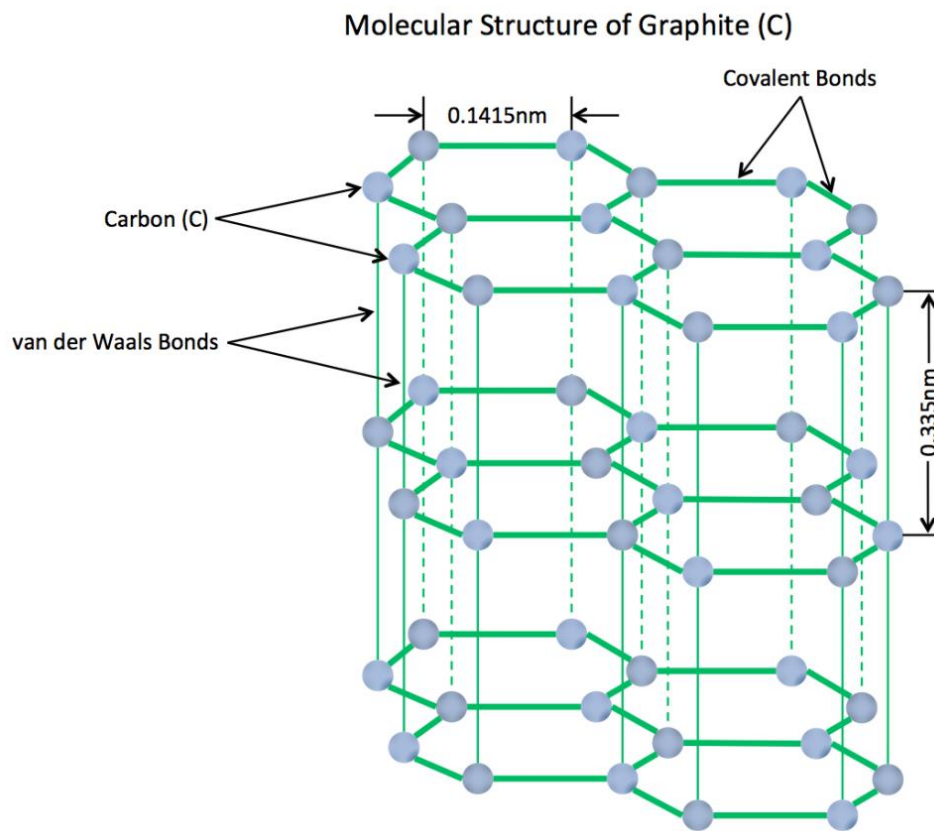
Figure 1.11: Illustration of the layered crystal molecular structure of graphite (C)

1.2.2.3 Hexagonal Boron Nitride

A lamellar solid with similar structural and lubricating properties as graphite is hexagonal boron nitride (hBN), also referred to as "white graphite" [70]. The layered crystal structure is shown in Fig. 1.12. It can be seen that the molecular structure resembles other lamellar solid lubricants such as graphite. This soft, white, lubricious

powder is derived from the reaction of boric oxide or boric acid with urea or ammonia at high temperatures ranging between 1073 and 1273 K. There are two crystal structures of boron nitride, cubic and hexagonal. Cubic boron nitride is extremely hard and wear resistant like diamond and is very abrasive. Hexagonal boron nitride, a synthetic inorganic solid lubricant, is a highly refractory and thermochemically stable material that maintains its lubricious qualities at high temperatures with negligible oxidation occurring below 1273 K. Moreover, hBN is chemically inert and resists attack by molten metals, oxides, glasses, slags, and fused salts. It is environmentally friendly and displays excellent electrical insulating properties, even under vacuum. The lubricating properties of hBN arise from its graphitic-like crystal structure where atomic planes arranged in two-dimensional arrays of boron and nitrogen atoms, configure in a honeycomb lattice as illustrated in Fig. 1.12. The bonding between atoms in a plane is the strong covalent bond and the bonding between each planar layer is the weak van der Waals bond.

Lubrication applications of hBN include compaction through hot pressing to create dense solid pieces or prepared as a solid polymer composite structure. Hexagonal boron nitride has been used as a dispersed additive to oils and greases to improve antiwear and antifriction properties as well as a self-lubricating coating where it is plasma/thermal-sprayed with ceramics [6, 17, 18, 71]. It can be used as metal-ceramic electro-deposition coatings, constituent in epoxy coatings, and has found uses in aqueous and oil dispersions as release agents in metalworking operations. The physical and chemical properties of hBN are similar to graphite, which allows it to function in a variety of similar applications under sliding contact in conditions involving high-load,

high-temperature, and extreme pressure [72, 73].
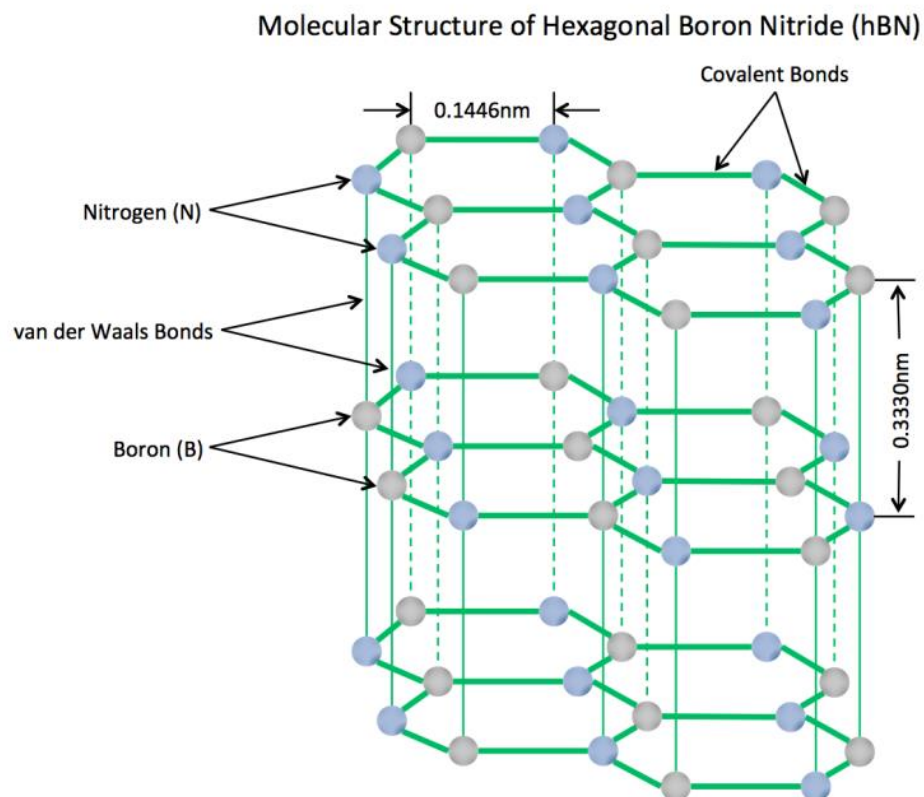
Figure 1.12: Illustration of the layered crystal molecular structure of hexagonal boron nitride (hBN)

1.2.3 Lubrication Mechanisms

The lubrication mechanisms that govern solid lubricants are controlled by intrinsic and extrinsic parameters. There are no solid lubricants that can provide both low friction and wear in all environments. The friction and wear performance of solid lubricants is influenced by inherent properties, environmental parameters, and application usage. Solid lubricants can be used as dry lubricants by themselves in which their physiochemical properties are dominant. They are used as additives in oils and greases

where their physical properties prevail and in coatings in which physiochemical reactions and adherence become critical. This section discusses the viability of solid lubricants based on their lubrication mechanisms and the lubricating environment.

Layered solid lubricants include lamellar solids (i.e. graphite, hBN, and H_3BO_3), transition-metal dichalcogenides (i.e. MoS_2 and WS_2), and metal-monochalcogenides (i.e. GaS, GaSe, or SnSe). The lubrication mechanisms of these various solid lubricants are controlled by their affinity for interfilm sliding, intrafilm flow, and interface slip, which are all dependent on the material's interlayer shear properties. As previously discussed in this chapter, all of these solids have layered crystal structures where atoms lying on the same plane are closely packed and strongly bonded through ionic, covalent, or hydrogen bonds and the layers themselves are bonded through weak van der Waals forces. The lubricity, wear resistance, and durability of these solid lubricants are derived from their strong interatomic bonding and packing within each layer that allows for the high in-plane strength. Furthermore, when these lubricants are entrained between two surfaces in relative motion, they are able to align themselves parallel to the relative motion and slide over one another with relative ease providing lubrication. Moreover, many of these layered solids coalesce in surface asperities creating a thin smooth transfer film that is able to accommodate the relative sliding velocity and dissipate frictional energy affording longer wear lives and greater performance.

The lubricity of solid lubricants is controlled by intrinsic properties, such as the layered crystal structure, interlayer distance, electrostatic attraction, and extrinsic parameters such as humidity, temperature, and environment. The intrinsic properties

contribute to the tribological performance of solid lubricants because the layered crystal structure allows the solids to shear with minimal resistance. The interlayer distance between layers is also important because as the interlayer distance increases, the ability of the van der Waals force to hold adjacent layers together decreases, thus the shearing resistance between layers weakens enhancing lubricity. For graphite and MoS_2 the interlayer distances are 0.335 nm and 0.296 nm respectively. In humid air, graphite can have a lower friction coefficient than MoS_2, however, in dry and vacuum environments MoS_2 has the lower coefficient of friction [7]. This shows how the lubricity and tribological performance of solid lubricants are largely controlled by extrinsic factors. Solid lubricants can be applied as dry lubricants or as additives in oils or greases. In either case, the physical mechanisms that control their lubricity and wear resistance are the same. Lamellar solids are able to coalesce in the valleys between asperities on rough or porous sliding surfaces while withstanding extreme contact pressures without being squeezed out of the contacting interface. In these situations, the solid lubricant develops into a thin lubricating transfer film that can protect a surface by accommodating the relative motion by easily shearing and carrying a portion of the asperity contact load, thus decreasing friction and minimizing wear. This physical behavior allows lamellar solids to be used as solid lubricants whether they are in the form of a granular powder, compressed pellet, or colloidal solution.

1.3 Conclusions

The advancements in lubricants have become an integral part of the development of machinery and various corresponding technologies. Lubricants and lubrication techniques are linked to numerous fields of expertise and without this interdisciplinary aspect, the progression of lubricants and many applications may have failed to achieve success. Lubrication is a vital segment of tribology with implications affecting world energy usage, system reliability, application feasibility, the environment, and financial stability. With more than 10,000 different types of lubricants and an abundance of additives, selecting the appropriate lubricant for a particular application is not obvious. Lubrication engineers must have an understanding of the performance demands of the application and the composition of the lubricating materials, before selecting a lubricant that has appropriate physicochemical properties that are not detrimental to the system.

Chapter 2 Science and Technology of Biolubricants

2.1. Introduction

In the lubrication industry there are nearly 10,000 different lubricant formulations of oils, greases, and other functional fluids to satisfy more than 90% of all lubricant applications. The primary function of these lubricants is to decrease friction, transmit energy, protect against corrosion and wear (attrition), remove heat, disperse wear debris, eliminate foreign contaminants, and act as a sealant [25]. The use of natural organic oils and fats derived from plants and animal-based raw materials (e.g. soybean, palm, tallow, and lard) dates back to the earliest days of lubrication for their ability to lower friction and prevent wear. In 1859, the first commercial oil well was drilled in Titusville, PA, USA, signaling the rise of the modern petroleum oil industry, which would eventually lead to the decline of the use of natural oils as lubricants. The advent of petroleum-based oils produced rapid advances in lubrication technology that quickly dominated other oils, such as natural plant and animal-based oils. During the mid-1930s, the properties of petroleum-based oils were significantly improved through the use of additives and new chemical synthesis and modification techniques that enhanced the load carrying capacity, lubricity, corrosive protection, and thermal-oxidative stability. These improvements in the properties of petroleum-based oils often surpassed similar properties of natural oils.

Over the last 150 years, petroleum-based oils have established themselves as the universal lubricant for most industrial, commercial, and personal applications. It is estimated that upwards of 50% of all lubricants worldwide enter the environment from

spills, improper disposal, accidents, volatility, and total loss applications such as chainsaw oils, two-stroke engines, concrete mould release oils, exhaust fumes in engines, and metal cutting and forming processes [74]. Of these leakage types the most problematic are the uncontrolled losses via broken hydraulic hoses or accidents whereby large quantities of fluids escape into the environment contaminating soil; surface, ground, and drinking water; as well as the air. It is estimated that 30 to 40 million tons of lubricant are consumed annually, with 20 million tons of this lubricant entering the environment, totaling to a 55% loss of lubricant [2]. Over 95% of these lubricants entering the environment are petroleum-based and harmful to the environment [75]. As a result of their high toxicity and low biodegradability, petroleum-based lubricants and functional fluids (hydraulic fluids) constitute a considerable threat to the environment. More astonishingly, it is estimated by some that over 90% of all petroleum-based lubricants could be replaced by biolubricants [76]. Illustrating the substantial potential biolubricants have to solve our environmental problems caused by toxic petroleum-based lubricants.

Lubricants are often classified into three categories: (1) mineral oils, that are predominantly petroleum-based lubricants and are the most common lubricants; (2) natural oils, that are derived from plant-based oils and animal-based fats or tallow; and (3) synthetic oils, that include polyalphaolefins (PAOs), synthetic esters, polyalkylene glycols (PAGs), alkylated aromatics, perfluoroalkylpolyethers (PFPEs), among others. In the last three decades natural and synthetic oils (not mineral oils) derived from bio-based feedstock have seen a resurgence for industrial purposes. The lubrication industry is

shifting to become more environmentally responsible with much of the attention centered around ecological conservation and sustainability through the use of bio-based lubricants for industrial purposes to be used as functional fluids. The term "biolubricant" has been ascribed to all lubricants, derived from bio-based raw materials (such as plant oils, animal fats, or other environmentally benign hydrocarbons), which are biodegradable and non-toxic to humans and other living organisms, particularly aquatic environments where the impacts are more detrimental [77]. In an effort to curb the use of petroleum-based lubricants, a primary focus has been on the development of technologies that incorporate biolubricants as biofuels and industrial lubricants because they are non-toxic, biodegradable, and renewable [78]. In the global lubrication market, the rise in biolubricants is a result of new environmentally friendly initiatives and economic factors such as protecting the environment from toxic substances; the depletion of the world's crude oil reserves; increasing crude oil prices; and increasingly stringent government regulations regarding use, operation, and disposal of petroleum-based oils [79, 80]. Furthermore, the emphasis placed on biolubricants is a result of the increase in demand for environmentally-friendly lubricants that are less toxic to the environment, renewable, and provide feasible and economical alternatives to traditional petroleum-based lubricants [81, 82].

Many biolubricants are comprised of plant oils, animal fats, or chemical modifications of these oils and are widely regarded as environmentally benign because of their superior biodegradability and renewable feedstock [77]. Although, mineral oils are classified according to their performance, biolubricants are classified according to their

base fluid composition. Traditionally, there are three groups of biolubricants: natural esters (type HETG), synthetic esters (type HEES), and polyglycols (type HEPG). The properties of these groups are listed in Table 2.1.

Table 2.1: Original classification of environmentally friendly biolubricants

Fluid	Base Fluid	Saturation	Feedstock
HETG	Natural ester	Unsaturated	Natural
HEES	Synthetic Ester	Unsaturated	Natural
		Saturated	Synthetic
HEPG	Polyglycol	…	Synthetic

For the purpose of this review, a more rudimentary classification of biolubricants will be imposed according to the synthesis process of the lubricant. Biolubricants will be classified in two categories: (1) natural oils and (2) synthetic oils. Natural oils (also known as natural esters) are biolubricants with the base-stock consisting of vegetable (plant-based) oils or animal fats. Synthetic oils (or synthetic esters) are biolubricants comprised of esters, diesters, genetically modified organisms, perfluoroalkylethers, ionic liquids, polyglycols, or any other lubricant consisting of chemical compounds that are artificially made [83]. Many biolubricants have superior lubricity and wear resistance that exceeds those of petroleum-based lubricants resulting in their increased usage as a base-stock for industrial oils and functional fluids, thus facilitating the biolubricant resurgence [84]. The largest drawback to biolubricants particularly natural oils are their poor thermal-oxidative stability and high pour points, which have led to the development of

synthetic biolubricants that undergo chemical modifications [84]. Ultimately, biolubricants formulated from bio-based feedstocks should offer the following advantages over petroleum-based oils [45]:

(1) higher lubricity lending to lower friction losses and improved efficiency affording more power output and better fuel economy

(2) lower volatility resulting in decreased exhaust emissions

(3) higher viscosity indices

(4) higher shear stability

(5) higher detergency eliminating the need for detergent additives

(6) high dispersancy

(7) rapid biodegradation resulting in decreased environmental and toxicological hazards

This review provides a summary of biolubricants detailing the types of biolubricants, discussing vulnerabilities, and revealing enhancement techniques. Further investigation examines the biodegradability and economy of biolubricants as well as recent advances in new technologies pertaining to their utilization.

2.2. Biolubricants

Biolubricants can be derived from a variety of bio-based feedstock, often this is a vegetable oil because they offer natural biodegradability and low toxicity. In other instances genetically-modified natural oils, such as high-oleic sunflower and canola (rapeseed), are being pursued for applications where higher oxidative stability is needed.

Synthetic esters derived from natural and artificial resources i.e. the hydrolysis of solid fats and low grade waste materials such as tallows to produce the constituent ester compounds are also common. Polyglycols (PGs) are another class of synthetic biolubricants similar to synthetic esters, yet PGs are the only type that is water-soluble. This property can be advantageous for biological degradation in water. On the contrary, this poses more of an environmental threat as polyglycol-contaminated water can penetrating more deeply into the soil layers, thus contaminating ground water. For this reason in some countries, PGs are not considered environmentally friendly fluids, thus their discussion will be limited in this review.

Similar to the development of environmentally friendly base fluids, new additives are also being developed. Ecofriendly initiatives, necessitate the development of additives for two reasons: (1) existing additives used for mineral oils deteriorate the performance properties in many biolubricants and (2) existing additives contain toxic substances leading to a significant deterioration of the biodegradability of the lubricant as a whole [85-89]. Other biolubricants are composed of environmentally benign solid particles in bio-based oil colloidal suspensions. The formulation of these two-phase lubricants means that biodegradable and low toxicity fluids i.e. natural oils are combined with biodegradable and low toxicity additives [76].

2.2.1 Natural Oils

The chemical composition of biolubricants derived from oils and fats affords them the ability to be used as fuels and lubricants for various applications. The sources of

bio-based oils and fats are numerous and encompass a wide variety of seeds, fruits, nuts, vegetables, animals, and marine life making them readily available, inexpensive, and environmentally benign [78]. Natural oils derived from plant-based oils are common because they have viscosity and surface tension properties similar to petroleum-based lubricants used in industrial applications for metal-stamping and metal-forming [24, 90]. Many plant-based oils are obtained by expeller methods and solvent extraction processes [81, 91-93]. There are a wide variety of plant-based oils such as avocado, canola (rapeseed), castor, coconut, corn, cottonseed, olive, palm, palm kernel, peanut, safflower, sesame, soybean, and sunflower, among many others that are native to particular regions of the world. The efficacy of natural oils and fats is determined by their chemical composition, where they predominantly consist of mixtures of fatty acid esters derived from glycerol. Inherently, these oils and fats are naturally occurring organic substances whose properties and utility vary based on biological factors such as nutrient availability, climate, light, temperature, humidity, and water as well as being influences based on different extraction methods [81, 91, 92, 94]. Despite their biologically inconsistent chemical composition, natural oils have superior wear properties, lower coefficients of friction, excellent biodegradabilitiy, higher flashpoints, sustainable and renewable feedstocks, and a lower ecotoxicity classification than mineral oils [95]. Additionally, it has been shown in the literature that natural oils derived from plants, with high-oleic acid (>80%) contents, surpass Group I petroleum-based lubricants at room temperature [96]. When comparing natural oils to mineral and synthetic oils they have a higher lubricity,

lower volatility, higher shear stability, higher viscosity index, higher load carrying capacity, and superior detergency and dispersancy [97].

Many of the accolades associated with natural oils are a result of their molecular structure, which affords superior lubrication properties. The attraction to natural oils is due to their chemical composition of approximately 98% triacylglycerol molecules made up of esters derived from glycerol and long chains of polar fatty acids. Natural oils also contain minor amounts of mono- and di-glycerols (0.5%), free fatty acids (0.1%), sterols (0.3%), and tocopherols (0.1%) [75]. Fatty acids themselves are carboxylic acids with long unbranched aliphatic chains (with 4 to 28 carbon atoms), composed of hydrogen atoms attached to the carbons, and in many instances contain other organic chemistry related functional groups and may be saturated or unsaturated. Due to the large amounts of unsaturated fatty acids in natural oils, they tend to suffer from a poor thermal stability with a limited temperature range.

The fatty acids in natural oils are desirable in boundary lubrication for their ability to adhere to metallic surfaces due to their polar carboxyl group, remain closely packed, and establish a monolayer film that is effective at reducing friction and wear by minimizing the metal-to-metal contact [98]. Much of the work with natural oils has concentrated on understanding the fundamentals of saturated and unsaturated fatty acids with the bulk of the attention focusing on the use of natural oils as neat lubricants, fatty acids as additives in mineral oils, and bio-based feedstock oils for chemically-modified lubricants [24, 90]. Additionally, new additives are being developed to extend the operable temperature range of natural oils to improve upon their thermal stability.

Recently, natural oils are finding uses as carrier fluids for lamellar particle additives in sliding contact [99].

2.2.2 Genetically Modified Lubricants

Genetically modified lubricants are as their name suggests lubricants derived from genetically modified organisms (GMOs). GMOs are organisms whose genetic material has been altered using genetic engineering techniques. In the lubrication industry, genetically modified lubricants are usually natural oils, in particular plant-based oils such as sunflower, soybean, and canola (rapeseed) oil. Plants are genetically engineered by manipulating the gene sequence within the organisms by causing a gene to be inoperative or "knocked out" or by attaching a gene to an identified region of DNA that initiates transcription of a particular gene thus acting as a "promoter". Genetically modified vegetable oils often focus on improving the thermal and oxidative stabilities of natural oils by decreasing the linoleic and linolenic acid amounts and increasing the oleic acid amounts, as will be explained further in the proceeding sections [100-102]. Genetically modified vegetable oils also seek to improve upon the cold flow properties of the lubricants where higher proportions of short-chain saturated or long-chain monounsaturated fatty acids lower the pour point [103, 104]. The objective of these manipulations is to create oils with higher degrees of saturation where by the oil is less susceptible to oxidative deterioration by means of exposed double bounds in the fatty acid molecules [105].

2.2.3 Synthetic Esters

Synthetic organic esters are a class of widely used lubricants that were once derived from glycerol molecules found in plant-based oils and animal fats. However, this causes synthetic esters to suffer from similar unsaturated performance issues as natural oils. Now, synthetic esters can be synthesized from long chain alcohols and acids, where the performance of synthetic esters is superior to natural ester fluids due to a more uniform molecular structure and the use of different alcohols. Using completely saturated esters, the resulting biolubricants tend to exhibit very stable aging characteristics. Additives used specifically for synthetic esters have been developed. Early synthetic esters possessed chemical structures similar to natural oils, however due to recent advancements there are now many choices of acids and alcohols available for the production of synthetic esters, affording them a wide variety of technical performance properties. Examples of synthetic esters feedstock include C6–C13 alcohols (i.e. n-hexanol, n-heptanol, isonal, and decanol), C5-C18 mono acids (i.e. valeric, heptanoic, pergalonic, and oliec acid) with neopentyl polyols, such as pentaerythritol (PE), polyol esters, diacids (i.e. adipic acid, azeleic, sebacic, and dodecanedioc) and various dimer acids [24, 55, 98, 106-111].

Esters are a type of biolubricant that provide better low temperature fluidity, low volatility, high flash points, and improved thermal-oxidative stabilities when compared to natural oils. Similar to natural oils, synthetic esters maintain an affinity for metal surfaces due to their high degree of polarity which affords them the ability to establish monolayers that minimize the surface contact and enhance the tribological properties. Esters are

inherently sensitive towards hydrolysis and thermal degradation, for this reason, their thermal properties have been improved by replacing the glycerol with other polyols such as neopentylglycol (NPG), pentaerythritol (PE), trimethylolpropane (TMP), Trimethylolhexane (TMH), and Trimethyloloethane (TME) [17, 81, 112-114]. A subgroup of esters known as complex or oligo esters are derived from mixtures of polyols and mono-, di-, and tri-carboxylic acids. Replacing the glycerol molecules with peresters of sugar (i.e. sucrose and sorbital), yield synthetic esters with enhanced oxidative stability, lubricity, and biodegradability [115]. These improved synthetic esters are strong candidates for replacing mineral oils in the food, pharmaceutical, and cosmetic industries; in fact, these esters could be used in many lubricant applications that require low toxicity due to potential contact with animals or humans [115, 116]. Esters such as the NPG were originally developed for the lubrication of aircraft jet engines whereas PE esters are derived from C5-C9 carboxylic acids and have found use in gas turbines. Still other esters such as TMP esters derived from oleic acid have found widespread use as automotive and marine engine oils, compressor oils (as replacement lubricants for hydrofluorocarbon systems), hydraulic fluids, gear oils, and grease formulations. The low toxicity, excellent biodegradability, moderate oxidative stability, and moderate price coupled with the high viscosity and good shear stability make synthetic esters attractive lubricants. More still, the use of appropriate additives to ester molecules improves their performance making them the optimal lubricant of choice for medium to heavy lubricant applications [24, 90, 93, 117, 118].

Another derivative of the synthetic ester is the diester, a biolubricant derived partly from renewable resources. Synthetic diesters are derived from dicarboxylic acid and monovalent alcohols. The dicarboxylic acid can be prepared from natural sources such as azelaic acid (ozonolysis of oleic acid), sebacic acid, dimeric fatty acid, isostearic acid, or from purely petrochemical sources such as adipic acid or malelic acid. Diesters generally consist of branched alcohols such as 2-ethylhexanol (iscooctanol), isodecanol, or guerbet alcohols to offer better low-temperature properties than conventional synthetic ester lubricants. Additionally, branched fatty acids for example 12-hydroxystearic acid derived from rhizinoleic acid can be utilized to form diester-based lubricants that also exhibit improved low temperature properties.

2.2.4 Perfluoroalkylethers

High performance applications that require a combination of high and low temperature properties, chemical or oxidative stability, low volatility, material compatibility, inertness, and non-flammability or non-combustibility simultaneously, will generally use synthetic lubricants known as perfluoroalkylethers (PFPEs) [119]. PFPEs are a new class of lubricants that are undergoing rapid advances to redesign them to be more environmentally friendly [120-122]. PFPEs are known for their superior thermal and oxidative stability. Once composed entirely of carbon, fluorine, chlorine and oxygen to produce a colorless, odorless, and completely inert functional fluid, they are now being derived from more environmentally benign feedstock that reduce their environmental impact. One such example are α,ω-Dialkoxyfluoropolyethers (DA-FPEs) which are

partially fluorinated polyethers that do not contain chlorine atoms and hence they do not contribute to ozone depletion [123]. The improvement in these lubricants is due to the incorporation of two alkoxy-groups that provide reactive sites, which act to minimize the atmospheric lifetime of these functional fluids [123-125]. Typically, PFPEs enter the environment as an aerosol by means of exhaust fumes or volatility. When compared with PFPEs, DA-FPEs have a lower environmental impact in terms of global warming potential as a result of atmospheric pollution by means of greenhouse gases in the form of carbon dioxide [123]. Furthermore, perfluorinated ether compounds derived from polymers maintain their properties of typical PFPEs such as high thermal and chemical stability, no acute toxicity, and excellent heat exchange properties [126]. Due to the presence of the alkoxy-groups in the DA-FPEs this has allowed these functional fluids to maintain excellent solvent properties with several organic liquids, such as ketones and alcohols [127].The appealing properties of DA-FPEs make them excellent candidates as CFC, perfluocarbon and halon substitutes in a number of applications, like foaming and fire extinguishing agents, cleaning agents for sophisticated electronic devices, heat transfer fluids, and lubricants in extreme applications [128-130].

2.2.5 Ionic Liquids

Ionic liquids (ILs), particularly those that are fluid at room temperature, represent a promising new class of biolubricants that show potential to improve the limitations associated with both petroleum-based lubricants and natural oils [131]. Room temperature ionic liquids are molten salts, which typically consist of combinations of a

bulky, asymmetric organic cation paired with an appropriate organic anion with melting points below 100°C and a liquid range beyond 300°C. The atomic structure of an IL is shown in Fig. 2.1.
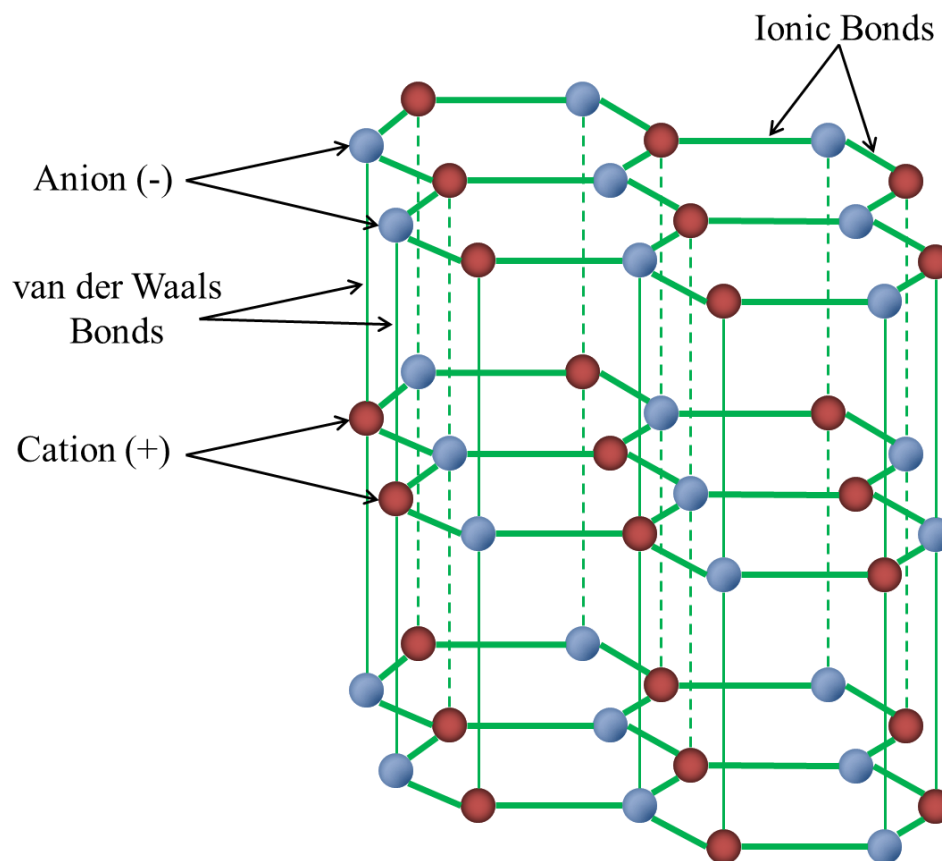
Figure 2.1: Atomic strucutre of an ionic liquid

This structure is similar to that of a typical lamellar solid particle, where the anions and the cations form ionic bonds to creating layers and these layers are held together with the weak van der Waals force. This structure provides ILs with their liquid lamellar crystal structure. ILs exhibit a number of unique and useful properties that make them well suited as the basis of a new family of biolubricants. The appeal of ILs as lubricants

becomes even more evident when one considers their many potential advantages over conventional lubricants including: (1) a broad liquid range (low melting and high boiling point); (2) negligible vapor pressure; (3) non-flammability and non-combustibility; (4) superior thermal stability; (5) high viscosity; (6) miscibility and solubility; (7) environmentally-benign (non-toxic); (8) lamellar-like liquid crystal structure; (9) long polar anion-cation molecular chains; and (10) economical costs [119, 132-142].

Additionally, ionic liquids have a consistent and easily tailorable chemical composition that affords them the ability to provide the level of thermal-oxidative stability and lubricity required for a variety of applications in the aerospace, automotive, manufacturing and magnetic storage industries. The consistent chemical composition of ILs allows them to have physicochemical properties that are readily reproducible. Further, they can be designed to be environmentally friendly by selecting both the cationic and anionic constituents to be non-toxic [143-145]. In many instances, ILs can be prepared from non-petroleum resources. Lastly, their capacity to overcome the variety of environmental, cost, and performance challenges faced by both petroleum-based and bio-based lubricants makes them a potentially attractive alternative biolubricant.

The possibility of preparing an ionic liquid capable of functioning as an efficient lubricant while exhibiting a variety of other useful properties is a result of their physicochemical characteristics, inherent tunability, and structural diversity of these novel compounds. Regarding the latter point, it has been estimated that as many as 10^{18} different combinations of anion and cation moieties are possible [146]. Clearly, this vast assortment of possibilities can pose a significant challenge in ionic liquid design. As the

number of desired properties increases, the number of possible candidate ILs declines dramatically. Here, for example, the desire for an environmentally friendly lubricant means that the use of highly fluorinated anions is unacceptable. Instead, the use of anions based on common food additives (e.g., benzoate and salicylate, are well known preservatives) or artificial sweeteners (e.g., saccharinate) are utilized. Similar considerations guide the choice of the cation and suggest that trihexyltetradecylphosphonium salts (i.e., $P_{666,14}$), some of which have been found to exhibit anti-microbial properties, can satisfy many of the desired criteria [147, 148]. Along these same lines, the objective of employing renewable feedstocks for the preparation of the ILs suggests the use of certain 1,3-dialkylimidazolium cations, such that can be derived from fructose [134, 149, 150]. The structures of these cations and anions are depicted in Table 2.2 and their atomic structures are shown in Table 2.3.

Table 2.2: Room temperature ionic liquid moiety structure
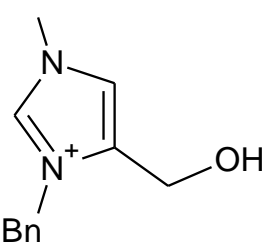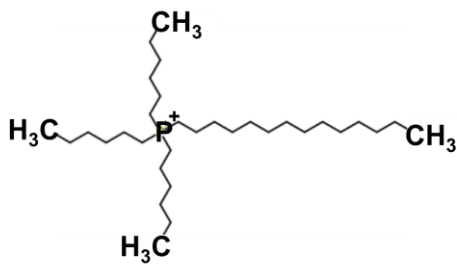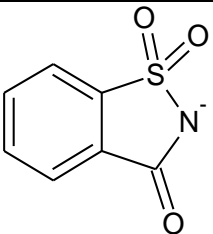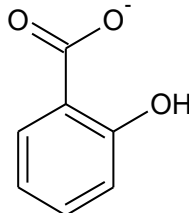
	Name and Structure
Cations	1,3-dialkylimidazolium trihexyltetradecylphosphonium ($P_{666,14}$)
Anions	saccharinate salicylate

Table 2.3: Self-assemblied anion and cation monolayer atomic structures

(A) Saccharinate; (B) Salicylate; (C) Benozate; (D) Tf_2N; (E) $P_{666,14}$;

(F) $C_{10}mim$; (G) C_8mim; and (H) C_6mim

Anion Monolayers	Cation Monolayers
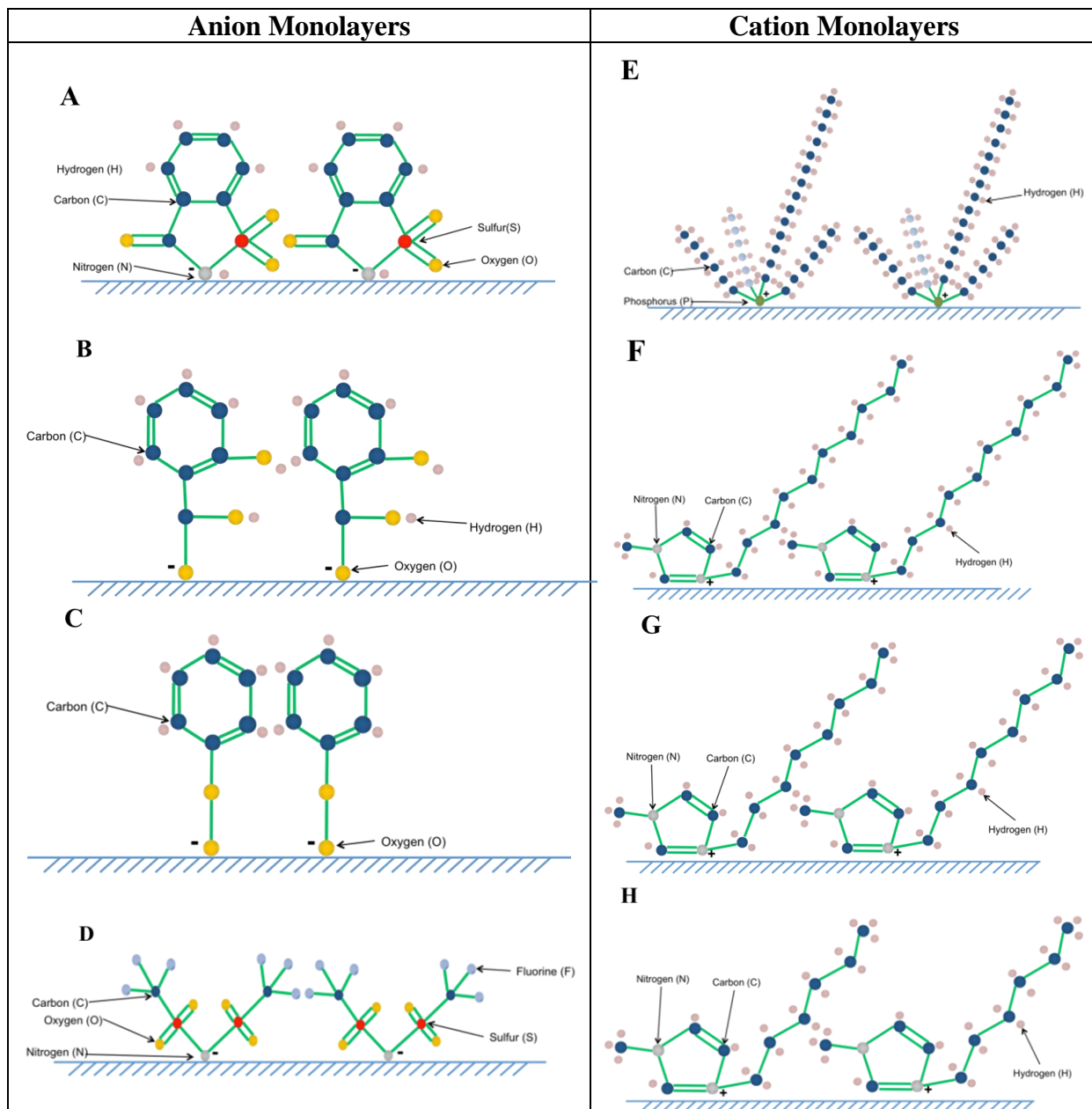
2.3. Drawbacks to Biolubricants

Bio-based lubricants have varying properties such as thermal-oxidative stability, viscosity, viscosity index, and low temperature behavior that are dependent on the structure of the molecules and the triacyclglycerol composition. Despite the many favorable attributes of biolubricants, the largest drawback to them are their poor thermal-oxidative stability, solidification at low temperatures (high pour points), biological (bacterial) deterioration, and hydrolytic instability (aqueous decomposition), and inconsistent chemical composition [132]. Additionally, many biolubricants particularly ester-based oils are susceptible to rapid oxidative degradation due to the presence of free fatty acids and the presence of double bonds in the carbon chains of the ester molecules.

2.3.1 Fatty Acids

The structures of the fatty acids affect the properties of the biolubricants in terms of thermal-oxidative stability, viscosity, viscosity index, and low temperature behavior. By increasing the length of the carbon chain, the fatty acid becomes more oily or fatty and increasingly less water-soluble. The short non-branched fatty acid chains having approximately 6 carbon atoms are more water-soluble due to the presence of the polar –COOH groups [133, 151]. If, in the carbon chain every carbon atom is attached to two hydrogen atoms, except those at the ends of the chain, which are attached to three hydrogen atoms, then the fatty acid is considered to be a fully saturated, geometrically configured in a linear shape, and referred to as a saturated fatty acid. When hydrogen

atoms are missing from adjacent carbon atoms, the carbons share a double bond instead of a single bond and have a nonlinear structure. This type of fatty acid is called an unsaturated fatty acids. These acids have lower thermal properties than saturated fatty acids as shown in Table 2.4 with the boil point values. The fatty acid is polyunsaturated if multiple double bonds occur. Therefore the classification of fatty acids are saturated, monounsaturated, and polyunsaturated with subcategories of diunsaturated and triunsaturated depending on the number of double bonds present. [134]. Investigations have revealed that the most important unsaturated fatty acids contained in natural oils are oleic acid (C18:1), linoleic acid (C18:2), and linolenic acid (C18:3). The most important saturated fatty acids are palmitic acid (C16:0) and stearic acid (C18:0) [152]. These fatty acids percentages are shown in Fig. 2.2 for several common vegetable oils. In this figure, safflower oil is a genetically modified organism. As can be seen from Fig. 2.2, natural oils are composed predominantly of oleic acid and linoleic acid with small trace amounts of other acids.
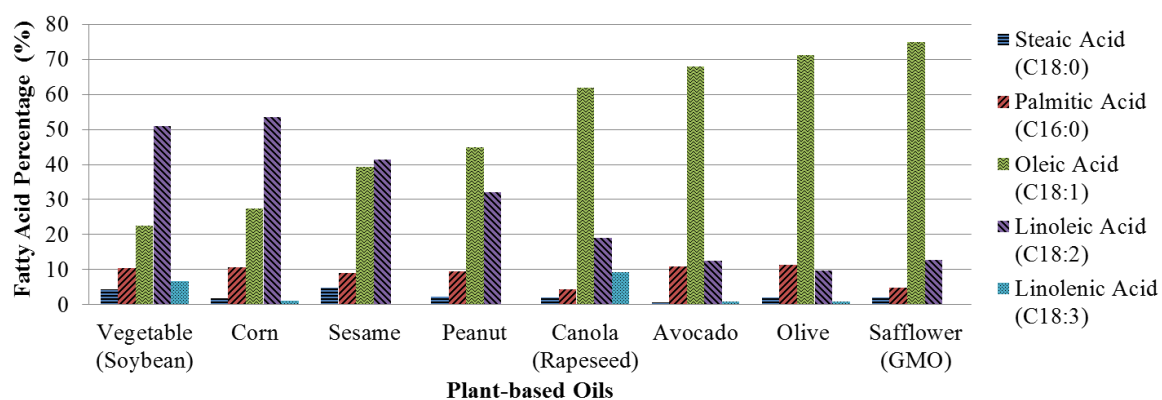
Figure 2.2: Fatty acid percentage for common plant-based oils

Table 2.4, details the characteristics between the most important fatty acids found in the natural oils. It can be seen in Table 2.4 that as the number of double bonds increases as denoted by the lipid number, the degree of unsaturation increases and the boiling point decreases. All of these properties influence the tribological performance of a lubricant when used as a base-stock or additive enhancement.

Table 2.4: Important fatty acids in plant-based oils

Fatty Acid Type	Common Name	Molecular Formula	Lipid Number	Degree of Unsaturation	Boiling Point (ºC)
Saturated	Palmitic Acid	$C_{16}H_{32}O_2$	C16:0	1	352
Saturated	Stearic Acid	$C_{18}H_{36}O_2$	C18:0	1	383
Monounsaturated	Oleic Acid	$C_{18}H_{34}O_2$	C18:1	2	360
Diunsaturated	Linoleic Acid	$C_{18}H_{32}O_2$	C18:2	3	230
Triunsaturated	Linolenic Acid	$C_{18}H_{30}O_2$	C18:3	4	228

2.3.2 Unsaturation Number

There is a balance that must be maintained in the biolubricants between the fatty acids to ensure functionality, for example stearic acid at room temperature is a solid in the form of a wax whereas oleic acid at room temperature is a liquid. For this reason, the saturation level describing the proportions of saturated and unsaturated esters must be optimal to ensure that the plant-based oil is liquid at room temperature and thus can serve as a functional fluid. To quantify the saturation level, the unsaturation number (UN) is

used. The UN of natural oils refers to the average number of double bonds within a triacylglycerol molecule. This provides a metric for quantifying the fatty acid concentrations within the natural oils. The greater the UN, the greater the degree of unsaturation in the natural oil. The UN is calculated from the fatty acid distribution using Eq. 2.1(a) and is summarized in Eq. 2.1(b).

$$UN =$$

$$\frac{1}{100}[(1 * \sum \text{monounsaturated Fatty Acids}) + (2 * \sum \text{diunsaturated Fatty Acids}) +$$

$$(3 * \sum \text{triunsaturated Fatty Acids})] \hspace{2cm} \text{Eq. 2.1(a)}$$

$$UN = \frac{1}{100}[\{1 * (C18\text{:}1 + C20\text{:}1 + C22\text{:}1)\} + \{2 * (C18\text{:}2 + C22\text{:}2)\} + \{3 * (C18\text{:}3)\}]$$

Eq. 2.1(b)

In Eq. 2.1(b) the *Cx:y* is the lipid number which represents the percentage of fatty acids within the plant-based oil with *x* representing the chain length and *y* representing the number of double bonds. Similarly, Eq. 2.1 could be used to calculate the UN for unsaturated esters or any other unsaturated hydrocarbon. Table 2.5 shows the UN for a variety of plant-base oils. Research has shown that natural oils with lower unsaturation numbers maintain a higher thermal-oxidative stability as well superior tribological properties.

Table 2.5: Natural oil unsaturation number

Natural Oil Type	Unsaturation Number (UN)
Olive	0.948
Avocado	0.985
Safflower (High Oleic)	1.010
Peanut	1.102
Sesame	1.232
Canola (Rapeseed)	1.287
Corn	1.381
Vegetable (Soybean)	1.451

2.3.3 Thermal-oxidative Stability

Previous research indicates that thermal-oxidative stability of natural oils requires a low percentage of polyunsaturated fatty acids (i.e. linoleic acid) [153-158]. Thus, the oxidative stability increases with decreasing amounts of polyunsaturated fatty acids. Furthermore monounsaturated fatty acids such as oleic acid having one double bond improve oxidative stability while simultaneously providing good low temperature properties and superior tribological properties. The best compromise between thermal-oxidative stability and low temperature properties are through the use of naturally high oleic acid oils or by genetically modifying the base-stock of low oleic acid oils to yield high oleic acid oils with concentrations above 80%, such as high oleic acid safflower oil (HOSO), canola oil, sunflower oil, or soybean oil all of which are commercially available and derived from genetically modified organisms (GMOs) [77]. An alternative method

would be to perform chemical modifications of the plant-based oil to achieve the desired stability. Fully saturated esters exhibit excellent oxidative stabilities, while partially unsaturated esters require modifications to be useful as engine and transmission fluids or hydraulic and compressor lubricants [159]. Moreover, fully saturated diester oils are highly stable towards oxidation, show good low temperature performance, and demonstrate a high viscosity-temperature index. By adjusting the chain length of the dicarboxylic acid the viscosity can be modified affecting the thermal stability as well as the hydrodynamic capabilities which influence the tribological performance.

2.3.4 Viscosity & viscosity index

The viscosity properties of biolubricants are important properties that influence the applicability of biolubricants as feasible alternatives to petroleum-based lubricants. Generally, bio-based oils derived from plants or animals are known for their high viscosity indices and can be considered multi-range oils. The influence of viscosity is particularly important when esters are used as lubricants because the acids being esterified do influence the viscosity of the lubricant. The viscosity and viscosity index of a biolubricant tends to increase with increasing chain length of the carboxyl acid or with an increase in molecular weight of the alcohol. In the case of polyols, the viscosity depends on the number of hydroxy functional groups present. Examining the effect of different polyols with identical fatty acid base fluids show the following series of viscosities where PE (40 mm^2/s) > TMH (31 mm^2/s) > TMP (27 mm^2/s) > TME (24 mm^2/s) > Glycerol (20 mm^2/s) > NPG (12 mm^2/s) as illustrated in Fig. 2.3 [160-163].
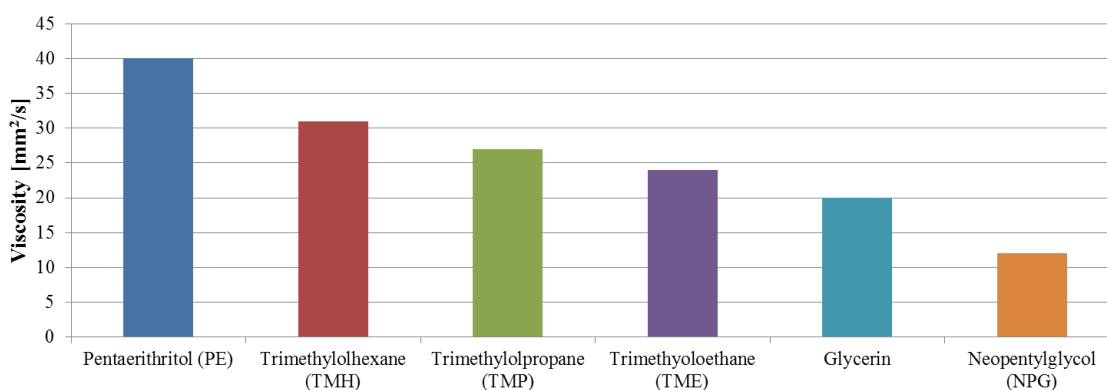
Figure 2.3: Viscosity of different polyol-esters with the same base acid [163]

The viscosity-index (VI) describes the dependence of viscosity with the temperature. The higher the VI, the smaller the changes in viscosity over a broader temperature range. The VI is also affected by branching where it has similar affects as double bonds. By increasing the branching in either the carboxyl acid or the alcohol while maintaining a constant carbon number, the viscosity and VI decrease. In contrast, an increase in chain length with the same structure, i.e. no branching results in an increase in viscosity. As more complex esters and acids are used to synthesize biolubricants there are diminishing returns, where the correlation between the viscosity and the carbon number declines. This is a result of the viscosity increase being compensated by the branching of the ester molecule and the increasing carbon number [164].

2.3.5 Low Temperature

Low temperature performance often refers to the pour point of a fluid. The pour point is the lowest temperature at which the fluid still flows before losing its flow characteristics. To achieve the desired low temperature properties necessary for most lubricants. Pour points for bio-based lubricants exhibit the same dependencies as observed with viscosity. With esters, short-chain branching of the alcohol with tertiary carbon or hydrogen atoms lowers the pour point, however this molecular structure also leads to a decrease in oxidative stability of the alcohol. For this reason, neopentyl-polyols are advantageous for the production of synthetic ester lubricants because their molecular structure is composed primarily of branched hydroxyl groups. Natural oils should have a low amount of saturated fatty acids and a shorter chain length or a branching chain length for optimal low pour points [43, 165, 166] as shown in Fig. 2.4. On the contrary, unsaturated fatty acids exhibit excellent low temperature properties, where monounsaturated fatty acids are optimal when compared to polyunsaturated fatty acids that are susceptible to high oxidation attacks due to the increase in double bonds. Although, double bonds positively influence the fatty acids by lowering the pour point as seen in Fig. 2.4, their vulnerability to oxidation negates much of the potential benefit. Short-chained saturated fatty acids are optimal for their cold flow properties, as the chain length increases to about 16-18 carbon atoms these fatty acids become solid at temperatures of 65-75°C [74]. Unfortunately, many natural oils are composed of palmitic acid (C16:0), stearic acid (C18:0), oleic acid (C18:1), linoleic acid (C18:2), and linolenic (C18:3) as shown in Fig. 2.2, and thus to achieve the desired low pour point temperatures,

maintain oil fluidity, and sustain a high oxidative stability a compromise must be made. Research has shown that oils with high amounts of oleic acid are the best compromise between sufficient cold flow properties and oxidative stability. High oleic acid oils such as HOSO has demonstrated low temperature properties with pour points of -35°C and TMP polyol-esters have demonstrated pour points as low as -50°C [55, 109].
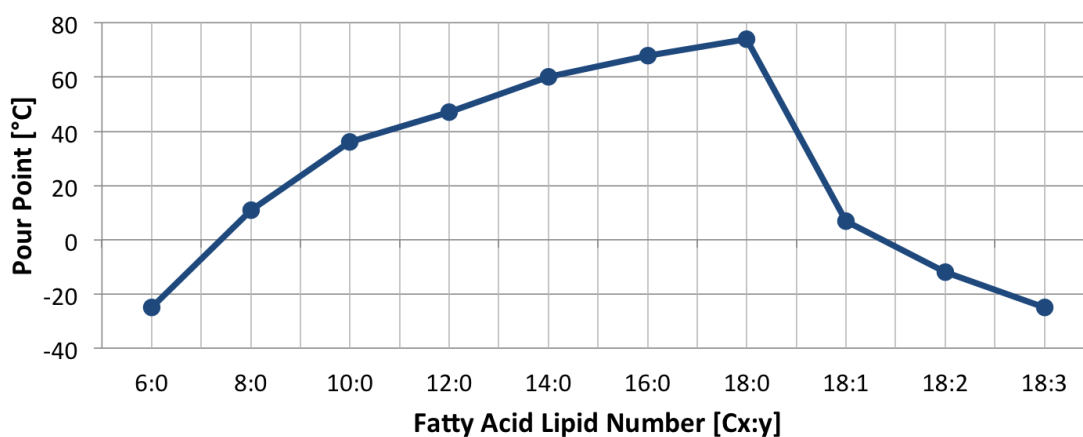
Figure 2.4: Dependence of pour point on fatty acid structure [167]

Further investigations into the pour point have shown that the position of the double bonds within the fatty acids has no significant influence of the cold flow properties. However, slight differences can be observed depending on the degree of distortion imparted by the double bonds on the molecules. Depending on the position of the double bond, the distance between molecules increases or decreases and this can influence the pour point. The influence of the double bond location is shown in Figure 2.5 for both the cis-configuration and the trans-configuration [167]. The cis-configuration has the hydrogen atoms on the same side of the double bond whereas the trans-

configuration has the hydrogen atoms on opposite sides of the double bond. As shown in Fig. 2.5, the steroconfiguration of the fatty acids influences the cold flow properties, where the cis-configuration has a consistently lower pour point than the trans-configuration.
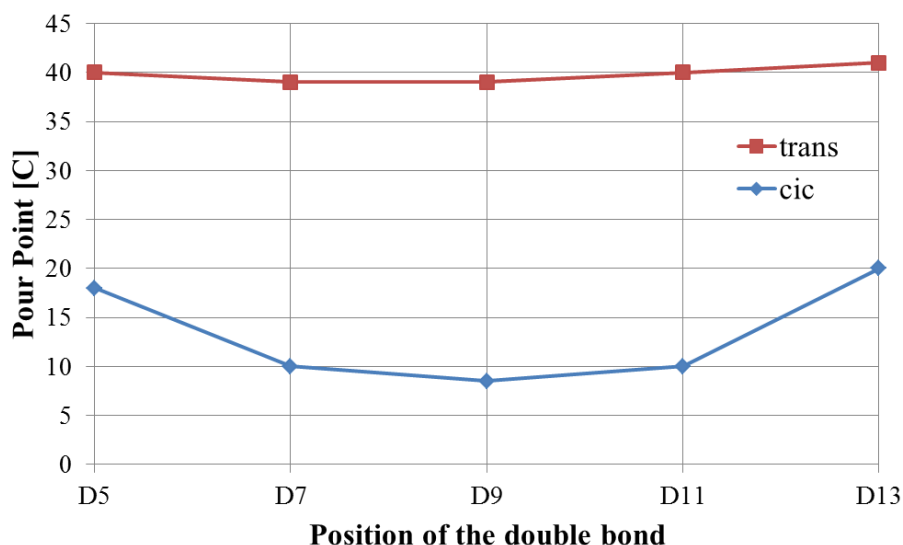
Figure 2.5: Influence of double bonds on the pour point [167]

2.3.6 Hydrolytic Stability

The degree of relative resistance to attack or cleavage of a molecule by water or water vapor is known as hydrolytic stability. This property is strongly dependent on the fatty acid ester and synthetic ester structure of bio-based fluids, because the chemical reaction for these molecules is an equilibrium reaction. Bio-based fluids cleave into their alcohol and acid components upon hydrolysis, which directly influences the ester bond. This process is also known as "hydrolytic splitting", which continues until the chemical

equilibrium is restored [164]. Thus, hydrolytic stability of an ester is influenced by its chemical structure. Biolubricants derived from saturated esters with straight chain components have a higher degree of hydrolytic stability than unsaturated or branched esters. The most stable derivatives are saturated dicarboxylic esters, arguably due to steric effects.

Steric hindrance is a natural phenomenon that occurs when a large quantity of methyl groups within a molecule prevent chemical reactions with other molecules with smaller quantities of methyl groups. This consequence of the ester bond improves hydrolytic stability. This protection is due to the presence of methyl groups instead of hydrogen atoms relative to the ester group. The methyl groups sterically protect the ester bond against an unwanted hydrolytic attack. Depending on the number of methyl groups positioned around the ester group, the reaction rate may be reduced many times. Table 2.6 illustrates the reaction rate as a function of the amount of alpha-carbon branching [168].

Table 2.6: Influence of alpha-carbon branching of the
oxygen ester on the rate of reaction [168]

Alkyl-substitution	Related Reaction Rate
CH_3	30
CH_3CH_2	1
$(CH_3)_2CH$	0.3
$(CH_3)_3C$	0

Biolubricants derived from saturated esters with straight chain components have than unsaturated or branched esters. The most stable derivatives are saturated dicarboxylic esters, arguably due to steric effects. Biolubricants demonstrate better hydrolytic stability through the use of linear short-chain mono-alcohols. Even the short alkyl chains in these alcohols yield improvements on the hydrolytic stability. When using branched alcohols larger than eight carbon atoms the resistance increases to the level of saturated linear mono-alcohols [164]. When using glycerol molecules in synthetic esters, the saturated esters behave with a higher degree of hydrolytic stability than stable unsaturated or branched esters. The level of hydrolytic stability is comparable to the stable mono-esters. The most stable derivatives are saturated dicarboxylic esters, arguably due to steric effects. Their stability is almost entirely independent of the chain length, branching, and the alcohol components used. Figure 2.6 depicts hydrolytic stabilities of different ester structures, where a low hydrolytic stability corresponds to a high acid number [164, 169, 170]. It can be seen in the figure that many saturated esters i.e. saturated linear mono-esters, saturated long chain mono-esters, saturated tri-glycerin-esters, dicarbon-acid-esters, and saturated polyol-esters exhibit superior hydrolytic stability. Although, biolubricants are often susceptible to hydrolytic stability, it is also this inherent property that affords these lubricants their high biodegradability. This is of special importance since hydrolysis is the starting reaction for biological degradation and reducing the effects of hydrolysis inherently reduce the rate of biodegradability. For this enigma, it follows that protecting an ester bond might be a disadvantage with regards to

the ecotoxicological properties, and thus a balance must be maintained when improving hydrolytic stability.
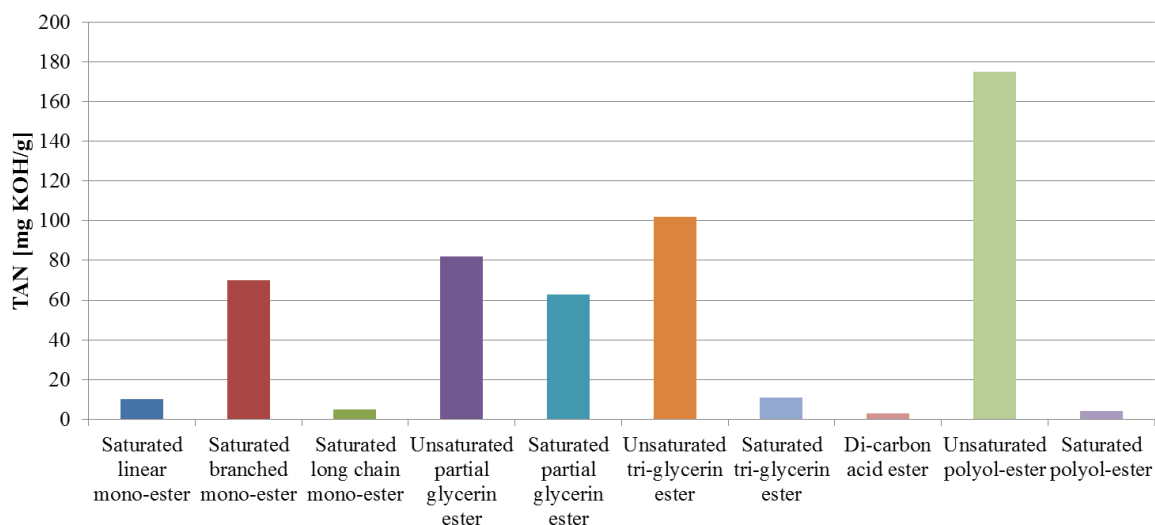
Figure 2.6: Hydrolytic stability of different ester structures [164]

2.3.7 Lubrication Mechanisms

Many biolubricants are amphiphilic in nature as they are composed of molecules with polar heads that are hydrophilic and nonpolar hydrophobic carbon chains [171]. These oils are primarily water insoluble due to the presence of the long hydrocarbon chains in the molecule. Depending on the type of bio-based feedstock, functional groups such as epoxies and hydroxides and various polar and nonpolar groups might be present in the hydrocarbon portion of the molecule which can impact the tribological properties as well as other important properties such as oxidation, low-temperature stability, and rheology [172]. The amphiphilic properties of biolubricants affect the boundary lubrication or additive properties while rheological or fluid properties affect the

hydrodynamic properties. For these reasons, the chemical composition of biolubricants is important because the combination of amphiphilic and rheological properties affect the performance of these lubricants in boundary, hydrodynamic, and mixed-film lubrication regimes [173].

When lubricants operate in the boundary lubrication regime their performance is often impacted by the ability of adsorption and tribo-chemical reactions to occur on the metal surface [174-179]. Adsorption refers to the ability of lubricant molecules specifically polar groups of molecules to attach to the friction surface, minimize asperity contact, and reduce the friction and wear as the interface. The ability of a lubricant to adsorb onto a surface is quantified using free energy of adsorption terms.

When lubricants operate in the hydrodynamic or mixed-film lubrication regime, their performance is often impacted by the ability to form tribo-chemical reactions in the tribo-interface. These reactions form tribo-films from the chemical reactions of the lubricants themselves and/or with other materials (e.g., oxygen, moisture, and metal) in the interface. Tribo-chemical reactions often occur as a result of high temperatures, pressures, and shearing of the lubrication process. This process in the interface is highly volatile and so complex that it is not fully understood. As a result, tribo-chemical reactions are often mistakenly blamed for mechanical failures resulting from oil degradation by oxidation and the generation of friction polymers [171].

2.4. Performance Enhancements

Biolubricant research has focused on thwarting the deficiencies of natural and synthetic oils while seeking to understand the relationship between chemical composition, molecular structure, and enhancements through chemical modifications such as epoxidation, metathesis, acylation, estolide formation, transesterification, and selective hydrogenation of biolubricants with polypols, and additivation [180, 181]. The potential use of biolubricants is far reaching, yet their major disadvantages militating against their widespread use in industrial applications are their sensitivity to hydrolysis, thermal degradation by elimination and oxidation caused by unsaturated molecular compounds. Investigations into the oxidative limitations of biolubricants have been researched and new techniques have been proposed to enhance the oxidative stability of biolubricants [152]. In some instances, through various chemical manipulations and enhancements biolubricants have been shown to offer higher oxidative stability than traditional petroleum-based lubricants [43-50, 52-56, 78, 182]. Still other researchers have investigated the stability of biolubricants when antioxidants are added [183-185]. Nonetheless, chemical modifications to biolubricants by addition reactions to the double bonds constitutes one of the most promising processes for obtaining commercially viable products from renewable raw materials. Thus to facilitate the use of lubricants derived from bio-based materials, additivation, chemical modifications, *de novo* synthesis, breeding of genetically modified organisms, and biotechnology will all play critical roles to ensure adequate functionability and stability as biolubricants and functional fluids [186-188].

2.4.1 Additivation

Commercial mineral oils can consist of 10 to 25% additives depending on the application [189]. Additives are necessary to impart properties that are application specific and beyond what oil-basestock can perform. Additives of biolubricants include antioxidants, metal deactivators, detergents, dispersants, corrosion inhibitors, demulsifiers, rust inhibitors, antiwear additives, extreme pressure additives, viscosity improvers, pour point depressants, hydrolysis protection, among others [184, 190-192]. Table 2.7, shows some of the common additives used with their water pollution classification. Additives are common practice in lubricants, but the toxicity of currently used additives requires research on the development and use of alternative bio-based environmentally-benign additives. Thus far, naturally occurring antioxidants such as tocopherol (vitamin E), L-ascorbic acid (vitamin C), esters of gallic acid (lauric alcohol and dodecanol), citric acid derivatives, or lipid modified ethylenediaminetetraacetic acid (EDTA) derivatives serve as synthetic metal scavengers and provide viable alternatives to the currently used toxic antioxidants [77].

Table 2.7: Commonly used additives

Additive	Compound	Water pollution class[*]
Antioxidants	BHT and other phenols	1
	Alkylsubstituted diphenylamines	1
Deactivators for Cu, Zn, etc.	Benzotriazoles	2
Corrosion inhibitors	Ester sulfonates	1
	Succinic acid esters	1
Anti-wear additives	Zn dithiophosphate	2(3)
Pour point depressants	Malan styrene copolymers	Not identified
	Polymethacrylates	Not identified
Hydrolysis protection	Carbodiimides	No identified

[*]0, no danger; 1, little danger; 2, danger; 3, strongly endangering

Other biolubricants additives function more as antiwear and extreme pressure additives and consist of environmentally benign solid particulate additives. Green solid lubricants are a class of "powder lubricants" consisting of lamellar crystal structures with low interlayer friction [6]. Examples of green solid lubricants include boric acid (H_3BO_3) and hexagonal boron nitride (hBN), which have similar properties to graphite (C), molybdenum disulfide (MoS_2), and tungsten disulfide (WS_2) [193]. Lamellar powder lubricants are superior additives due to their crystal structure, in which atoms lying on the same layer are closely packed and strongly bonded together by covalent bonds, and the layers are relatively far apart due to the weak van der Waals force [25]. When entrained between sliding surfaces, these lamellar powders can adhere to the surface, form a

protective boundary layer, and minimize contact between opposing surface asperities to prevent wear. The protective boundary acts as a lubricant in sliding contacts by accommodating relative surface velocities. The lamellar powder lubricants accomplish this by aligning their layers parallel to the direction of motion and sliding over one another to minimize friction. Moreover, these powder lubricants can lubricate in extreme conditions such as high or low temperatures and pressures [11, 16, 92, 113, 194-196].

Although there are many solid powder lubricants that can be used as additives, there are far less that are environmentally benign. Hexagonal boron nitride and boric acid powder represent some of the greener more environmentally-friendly additives that are inert to most chemicals [152]. They have been studied extensively because they are highly refractory materials with physical and chemical properties similar to that of graphite [9, 92, 93, 197]. These powder are extremely lubricious with attractive performance-enhancing attributes similar to other lamellar solids, making them attractive alternatives to other inorganic solid lubricants. Boric acid is found naturally, however boron nitride is not naturally occurring, it is synthesized from boric oxide or boric acid compounds. Generally, boron-based compounds are extremely stable and do not breakdown to form other hazardous materials under normal operation; thus, they are safe to handle and feasible to use in industrial applications with no hazardous effects or limitations on their use. There are no reports issued by the National Toxicology Program, International Agency for Research on Cancer, Occupational Safety and Health Administration (OSHA), or American Conference of Government and Industrial Hygienists that indicate boron nitride or other boron compounds are carcinogens or pose

any toxic hazard [113]. Boron compounds are not considered hazardous chemicals by the EPA or under the Superfund Amendments and Reauthorization Act (SARA) guidelines, and no regulations exist regarding their use, storage, transport, or disposal. For these many reasons, boron nitride and boric acid can be considered an environmentally benign substance with no limitations on its operational use [198].

Research has indicated that powder-based biolubricants can be problematic because they can be forced out of the contact zone during dry sliding contact [198]. In an attempt to remedy this problem, biolubricant colloidal mixtures composed of powder additives such as boric acid or boron nitride with natural oils such as canola (rapeseed) or soybean oil create a more environmentally friendly lubricant [118]. Here, the natural oil is a bio-based carrier fluid used to circulate the green powder additives allowing them to remain in the contacting pin-disk interface without degrading over time [199, 200]. These powder-based biolubricants demonstrate improved friction and wear reduction and promote ecological sustainability [90, 93, 95, 113].

2.4.2 Oxidation

Many natural oils and bio-based feedstock are composed of fatty acids that are derived from triacylglyceride molecules, which contain glycerol. The presence of glycerol in bio-based materials gives rise to a tertiary β-hydrogen (secondary hydrogen) attached to the β-carbon (secondary carbon) of the functional hydroxyl group, as illustrated in Fig. 2.7 at location (a).
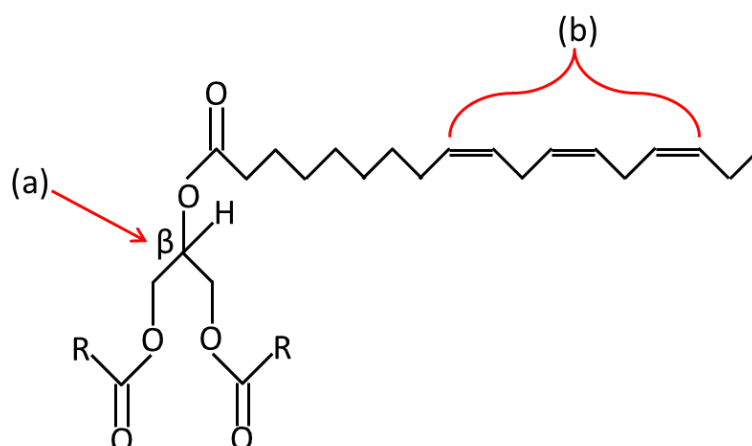
Figure 2.7: Critical positions in triacylglycerides susceptible to chemical modifications (a) β-hydrogen position, (b) double bond position

The β-hydrogen present in the unsaturated fatty acids is known to have oxidative instability and therefore is a cause for the fast oxidation of natural oils in process known as autoxidation. The β-hydrogen is also the location where most bio-based feedstock are chemically modified [81]. Additionally, the bis-allylic hydrogen, which attaches to the double bonded carbon atoms in polyunsaturated fatty acids are particularly susceptible to free radical attacks, peroxide formation, and production of polar oxidation products similar to that of hydrocarbon mineral oils, except at an expedited rate in natural oils [10, 201-203]. Oxidative instability also arises from the presence of the double bonds present in the triacylglycerol molecule as depicted in Fig. 2.7 at location (b) [19, 81, 92, 196, 204-209]. Figure 2.8, shows how the oxidation stability of vegetable oils is influenced by the number of double bonds by the Rancimat method [210]. Here, the strong dependency of the stability on the amount of double bonds is apparent.
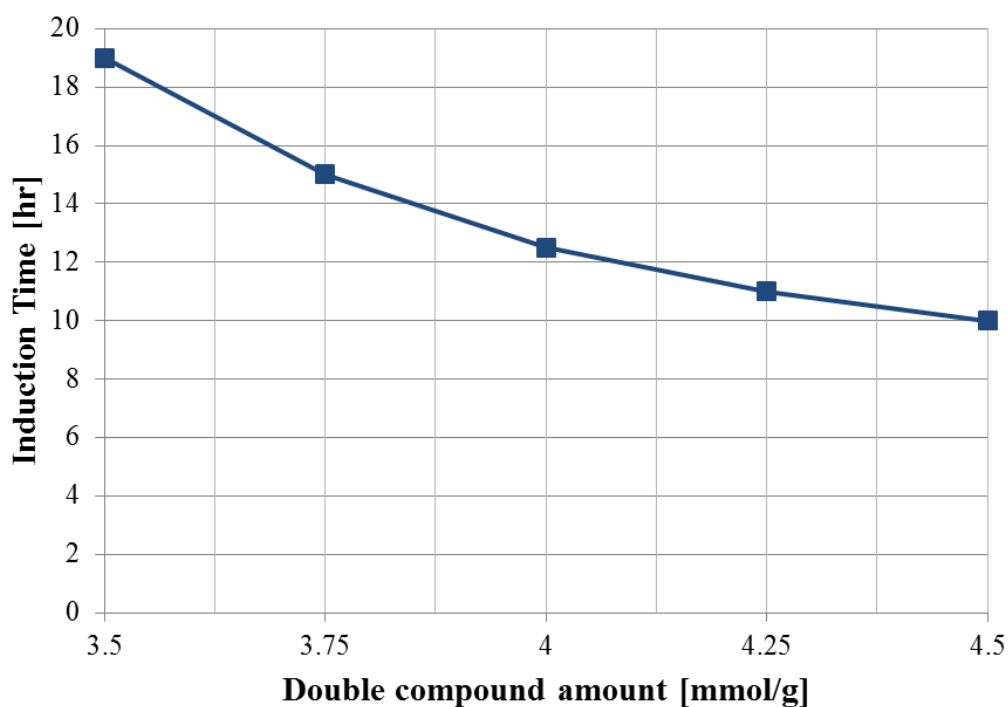
Figure 2.8: Influence of oxidation stability on the amount of double bonds with the Rancimat method [210]

Additionally, the degree of unsaturation of ester molecules also has a profound effect on the oxidation stability of synthetic lubricants. The effect of oxidation on three different saturated polyol-esters is depicted in Figure 2.9. The oxidation stability of these fluids was determined by the viscosity increase after an aging process according to the Baader-test (DIN 51587) [210].
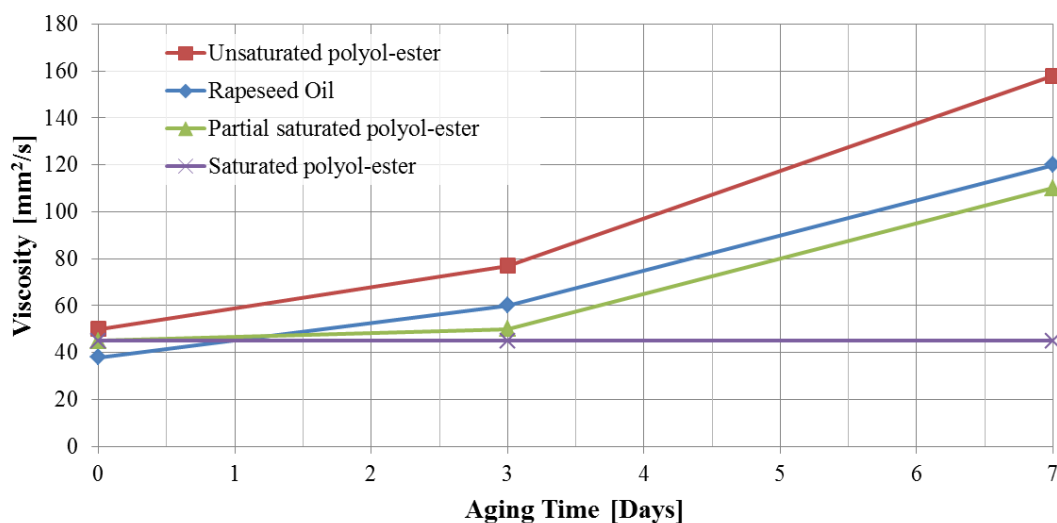
Figure 2.9: Influence of saturation on oxidation stability [210]

As a precaution saturated alcohols and acids are used for the production of lubricants. The deficiencies of bio-based lubricants can cause the development of insoluble deposits and increases in oil acidity, viscosity, and poor corrosion protection to occur. Moreover, the existence of unsaturated ester compounds in biolubricants causes hydrolytic degradation, which also increases oxidation [44, 102, 152, 211-213]. Oxidation stability can also be enhanced by sterically protecting the double bonds by means of branching. The effects of branching on oxidation are similar to the effects of increased hydrolytic stability through branching.

These problems become negligible in oxygen-free environments because the critical β-hydrogen and the bis-allylic hydrogen are no longer susceptible to oxidative degradation by elimination (e.g. esterification or hydrolysis) and can therefore withstand the higher temperatures affording increased thermal stability of the biolubricants. The

thermal degradation temperatures of biolubricants in an oxygen-free atmosphere are significantly higher than that in an open air oxygenated environment, where the process of oil oxidation lowers the thermal stability and influences the performance of the tribological properties within the natural oils [214-216]. For example, a thermogravimetric analysis (TGA) in a nitrogen environment has revealed thermal-oxidative stabilities 20º to 100ºC higher when compared to a TGA performed in an oxygen environment as performed on fatty acid-based oils by Salih et al. [44, 152, 211, 212], vegetable-base oils by Erhan et al. [217], and synthetic ester basestocks by Salimon et al. [218]. To further quantify the susceptibility of the biolubricants to thermal and oxidative vulnerabilities an unsaturation analysis of biolubricants is often performed. In general, decreasing the unsaturation levels, increases the thermal oxidative stability.

2.4.3 Esterification

There are two locations in bio-based lubricants where chemical modifications can be effective (Fig. 2.7): (a) the first position is at the ester moieties in the triacylglycerides where the β-hydrogen exists and (b) the second position is at the C-C double bonds along the fatty acid chains [55]. Esterification or transesterification is the modification of the ester moieties present in the triacylglycerides, which have glycerol as the alcohol component and have the critical β-hydrogen, which is susceptible to thermal degradation by elimination. In this process the glycerol is replaced with polypols such TMP, NPG, or PE, effectively creating a synthetic ester. Results indicate that hydrolytic and oxidative stability are increased considerably for biolubricants if the fatty acid portion consists

entirely of oleic acid. High oleic acid vegetable oils have shown high stabilities similar to standard oleic acids (68-72%) with TMP, indicating the feasibility of neat vegetable oils without the need of any modifications. These results are promising and continue to be investigated [109].

2.4.4 Epoxidation

Epoxidation is the second chemical modification and one of the most important functionalization reactions of the C-C double bonds to improve the oxidative stability, lubricity, and low temperature behavior of biolubricants [219]. The chemical modification of epoxidized fatty acids is often used as a precursor to ring opening reactions as seen in Fig. 2.10 [44, 121, 152, 212]. The chemistry of epoxidation of unsaturated fatty acids is a well-known technique for improving the oxidative stability dating back almost seventy years [152]. A number epoxidation methods have transpired utilizing classical chemical methods via peroxy acids, dioxiranes, peracids, and through the use of alkyl hydroperoxides [220]. Other epoxidation techniques utilize a chemoenzymatic self-epoxidation process as well as an in situ performic acid procedure [221]. In recent attempts to chemically modify the fatty acid chain of natural oils was the development of diester compounds synthesized from oleic acid and common fatty acids [222]. A multi-step process of oleochemical diesters begins with epoxidation, followed by ring opening of epoxidized oleic acid with fatty acids using a *p*-toluenesulfonic acid (PTSA) as a catalyst to yield mono-ester compounds. The process ends with the estification reaction of these compounds producing the desired diester compounds [223-

228]. These diesters compounds have demonstrated enhanced low temperature behavior due to the increased ability of the long chain esters to disrupt macrocrystalline formation at low temperatures.

In addition to epoxidation, a number of other chemical modifications can be employed to manipulate the C-C double bond such as alkylation, radical addition, acylation, enereaction, aminoalkylation, hydroaminomethylation, acyloxylation (with the addition of carboxylic acids), co-oligomerization, and hydroformylation [229-231]. Many of these reactions have been investigated using oleic acid esters and other derivatives for their wide applicability and performance enhancements to biolubricants.

Figure 2.10: Diagram of various chemical modification techniques for vegetable and animal oils [232]
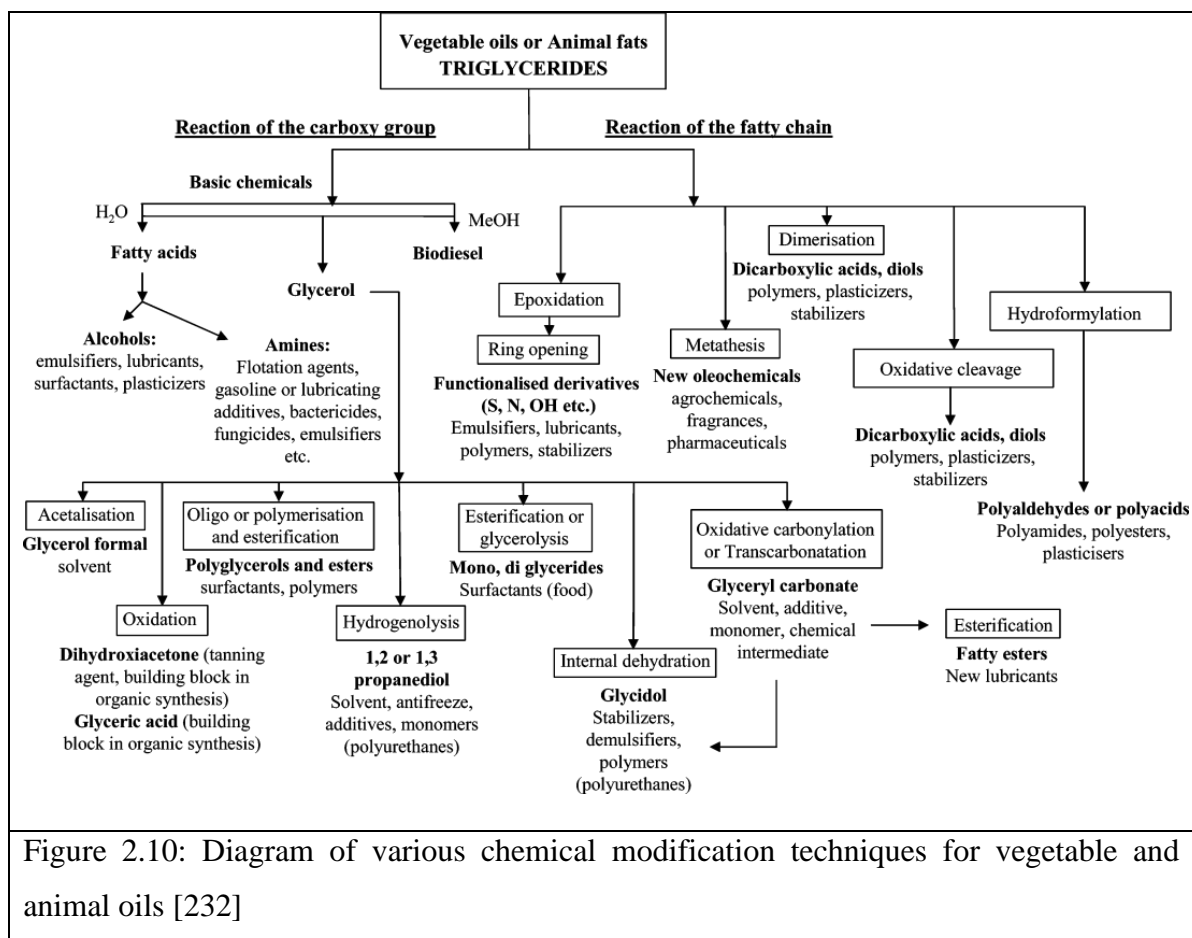
2.4.5 Estolides of Fatty Acids

Estolides are a class of esters derived from natural and synthetic compounds synthesized from fats and oils at the location of the carbon-to-carbon double bond (unsaturation point) where they form a carbocation. The estolide structure consists of a secondary ester linage between one fatty acid acyl molecule to another fatty acid alkyl molecule [166, 233-235]. The carbocation on the estolide can undergo nucleophilic attacks by other fatty acids, with or without carbocation migration along the length of the chain, to form an ester linkage, thus inherently promoting the formation of estolides [122, 236-247]. Estolides can be found in free acids, esters, or triacylglycerides. Estolides were primarily developed to overcome the thermal oxidative instabilities and poor low temperature properties of natural oils [221]. In some instances, estolides are enhanced with additives, however at the expense of biodegradability, cost, and toxicity. Recent research in estolides have revealed their synthesis from saturated mono-estolide methyl esters and enriched saturated mono-estolide 2-ethyl hexyl esters from oleic acid, lauric acid, and free estolides [248]. Results indicate that chain length and estolide number affect low temperature properties and tribological performance.

2.4.6 Selective Hydrogenation

As described previously, the multiple double bonds present in polyunsaturated fatty acids is disadvantageous for the utility of biolubricants because of their susceptibility towards oxidation attacks. Monounsaturated fatty acids with only one isolated *cis* double bond such as oleic acid (C18:1) are considerably more stable towards

thermal-oxidation stability by an order of magnitude or more. Despite this, it seems that the ideal situation would be to remove all unsaturation by catalytic hydrogenation. This however would "harden" the lubricate leaving it with saturated fatty acids such as stearic acid that would turn the (liquid) oil to a (solid) fat rendering it useless as a lubricant or hydraulic fluid. For this reason, it is necessary to leave monounsaturated fatty acids in the oil to ensure optimal lubricity, viscosity, and pour point.

Selective hydrogenation is a process of converting polyunsaturated fatty acids to saturated and monounsaturated fatty acids by removing all or all but one of the double bonds. For example linolenic acid (C18:3) and linoleic acid (C18:2) would each lose two and one of the *cis* double bonds respectively, thus being converted to oleic acid (C18:1) and its positional isomers, each of which carrying only one isolated *cis* double bond. Hydrogenation can occur through a variety of catalysts [77]. Although these processes are still in their infancy as reactions of linolenic acid and linoleic acid were reduced but not strictly to oleic acid, some of the reaction isomerized to elaidic acid (*trans* C18:1) which has similarly properties as stearic acid (C18:0), that are undesirable, and thus rendering the process unsubstantiated. Through continued efforts this process does have potential to allow the improvement of readily available natural oils, however more research is needed.

2.4.7 Branched Fatty Acids

Biolubricants synthesized from branched fatty acid such as iostearic acid exhibit superior low temperature behavior such as low pour point, low viscosity, high chemical

stability, and high flashpoint. Isostearic acid is procured from the thermal isomerization of polyunsaturated C-18 fatty acids followed by hydrogenation. The branching points are limited to the interior portion of the molecule [131, 249]. In a similar fashion 12-hydroxystearic acid derived from rhizonoleic acid by hydrogenation can also be used. As previously discussed, removing the double bonds and the glycerol molecules from the triacylglycerides enhances biolubricant performance. Compromises will always be made between tribological performance, oxidative stability, low-temperature performance, and biodegradability. For example, biolubricants synthetized from branched fatty acids maintain low temperature capabilities that must be present in the oils for many industrial applications, however branched fatty acids decrease biodegradability of the lubricant.

The forgoing discussion on the enhancements of biolubricants aims at providing an overview of the molecular structure and physical constraints that must be considered when evaluating their performance. In an effort to provide the reader with a broad scope, Fig. 2.11, summarizes the influence of structure on the chemical and physical properties.

As it relates to	Increase of branching of alcohol	Increase of branching of acid	Increase of saturation of acid	Increase of molecule weight	Increase of linearity
Hydrolytic stability	↑	↑	↑	↑	↓
Viscosity	↑	↑	↑	↑	↑
Low temperature viscosity	↑	↑	↓	↓	↑
Oxidation stability	↑	↑	↑	↑	↑
Viscosity index	↓	↓	↓	↑	↑

Figure 2.11: Summarized table of the influence of structure on chemical and physical properties

2.5. Evaluating Biodegradability and Ecotoxicity

2.5.1 Biodegradability

As the lubrication industry shifts towards the use of "greener" lubricants, two major prerequisites are remaining that biolubricants must meet: (1) a high biodegradability and (2) a low ecotoxicity. One of the primary attributes of bio-based lubricants is their inherent biodegradability. Biodegradation is the chemical dissolution by which organic substances are broken down by the enzymes produced by living organisms. This means that biolubricants based on renewable raw materials derived from CO_2 and H_2O via photosynthesis, following their use, are ultimately returned to the earth as CO_2 and H_2O through biodegradation [250]. Organic material can be degraded aerobically, with oxygen or anaerobically, without oxygen. By definition, biodegradation is the chemical transformation of a substance by organisms or their enzymes [251-254].

Biodegradation, once a term reserved for ecology, waste management, and environmental remediation (bioremediation), has now become ubiquitous within the lubrication industry.

Biodegradability of a lubricant can be separated into two types, primary and ultimate biodegradation. Primary degradation refers to the disappearance of the original organic compound and may or may not indicate that a substance will biodegrade completely. This method is measured by evaluating the infrared (IR) bands of the C-H bonds through a method listed as CECL-33-A-93 (CEC, Coordinating European Council) [255, 256]. This method of testing biodegradability has yet to become widely accepted due to the obscurity in the compound disappearance [257]. Ultimate degradation also known as total degradation describes the conversion of the original organic compound to carbon dioxide (CO_2) and water (H_2O) by biodegradation within 28 days. This method is measured by the OECD 301 B (OECD, Organization of Economic Cooperation and Development) test method, which has gained worldwide acceptance [258]. Currently, there are numerous standardized test methods available that have been reviewed for assessing biodegradability, with many biolubricants themselves being tested under a variety of operating conditions [259]. Interestingly, results indicate that biodegradability is not affected by usage and that antioxidant additives have a positive effect.

2.5.2 Ecotoxicity

Ecotoxicity is an important property in the discussion of biolubricant usage. With upwards of 50% of all lubricants (most being petroleum-based) entering the environment via waste streams, spills, normal usage, and improper disposal their presence in the

environment is toxic with compounding effects that are detrimental to plants, animals, and humans. These effects are strikingly more severe in aquatic ecosystems due to their high sensitivity. For these reasons, it is important to test the aquatic toxicity of lubricants by measuring the extent to which they poison particular environmental species such as green algae, *Pseudokirchneriella subcapitata* or *Desmodesmus subspicatus* (OECD 201); freshwater fleas, *Daphina magma* (OECD 202-12); rainbow trout minnows, *Oncorhynchus mykiss* or zebrafish minnows, *Brachydanio rerio* (OECD 203-13); bacteria, *Pseudomonas putida* (OECD 209); and laboratory rats, *Sprague Dawley* (OECD 401).

Qualification of a lubricant to be classified as biodegradable means the lubricant biodegrades by at least 80% within 28 days (CECL-33-A-93) or by 60% after 28 days (OECD 301B). Toxicity measurements are based on the LD_{50} value, which is a measurement used to determine the potential impact of toxic substance on different types of organisms. It provides an objective measure to compare and rank the toxicity of substances based on the median lethal dose (LD) of a substance, or the amount required to kill 50% of a given test population. In ecotoxicity studies a lubricant is deemed ecofriendly (non-toxic) if its LD_{50} value is greater than 1000ppm ($LD_{50}>1000ppm$).

2.5.3 Biolubricant Environmental Definitions

Despite the criteria for evaluating biodegradability and ecotoxicity, many lubricants are still deemed biolubricants that are *environmentally acceptable* even if they are not properly formulated. For example, if a lubricant consists of a bio-based fluid in combination with a toxic additive, the "environmentally-friendliness" of the lubricant is

thus compromised and should be referred to as *not* environmentally acceptable, even while the bulk of the fluid is indeed biodegradable, the overall lubricant is not. For this reason, it is useful to classify lubricants according to environmental risk as shown in Table 2.8 [260].

Table 2.8: Classification of terminology regarding lubricants and environment risk

Term	Definition
Environmentally positive	Non-injurious
Environmentally-friendly	Eco-friendly
Environmentally-sociable	Socially Friendly
Environmentally-justified	Environmentally favorable
Environmentally careful	Environmentally conservative
Environmentally neutral	Harmless to the environment
Environmentally protective	Preserves the environment
Environmentally conformable	Respectful of the environment

Moreover, it is equally important to organize the lubricant classifications by environmental risk (Table 2.9). According to this categorization, no lubricant can be regarded as *truly* environmentally friendly, because this in turn implies an improvement to the environmental conditions. Therefore, one must be content with the fact that a lubricant is environmentally acceptable and that it affects the environment to a less pronounced degree [261]. To this point, several European countries have begun eco-labeling lubricants as environmentally acceptable such as the Blue Angel label in Germany, the Nordic Swan in Nordic countries, the new Euro Margerite eco-label seen in

various European countries, and most recently the BioPreferred program in the United States [181, 262-265].

Table 2.9: Rank of terminology regarding environment risk

Term	Definition
Friendly	Improves the environment
Neutral	Unimportant, harmless
Threshold of Perception	
Sociable	Low, Unsuitable
Start of Legal Regulation	
Annoying	Disagreeable, unpleasant, impairing
Irksome	Troublesome, inconvenient
Limit of Burdening	
Endangering	Excessive, unimputable
Harmful	Dangerous, irreversible effects

2.5.4 Evaluation methods

Since the testing of biolubricants varies substantially from those of conventional petroleum-based lubricants, extensive testing is required. To qualify biolubricants for their intended applications, special laboratory tests are required to ensure that they will withstand the pressures and temperatures encountered, while maintaining adequate tribological performance. Many of the conventional chemical and physical test procedures were developed for mineral oils and are not applicable for biolubricants, so many new test procedures have been developed. In particular, new test methods to access

the thermal-oxidative stability, biodegradability, and ecotoxicity of biolubricants have been developed. Various test methods exist for evaluating many of the properties of biolubricants. As described previously biodegradability can be measured by CECL-33-A-93 and OECD 301 tests and ecotoxicity can be measured according to OECD 201 through 213 tests. Other performance tests involve the quantification of a lubricant's oxidative stability, viscosity, viscosity index, and hydrolytic stability, among many other properties that are pertinent to biolubricants. There are a number of standardized oxidative stability tests for lubricants such as the Baader Oxidation Test (DIN 51553 part 3), Two One-Sided Tests (DIN 51587), Rancimat method, and various Standard Test Methods for Oxidation Stability (ASTM D2112-93, ASTM D2272, and ASTM D943). Kinematic Viscosity and the viscosity index can be studied according to ASTM standards D445 and D2270, respectively. Standard test methods for examining hydrolytic stability are ASTM D2619, known as the 'beverage bottle test', and ASTM D943 where it describes a TOST test measuring hydrolytic stability [77]. More specialized tests exist for particular applications and the needs of a lubricant, however a detailed summary of all these methods is beyond the scope of this review [266].

2.6. Laws, regulations, and the state of biolubricants

Most industrialized countries have laws, which are designed to protect water resources, the ground, work places, and the air from pollution. In most countries, except Portugal and Austria, there are no compulsory legislative measures regarding the use of biolubricants. Portugal was the first country to institute a mandate requiring outboard

two-stoke engines to run off a two-thirds biodegradable lubricant, the minimum requirements of biodegradability according to CECL-33-T-82. In Austria, the use of a plant-derived lubricant for chain saw oils is a federal regulation. Recommendations for the use of bio-based lubricants and functional fluids exist in the United Kingdom and Canada [23, 267, 268]. In the United States, the Department of Agriculture (USDA) has established guidelines for designating and promoting items made from biobased products (including plant based lubricants) through two initiatives: (1) Product Labeling, where the government seeks to qualify products to increase consumer recognition and (2) the Federal Procurement Preference, where the USDA designates categories of biobased products. Here, the USDA has a BioPreferred program whose primary focus is to "promote the increased purchase and use of biobased products" [269]. This program aims at creating economic development by generating new jobs and building new markets for farm commodities. The USDA believes that an increase in the development, purchase, and use of bio-based products will reduce the nation's reliance on petroleum. The underlying goal is to increases the use of renewable agricultural resources in hopes of reducing adverse environmental and health impacts from the nearly 20 million tons of petroleum-based lubricant entering the environment annually. Currently, many state and local community regulations are voluntarily trying to convince contractors and subcontractors to use environmentally acceptable lubricants and functional fluids. However, the decision to use biolubricants remains with the contractor as well as the financial burden.

The price of biolubricants is an issue that affects their widespread use. On average

biolubricants cost approximately three times more than traditional petroleum-based lubricants. Vegetable oils and synthetic esters can range anywhere from 1.5 to 5 times more expensive than mineral oils [76]. For this reason, their must be an economic and environmental balance in order to minimize the cost, where the difference between economic cost and true cost are on the same order of magnitude. This can be accomplished by government funded subsidies for original equipment manufacturers (OEMs) to invest in biolubricants without assuming all of the financial liability.

To bring biolubricants to the forefront of the lubrication industry there needs to be economic incentives where government legislature puts a value on protecting the environment. Increasing legislative pressure would promote the use of biolubricants. In order for this to occur, lawmakers would have to quantifiably decide, with a similar logic as presented in Table 2.9, if the release of lubricants into the environment is tolerable or hazardous in the sense of pollution. Without a decision on these terms and the lack of appropriate incentives, the consumer, industrial companies, contractors, and other stakeholders involved in the lubrication industry would have little reason to use the more expensive biolubricants over petroleum-based lubricants. Currently, many lubrication engineers first base their decision to use a lubricant on price, then on performance, and lastly by environmental consideration.

More still, legislative pressure and government subsidiaries are necessary to encourage the use of biolubricants because this will incentivize OEMs to design and test their machinery and hydraulic equipment for use with biolubricants. This is important because it ensures a customer that their equipment is covered under warranty if it uses a

biolubricant and it helps drive down prices of bio-based lubricants and functional fluids. For example, currently the market share of biolubricants is 2-5% and many OEMs do not see the immediate value of using a biolubricant because it is more expensive, however a government subsidy could help to encourage more OEMs to create products with biolubricants. This would in turn reduce the price of biolubricants through increased market saturation.

2.7 Conclusions

Biolubricants can provide economical and feasible alternatives to petroleum-based lubricants while promoting energy conservation and sustainability. Their ability to be non-toxic and renewable as well as potentially satisfy the combination of environmental, health, economic, and performance challenges of conventional lubricants illustrates the vast potential of bio-based lubricants. When developing bio-based lubricants a compromise must be maintained between synthesizing a lubricant with optimal environmental and tribological properties as well as ensuring a competitive price. Although many biolubricants often suffer from poor thermal-oxidative stability, solidification at low temperatures, biological deterioration, and hydrolytic instability, there remains to be many techniques to rectify these drawbacks through a multidiscipline understanding of the relationships between chemical composition, molecular structure, and various chemical modification techniques. In this review, biolubricants were examined from a macroscale perspective with their deficiencies and advantages being highlighted. Biolubricants have progressed tremendously over the last thirty years and

hopefully in the next thirty years they can become as prevalent and ubiquitous as mineral oil, thus supporting many of the global environmental initiatives.

Chapter 3 Experimental Details

3.1 Materials

3.1.1 Natural Oils
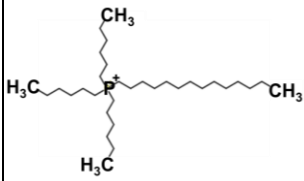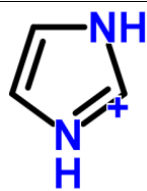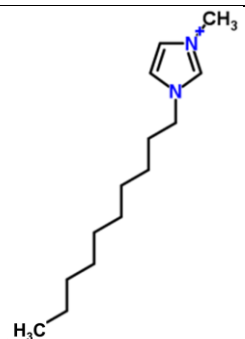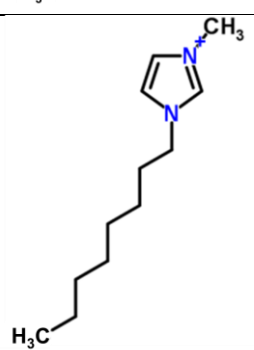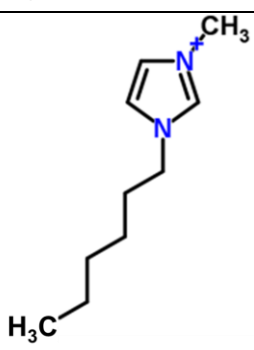
In the present investigation, eight commercially available natural oils were selected as neat lubricants: avocado, canola (rapeseed), corn, olive, peanut, safflower (derived from genetically modified organisms), sesame, and vegetable (soybean) oil. These oils were chosen because they represent oils with a variety of saturated, monounsaturated, and polyunsaturated fatty acid compositions. The natural oils are derived from a broad range of bio-based feedstocks with minimal refinement and are readily available and inexpensive. Additionally, they have viscosity indices and surface tension properties similar to petroleum-based lubricants and transmission fluids used in sheet metal stamping and metal-forming processes [17, 81, 91, 92, 95, 196]. In addition, as a basis for comparison a commercial soybean derived biolubricant and a petroleum-based lubricant SAE 10W-30 synthetic motor oil were tested.
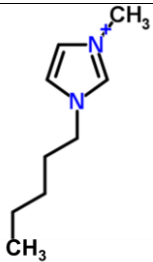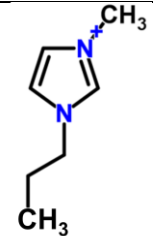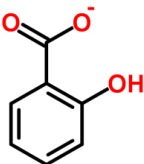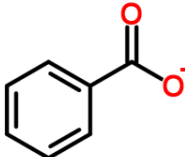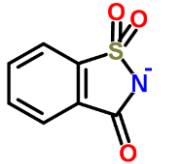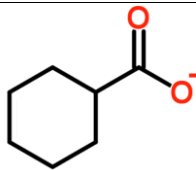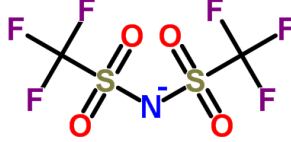
3.1.2 Ionic Liquids

In this investigation, the ionic liquids examined consist of anions such as salicylate⁻, saccharinate⁻, benzoate⁻, cyclohexane carboxylate⁻, chlorine⁻, and bis(trifluoromethylsulfonyl)imide, designated as Tf_2N^- *(anion charges will now be omitted)*. Salicylate, saccharinate, and benzoate are considered to be environmentally benign anions due to their potential bio-based derivation. The cations consisted of

trihexyl(tetradecyl)phosphonium ($P_{666,14}^+$) and 1,3-diakylimidazolium (C_xmim^+) of varying chain lengths, where the x denotes 10, 8, 6, 5, and 3 carbon atoms representing the 1-decyl, 1-octyl, 1-hexyl, 1-pentyl, and 1-propyl analogs *(cation charges will now be omitted)*. The names, properties, and molecular structure of the anions and cations are depicted in Table 3.1. The 1,3-diakylimidazolium-based ionic liquids were prepared via either conventional anion metathesis reactions or microwave synthesis involving either the conjugate acid or sodium salt of the desired anion, then purified and characterized using established methods [138, 270-272]. The phosphonium-based ionic liquids consisting of a trihexyl(tetradecyl)phosphonium (more commonly referred to as phosphonum) cation paired with a benzoate, salicylate, saccharinate or Tf_2N anion were synthesized, purified, and characterized according to published methods [272] with slight modifications. In the synthesis process, a dichloromethane solution of $P_{666,14}Cl$ was contacted for two hours at room temperature with a saturated aqueous solution (in D.I. water) of either the sodium or lithium salt of the anion of interest to permit ion exchange. The IL (lower) layer was separated from the aqueous phase (upper) and washed three times with D.I. water to ensure complete removal of NaCl (or LiCl). The methylene chloride was then removed at 80°C and the chemical composition of the residue remaining (i.e. the IL) was determined by ^{1}H NMR.

Table 3.1: Names, properties, and molecular structure of

various ionic liquid anion and cation constituents

Systematic Name	Common Names	Details	Structure
Trihexyl(tetradecyl) phosphonium	trihexyl(tetradecyl)phosphonium Tetradecyl(trihexyl)phosphonium Phosphonium $P_{666,14}$	Cation (+) Molecular Formula: $C_{32}H_{68}P$ Molar Mass: 483.86 Da	
1H-Imidazol-3-ium	1,3-dialkylimidazolium $C_x$mim	Cation (+) Molecular Formula: $C_3H_5N_2$ Molar Mass: 69.08 Da	
1-Decyl-3-methyl-1H-imidazol-3-ium	1-Decyl-3-methylimidazolium C_{10}mim	Cation (+) Molecular Formula: $C_{14}H_{27}N_2$ Molar Mass: 223.38 Da	
1-Methyl-3-octyl-1H-imidazol-3-ium	1-Methyl-3-octylimidazolium 1-Octyl-3-methylimidazolium 3-Methyl-1-octylimidazolium C_8mim	Cation (+) Molecular Formula: $C_{12}H_{23}N_2$ Molar Mass: 195.32 Da	
1-Hexyl-3-methyl-1H-imidazol-3-ium	1-Hexyl-3-methylimidazolium C_6mim	Cation (+) Molecular Formula: $C_{10}H_{19}N_2$ Molar Mass: 167.27 Da	

3-Methyl-1-pentyl-1H-imidazol-3-ium	3-Methyl-1-pentylimidazolium C_5mim	Cation (+) Molecular Formula: $C_9H_{17}N_2$ Molar Mass: 153.24 Da	
1-Allyl-3-methyl-1H-imidazol-3-ium	1-Allyl-3-methylimidazolium C_3mim	Cation (+) Molecular Formula: $C_7H_{11}N_2$ Molar Mass: 123.18 Da	
Salicylate	Salicylate	Anion (-) Molecular Formula: $C_7H_5O_3$ Molar Mass: 137.11 Da	
Benzoate	Benzoate	Anion (-) Molecular Formula: $C_7H_5O_2$ Molar Mass: 121.11 Da	
1,1-Dioxo-1,2-benzothiazol-2-id-3-one	Saccharinate	Anion (-) Molecular Formula: $C_7H_4NO_3S$ Molar Mass: 182.18 Da	
Cyclohexane carboxylate	Cyclohexane carboxylate	Anion (-) Molecular Formula: $C_7H_{11}O_2$ Molar Mass: 127.16 Da	
Bis((trifluoromethyl)sulfonyl)azanide	Bis(trifluoromethylsulfonyl)amide Bistriflylimide anion Tf_2N	Anion (-) Molecular Formula: $C_2F_6NO_4S_2$ Molar Mass: 280.15 Da	
Chloride	Chloride	Anion (-) Molecular Formula: Cl Molar Mass: 35.45 Da	

3.1.3 Particulate Additives

In the present investigation the lubricants were mixed with various particulate additives such as hexagonal boron nitride (hBN), molybdendum disulfide (MoS_2), tungsten disulfide (WS_2), graphite (C), and multi-walled carbon nanotubes (MWNTs). These additives ranged in size from nanometers to microns. Table 3.2 showcases the various additives used throughout this experimental investigation. During particulate lubricant mixture tests, 5 to 10 mL of lubricant were mixed with the particulate additives at 5% by weight. The individual particles and their mixtures were combined with the neat lubricants using a vortex generator to form a homogenous colloidal mixture. In trials where two particles were mixed, the percentage of each additive was decreased in half to 2.5%, resulting in a total addition of 5% by weight. These solid particle lubricant suspensions were tested in identical manners to the neat lubricants using a pin-on-disk tribometer.

Table 3.2: Particle additives mixed with the lubricants

Additive Name	Additive Composition	Size (μm)	Structure
Boron Nitride	h-BN	0.07	Lamellar
Boron Nitride	h-BN	0.50	Lamellar
Boron Nitride	h-BN	1.50	Lamellar
Boron Nitride	h-BN	5.00	Lamellar
Tungsten Disulfide	WS_2	0.055	Lamellar
Tungsten Disulfide	WS_2	0.60	Lamellar
Graphite	C	0.05	Lamellar
Molybdenum Disulfide	MoS_2	2.00	Lamellar
Multi-Walled Carbon Nanotube	C	O.D. x L 0.006-0.009 x 5.0	Cylindrical

O.D. = Outside Diameter

L = Length

3.1.4 Pin and Disk Materials

Throughout this experimental investigation three materials were consistently used for the construction of the pins and disks used in the tribo-interface, 440C stainless steel, 2024 aluminum alloy, and oxygen-free electronic copper (C101) (99.99 wt. % purity of copper) [112]. The chemical composition of the steel and aluminum material is shown in Tables 3.3 and 3.4, respectively [112, 198]. The pin and disk materials were specifically chosen to match prior experiments conducted by the authors [81, 90, 93, 118]. Additionally, these materials are used to manufacture components for metal-forming, drilling, and machining operations as well as extensive use in a broad set of applications within the manufacturing and automotive industries. They are also used to produce a

wide variety of parts including dies, molds, bearings, brake valves, and bushings [95, 273-277].

Table 3.3: Chemical compositions of 440C stainless steel [112]

Element	Percent (%)
Fe	79.89
Cr	17
Ni	0.375
C	1.075
Mg	0.5
Cu	0.25
Mo	0.375
Si	0.5
S	0.015
P	0.02
Other, total	None

Table 3.4: Chemical compositions of 2024 Al alloy [112]

Element	Percent (%)
Al	91.9
Cu	4.35
Mg	1.50
Mn	0.60
Fe	0.50
Si	0.50
Zn	0.25
Ti	0.15
Cr	0.10
Others, total	0.15

The pins were machined to dimensions of 6.35 mm in diameter and 50 mm in length with a hemispherical tip. The disks were made having dimensions of 70 mm in diameter and 6.35 mm in thickness. The disks were originally machined to a surface roughness having an arithmetic average, R_a, of 0.3 ± 0.05 μm. The surface roughness measurements were conducted using a 2-dimensonal contact-type profilometer for a 10 mm scan length. In some experiments the surface roughness was altered. These details will be provided in the subsequent chapters.

3.2 Experimentation

3.2.1 Tribological Testing

Pin-on-disk tests at ambient (23°C) and high temperature (100°C) conditions were conducted to characterize the tribological properties of the various lubricants. Table 3.5 presents the basic testing conditions used throughout each experiment.

Table 3.5: Test parameters

Parameter	Selected Value
Normal load (N)	10
Sliding velocity (mm/s)	36
Angular velocity (rpm)	21.5
Distance traveled (m)	Variable i.e. test dependent
Environment	Ambient (23°C) or high temperature (100°C)
Lubricant quantity (mL)	5 - 10

During each of the tests the surface of disk was completely submerged by the lubricant mixture, thereby continually lubricating the pin-disk interface throughout the duration of the test. The pin and disk specimen were cleaned before and after each test using an ultrasonic cleaner with soap, acetone, and hexane solutions. Each test was repeated a minimum of three times to ensure repeatability and accuracy of the results. The normal load and friction force measurements were monitored for each test using a two beam type load cells that read the normal load from a static hanging mass and the friction force from as the tangential force off the pin holder. The linear wear-loss was acquired through a linear variable differential transducer (LVDT) with an encoder, which recorded the

vertical displacement of the pin. The linear wear displacement of each pin was converted into a volumetric wear loss using Eq. (3.1) derived from the geometry of a spherical cap [278].

$$V = \frac{\pi h^2}{3}(3r - h) \qquad\qquad \text{Eq. (3.1)}$$

In Eq. (3.1), h is the linear displacement (mm) in the vertical (longitudinal) axis for the pin, r is the pin radius (mm), which is assumed to be constant throughout the test, and V is the volumetric wear loss (mm^3). The tribometer was configured with a data acquisition system that recorded all the data in situ throughout the duration of each test. After each test, the pin specimens were examined using a scanning electron microscope to study the deformation and damage on the worn surface of the pins.

3.2.2 Thermogravimetric Analysis

A thermogravimetric analysis (TGA) in a nitrogen (N_2) atmosphere was performed on the lubricants to determine the thermal stability by measuring the decomposition temperatures in the absence of oxygen. This analysis was performed by first heating up 8.5 ± 0.5 mg of the natural oils to 60ºC for 20 hours under a vacuum of 948 mbar (711 mm Hg) to remove any residual water to minimize the error in the decomposition data measurements. The TGA was performed by measuring the mass loss for both the dynamic and isothermal decomposition tests using a platinum pan with a N_2 flow rate greater than or equal to 40 mL/min. During the dynamic decomposition tests, the samples were heated at a rate of 10ºC/min from room temperature to a maximum of

1000ºC. The TGA was stopped after reaching the maximum thermal decomposition temperature when a temperature plateau was observed for at least 200ºC as shown in Fig. 3.1 for peanut oil undergoing a dynamic decomposition analysis. In this figure, the onset of decomposition, $T_{d(onset)}$ is 378ºC. By taking the derivative of the onset of decomposition with respect to temperature, the maximum thermal decomposition, $T_{d(max)}$ is determined. In Fig. 3.1, $T_{d(max)}$ is calculated to be 411ºC at the peak. In the isothermal decomposition tests, the samples were heated at a rate of 20ºC/min up to 50ºC and 100ºC below the onset of decomposition temperature, $T_{d(onset)}$ of 378ºC. In these tests, the samples were held for 480 minutes at approximately 327ºC and 277ºC, in order to reveal thermal mass loss in a constant heat environment, as illustrated in Fig. 3.2 for peanut oil. It can be seen in Fig. 3.2 that with a temperature of 327ºC, 92% of the peanut oil has decomposed and with a temperature of 277ºC, 19% of the peanut oil has decomposed within the 480 min.
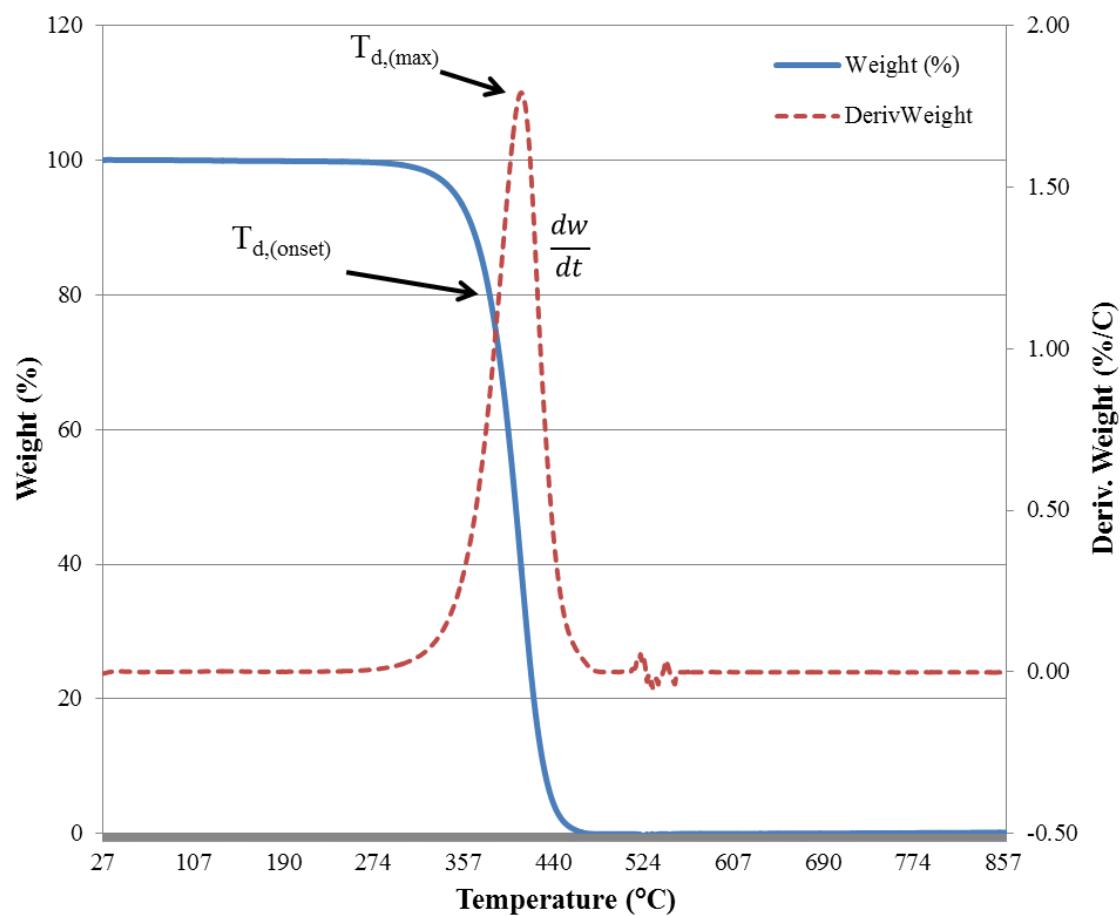
Figure 3.1: Dynamic decomposition plot for peanut oil
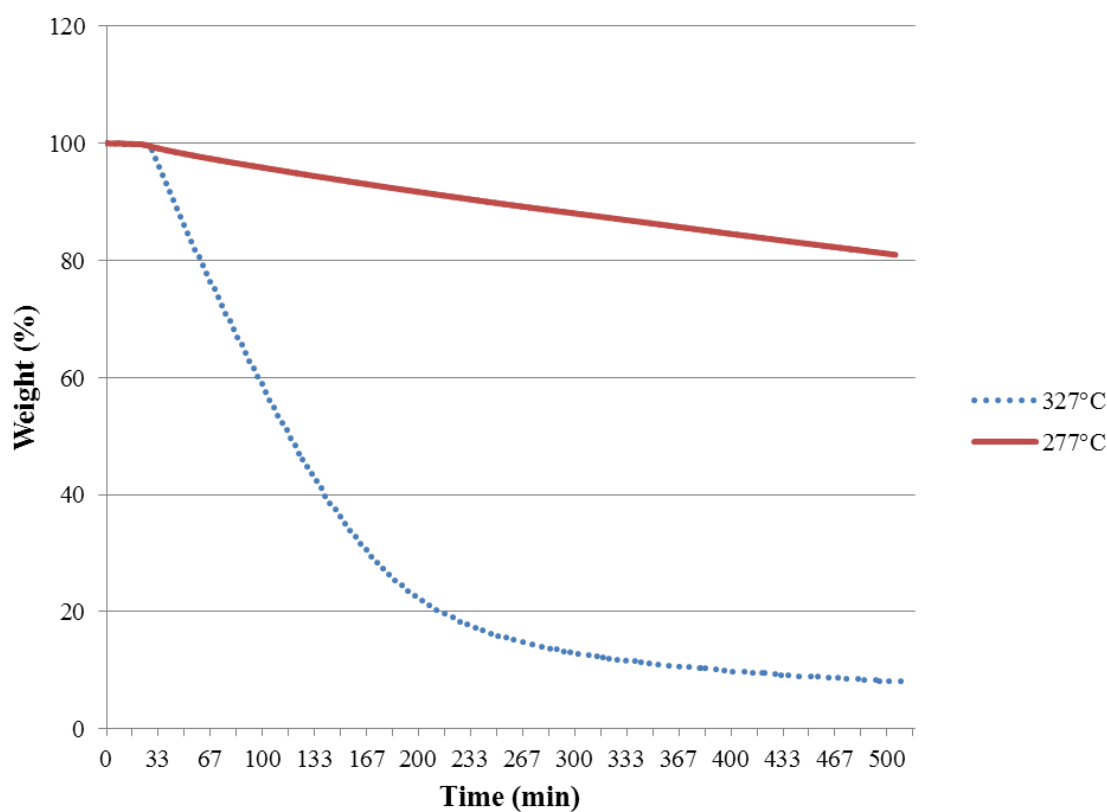
Figure 3.2: Isothermal decomposition plot for peanut oil at two different temperatures

3.2.3 Statistical Analysis

After the experiments, data-driven statistical correlation assessments were conducted through a linear regression by examining the Pearson Product-Moment Correlation Coefficient (R). Here, the Pearson Product-Moment Correlation Coefficient or sample correlation coefficient is a numerical indicator of the linear relationship between two variables. Through this statistical analysis multiple correlation coefficients were determined using predictor variables such particle additive size, fatty acid chain

lengths, unsaturation numbers, fatty acid compositions, thermal degradation temperatures, anion and cation molecule size, ionic liquid additive amounts, surface roughness, and tribological properties such as coefficient of friction and wear rate. This analysis was calculated by comparing a sample of paired predictor variables in the form of X_i and Y_i and inserting them into Eq. (3.2) [278].

$$r = \frac{\sum_{i=1}^{n}(X_i - \bar{X})(Y_i - \bar{Y})}{\sqrt{\sum_{i=1}^{n}(X_i - \bar{X})^2 \sum_{i=1}^{n}(Y_i - \bar{Y})^2}} \qquad \text{Eq. (3.2)}$$

Here, r (also written as R, or R-value) is the sample correlation coefficient. Properties of the correlation coefficient are as follows and an example calculation is performed in Appendix A:

1. $-1 \leq R \leq 1$ or, equivalently, $|R| \leq 1$.

2. R is positive or negative according as Y tends to increase or decrease respectively as X increases.

3. The closer $|R|$ is to 1, the stronger, the linear relationship between the variables X and Y, indicating a high correlation (i.e. dependence) between X and Y.

4. The closer $|R|$ is to 0, the weaker, the linear relationship between the variables X and Y, indicating a low correlation between X and Y. If $R = 0$, there is no correlation and the variables are independence of each other.

This analysis allowed for a deeper exploration of the causal relationships between particle size, fatty acid composition, thermal stability, oxidative stability, anion-cation moieties, surface roughness, friction, and wear. Through this assessment individual factors could

be isolated and examined to understand their specific influences on the tribological and thermal performance of the lubricants.

3.3 Surface Texturing

The disks were polished using one of three methods in order to vary the surface roughness with a random surface texture: (1) dry SiC emery paper with grit sizes of 80, 220, 320, 600, and 1200; (2) slurry SiC paste with a grit size of 1200; and (3) a 1.0 μm aqueous diamond slurry polish. A two-dimensional contact-type profilometer was used to study the surface roughness of the disks. Table 3.6 shows the initial arithmetic average surface roughness (R_a) values of the disks before the experiments and the techniques used to polish the surfaces. Figure 3.3 shows the SEM surface images of selected disks polished with the 80 grit, 320 grit, 1200 grit SiC dry emery paper as well as a disk polished with the 1μm diamond slurry before testing. It is revealed that the disk polished with the 80 grit paper had the roughest surface. Subsequent disk surfaces polished with the 320 grit paper, 1200 grit paper, and 1200 grit slurry showed a decrease in surface roughness with their values shown in Table 3.6.

Table 3.6: Preparation techniques and initial surface roughness values

of the test disks at the start of the experiment

Grit Size	Polishing Type	R_a value (μm)
C101 Copper Disk		
80	Dry SiC Emory Paper	1.25 ± 0.14
320	Dry SiC Emory Paper	0.49 ± 0.03
600	Dry SiC Emory Paper	0.20 ± 0.02
1200	Slurry SiC Paste	0.11 ± 0.02
1200	Dry SiC Emory Paper	0.11 ± 0.02
N/A	1 μm Diamond Slurry Polish	0.09 ± 0.04
2024 Aluminum Alloy		
220	Dry SiC Emory Paper	0.43 ± 0.02
600	Dry SiC Emory Paper	0.27 ± 0.03
1200	Dry SiC Emory Paper	0.22 ± 0.02
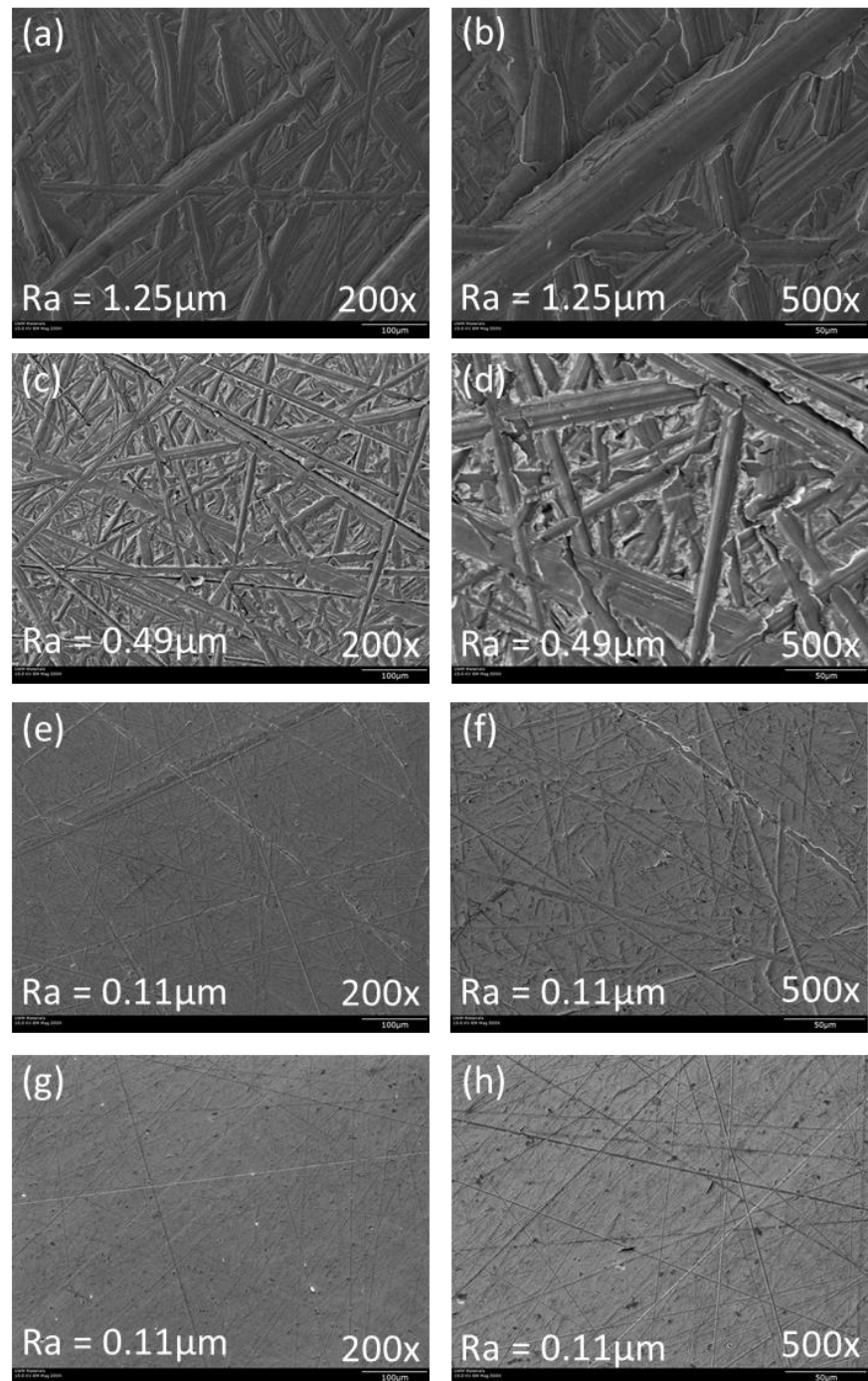
Figure 3.3: SEM micrographs of selected disk surfaces after SiC polishing and before testing (a) & (b) 80 grit polish, (c) & (d) 320 grit polish, (e) & (f) 1200 grit polish, (g) & (h) 1 μm diamond slurry polish

3.4 Instruments

Ionic liquid characterization was carried out by NMR spectroscopy. All spectra were acquired on a Bruker DPX300 NMR spectrometer operating at 300.13 MHz for protons. Spectra were obtained using solutions in chloroform-d (Acros, 100.0% atom D) and all chemical shifts were reported relative to tetramethylsilane. A thermogravimetric analysis (TGA) was performed using a TA Instruments Q50. Experiments were run in a nitrogen atmosphere from room temperature to 600°C using a platinum pan at a temperature scan rate of 10°C/min using 8.35 ± 0.35 mg samples. Pin-on-disk testing and friction and wear measurements were conducted using a Ducom Instruments (Bangalore, India) Material Characterization System tribometer (up to 20 N) containing a horizontally oriented unidirectional rotational disk spinning against a vertically placed pin). The Ducom Instruments tribometer utilized a hanging mass load with a linear variable differential transformer (LVDT) to measure the wear rate. The tribometer was outfitted with a Hotset Multi K-type thermocouple heating chamber furnace with a temperature feedback loop with the ability to maintain a temperature accuracy of $1°C \pm 1\%$ of the measured temperature. Additionally, scanning electron microscopy (SEM) along with energy dispersive X-ray spectroscopy (EDS) where conducted to analyze the surface roughness of the test specimen before and after testing. The EDS was also used to assess the potential for transfer layer formation after the pin-on-disk testing.

3.5 Lubrication Regime Determination

Investigating the lubrication regime for the following experiments is an important preliminary step when characterizing the friction mechanisms between the pin and the disk surfaces. This can be achieved by utilizing the elastohydrodynamic minimum film thickness equation developed by Hamrock and Dowson [279] as referenced in other sources [40, 280, 281], which is applicable in many material combinations for a variety of contact geometries including point contact of a hemisphere on a flat surface as is the geometry for the pin-on-disk testing as shown in Fig. 3.4.
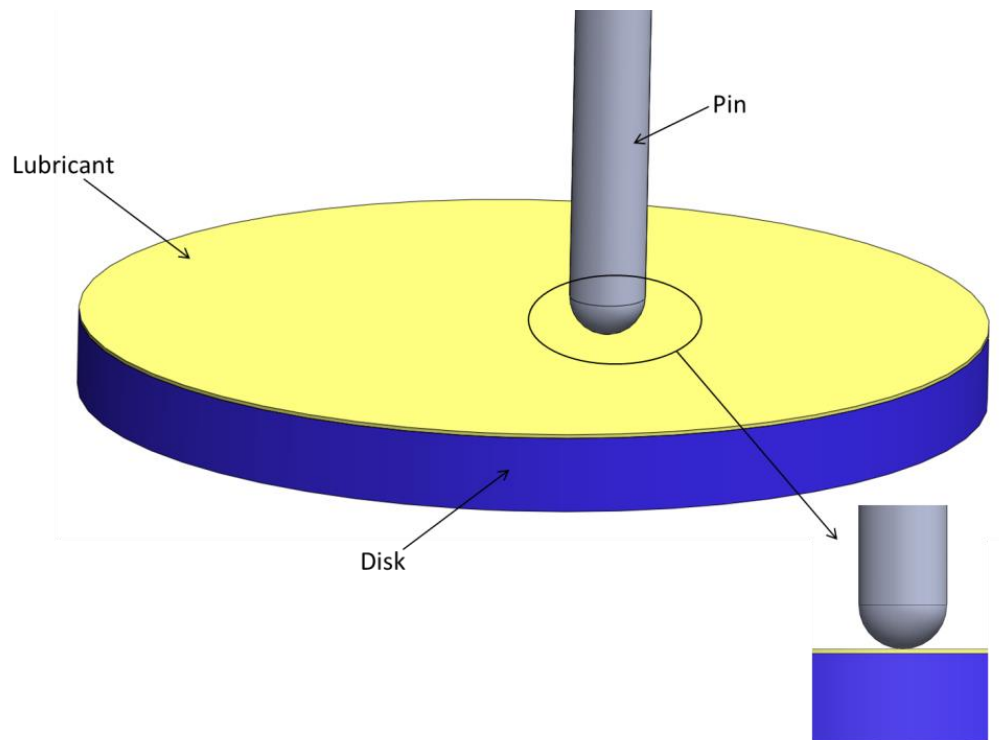
Figure 3.4: Schematic of pin-disk interface with a lubricant film covering the disk

The numerically derived formula for the minimum film thickness is expressed in the following form:

$$\frac{h_o}{R'} = 3.63 \left(\frac{U\eta_o}{E'R'}\right)^{0.68} (\alpha E')^{0.49} \left(\frac{w}{E'R'^2}\right)^{-0.073} \left(1 - e^{-0.68k}\right) \qquad \text{Eqn. (3.2)}$$

where:

h_o is the minimum film thickness (m);

U is the entraining surface velocity (m/s), i.e. $U = \frac{(U_a + U_b)}{2}$, where the subscripts 'a' and 'b' refer to the velocities of bodies 'a' and 'b' respectively;

η_o is the viscosity at atmospheric pressure of the lubricant (Pa s);

E' is the reduced Young's modulus (Pa), i.e. $\frac{1}{E'} = \frac{1}{2}\left(\frac{1-v_a^2}{E_a} + \frac{1-v_b^2}{E_b}\right)$, where v is Poisson's ratio and E is Young's modulus for the respective pin and disk specimen;

R' is the reduced radius of curvature (m) for a pin on flat, i.e. $\frac{1}{R'} = \left(\frac{1}{R_{ax}} + \frac{1}{R_{ay}}\right)$, where R_a is the radius of curvature for the pin in the x and y directions

α is the pressure-viscosity coefficient (m^2/N), i.e. $\alpha = (0.6 + 0.965 \log_{10} \eta_o) \times 10^{-8}$

w is the normal load (N)

k   is the ellipticity parameter defined as k = a/b, where 'a' is the semiaxis of the contact ellipse in the transverse direction (m) and 'b' is the semiaxis in the direction of motion (m), however in this calculation the value of the ellipticity parameter for point contact is k = 1.

To determine which lubrication regime is occurring in the experimental investigation a calculation of the minimum oil film thickness to surface roughness ratio is determined based on the following equation as described in Chapter 1, $\lambda = \frac{h_o}{\sigma^*}$. In the present experimental conditions the pin tip radius is 3.175mm, the sliding speed is 36mm/s, and the normal load is 10N. Table 3.7, shows the various mechanical properties for selected materials. Applying the parameters listed in Table 3.7 for the current system, Hamrock and Dowson's elastohydrodynamic film thickness equation predicted a minimum film thickness ratio of 2.36×10^{-6} or less. These values are significantly less than unity and place the current experimental investigation in the boundary lubrication regime where plowing components of friction dominant and hydrodynamic effects are negligible [282]. Moreover it can be inferred that for the variety of testing conditions presented in this experimental study the lubricating regime will remain in the boundary lubrication where large hydrodynamic effects will not prevail.

Table 3.7: Mechanical properties for pin-disk materials and lubricants [281, 283-285]

Mechanical Property	440C Stainless Steel	C101 Copper	2024 Aluminum Alloy
Poisson's ratio	0.285	0.348	0.325
Young's modulus (GPa)	200	117	75
Surface Roughness, Ra (μm)	0.25 to 0.35	0.09 to 1.25	0.22 to 0.43

Lubricant	Kinematic Viscosity (mPa∘s)		
Canola oil (at 40°C)	7.22 to 32.21		
Canola oil (at 100°C)	2.18 to 7.85		
$P_{666,14}$Salicylate (at 25°C)	56,700		
$P_{666,14}$Benzoate (at 25°C)	67,400		
$P_{666,14}$Saccharinate (at 25°C)	158,500		
$P_{666,14}$Tf$_2$N (at 25°C)	31,550		
$P_{666,14}$Cl (at $25°$C)	175,900 to 195,000		

Chapter 4 The Influence of Fatty Acids on the Tribological and Thermal Properties of Natural Oils as Sustainable Biolubricants

4.1 Introduction

Pure natural oils have been known to be good lubricants since ancient times in lowering friction and preventing wear. In 1859, the first commercial oil well was drilled in Titusville, PA, USA, this lead to the rise of the modern petroleum oil industry, which would eventually decline the use of pure natural oils as lubricants. The advent of petroleum-based oils produced rapid advances in lubrication technology that quickly dominated other oils, such as natural oils in the lubrication industry. During the mid-1930s, the properties of petroleum-based oils were significantly improved through the use of additives in the oil to enhance the load carrying capacity, lubricity, corrosive protection, and thermal-oxidative stability. These improvements in properties of petroleum-based oils often surpassed similar properties of natural oils.

Since the beginning of the 20th century, investigations into the properties of natural oils have received much attention [24, 90, 106, 107, 110, 111, 117]. This revival is due to the fact that 50% of all lubricants worldwide end up in the environment through usage, spill, volatility, or improper disposal [222, 286]. Many of these lubricants entering the environment are derived from petroleum-based oils and are deleterious to sensitive biological ecosystems [82]. More recently, in an effort to curb the use of petroleum-based lubricants due to concerns of protecting the environment, depletion of oil reserves, and increases in oil price, natural oils have witnessed a resurgence. Furthermore, the

emphasis placed on natural oils is a result of the increase in demand for environmentally-friendly lubricants that are less toxic to the environment, renewable, and provide feasible and economical alternatives to traditional lubricants [81, 82].

Recently, the industrial market has been shifting to become more ecologically responsible with much of the attention focused on energy conservation and sustainability through the use of natural oils for industrial purposes to be used as functional fluids. A primary focus has been on the development of technologies that incorporate plant oils as biofuels and industrial lubricants because they are non-toxic, biodegradable, and renewable [78]. In the lubrication market, the term "biolubricants" refers to all lubricants derived from bio-based raw materials (plant oils and animal fats), which are biodegradable and non-toxic to humans and other living organisms, particularly aquatic environments where the impacts are more detrimental. Many biolubricants are comprised of plant oils, animal fats, or chemical modifications of these oils and are widely regarded as environmentally benign because of their superior biodegradability and renewable feedstock [77]. Moreover, many bio-based oils have superior lubricity and wear resistance that exceeds similar properties of petroleum-based oils resulting in the increased usage of biolubricant base-stock for industrial oils and functional fluids, thus 'fueling' the biolubricant resurgence in the industrial market [84].

Natural plant oils have a higher lubricity, lower volatility, higher shear stability, higher viscosity index, higher load carrying capacity, and superior detergency and dispersancy when compared to mineral and synthetic oils [24, 90]. Many of the accolades associated with natural oils are a result of their molecular structure, which affords

superior lubrication properties. The attraction to natural oils is due to their chemical composition of triacylglycerol molecules made up of esters derived from glycerol and long chains of polar fatty acids. The fatty acids are desirable in boundary lubrication for their ability to adhere to metallic surfaces due to their polar carboxyl group, remain closely packed, and create a monolayer film that is effective at reducing friction and wear by minimizing the metal-to-metal contact [24, 55, 98, 106-111]. Much of the work with bio-based oils has concentrated on understanding the fundamentals of saturated and unsaturated fatty acids with the bulk of the attention focusing on the use of natural oils as neat lubricants, fatty acids as additives in mineral oils, and bio-based feedstock oils for chemically-modified lubricants [17, 81, 112-114].

Despite these favorable attributes, the largest drawback to bio-based oils are their price (costing three times more than traditional lubricants), poor thermal-oxidative stability, solidification at low temperatures (high pour points), biological (bacterial) deterioration, and hydrolytic instability (aqueous decomposition) [109, 153-158]. Additionally, many biolubricants are susceptible to rapid oxidative degradation due to the presence of free fatty acids and the presence of double bonds in the carbon chains of the triacylglyceride molecules. Previous research [160-162] indicates that thermal-oxidative stability of natural oils requires a low percentage of polyunsaturated fatty acid (i.e. linoleic acid). Thus, the oxidative stability increases with decreasing amounts of polyunsaturated fatty acids. Furthermore, monounsaturated fatty acids such as oleic acid having one double bond improve oxidative stability while simultaneously providing good low temperature properties and superior tribological properties. The best compromise

between thermal-oxidative stability and low temperature properties are through the use of naturally high oleic acid oils or by genetically modifying the base-stock of low oleic acid oils to yield high oleic acid oils, such as high oleic acid safflower oil (HOSO), canola oil, sunflower oil, or soybean oil all of which are commercially available and derived from genetically modified organisms (GMOs) [55, 109].

Although biolubricants and bio-based functional fluids have their shortcomings, they have many uses ranging from basic lubrication; transmission of energy; protection against corrosion and wear (attrition); and the removal of heat, wear debris, and foreign contaminants [25]. Recently, natural oils are finding uses as carrier fluids for lamellar particle additives in sliding contact [24, 90, 93, 117, 118]. The efficacy of natural oils is determined by their fatty acid composition, which affects their specific properties allowing them to be used as lubricants, fuels, and functional fluids. The sources of bio-based oils are numerous and encompass a wide variety of vegetables, nuts, fruits, animals, and marine sources. Inherently, bio-based oils are naturally occurring organic substances primarily composed of triacylglycerol whose properties and utility vary based on biological factors such as nutrient availability, climate, light, temperature, and water, which can influence their tribological properties [97]. Notwithstanding their inconsistent and widely variable chemical composition, biolubricants remain to have superior wear resistance, lower coefficients of friction, lower volatility, higher viscosity index, excellent biodegradability, higher flashpoints, sustainable and renewable feedstock, and a lower ecotoxicity classification than mineral oils [75]. Furthermore, research has focused on thwarting the deficiencies of natural oils and other biolubricants while seeking to

understand the relationship between chemical composition, molecular structure, and properties through chemical modifications such as epoxidation, metathesis, acylation, estolide formation, transesterification, and selective hydrogenation of plant oils with polypols, and additivation [43-49, 52-56, 182, 287].

In this study, various natural oils were selected to represent a broad range of saturated and unsaturated fatty acid compositions within bio-based oils. These oils were investigated to understand the effects of fatty acid composition on friction and wear performance under ambient conditions using a pin-on-disk apparatus. Further, a thermogravimetric analysis was used to determine the correlations between the fatty acid composition, tribological performance, and the thermal response of the natural oils.

4.2 Experimentation

In this investigation, eight natural oils were evaluated as base fluids: avocado, canola (rapeseed), corn, olive, peanut, safflower, sesame, and vegetable (soybean) oil. Pin-on-disk tests at ambient conditions were conducted to characterize the tribological properties of the natural oils. During this study, oxygen-free electronic copper (C101) was used as the pin material [112] and the disks were made from 2024 aluminum alloy. The disks were polished to a surface roughness having an arithmetic average, R_a, of 0.3 ± 0.05 μm. The tests were conducted for a duration of 23.2 hours and a sliding distance of approximately 3000 m. Table 4.1 presents a list of the saturated and unsaturated fatty acid percentages of the natural oils tested. As previously mentioned in Chapter 3, these oils were selected for their variety in fatty acid composition. The pin and disk specimen were

cleaned before and after each test using an ultrasonic cleaner with soap, acetone, and hexane solutions. During each test, the linear wear loss was continually measured by use of Center for Tribology (CETR) Universal Material Tester (UMT) outfitted with a pin-on-disk module composed of a high precision ball screw actuator with encoder that measured the vertical displacement of the pins. A thermogravimetric analysis (TGA) in a nitrogen (N_2) atmosphere was performed on each natural oil to determine the thermal stability by measuring the decomposition temperatures in the absence of oxygen.

Table 4.1: Saturated and Unsaturated Fatty Acid Percentages of Natural Oils Tested

Natural Oils	Saturated Fatty Acid Percentage (%)	Monounsaturated Fatty Acid Percentage (%)	Polyunsaturated Fatty Acid Percentage (%)
Avocado Oil	11.560	70.554	13.487
Canola Oil	7.365	63.275	28.142
Corn Oil	12.949	27.576	54.676
Olive Oil	13.808	72.960	10.523
Peanut Oil	16.900	46.200	32.000
Safflower Oil	7.541	75.220	12.820
Sesame Oil	13.700	39.700	41.600
Vegetable Oil	15.651	22.783	57.741

4.3 Results and Discussion

4.3.1 Friction Analysis

Figure 4.1(a) depicts the variation of the coefficient of friction with sliding distance for various natural oils under ambient conditions. It can be seen that a general trend exists where there is a decrease of the coefficient of friction (COF) significantly at

the start of each experiment. The COF of the natural oils reaches steady-state at a sliding distance of approximately 2,000 m. The experimental results show a clear distinction between the oils where the avocado, olive, canola, and peanut oils all have the lowest COF values (between 0.02 and 0.10), while sesame, vegetable, corn, and safflower oils all have the highest COF values (between 0.30 to 0.50). Figure 4.1(b) shows the variation of the COF for various natural oils at the completion of the test. Here, it is clearly illustrated that avocado oil has the lowest COF value of the natural oils tested. Interestingly, safflower oil (being the only GMO) has the highest COF.
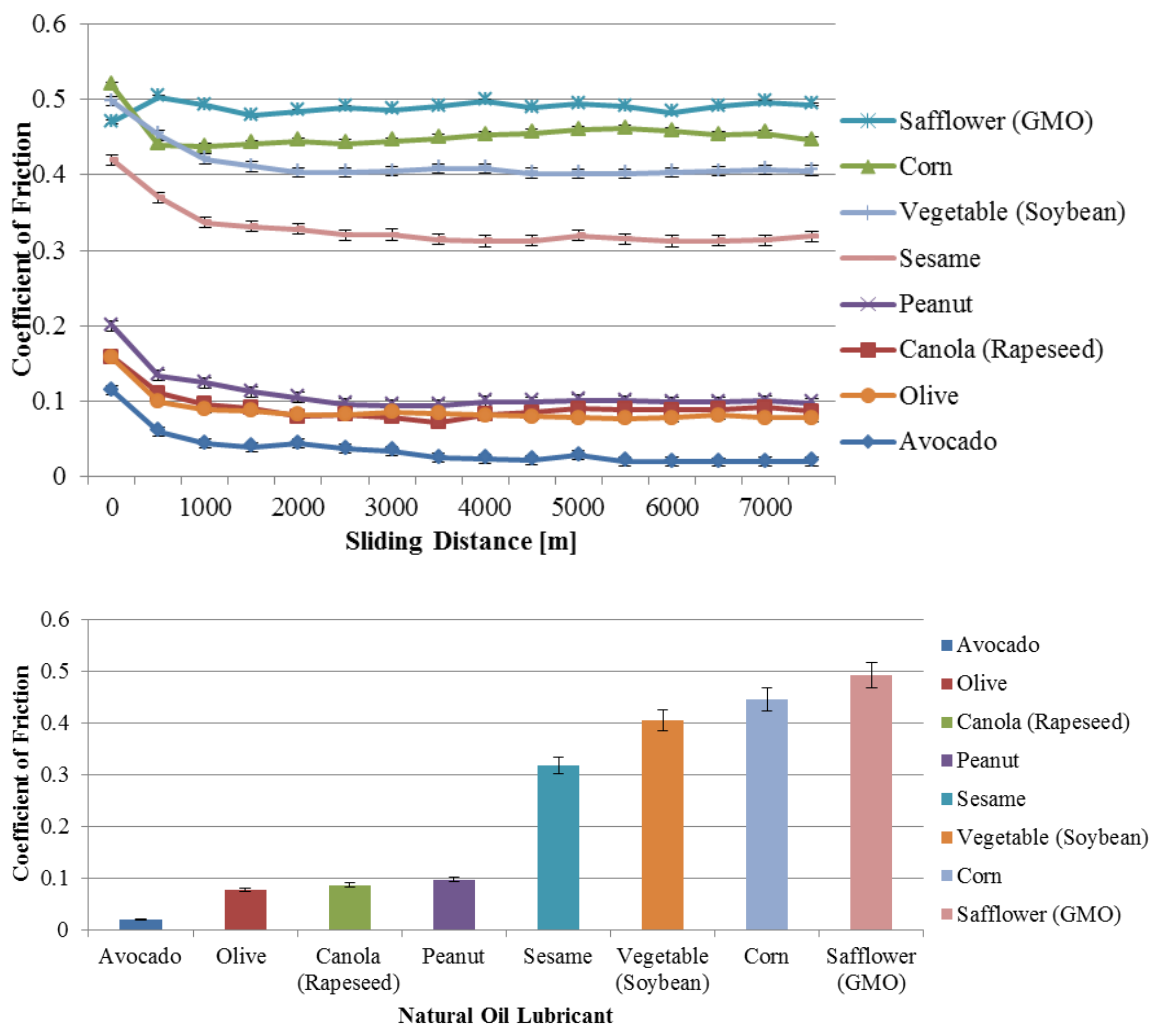
Figure 4.1: Variation of coefficient of friction during ambient conditions (a) for natural oils with sliding distance (b) for natural oils at completion of tests

Figure 4.2 depicts the variation of COF during high temperature testing of 350°C for (a) natural oils with sliding distance and (b) natural oils at the completion of the tests. In Fig. 4.2(a) the natural oils show significant fluctuations in the first 70 m of the test before the COF begins to decline with sliding distance. Figure 4.2(b) shows similar

natural oil performance trends as in Fig. 4.1(b), where avocado, peanut and olive oil have the lowest COF values between (0.06 and 0.09) and sesame, safflower, corn and vegetable oil all have the highest COF values (between 0.14 and 0.18). Canola oil under high temperature testing witnessed an increase in its COF and demonstrated a moderate friction value. The friction results suggest that the natural oil compositions influence the friction in sliding contact under ambient and high temperature conditions.
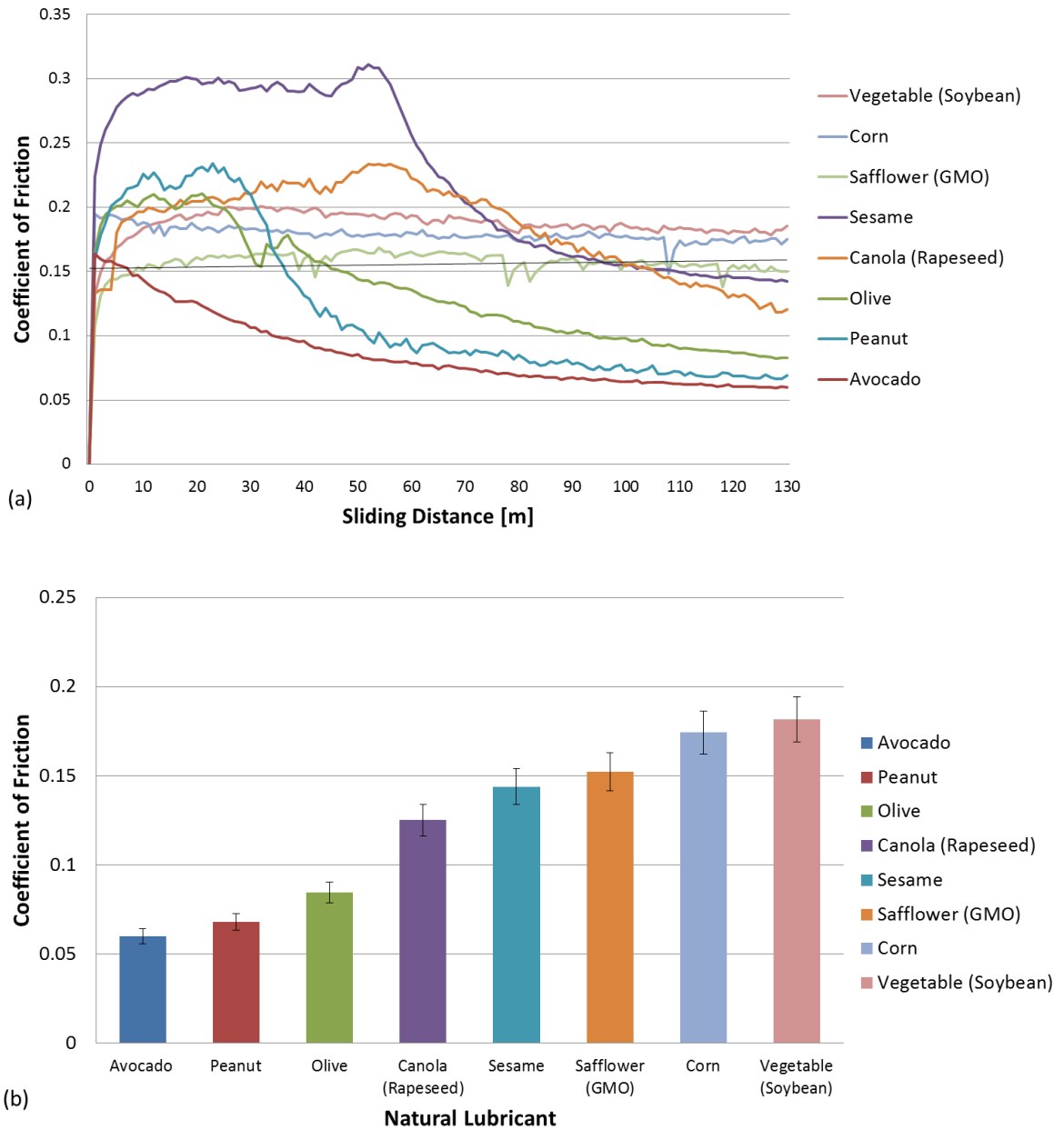
Figure 4.2: Variation of coefficient of friction during high temperature (350℃) testing (a) for natural oils with sliding distance (b) for natural oils at completion of tests

4.3.2 Wear Analysis

Figure 4.3(a) depicts the variation of the pin wear volume with sliding distance for various natural oils. It can be seen that the wear volume increases significantly within a sliding distance of the first 1000 m. Afterwards the rate of change in wear volume decreases with sliding distance. This transition is due to the abrasive nature of the surfaces which begin to conform the longer they are in sliding contact with each other. As a result of this contact, blunting of the surfaces leads to two-body wear and clogging of the surfaces by abraded debris causing the worn surfaces to eventually enter into a steady wear state [25]. Figure 4.3(b) shows the variation of the wear volume for various natural oils at the completion of the tests, where the distinctions in wear volume for the different oils tested is illustrated. As shown in the figure, avocado oil has the lowest wear volume and vegetable and corn oil have the highest wear volume. Peanut, olive, safflower, canola, and sesame oil all have a moderate wear volume.
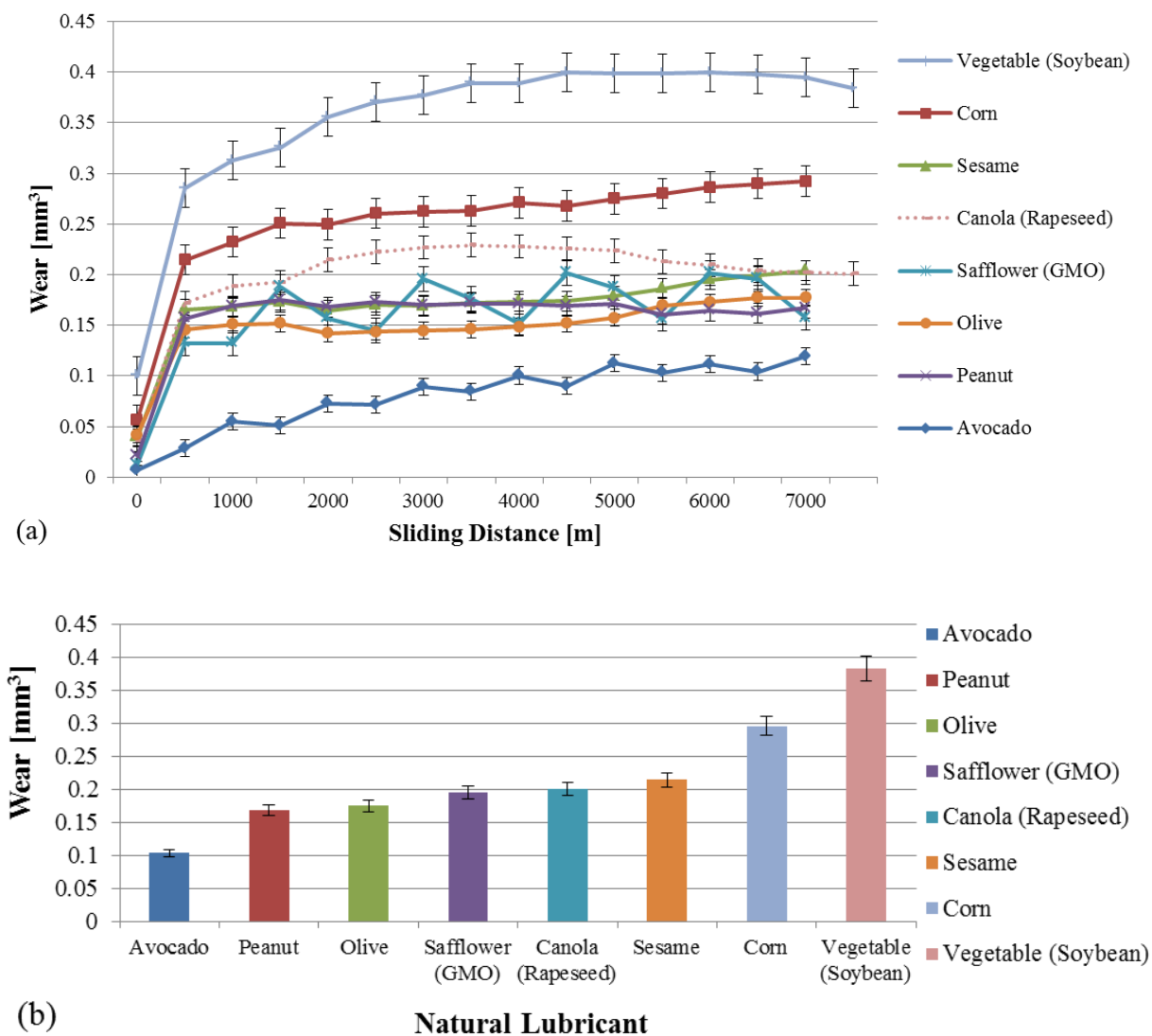
Figure 4.3: Variation of wear volume during ambient conditions (a) for natural oils with sliding distance (b) for natural oils at completion of tests

Figure 4.4 depicts the variation of wear volume during high temperature testing of 350°C for (a) natural oils with sliding distance and (b) natural oils at the completion of the tests. The influence of temperature is exacerbated in the wear results as seen through the significant fluctuations in the first 70 m of the tests as shown in Fig. 4.4(a), where degradation within the natural oils was observed for example corn and vegetable oil darkened during their tests, indicative of thermal degradation effects. Figure 4.4(b) shows the final wear volume of the tests. It can be seen in the figure that avocado, peanut, and olive oil have the lowest wear volumes. Canola and safflower oil maintain moderate wear volumes and sesame, corn and vegetable oil demonstrate high wear volumes at elevated temperatures. The trends shown in Fig. 4.4(b) are in agreement with Fig. 4.3(b), where avocado oil demonstrates the lowest wear rate and corn and vegetable oil demonstrate the highest wear rate at both ambient and high temperature testing conditions. These wear results suggest that the natural oil compositions influence the wear rate in sliding contact under ambient and high temperature conditions.
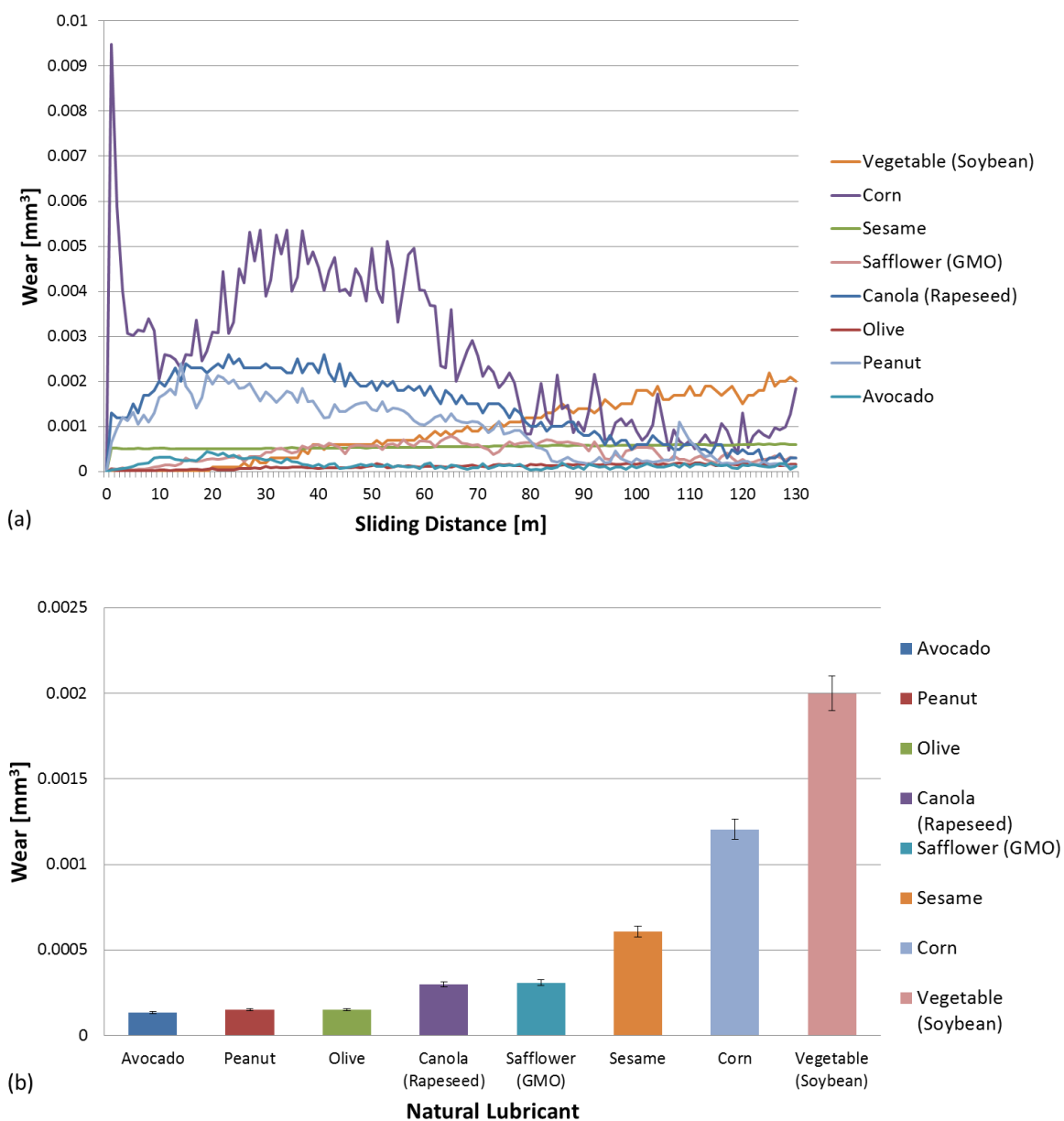
Figure 4.4: Variation of wear volume during high temperature (350°C) testing (a) for natural oils with sliding distance (b) for natural oils at completion of tests

4.3.3 Surface Analysis

Figures 4.5 and 4.6 show the scanning electron micrographs of the worn pin surfaces under ambient conditions at the completion of the tests under low and high magnification. Figure 4.5(a) and (b) show the pin surfaces that were lubricated with avocado oil and Figs. 4.5(c) and (d) show the pin surfaces that were lubricated with olive oil during the experiments. The avocado and olive oils have demonstrated low friction and low wear (as shown in Figs. 4.1 through 4.3) and can be seen in the micrographs to have a relatively smooth surface finish with fine grooves along the sliding direction. Figure 4.6(a) and (b) show the pin surfaces that were lubricated with vegetable oil and Figs. 4.6(c) and (d) show the pin surfaces that were lubricated with corn oil during the experiments. The vegetable and corn oils have demonstrated high friction and high wear (as shown in Figs. 4.1 and 4.3) and can be seen in the micrographs to have a relatively rough surface finish with deep grooves along the sliding direction. The SEM images shown in Figs. 4.5 and 4.6 also illustrate the effect of the wear volume. Avocado and olive oil have the lowest friction, resulting in smoother surface finishes. This led to a smaller contact area on the worn pin surface where at similar magnifications of 30x, Fig. 4.5(a) and (c), as the cross-sectional diameters of the avocado and olive oil pin worn surfaces are approximately 1.4 mm. As a result, the avocado and olive oil pin worn surfaces showed a low wear rate as shown in Fig. 4.3. In comparison, vegetable and corn oil have the higher friction values, resulting in rougher surface finishes. This led to a larger contact area where at their corresponding 30x SEM images shown in Fig. 4.6(a) and (c), the cross-sectional diameters of the vegetable and corn oil pin worn surfaces are

approximately 2.4 mm. Here, the surface contact area is increase by 66% when compared to the avocado or olive oil tests. As a result, the vegetable and corn oil pin worn surfaces showed a high wear rate as shown in Fig. 4.3. Further, the SEM images verify there is a strong correlation between friction and wear. The investigation reveals a strong correlation coefficient (R-value) of 0.876 between friction and wear. The friction, wear, and surface analysis demonstrate that the underlying chemical composition differences between the oils, more specifically their fatty acid composition, maintain a direct influence on the tribological properties. Hence, it is important to study the chemical analysis of the oils and show the relationship between chemical composition and tribological performance.
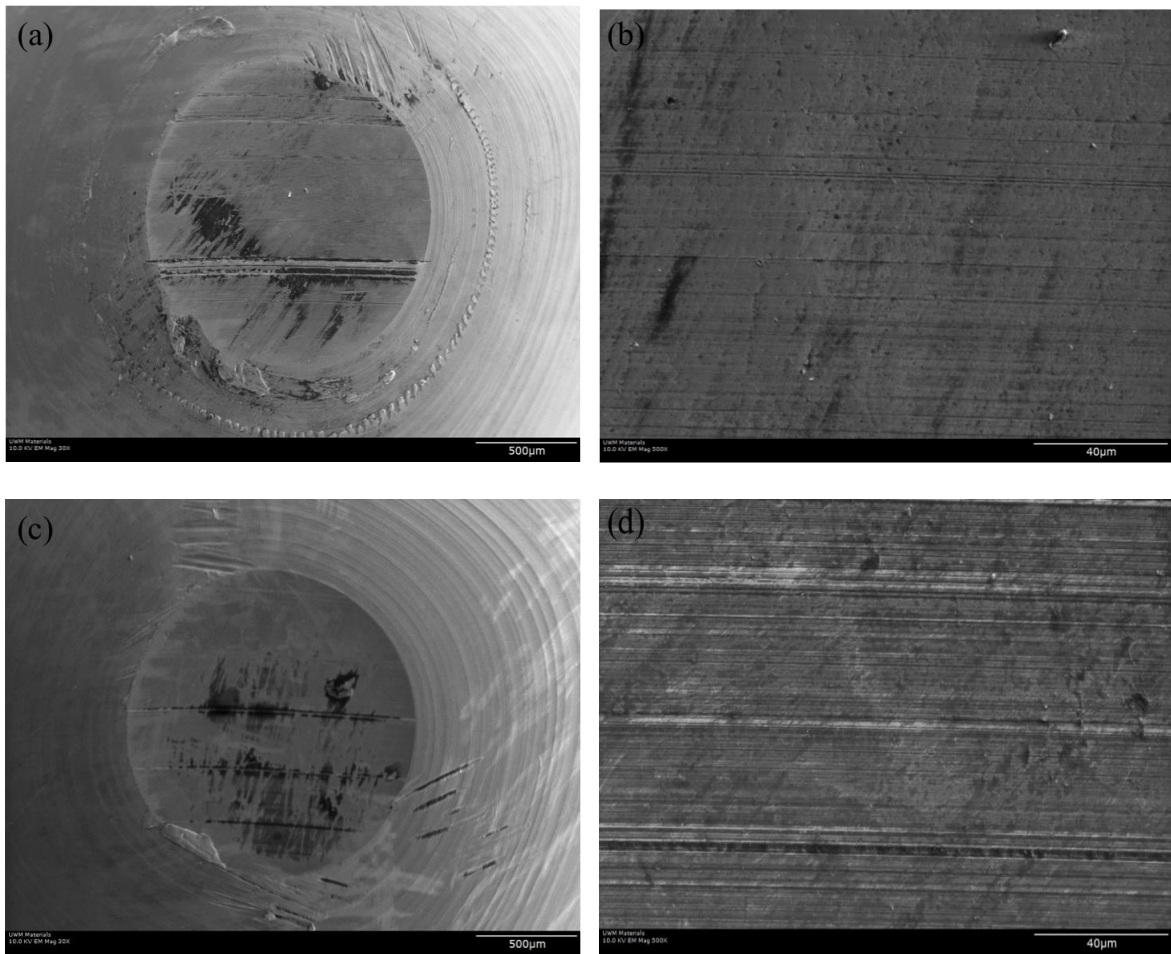
Figure 4.5: Scanning electron micrographs of a worn pin surface lubricated with (a) avocado oil at 30x magnification; (b) avocado oil at 500x magnification; (c) olive oil at 30x magnification; and (d) olive oil at 500x magnification
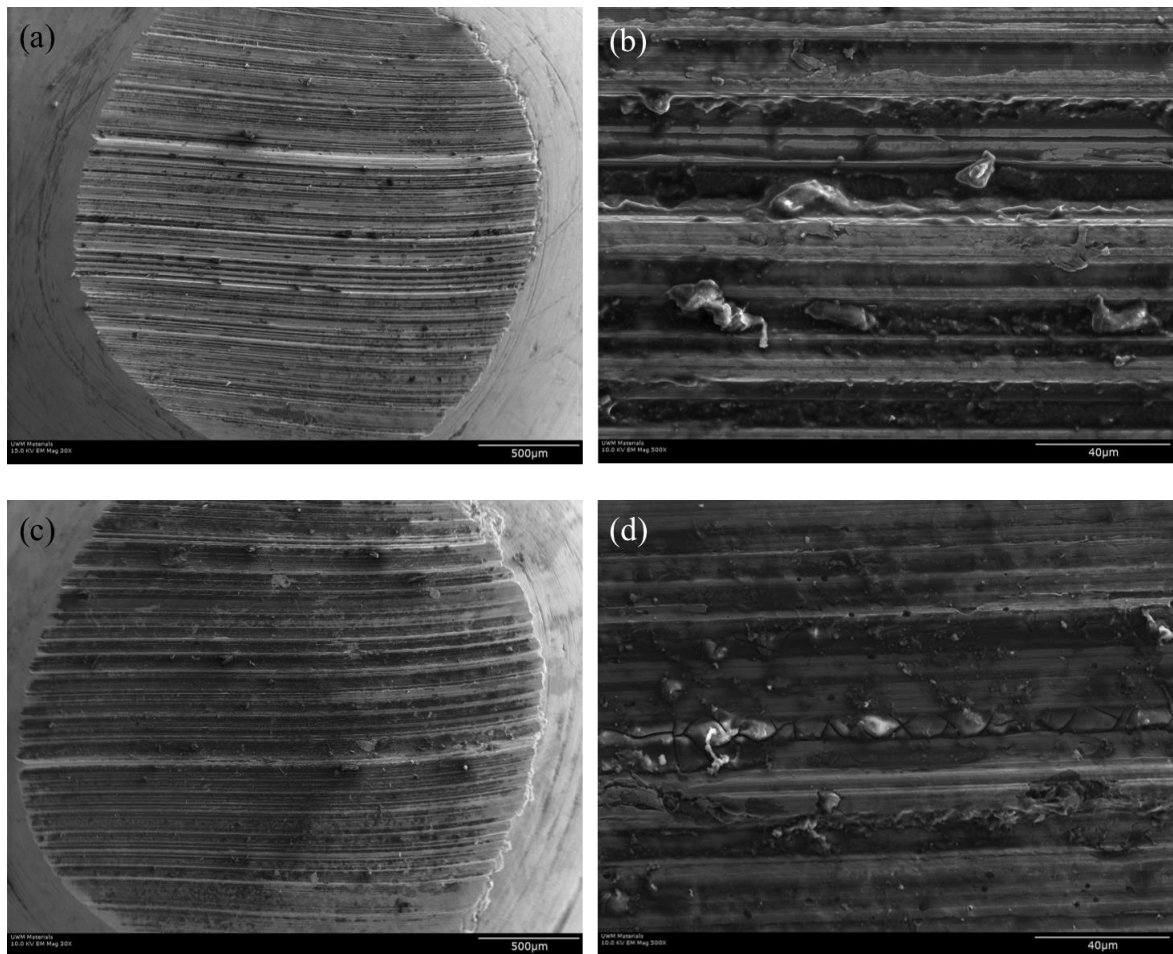
Figure 4.6: Scanning electron micrographs of a worn pin surface lubricated with (a) vegetable oil at 30x magnification; (b) vegetable oil at 500x magnification; (c) corn oil at 30x magnification; and (d) corn oil at 500x magnification

4.4 Chemical Composition Analysis

Figure 4.7 presents the predominant fatty acid percentages for each lubricant used in the present study. The fatty acid content was retrieved from the United States Department of Agriculture's National Agricultural Library, which publishes compositional data in their Nutrient Database. The natural oils investigated in this study are composed entirely of triacylglycerol with approximately 95% to 99% fatty acids which includes both saturated and unsaturated. There are minimal amounts of saturated fatty acids in each of the natural oils with palmitic acid (C16:0) and stearic acid (C18:0) occurring around 11% or less when combined. Unsaturated acids dominate the triacylglycerol composition with a trade-off between monounsaturated fatty acid, i.e. oleic acid (C18:1) and polyunsaturated fatty acid, i.e. linoleic acid (C18:2). It can be seen in Fig.4.7 that as the oleic acid increases, the linoleic acid decreases, revealing their inverse proportionality. In fact, the correlation coefficient (R-value) between oleic acid and linoleic acid is -0.987, signifying a strong inverse correlation.
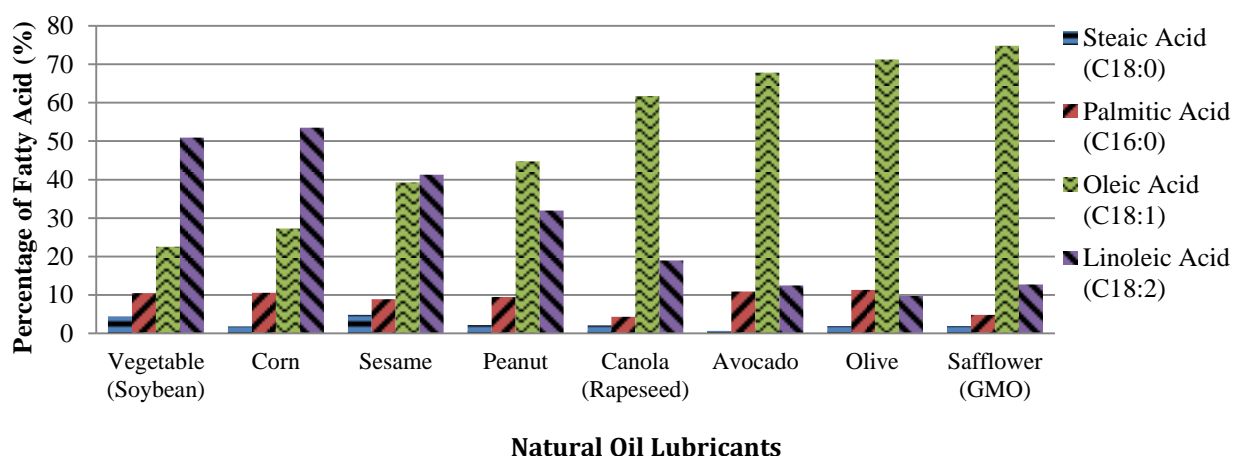
Figure 4.7: Fatty acid concentration for various natural oil

Within the natural oils examined, the high oleic acid safflower oil (HOSO) was derived from the breeding of genetically modified organisms (GMOs) that have higher than normal oleic acid concentrations. The avocado and olive oil also have large percentages of oleic acid, above 65%. Investigations have revealed that the most important fatty acids contained in natural oils are unsaturated fatty acids such as oleic acid and linoleic acid and the most important saturated fatty acids are palmitic acid and stearic acid [152]. However, there is a balance that must be maintained in the natural oils, because stearic acid at room temperature is a solid whereas oleic acid at room temperature is a liquid. For this reason, the saturation level describing the proportions of saturated and unsaturated oils must be optimal to ensure that the natural oil is liquid at room temperature and thus can serve as a functional fluid. To quantify the saturation level, the unsaturation number (UN) is used. The UN of the natural oils refers to the average number of double bonds within a triacylglycerol molecule. This provides a metric for quantifying the fatty acid concentrations within the natural oils. The greater the UN, the greater the degree of unsaturation in the natural oil. The UN is calculated from the fatty acid distribution using Eq. 4.1(a) and is summarized in Eq. 4.1(b) [171].

$UN =$

$\frac{1}{100}[(1 * \sum \text{monounsaturated Fatty Acids}) + (2 * \sum \text{diunsaturated Fatty Acids}) +$

$(3 * \sum \text{triunsaturated Fatty Acids})]$

Eq. 4.1(a)

$UN = \frac{1}{100}[\{1 * (C18:1 + C20:1 + C22:1)\} + \{2 * (C18:2 + C22:2)\} + \{3 * (C18:3)\}]$

Eq. 4.1(b)

In Eq. 4.1(b) the *Cx:y* is the percentage of fatty acids within the natural oil with *x* representing the chain length and *y* representing the number of double bonds. The results are shown in Table 4.2 along with the final COF and wear volume results. The analysis between the fatty acid composition and friction values as well as the fatty acid composition and wear volume for the natural oils are presented in the following sections.

Table 4.2: Unsaturation number, thermal decomposition, coefficient of friction, and wear volume values for various natural oils in both ambient and high temperature conditions

Natural Oil Type	Unsaturation Number (UN)	Dynamic $T_{d(onset)}$ (°C)	Isothermal Percent Decomposition ($T_{d(onset)}$-50°C)	COF (23°C)	Wear Volume (mm³) (23°C)	COF (100°C)	Wear Volume (mm³) (100°C) x10⁻⁴
Avocado	0.985	376	82	0.0201	0.1037	0.0601	1.328
Canola (Rapeseed)	1.287	377	79	0.0868	0.2009	0.1250	3.000
Corn	1.381	372	76	0.4458	0.2965	0.1742	1.205
Olive	0.948	377	86	0.0778	0.1753	0.0846	1.509
Peanut	1.102	378	92	0.0975	0.1682	0.0679	1.512
Safflower (High Oleic)	1.010	376	91	0.4936	0.1948	0.1523	6.076
Sesame	1.232	370	72	0.3184	0.2151	0.1438	3.092
Vegetable (Soybean)	1.451	371	76	0.4059	0.3839	0.1814	2.000
R-value	N/A	-0.676	-0.706	0.830	0.882	0.925	0.843

4.4.1 Fatty Acid-COF Analysis

It can be seen from the friction results (see Figs. 4.1 and 4.2) and fatty acid concentrations (see Fig. 4.7) that the natural oils, namely avocado, olive, canola, and peanut oil have lower COF values and higher amounts of oleic acid. The corn, vegetable and sesame oils correspond to natural oils having lower amounts of oleic acid and higher friction coefficients. When comparing ambient temperature to high temperature conditions, the avocado, olive, and peanut oils standout for their consistently low friction, particularly the avocado oil as it maintained the lowest COF oil. Examining the correlation coefficient (R-value) between the UN and the COF at both ambient and high temperature conditions, as shown in Table 4.3, reveals strong correlations having R-

values of 0.830 and 0.92, respectively. The unsaturated fatty acids (oleic acid and linoleic acid) and COF at ambient conditions have strong correlation coefficients of -0.918 and 0.944 as shown in Table 4.3. Similarly in Table 4.3, the correlation coefficients between the unsaturated fatty acids and the COF at high temperature conditions have R-values of -0.801 and 0.825.

Table 4.3: Correlation coefficient R-value between fatty acid percentage and coefficient of friction for the natural oils in both ambient and high temperature conditions

Parameter	Lipid Number	R-value (23°C)	R-value (100°C)
Unsaturation Number	NA	0.830	0.925
Palmitic Acid	C16:0	0.202	-0.099
Stearic Acid	C18:0	0.621	0.632
Oleic Acid	C18:1	-0.918	-0.801
Linoleic Acid	C18:2	0.944	0.825

In comparison, the correlation coefficients between the saturated fatty acids (palmitic acid and stearic acid) acid and the COF indicate low and moderate R-values of 0.202 and 0.621 at ambient conditions and -0.099 and 0.632 at high temperature conditions. The high correlation values of 0.830 and 0.925 between the UN and the COF at ambient and high temperature reveals that the fatty acid composition within the natural oils has a significant effect on the COF. The general trend of low COF with high percentages of oleic acid and low percentages of linoleic acid and the inversely proportional trend of high friction with high percentages of linoleic acid and low percentages of oleic acid are a result of the structure of the fatty acids. The oleic acid has one double bond in contrary to linoleic acid having two double bonds. The presence of a

double bond decreases the density of the fatty acid monolayer [24, 93, 117]. An effective fatty acid monolayer can be established by saturated and monounsaturated fatty acids, which act to limit the metal-to-metal contact thereby minimizing the friction force. [24, 55, 288]. Safflower oil seems to be an outlier to the witnessed trend, as it has the highest oleic acid composition and the highest COF. This could be due to the fact that safflower oil being the only natural oil derived from the breeding of GMOs and thus the structure of the fatty acids does not follow the trends of the other natural oils.

4.4.2 Fatty Acid-Wear Analysis

Investigating the correlation coefficient between the UN and the wear volume at ambient and high temperature conditions as shown in Table 4.1, reveals strong correlation coefficients having R-values of 0.882 and 0.843, respectively. This indicates that generally as the wear volume increases the unsaturation number also increases. This relationship corresponds well with the wear results because as seen in Figs. 4.3 and 4.4, the natural oils with lower wear volumes such as avocado, olive, and peanut oil have higher amounts of oleic acid as shown in Fig. 4.7 and thus lower UNs. Conversely, natural oils with higher wear volumes such as corn, vegetable and sesame oils have a lower amount of oleic acid and higher UNs. There wear results indicate that the fatty acid percentages directly influence the pin wear volume at ambient and high temperatures. Table 4.4 examines the relationship between the fatty acid percentage and the pin wear volume for the various natural oils tested. The saturated fatty acids, palmitic acid and

stearic acid have low and moderate correlation coefficients of 0.074 and 0.625 at ambient temperatures and 0.207 and 0.578 at high temperatures, respectively.

Table 4.4: Correlation coefficient R-value between fatty acid percentage and pin wear volume for the natural oils for the natural oils in both ambient and high temperature conditions

Parameter	Lipid Number	R-value (23°C)	R-value (100°C)
Unsaturation Number	NA	0.882	0.843
Palmitic Acid	C16:0	0.074	0.207
Stearic Acid	C18:0	0.625	0.578
Oleic Acid	C18:1	-0.846	-0.849
Linoleic Acid	C18:2	0.822	0.819

It can be seen from Figs. 4.3 and 4.4 for wear results and Fig. 4.7 for fatty acid composition that as the wear volume increases, the monounsaturated fatty acid (e.g. oleic acid) percentage decreases and has a correlation coefficient of -0.846 at ambient conditions and -0.849 at high temperature conditions, revealing their strong inverse relationship. This trend is reversed for the polyunsaturated fatty acid percentage (e.g. linoleic acid), which increases with an increase in wear volume and has a strong correlation coefficient of 0.822 at ambient conditions and 0.819 at high temperature conditions. The high R-values for the unsaturated fatty acids is due to their higher percentages within the natural oils and the presence of the double bonds in the oleic

(C18:1) and linoleic (C18:2) acids which have one and two double bonds, respectively. The greater the quantity of double bonds prevents the carbon chains from forming densely packed bundles, therefore weakening the protective layer [117]. Oleic acid (C18:1) having one double bond is more densely packed and forms a superior protective monolayer that results in less metal-to-metal contact between the surface asperities, whereas linoleic acid (C18:2), which has two double bonds results in an increase in metal-to-metal contact. Natural oils that have a higher wear volume tend to have a low oleic acid content, a high linoleic acid content, and a higher UN as demonstrated in Tables 4.1. This is indicative of a weak protective monolayer on account of the increased number of double bonds in the fatty acids. These results are in agreement with previous studies on natural oils where high oleic acid content oils were revealed to have low COF and wear rate due to their effective monolayer development [24, 55, 90, 102, 219]. The tribological results and the relationships with the fatty acids particularly oils with high oleic acid concentrations have shown improved lubricity and oxidative stability that in some cases surpasses Group I petroleum-based oils [106, 289]. The various fatty acid percentages within the natural oils not only influence the friction and wear properties, but it can also have a tremendous impact on the thermal-oxidative response of the natural oils. As with many oils, thermal and oxidative stability are important properties that must be considered when characterizing the performance of a lubricant and thus a TGA is beneficial to studying the properties.

4.4.3 Thermogravimetric Analysis

The TGA results depicted in Fig. 4.8 reveal the thermal degradation temperature for various natural oils in a nitrogen environment. In the figure, $T_{d(max)}$ indicates the temperature at which the maximum weight percentage of the lubricant decomposes and $T_{d(onset)}$ indicates the temperature when thermal degradation of the lubricant first begins to occur. Due to the nitrogen atmosphere three phenomena were witnessed, (1) a lack of thermal variability, (2) higher thermal degradation temperatures, and (3) a dependence on individual fatty acids. With respect to the variation of $T_{d(max)}$, there is less than a 1% difference in temperature and approximately a 2% difference in the variation of $T_{d(onset)}$ among various natural oils investigated and found a strong correlation with a R-value of 0.894 exists between $T_{d(max)}$ and $T_{d(onset)}$.
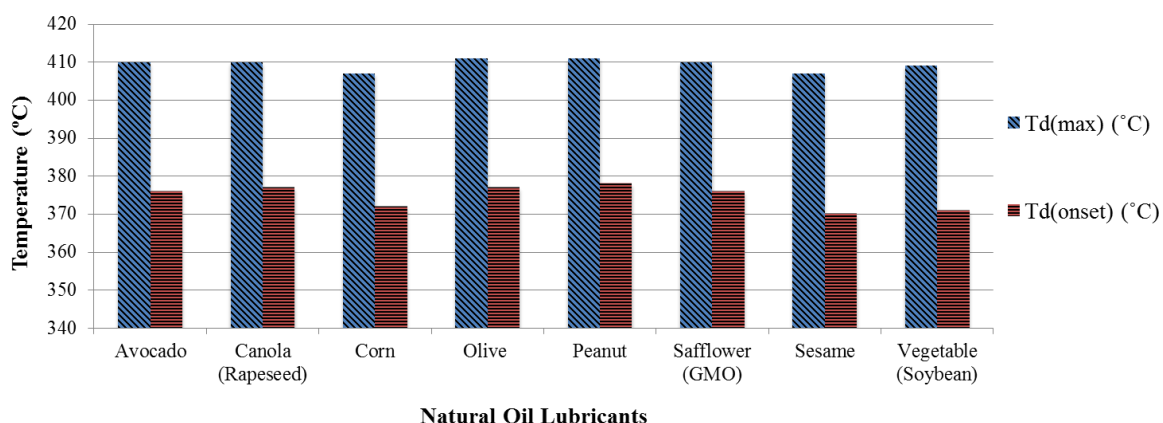
Figure 4.8: Thermal degradation temperature for various natural oils in a nitrogen environment

Despite the low variability in the TGA results, their remains to be a trend with the fatty acid compositions and the decomposition temperatures. Figure 4.9 is a graph of the fatty acid profiles, where the fatty acid percentages are plotted against the onset of decomposition temperatures, $T_{d(onset)}$. Table 4.5 shows the corresponding correlation coefficients (R-value) for the fatty acid percentages and the onset of decomposition temperatures.

Table 4.5: Correlation coefficient R-value between
decomposition temperature and fatty acid

Fatty Acid Type	Common Name	Molecular Formula	Lipid Number	R-value	Degree of Unsaturation	Boiling Point (ºC)
Saturated	Stearic Acid	$C_{18}H_{36}O_2$	C18:0	-0.739	1	383
Monounsaturated	Oleic Acid	$C_{18}H_{34}O_2$	C18:1	0.737	2	360
Polyunsaturated	Linoleic Acid	$C_{18}H_{32}O_2$	C18:2	-0.781	3	230
Saturated	Palmitic Acid	$C_{16}H_{32}O_2$	C16:0	-0.269	1	352

From Fig. 4.9, it can be seen that the higher the oleic acid percentage (or the lower the linoleic acid percentage), the higher the thermal decomposition temperature. The trends with the stearic and palmitic acid are less discernable in Fig. 4.9, due to their low percentages. From Table 4.5, the fatty acids having 18 carbon atoms: stearic acid, oleic acid, and linoleic acid have a strong correlation between them and the decomposition temperatures with R-values of -0.739, 0.737, and -0.781, respectively. Palmitic acid has a weak correlation with a R-value of -0.269. The trends found for the 18 carbon fatty acids agree with similar results found in the literature for thermal decomposition temperatures in "open air" oxygen environments [55, 109, 165, 218, 219, 290]. In open air

environments, oxidation of natural oils becomes a primary concern due to vulnerabilities in the fatty acid molecular compounds. As the TGA results have demonstrated that natural oils are susceptible to thermal degradation at high temperatures where the natural oil breaks down. More still, these vulnerabilities became noticeable in the high temperature testing at 350°C (below the $T_{d(onset)}$) as seen in Figs. 4.2 and 4.4, where there was significant variability in the friction and wear results with sliding distance when compared to the ambient condition testing. During the high temperature testing, it was observed that the corn and vegetable oil burned slightly and became a darker brown, indicating a form of thermal-oxidative degradation. It can therefore be inferred that these vulnerabilities may exist within the fatty acid compounds of the natural oils and are investigated as follows.
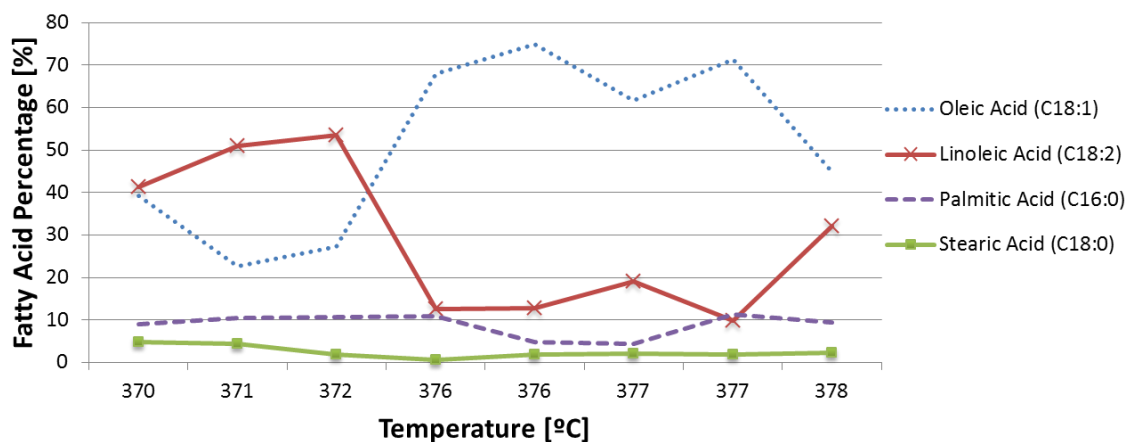
Figure 4.9: Fatty acid profiles for decomposition temperatures

4.4.4 Oxidation Analysis

The natural oils used in this investigation are predominately composed of fatty acids with boiling points of approximately 230ºC for linoleic acid, 352ºC for palmitic acid, 360ºC for oleic acid, and 383ºC for stearic acid [291] and the data is shown in Table 4.5. However, the TGA results shown in Fig. 4.8 reveal the natural oils remaining intact up to about 370ºC with maximum degradation temperatures above 400ºC, which are in accordance with other studies [165, 218, 290]. The reason for such high degradation temperatures (beyond what was observed in the current high temperature pin-on-disk testing) is a result of the nitrogen atmosphere in the TGA and lack of oxygen. The natural oils investigated are composed of fatty acids that are derived from triacylglyceride molecules, which contain glycerol. The presence of glycerol in the natural oils gives rise to a tertiary β-hydrogen (secondary hydrogen) attached to the β-carbon (secondary carbon) of the functional hydroxyl group, as illustrated in Fig. 2.7 at location (a). The β-hydrogen present in the unsaturated fatty acids is known to have oxidative instability and therefore is a cause for the fast oxidation of natural oils as known as autoxidation. The β-hydrogen is also the location where most bio-based lubricants are chemically modified [44, 102, 152, 211-213]. Additionally, the bis-allylic hydrogen, which attaches to the double bonded carbon atoms (in region b in Fig. 2.7) in polyunsaturated fatty acids are particularly susceptible to free radical attacks, peroxide formation, and production of polar oxidation products similar to that of hydrocarbon mineral oils, except at an expedited rate in natural oils [109, 214-216]. Oxidative instability also arises from the presence of the double bonds present in the triacylglycerol molecule as depicted in Fig.

2.7 at location (b) [44, 152, 211, 212]. These deficiencies can cause the development of insoluble deposits and increases in oil acidity, viscosity, and poor corrosion protection properties in oil. Moreover, the existence of ester compounds in natural oils causes hydrolytic degradation [217]. These problems become negligible in the nitrogen environment because the critical β-hydrogen and the bis-allylic hydrogen are no longer susceptible to oxidative degradation by elimination (e.g. esterification or hydrolysis) and can therefore withstand the higher temperatures affording increased thermal stability of the natural oils. The thermal degradation temperatures of the natural oils in the nitrogen atmosphere are significantly higher than that in an oxygen environment, where the process of oil oxidation lowers the thermal stability and influences the performance of tribological properties within the natural oils [218]. For example, the current $T_{d(onset)}$ results shown in Fig. 4.8 are anywhere between 20º and 100ºC higher when compared to the oxidative stability tests performed on fatty acid-based oils by Salih et al. [55], vegetable-base oils by Erhan et al. [109], synthetic ester basestocks by Salimon et al. [219] , or by the current tribological investigations shown in Figs. 2 and 4 in an oxygen environment. To further quantify the susceptibility of the natural oils to thermal and oxidative vulnerabilities, an unsaturation analysis of the natural oils is performed. This analysis will further compare the influence of the various fatty acid compositions in the natural oils to the thermal and oxidative instabilities of the natural oils.

4.4.5 Unsaturation Analysis

The degree of unsaturation for the fatty acids was calculated using Eq. 4.2, based on an organic compound with the following formula: $C_aH_bN_cO_dX_e$, where a = number of carbon atoms, b = number of hydrogen atoms, c = number of nitrogen atoms, d = number of oxygen atoms, X = halogen atom (i.e. F, Cl, Br, or I), and e = number of halogen atoms [292, 293].

$$\text{Degree of unsaturation} = \frac{1}{2}(2 + 2a - b + c - e) \qquad \text{Eq. 4.2}$$

The degree of unsaturation is used to compare the number of hydrogen atoms to bond types in a fatty acid, where double bonds count as one degree of unsaturation and triple bonds count as two degrees of unsaturation. From Table 4.5, the fatty acids with 18 carbon atoms (stearic, oleic, and linoleic acid) all have relatively similar and strongly correlated relationships between decomposition temperature and fatty acid content, despite having different degrees of unsaturation. The oxidative instability arises from the presence of the β-hydrogen, bis-allylic hydrogen, and double bonds present in the fatty acids. Typically, increasing oxidative instability occurs with increasing unsaturation, which is particularly present in the polyunsaturated fatty acids that have high degrees of unsaturation. These results reveal that in oxygen-free environments, oxidation becomes negligible, and thermal stability of natural oils becomes independent of the degree of unsaturation as shown in Fig. 4.8 where the natural oils all have similar decomposition temperatures. This phenomenon occurs as a result of the fatty acids (excluding palmitic acid) having similar structures with 18 carbon atoms which result in uniform thermal decomposition properties as substantiated by the high R-values in Table 4.5. As a direct

consequence, the natural oils show limited variability in their thermal degradation properties in a nitrogen environment (with a 2% or less variation in the thermal degradation temperatures as shown in Fig. 4.8), despite having a wide variety of fatty acids compositions (with variations of 62% for palmitic acid, 86% for stearic acid, 70% for oleic acid, and 82% for linoleic acid as calculated from Fig. 4.7). For these reasons, the different fatty acid compositions in the natural oils have a negligible influence on the thermal decomposition properties, because three (i.e. stearic acid, oleic acid, and linoleic acid) of the four predominant fatty acids behave the same when oxygen is not present. This suggests that the influence of the fatty acid compositions in the natural oils were not effective due to the lack of oxygen in the TGA. Thus, it can be inferred that thermal stability of the natural oils is independent of the fatty acid composition in a nitrogen environment. The current TGA results are in accordance with previous studies in the literature [109, 161, 294, 295] where the research has demonstrated that the thermal stability of the natural oils is independent of the fatty acid composition and is strongly correlated to individual fatty acids particularly oleic acid due to its high concentration within each individual natural oil. The oxidative stability of the natural oils in an oxygen environment is dependent on the fatty acid composition (i.e. unsaturation number), because oxidation can occur at lower temperatures, which can lower the thermal stability. This causes the thermal stability and oxidative stability to become coupled in oxygenated environments where thermal stability is dependent on oxidative stability. This phenomenon was present in the high temperature testing, where the friction and wear results showed significant fluctuations throughout each test as some of the natural oils

deteriorated, degraded, and even burned. Other natural oils with low UNs such as avocado oil maintained superior tribological performance at both low and high temperatures due to their high thermal-oxidative stability.

4.3.5 Natural Oil Analysis

Analyzing the UN for the natural oils (Table 4.2) reveals that olive, avocado, safflower, and peanut oil have lower unsaturation numbers because they are primarily composed of oleic acid, which has one double bond. Vegetable, corn, and sesame oil have higher unsaturation numbers because they are primarily composed of linoleic acid, having two double bonds. Canola oil is a slight outliner because although it is primarily composed of oleic acid (C18:1) it has a higher UN. This is due to the fact that the canola oil being composed of a relatively high amount, 9.14% of linolenic acid (C18:3), which has three double bonds. The only other oil that has significant amounts of linolenic acid is vegetable oil with 6.79% and it has a high UN because it is composed primarily from linoleic acid (C18:2). Table 4.2 shows moderate correlations having R-values of -0.676 and -0.706 for the relationship between the unsaturation number and the onset decomposition temperature, $T_{d(onset)}$ (dynamic) and for the weight percent decomposition at $T_{d(onset)}$-50˚C (isothermal) for the various natural oils. This is expected because in the nitrogen environment the thermal stability of the natural oils is independent of the fatty acid composition and dependent on the particular 18 carbon atom fatty acids that behave the same in oxygen-free environments. Since all of the oils tested are primarily composed of stearic, oleic, and linoleic acid that have strong correlation coefficients with

decomposition temperatures, the amount of each of these acids within the natural oils becomes irrelevant. In effect, this causes all the natural oils to have similar thermal properties with minimal variability as observed in the TGA.

In an oxygen environment, natural oils having high unsaturation numbers are more susceptible to rancidification through hydrolysis or oxidation as well as having higher pour points that limit their use in low temperature environments. To improve the oxidative stability of the natural oils, the ideal situation would be to remove all unsaturation by catalytic hydrogenation or by other chemical modifications. This, however, would "harden" the lubricant leaving it with saturated fatty acids that would turn the lubricant from a liquid oil to a solid fat rendering it useless as a functional fluid. For this reason, it is necessary to leave unsaturated fatty acids in the oil. Monounsaturated fatty acids particularly, oleic acid are the best compromise between thermal and oxidative stability because oleic acid provides superior tribological performance with optimal lubricity, minimal wear, ideal viscosity, less thermal decomposition, and low temperature properties [16, 24, 55, 109].

4.5 Conclusions

Natural oils are non-toxic, renewable, and feasible alternatives to petroleum-based lubricants that can satisfy the combination of environmental, health, economic, and performance challenges of modern lubricants. The current investigation examined the mechanisms governing the improved tribological performance and thermal response of the natural oils. The prevailing trend with the natural oils is that high oleic acid concentrations improve friction and wear performance by establishing densely packed

monolayers on the lubricating surface. Moreover, in an oxygen-free environment, the thermal stability of the natural oils is independent of the fatty acid composition and the degree of unsaturation. It was shown that natural oils with low unsaturation numbers as a result of high monounsaturated fatty acid content particularly oleic acid provide the optimal balance between thermal and oxidative stability. Through a chemical composition analysis, tribological analysis, and thermogravimetric analysis, the influence of fatty acid content in natural oils revealed the following conclusions:

- Avocado oil was shown to have the best tribological properties with the lowest friction and wear at ambient and high temperature conditions.

- Natural oils with high percentages of oleic acid maintain low COF values and low wear rates because the oleic acid establishes a denser fatty acid monolayer that minimizes the asperity contact and protects the metallic surfaces.

- Natural oils with high percentages of monounsaturated fatty acids such as oleic acid are optimal to ensure superior thermal-oxidative stability in ambient and high temperature environments.

- In an oxygen-free environment, the thermal stability of natural oils is dependent on individual fatty acid (stearic, oleic, and linoleic acids) percentages and independent of the degree of unsaturation of the natural oil.

- In an oxygen environment, the oxidative stability of natural oils is dependent on the fatty acid composition or unsaturation number of the natural oil and it becomes coupled with thermal stability.

Chapter 5 The Size Effect of Boron Nitride Particles on the Tribological Performance of Biolubricants for Energy Conservation and Sustainability

5.1 Introduction

The United States consumes more petroleum-based oil than any other country in the world, with 54% of the oil consumed as automotive lubricants (engine oils and transmission fluids) and 44% used as industrial lubricants (hydraulic fluids and gear oils) [90, 296-298]. It has been reported that 50% of all lubricants worldwide end up in the environment through usage, spillage, volatility, or improper disposal [286]. These oils typically are not environmentally friendly or biodegradable and are toxic to the environment by contaminating soil, air, and drinking water [82, 286]; they also have long-term effects that are deleterious to plants, fish, humans, and other ecological systems. As a result, the U.S. Environmental Protection Agency (EPA) and other government agencies have imposed more stringent regulations regarding the use, containment, and disposal of petroleum-based oils [153]. Moreover, concerns for the depletion of crude oil reserves and increases in the price of oil have had an impact on the use of petroleum-based oils. These factors have caused the lubrication industry to develop and implement environmentally friendly lubricants. These 'green' lubricants are typically derived from organic materials that are non-toxic, renewable, and provide feasible and economic alternatives to traditional lubricants [81, 82]. As described in the literature, a lubricant formulated from bio-based feedstock offers several advantages over

petroleum-based oils including a higher lubricity, lower friction losses, improved efficiency, more power output, and better fuel economy [78]. For this reason, there has been a revival in the development of environmentally friendly or environmentally benign lubricants that satisfy the combination of environmental, health, economic, and performance challenges of modern lubricants. Fundamental research is an important step for scaling-up the development and industrial use of biolubricants for energy conservation and sustainability.

Green liquid lubricants derived from pure natural oils have been utilized since ancient times for their ability to lower friction and reduce wear. Many pure natural oils are derived from vegetables, fruits, or nuts. These oils, composed of triacylglycerides, are made up of esters that are derived from glycerol and three fatty acids: saturated, monounsaturated, and polyunsaturated. Natural oils have a varied chemical composition due to biological effects stemming from the type of plant, climate, weather, and abundance of nutrients. The attraction of natural oils in recent decades is due to the structure of the triacylglycerol, which contains long chains of polar fatty acids that are desirable in boundary lubrication because they adhere to metallic surfaces, remain closely packed, and create a thin monolayer that is effective at reducing friction and wear [24, 107, 117].

In the twentieth century, scientists and engineers began investigating vegetable oils for their fatty acid composition in an attempt to further understand how fatty acids influence friction and wear. [24, 90, 106, 107, 110, 111, 117]. Vegetable oils meet many of the requirements as alternatives to traditional petroleum-based lubricants because they

are renewable, biodegradable, non-toxic, and have minimal environmental pollution and production costs [106]. Vegetable oils also exhibit higher lubricity, lower volatility, higher shear stability, higher viscosity index, higher load carrying index, and superior detergency and dispersancy when compared with mineral and synthetic oils [24, 43, 81, 90]. Despite the environmental advantages to using pure natural oils, they do suffer from poor thermal and oxidative stability, biological (bacterial) deterioration, hydrolytic instability, poor fluid flow behavior, solidification at low temperatures, and on occasion high wear rates [109, 153-158]. They are also susceptible to oxidative degradation due to the presence of free fatty acids and the presence of double bonds in the carbon chain.

Research focusing on the physicochemical structure of triacylglycerides and the influence of fatty acids has shown promising tribological performance in biolubricants for industrial applications. Experiments indicate that the existence of polar groups such as carboxylate in fatty acids promote strong molecular adherence of the fatty acids to metallic surfaces [24, 108, 117]. The long carbon chains of the fatty acids orient themselves perpendicular to a surface forming tightly packed bundles where slimmer more saturated molecules allow for closer packing, stronger intermolecular interactions, and provide a stronger protective film [24, 106, 117]. Additional research has focused on thwarting the deficiencies of vegetable oils while seeking to understand the relationship between chemical composition, molecular structure, and properties through chemical modifications such as epoxidation, metathesis, acylation, estolide formation, transesterification, and selective hydrogenation of plant oils with polyols, and as investigated with lamellar powder additives [43, 45-49, 51-56, 287, 299].

5.2 Green Solid Lubricants: Boron Nitride

Green solid lubricants are a new class of "powder lubricants" consisting of lamellar crystal structures with low interlayer friction. Examples of green solid lubricants include boric acid (H_3BO_3) and hexagonal boron nitride (hBN), which have similar properties to graphite (C), molybdenum disulfide (MoS_2), and tungsten disulfide (WS_2) [9, 92, 93, 197]. Lamellar powder lubricants are known for their crystal structure, in which atoms lying on the same layer are closely packed and strongly bonded together by covalent bonds, and the layers are relatively far apart due to the weak van der Waals force, as illustrated for boron nitride in Fig. 5.1 [113]. When entrained between sliding surfaces, the lamellar powders can adhere to the surface, forming a protective boundary layer that minimizes contact between opposing surface asperities to prevent wear. The protective boundary acts as a lubricant in sliding contacts by accommodating relative surface velocities. The lamellar powder lubricants accomplish this by aligning their layers parallel to the direction of motion and sliding over one another to minimize friction. Moreover, these powder lubricants can lubricate in extreme conditions such as high or low temperatures and pressures [11, 90-92, 113, 194, 195].
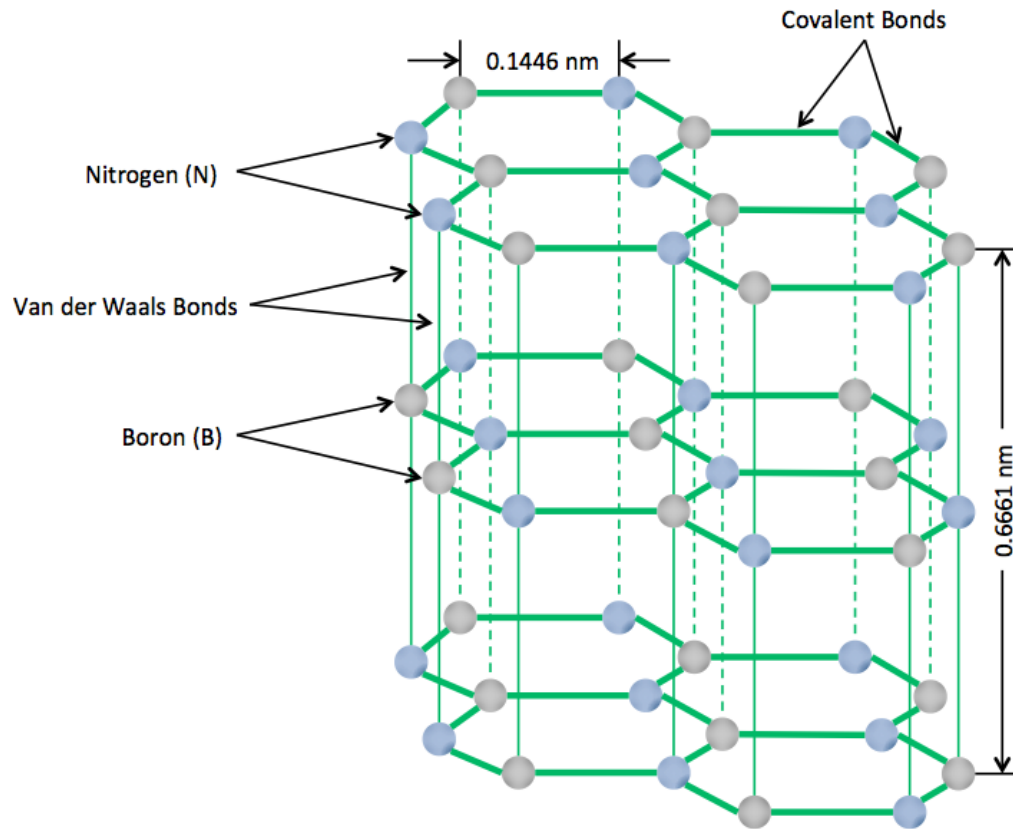
Figure 5.1: Hexagonal boron nitride structure

Although there are many green powder lubricants, hexagonal boron nitride powder will specifically be considered in this investigation. Boron nitride is a highly refractory material with physical and chemical properties similar to that of graphite [198]. Boron nitride powder is soft, white, and lubricious with attractive performance-enhancing attributes similar to other lamellar solids, making it an attractive alternative to other inorganic solid lubricants. It is also environmentally-friendly and inert to most chemicals [198]. Boron nitride does not occur naturally; it is synthesized from boric oxide or boric acid in the presence of urea or urea derivatives and ammonia at temperatures ranging between 800 and 2000°C. Boron nitride is an extremely stable compound that does not breakdown to form other hazardous materials under normal operation; thus, it is safe to handle and feasible to use in industrial applications. High-purity, commercial-grade boron nitride powder does not contain free boron, but retains it in the form of a nitride or borate, which has no hazardous effects or limitations on its use. There are no reports issued by the National Toxicology Program, International Agency for Research on Cancer, Occupational Safety and Health Administration (OSHA), or American Conference of Government and Industrial Hygienists that indicate boron nitride or other boron compounds are carcinogens or pose any toxic hazard [199]. Boron compounds are not considered hazardous chemicals by the EPA or under the Superfund Amendments and Reauthorization Act (SARA) guidelines, and no regulations exist regarding their use, storage, transport, or disposal. For these many cited reasons, boron nitride can be considered an environmentally benign substance with no limitations on its operational use [200].

Previous research has indicated that powder-based lubricants, such as boric acid, graphite, and MoS_2 can be problematic because they can be forced out of the contact zone during dry sliding contact [113]. In an attempt to remedy this problem, a carrier fluid was used, such as paraffin oil, which demonstrated improved tribological properties with the powder-based lubricants [10, 201-203]. From an ecological sustainability perspective, a more environmentally friendly lubricant such as canola oil was used instead of traditional grease or oil [81]. Canola oil has a viscosity and surface tension similar to the functional fluids used in industrial applications such as metal-stamping and metal-forming operations, and it has been speculated to serve as an automotive lubricant for gears or bearings [95]. In this study, canola oil was specifically chosen because it is readily available, inexpensive, environmentally benign, and tested previously by the authors [81, 91-93]. Additionally, it has been shown in the literature that canola oil derived from rapeseed plants, with high-oleic acid (>80%) content, surpasses Group I petroleum-based lubricants at room temperature [98]. Pin-on-disk studies show molybdenum disulfide and boric acid with micron- and nano-sized particle additives in canola oil establish a colloidal mixture leading to improved friction and wear reduction [19, 81, 92, 196, 204-209]. Investigations revealed that the use of a carrier fluid allows the particle additives to remain in the contacting pin-disk interface without degrading over time [90, 93, 95]. The presence of the nano-sized particulate mixtures by themselves or in combination with submicron-sized particles provides improved tribological performance [113, 196].

5.3 Experimental Procedure

In the present investigation, canola oil with boron nitride powder additives was studied using a pin-on-disk tribometer to determine its feasibility as a biolubricant. The performance of this lubricant was studied by varying the particle size of the powder additives in the base oil. Four hBN particle sizes were considered: 70 nm, 0.5 μm, 1.5 μm, and 5.0 μm. A commercial third party manufacturer - who specializes in the production of solid lubricants, generated the hBN particles used in the present study. The particles were synthesized through a proprietary boric acid-based chemical synthesis process that included jet milling to maintain quality control with a 20% tolerance on all particle sizes. The average particle size of the hBN particles, as prescribed by the manufacturer, was determined through transmission electron microscopy and scanning electron microscopy. Furthermore, in the present investigation, the particles were analyzed using SEM. Figs. 5.2(a) – (d), show the scanning electron micrographs of the various hBN particles. It was found that the particle sizes observed in the micrographs were in the same range as their average particle size descriptions given by the manufacturer. These micrographs further reveal that the spherical nature of the particles decreases as the average particle size increases. In Fig. 5.2(a) the 70 nm particles are fully spherical, while Figs. 5.2(b) and 5.2(c) show a transformation to a less spherical geometry in the 0.5 and 1.5 μm particles. In Fig. 5.2(d), the 5.0 μm particles have transformed into a plate-shaped geometry. During each test, 10 mL of canola oil were mixed with hBN particles at 5% by weight.
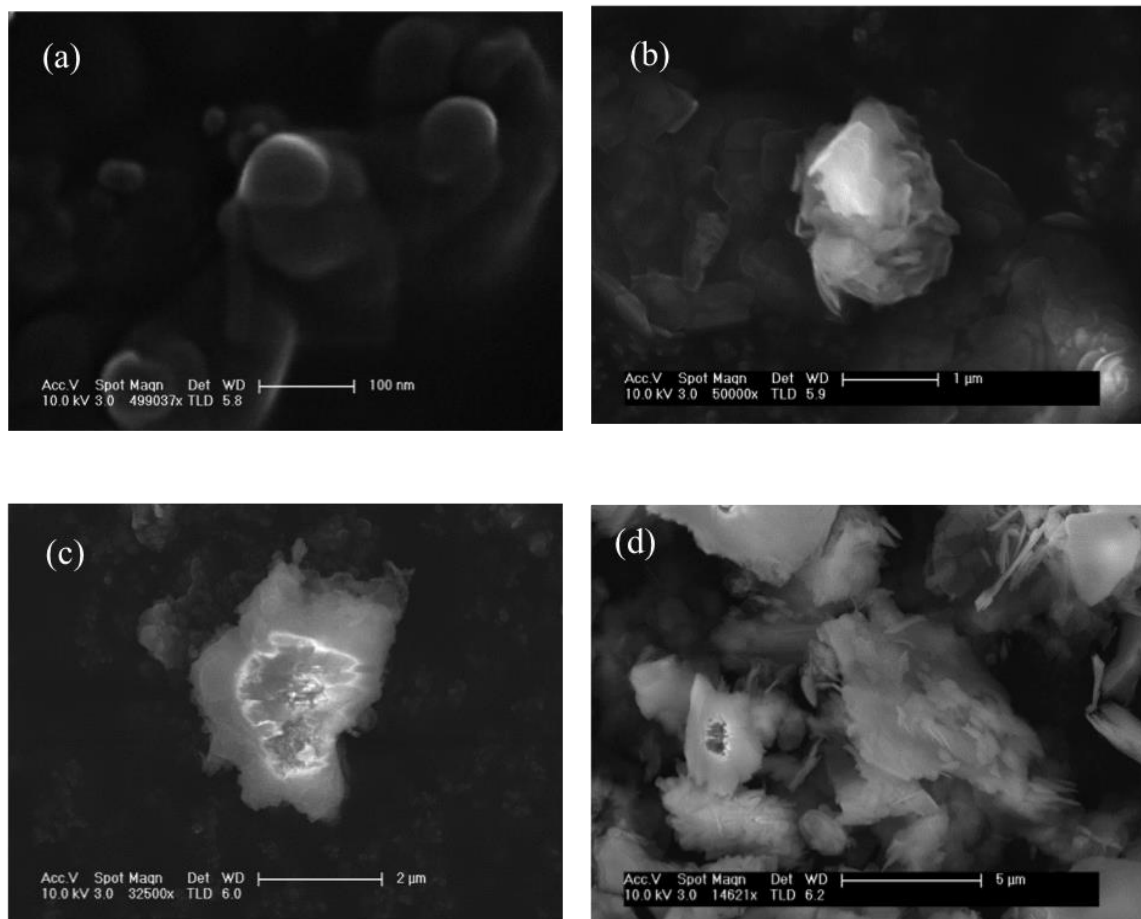
Figure 5.2: Scanning electron micrographs of hBN particles with size (a) 70 nm, (b) 0.5 μm, (c) 1.5 μm, and (d) 5.0 μm

The individual particles and their mixtures were combined with the canola oil using a vortex generator to form a homogenous colloidal mixture. The various lubricant compositions that were used in the tests are shown in Table 5.1. In trials 6 through 11, it can be seen that 2.5% of each particulate size was added into the canola oil, resulting in a total addition of 5% hBN by weight.

Table 5.1: Lubricant mixture composition for pin-on-disk tests

Trial number	Particulate mixture composition
1	Pure Canola Oil (No hBN)
2	70 nm hBN (5% Wt.%) in Canola Oil
3	0.5 m hBN (5% Wt.%) in Canola Oil
4	1.5 m hBN (5% Wt.%) in Canola Oil
5	5.0 m hBN (5% Wt.%) in Canola Oil
6	70 nm hBN (2.5% Wt.%) + 0.5 μm hBN (2.5% Wt.%) in Canola Oil
7	70 nm hBN (2.5% Wt.%) + 1.5 μm hBN (2.5% Wt.%) in Canola Oil
8	70 nm hBN (2.5% Wt.%) + 5.0 μm hBN (2.5% Wt.%) in Canola Oil
9	0.5 m hBN (2.5% Wt.%) + 1.5 μm hBN (2.5% Wt.%) in Canola Oil
10	0.5 m hBN (2.5% Wt.%) + 5.0 μm hBN (2.5% Wt.%) in Canola Oil
11	1.5 m hBN (2.5% Wt.%) + 5.0 μm hBN (2.5% Wt.%) in Canola Oil

In the pin-on-disk tribometer, an oxygen-free electronic copper (C101) pin was fabricated to slide against a 2024 aluminum disk to obtain the friction and wear properties of the lubricants. The pin and disk materials were specifically chosen to match prior experiments conducted by the authors [81, 90, 93]. The copper pin dimensions were 6.35 mm in diameter and 50 mm in length, and had a hemispherical tip. The aluminum disk dimensions were 70 mm in diameter and 6.35 mm in thickness, and were polished to a surface roughness having an arithmetic average, Ra, value of 0.3 ± 0.05 μm. Table 5.2,

presents the specified testing parameters used during each experiment. This experimental study also used the Center for Tribology (CETR) Universal Material Tester (UMT) mounted with a pin-on-disk module. The friction force and linear wear-loss measurements were acquired for each test using a dual axis force transducer and a high-precision ball screw actuator with encoder, which recorded the vertical displacement of the pin. The tribometer was configured for a data acquisition rate of 10 Hz. Prior to each experiment, all test specimens were cleaned with a soap, acetone, and hexane solution in an ultrasonic cleaner. During each of the tests the disk was completely submerged by the lubricant mixture, thereby continually lubricating the pin-disk interface throughout the duration of the test. Each test was repeated a minimum of three times to ensure repeatability and accuracy of the results.

Table 5.2: Test parameters

Parameter	Selected value
Normal Load (N)	10
Sliding Velocity (mm/s)	36
Angular Velocity (rpm)	21.5
Distance Traveled (m)	3000
Duration (hours)	23.2
Environment	Ambient conditions
Lubricant Amount (mL) Canola Oil	10
Additives	5% Wt. hBN
Additive Particle Sizes	5.0 μm, 1.5 μm, 0.5 μm, & 70 nm

5.4 Results and Discussion

5.4.1 Friction Results

Figures 5.5(a) and (b) show the variation of the coefficient of friction with sliding distance for the various single particle-size and multiple particle-size particulate mixtures, respectively. It can be seen that generally the coefficient of friction decreases with sliding distance as a result of the tribo-contacts conforming to each other. In Fig. 5.3(a), the 70 nm particulate mixture has the lowest coefficient of friction and the 5.0 μm particulate mixture has the largest. The presence of 70 nm particles in combination with micron- or submicron-sized particles shown in Fig. 5.3(b), resulted in a significantly lower friction than particulate mixtures without the 70 nm particles. For example, the combination of the 70 nm and 5.0 μm particulate mixture has a lower coefficient of friction than the individual 5.0 μm particulate mixture. This observation is highlighted in Fig. 5.3(c), which depicts the various particulate mixtures and their coefficient of friction values at the completion of the test. It can be seen from Fig. 5.3(c) that the 70 nm particulate mixture continually has the lowest coefficient of friction, followed by the particulate mixture containing the combination of 70 nm and 1.5 μm hBN particles. The 5.0 μm particulate mixture has the highest friction coefficient, followed by the 0.5 μm particulate mixture. These results reveal the important role that the boron nitride particles play in filling the inter-asperity valleys. The filling of the asperities establishes a thin transfer film that allows the particles to align themselves parallel to the relative motion and slide over one another with relative ease providing lubrication.

(a)

(b)

Coefficient of Friction vs Sliding Distance [m]

Legend:
- 70nm+1.5μm
- 70nm+0.5μm
- 70nm+5.0μm
- 1.5μm+0.5μm
- 5.0μm+0.5μm
- 5.0μm+1.5μm
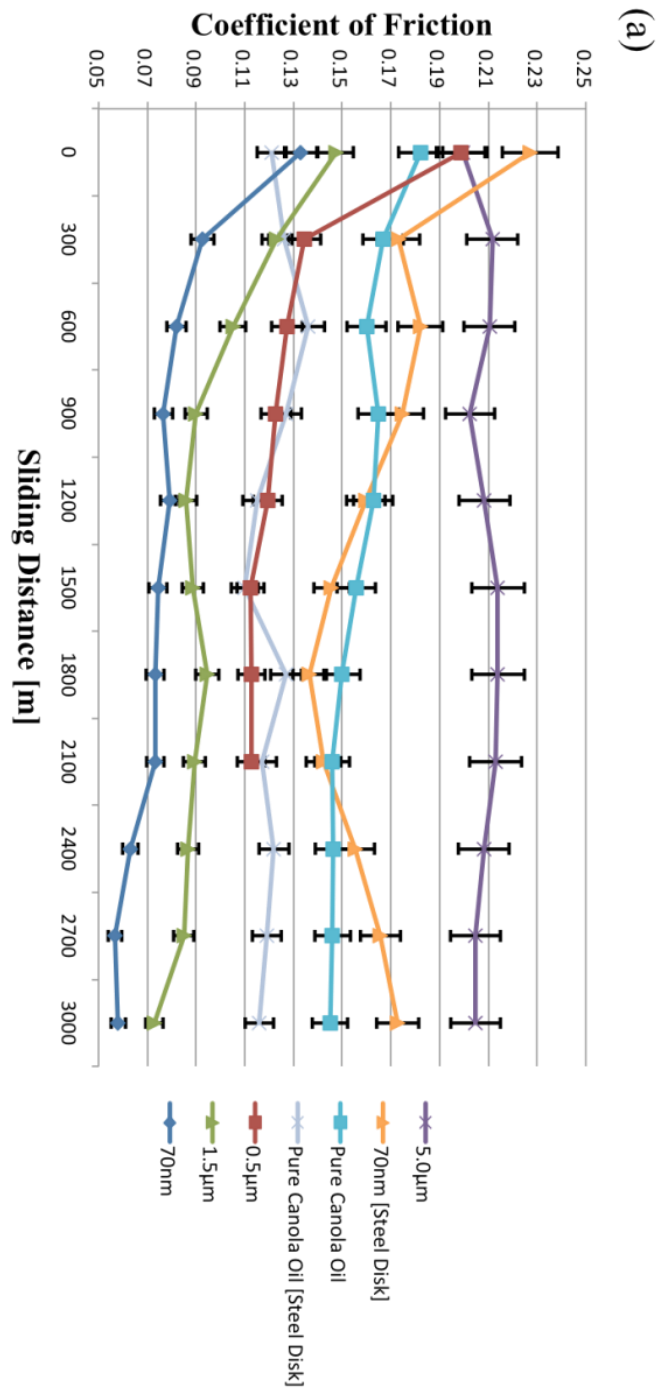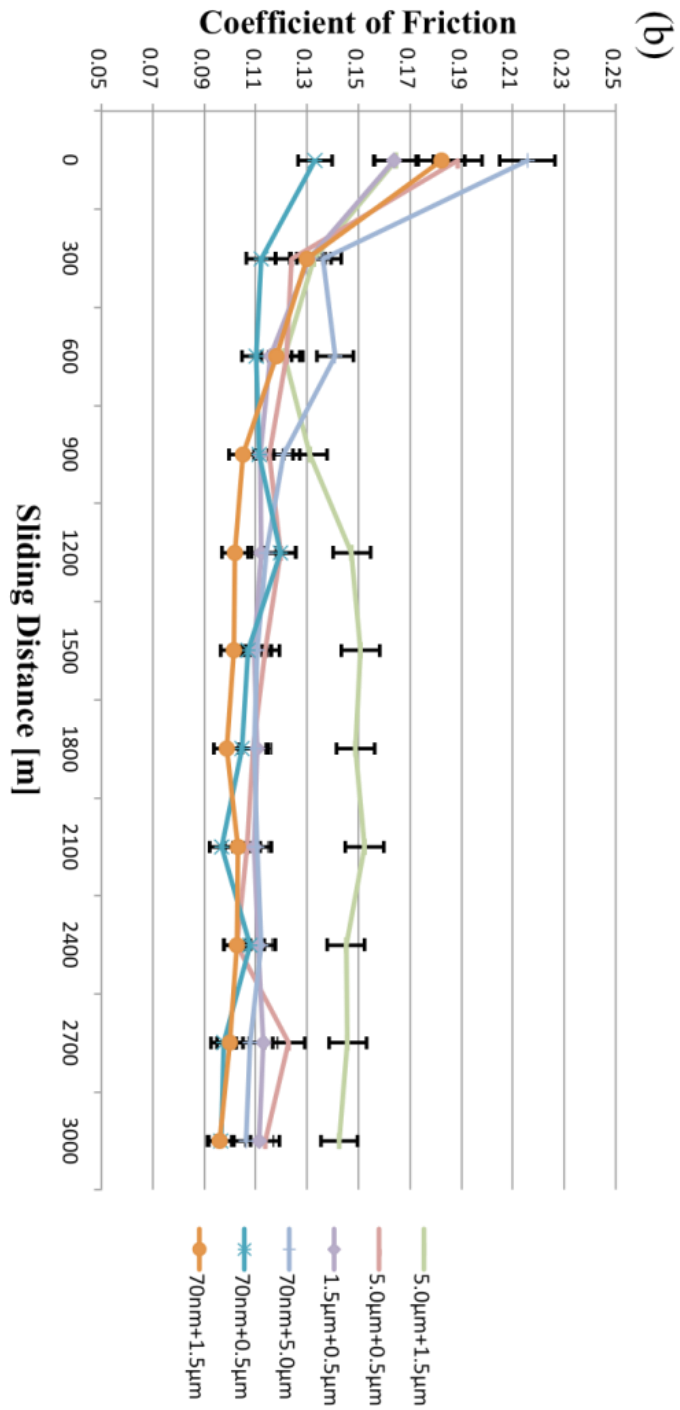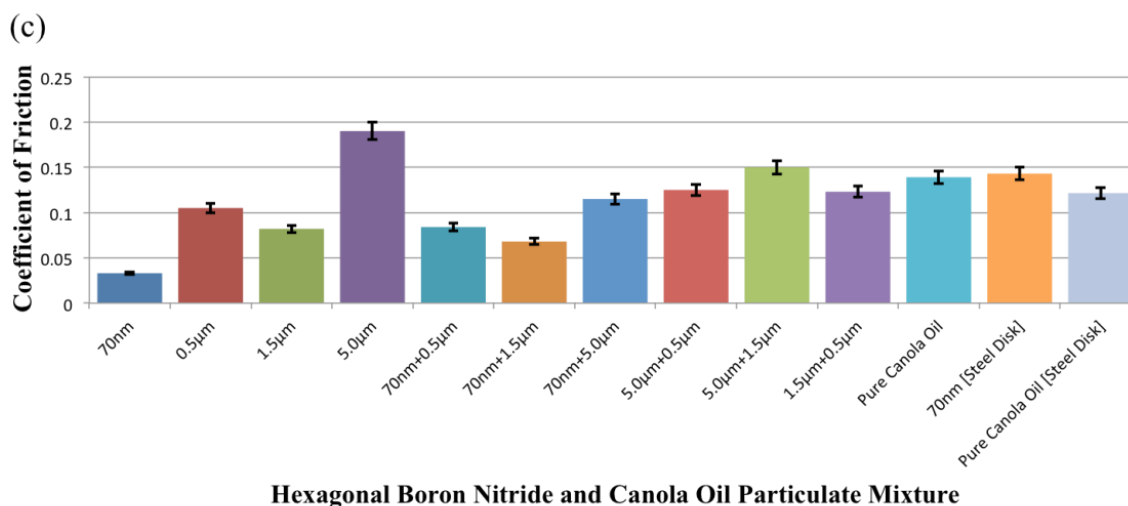
Figure 5.3: (a) Variation of coefficient of friction with sliding distance for single particle-size particulate mixtures, (b) Variation of coefficient of friction with sliding distance for multiple particle-size particulate mixtures, (c) Variation of coefficient of friction for various particulate mixtures at the end of the experiments

An illustration of the boron nitride particles in the tribo-interface is shown in Fig 5.4. This graphic represents a true-scale schematic between the disk surface asperities and the particle sizes with the particle shape geometry depicted. Fig 5.4(a) shows the spherical 70 nm particles in the contact zone and schematically demonstrates how they particles fill the inter-asperity valleys to establish a thin powder transfer film. Based on the experimental results, it can be deduced that the ability of the smaller particles to lower friction is more important than the ability of the larger hBN particles to support the contact loads between the asperities (see Table 5.3). The table illustrates the influence of particle size on the coefficient of friction as substantiated in the tests involving combinations of particle sizes. Particulate mixtures containing 70 nm particles had the largest reductions of the coefficient of friction compared with mixtures with the larger

particle sizes. For example, the 0.5 µm particle mixture had a 20% reduction; the 1.5 µm particulate mixture had a 17% reduction; and the 5.0 µm particle mixture had a 39% reduction in coefficient of friction when mixed with the 70 nm particles.
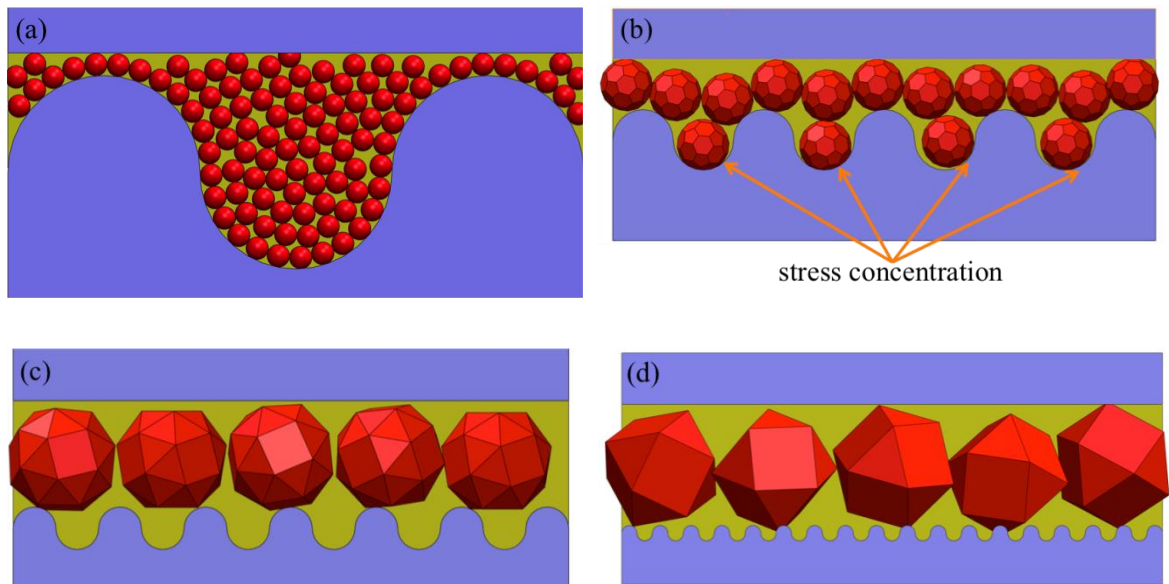
Figure 5.4: Schematic diagram of boron nitride and canola oil particulate mixtures with size (a) 70 nm, (b) 0.5 µm, (c) 1.5 µm, (d) 5.0 µm at the tribo-interface

The 5.0 µm hBN particles are considered to behave more like a third-body abrasive particle when sliding along the aluminum disk, because of their plate-like geometry, which damages the softer disk surface by plastic deformation, resulting in the high coefficient of friction values. A diagram of these particles in the contacting interface is shown in Fig. 5.4(d). The 0.5 µm particles also behave abrasively, resulting in a high coefficient of friction value, possibly because their size is on the same order of magnitude as the surface roughness of the aluminum disk, which has an R_a value of 0.3 µm. As

shown in Fig. 5.4(b), the 0.5 μm particles easily coalesce among the asperities but are thought to have high stress concentrations, as the particles in the asperity valleys remain entrapped, thereby limiting the motion of the neighboring particles and generating larger amounts of force, which leads to the abrasive behavior. For these reasons, the 0.5 μm hBN particles have larger coefficient of friction values. The 1.5 μm particles depicted in Fig. 5.4(c) are unique, because they are larger than the surface asperities and have a more rounded particle geometry; therefore, they can effectively support the asperity contact loads and accommodate the relative velocity with minimal resistance, thus providing a lower coefficient of friction. Table 5.3 reveals that the addition of 0.5 μm, 1.5 μm, or 5.0 μm particles to either the 70 nm, 0.5 μm, or 1.5 μm particles increase the coefficient of friction anywhere from 17 to 248%. This is observed in the case of the 0.5 μm particulate mixture, which has a lower coefficient of friction than the particulate mixture containing both 0.5 μm and 1.5 μm.

Table 5.3: Influence of particle size on coefficient of friction

Base Particles	Additive Particle			
	70nm	0.5 micron	1.5 micron	5.0 micron
70 nm	X	155%	106%	248%
0.5 micron	-20%	X	17%	19%
1.5 micron	-17%	50%	X	83%
5.0 micron	-39%	-34%	-21%	X

Note: (+) is an increase in COF and (-) is a decrease in COF

The ability of the boron nitride particles to remain in the pin-disk interface is an important factor contributing to their friction reducing capabilities [90]; therefore, examining the continual renewal of the hBN particles in the pin-disk interface is critical. The experiments involving canola oil with and without the 70 nm particles were used in a comparative study between a copper pin sliding against an aluminum disk and a copper pin sliding against a 440C stainless steel disk. The results revealed in Fig. 5.3 indicate the effectiveness of the boron nitride particles to act as a lubricant when present in the lubricating interface. In the case of the aluminum disk, the coefficient of friction is low because the copper pin is harder than the aluminum disk, allowing abrasive wear to occur and thus plastic deformation of the disk material. Here the copper pin deforms the aluminum disk, creating a series of grooves as it establishes a wear track. The wear track allows the 70 nm hBN particles to remain in the contacting (pin-disk) interface, providing adequate lubrication. On the contrary, in the case of the copper pin against the steel disk, the increased hardness of the steel disk hinders the formation of a wear groove by plastic deformation in the disk; therefore the hBN particles cannot accumulate in a groove, resulting in a higher coefficient of friction. In the case of the steel disk with the 70 nm hBN particles in canola oil, the boron nitride particles escape from the pin-disk interface, resulting in a condition similar to the steel disk lubricated by pure canola oil with a comparable final coefficient of friction, as shown in Fig. 5.3(c). These results validate the importance of the hBN particles to remain in the contacting interface to provide adequate lubrication throughout the test duration.

5.4.2 Wear Volume Results

During the tests the linear wear displacement of each pin was measured and converted into a volumetric wear loss using Eq. (5.1) derived from the geometry of a spherical cap [278].

$$V = \frac{\pi h^2}{3}\left(3r\text{-}h\right) \qquad\qquad \text{Eq. (5.1)}$$

In Eq. (5.1), h is the linear wear displacement (mm) in the vertical direction for the pin, r is the pin radius (mm), which is assumed constant throughout the test, and V is the volumetric wear loss (mm^3). Fig. 5.5(a) shows the variation of the pin wear volumes with sliding distance for the all the particulate mixtures.

(a)

(b)

Hexagonal Boron Nitride and Canola Oil Particulate Mixture
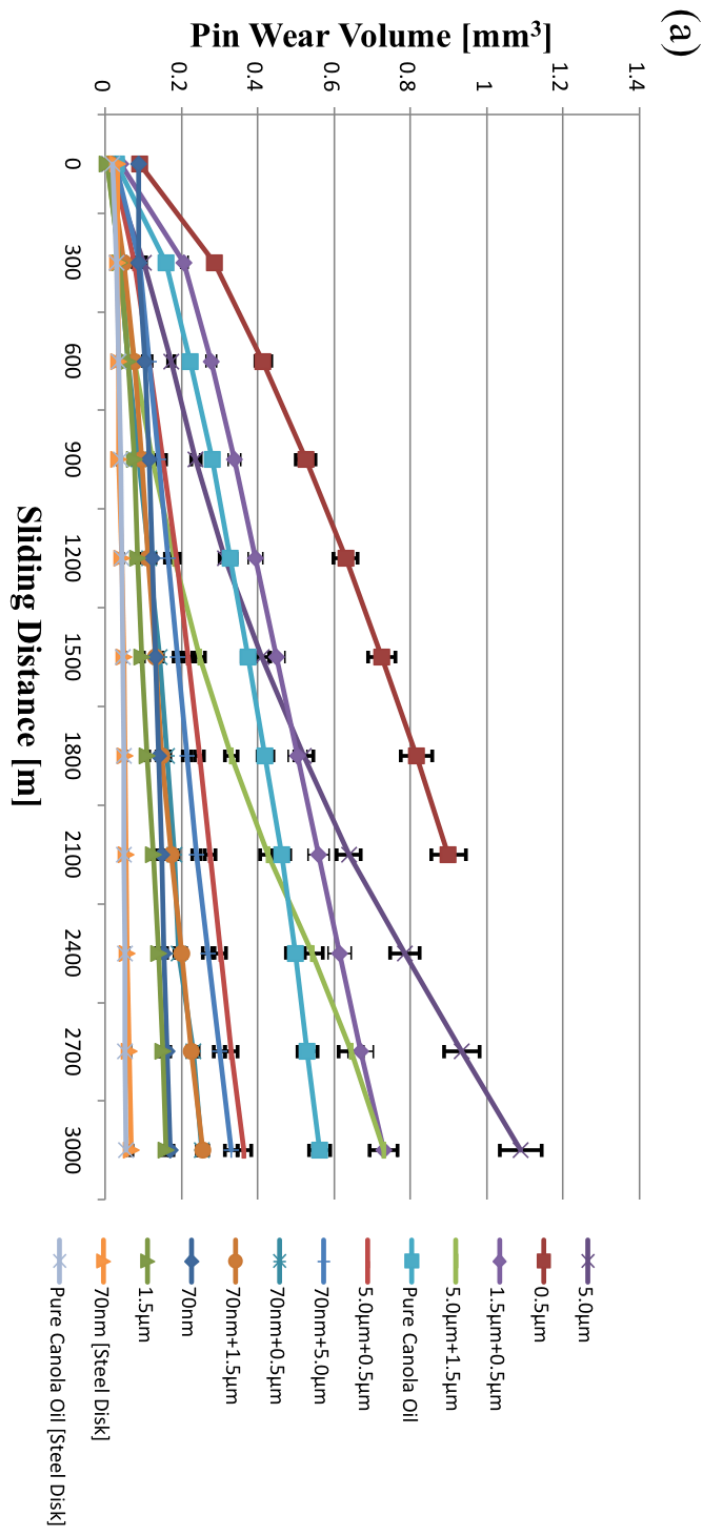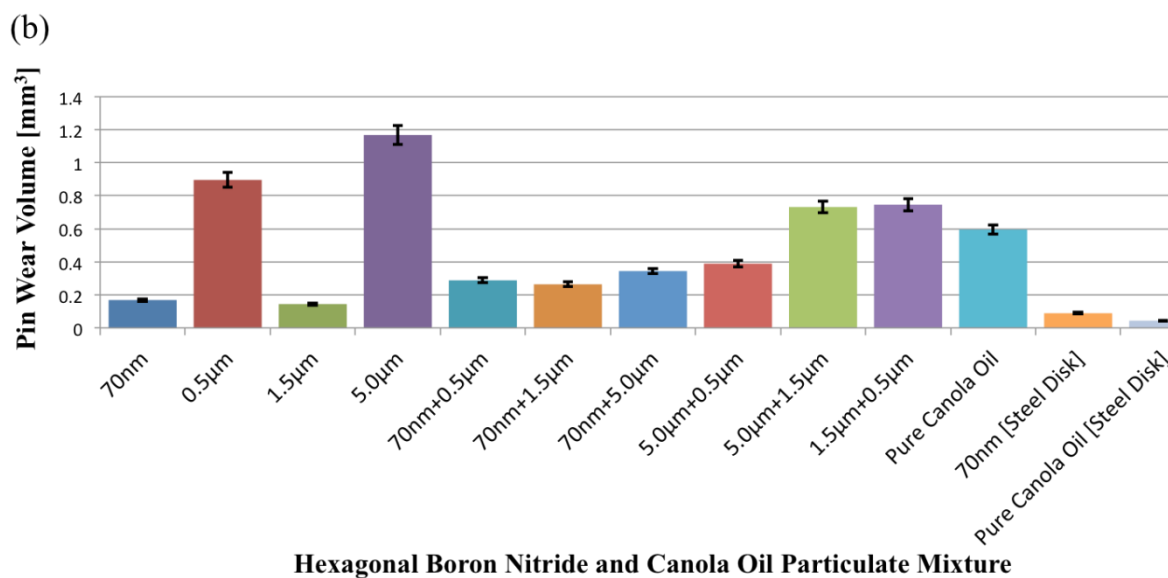
Figure 5.5: (a) Variation of pin wear volume with sliding distance for particulate mixtures, (b) Variation of pin wear volume for various particulate mixtures at the end of the experiments

It can be seen that the pin wear volume increases with the sliding distance for various particulate mixtures. The 5.0 μm and 0.5 μm particle mixtures have the highest wear volumes and the 70 nm and 1.5 μm particulate mixtures have the lowest wear volumes; these results are similar to the trends seen in the coefficient of friction behavior. Lubricants containing mixtures of two particle sizes resulted in pin wear volumes that fluctuate between the maximum and minimum pin wear volumes for individual particulate mixtures. The 0.5 μm and 5.0 μm particle mixtures have the highest wear rates, which support previous claims that these particles behave abrasively. Fig. 5.5(b) depicts the various particulate mixtures and the pin wear volumes upon the completion of the test. It can be seen from Table 5.4 that the addition of the 70 nm or the 1.5 μm particles to the

0.5 μm or 5.0 μm particulate mixtures lowers the amount of wear. In fact, any combination of particles added to either the 0.5 μm or 5.0 μm particulate mixtures decreases the amount of wear and any combination of particles added to either the 70 nm or 1.5 μm particulate mixture increases the amount of wear.

Table 5.4: Influence of particle size on pin wear volume

Base Particles	Additive Particle			
	70nm	0.5 micron	1.5 micron	5.0 micron
70 nm	X	71%	56%	104%
0.5 micron	-68%	X	-17%	-57%
1.5 micron	83%	417%	X	407%
5.0 micron	-71%	-23%	-37%	X

Note: (+) is an increase in wear and (-) is a decrease in wear

These results indicate the presence of the 70 nm particles to produce a thin lubricating transfer film, as shown in Fig. 5.4(a), and the 1.5 μm particles to carry the asperity contact loads, as shown in Fig. 5.4(c), limit the amount of wear that occurs. The influence of the 70 nm particles to lower the wear is far greater than that of the 1.5 μm particles. For example, by examining the two particle mixtures with the highest wear volume (0.5 μm and 5.0 μm), the presence of the 70 nm particles with the 0.5 μm particles lowers the wear volume by 68% when compared to the 1.5 μm and 0.5 μm particulate mixture, which reduced the wear volume by 17% (Table 5.4). Furthermore, the influence of the 70 nm particles with the 5.0 μm particles lowered the wear volume by

71% compared with the 1.5 μm and 5.0 μm particulate mixtures, which had only a 37% decrease (Table 5.4). This supports the claim that the influence of the 70 nm particles to coalesce in the asperity valleys and establish a thin lubricating film to minimize friction and wear is more important than the ability of the larger particles to support the asperity contact.

The importance of the hBN particles to remain in the lubricating interface was again evaluated using the 70 nm particulate mixture with the copper pin sliding on an aluminum disk. These results were compared with that of a copper pin sliding on the 440C stainless steel disk. In this analysis, the influence of the disk material on the wear volume was examined. The hardness of the steel disk is more than that of the aluminum disk, therefore less wear occurs for the case of the steel disk. Significant research has gone into understanding the influence of the hardness ratio on the wear rate of mating materials. In addition, substantial work has gone into determining the effects of crystal structure, yield strength, and other material properties on a materials wear rate [38, 300-316]. The influence of the crystal structure affects the wear rate, for example the steel disk has a body-centered cubic (BCC) crystal structure with a lower number of slip systems when compared with the aluminum disk, which has a face-centered cubic (FCC) crystal structure. Here, the BCC crystal structure has 48 possible slip systems, but since the planes are not so closely packed, they require higher amounts of stress to cause slip. On the contrary, the FCC crystal structure is closely packed and has 12 possible slip systems that require less stress than the BCC to cause slip [317]. The limited number of slip systems in the steel decreases the occurrence of plastic deformation in the material,

thereby severely limiting the real area of contact in the pin-disk interface; for this reason, less wear occurs with the steel disk when compared with the aluminum disk. It is reported in the literature that a higher hardness difference between mating pairs results in a higher wear rate. In the present study, the aluminum disk had a Brinell hardness of 120 and a yield strength of 310 MPa, whereas the steel disk had a Brinell hardness of 230 and a yield strength of 448 MPa [318, 319]. The copper used for the pins had a hardness that was in between the aluminum and the steel disks with a Brinell hardness value of 179 and a yield strength of 310 MPa [318, 319]. The hardness ratio, R is defined as the ratio of the hardness of the disk material to the hardness of the pin material as shown in Eq. (5.2) [7].

$$Hardness\ Ratio = \frac{hardness\ of\ disk\ material}{hardness\ of\ pin\ material} \qquad \text{Eq. (5.2)}$$

From Eq. (5.2), the hardness ratio, R for the material pairs is as follows: for the aluminum disk and copper pin, R = 0.67 and for the steel disk and the copper pin, R = 1.28; where a lower hardness ratio results in a higher wear rate of mating materials. Thus, from Eq. (5.2) the aluminum-copper material pair has a lower hardness ratio and a greater hardness difference, so it would be expected that it would exhibit a higher wear rate when compared to the steel-copper material pair. In the present investigation, the variation in the wear rate is substantial between the aluminum and the steel disks when sliding against the copper pins. This is because in the case of the copper pin sliding against an aluminum disk, the wear grooves are formed on the aluminum disk as a result of plastic deformation, since the aluminum disk is softer than the copper pin. The boron nitride particles in the

canola oil in this scenario were able to remain in the wear groove and provide adequate lubrication leading to relatively low wear rates, especially in the cases involving the 70 nm and 1.5 μm particle sizes. In the case of the copper pin sliding against a steel disk, wear grooves were not able to develop to constrain the boron nitride particles which are present in canola oil in the interface because the hardness of the steel-disk is much greater than that of the copper. It is for this reason that the boron nitride particles were able to flow out of the pin-disk interface, starving it of any hBN particles, and enter a pure canola oil scenario, thus leading to a deficiency in the lubricant. This can be seen in Fig. 5.5(b), where the steel disk was lubricated with both a 70 nm hBN particulate mixture and pure canola oil, which resulted in similar wear rates. Here, the lower wear rate in the case of the steel disk is directly caused by the greater hardness ratio and lower hardness difference between steel disk and the copper pin, rather than the influence of the boron nitride particles as seen in the aluminum disk.

5.4.3 Surface Analyses

To further evaluate the influence of the particle size on friction and wear, an optical profilometer and scanning electron microscope (SEM) were used to analyze the worn pin surfaces. An optical profilometer was used to measure surface roughness parameters including the arithmetic average. Fig. 5.6(a) shows three-dimensional worn pin surfaces recorded by the optical profilometer for the 70 nm particulate mixture, and Fig. 5.6(b) for the 5.0 μm particulate mixture.
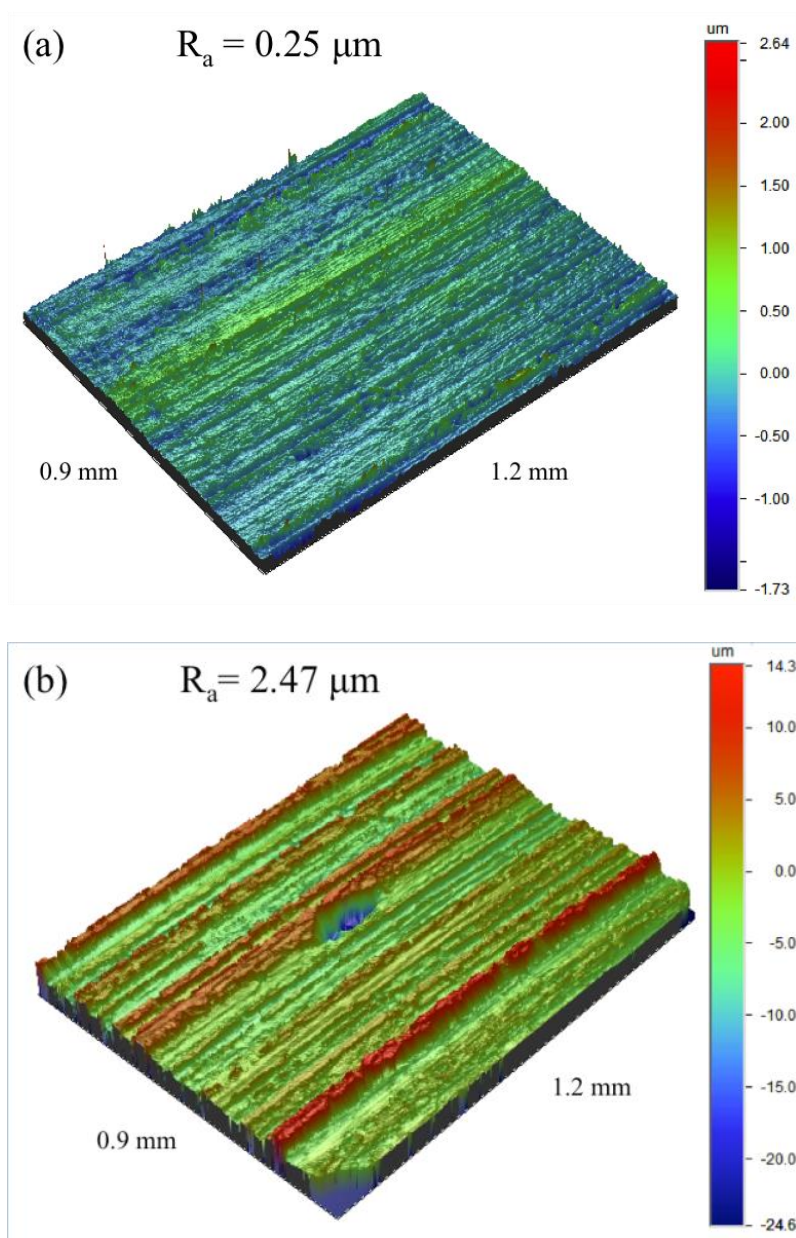
Figure 5.6: 3D Optical profilometer images of worn surface of the pin for the (a) 70 nm, (b) 5.0 µm experiments

Figure 5.7 shows scanning electron micrographs of worn pin surfaces at low and high magnifications for the particulate mixtures containing 70 nm, 5.0 μm, and the combination of 70 nm and 5.0 μm hBN particles. This analysis reveals that the worn pin surface for the 70 nm particle mixture, Figs. 5.6(a), 5.7(a), and 5.7(b), has a relatively smooth surface with an Ra value of 0.25 μm and a uniform worn surface. The pin surface used in the 5.0 μm particle mixture, Figs. 5.6(b), 5.7(c), and 5.7(d), is severely abraded, having a Ra value of 2.47 μm, which is significantly rougher than in the 70 nm particulate mixture test. This is consistent with the friction and wear results, because the 5.0 μm particle test had a higher coefficient of friction (COF) and wear volume than the 70 nm particle test. Finally, the combination of the 70 nm and 5.0 μm particulate mixture, Figs. 5.7(e) and 5.7(f), reveal that the surface roughness decreases with the presence of nano-sized particles with a Ra value of 0.42 μm, which is again consistent with the friction and wear results. In fact, in this trial the presence of the 70 nm particles lowered the COF by 39%, the pin wear volume by 71%, and the surface roughness by 83%. These results further verify that the 70 nm hBN particles have the ability to form a protective coating on a surface that lowers the coefficient of friction, wear volume, and surface roughness. The abrasive nature of the 0.5 μm and 5.0 μm particles with high friction coefficients and wear volumes generate rough surfaces and thus may not be suitable additives in the present canola oil-particulate mixtures.
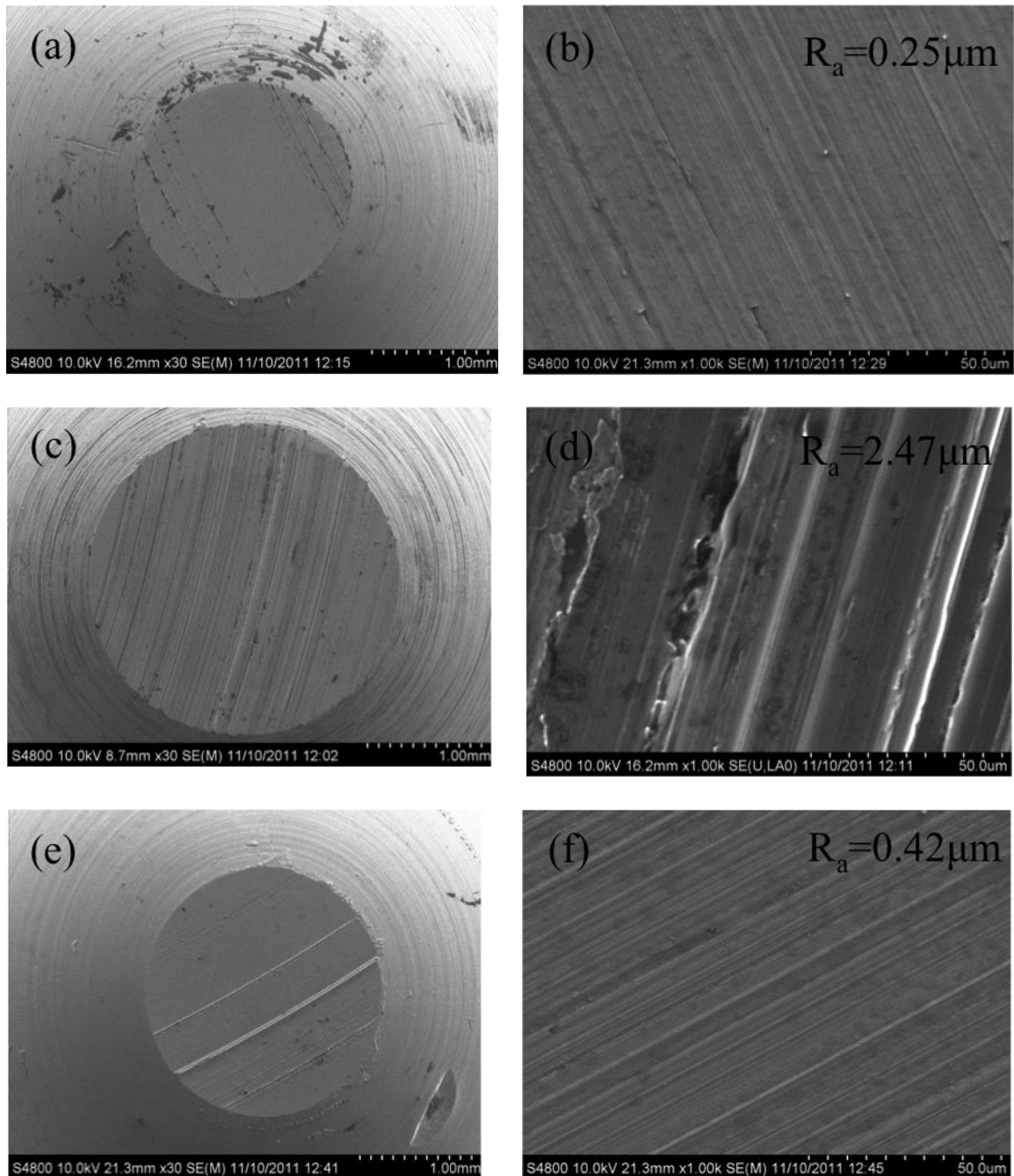
Figure 5.7: Scanning electron micrographs of worn pin surfaces for various particulate mixtures (a, b) 70 nm, (c, d) 5.0 μm, and (e, f) 70 nm + 5.0 μm, in canola oil under low magnification (a, c, e) and high magnification (b, d, f)

The Ra values for the worn pin surfaces for various particulate mixtures are depicted in Fig. 5.8, which shows two relationships between the surface roughness and particle size. The first relationship is present in the experiments involving the single particle-size particulate mixtures—the larger the difference between the particle size and the initial surface roughness of the disk, the greater the surface roughness of the worn pin surface. The second relationship occurs in the experiments involving multiple particle-size particulate mixtures—the larger the difference between the two particle sizes, relative to the larger one, the smoother the worn pin surface (i.e. less surface roughness).
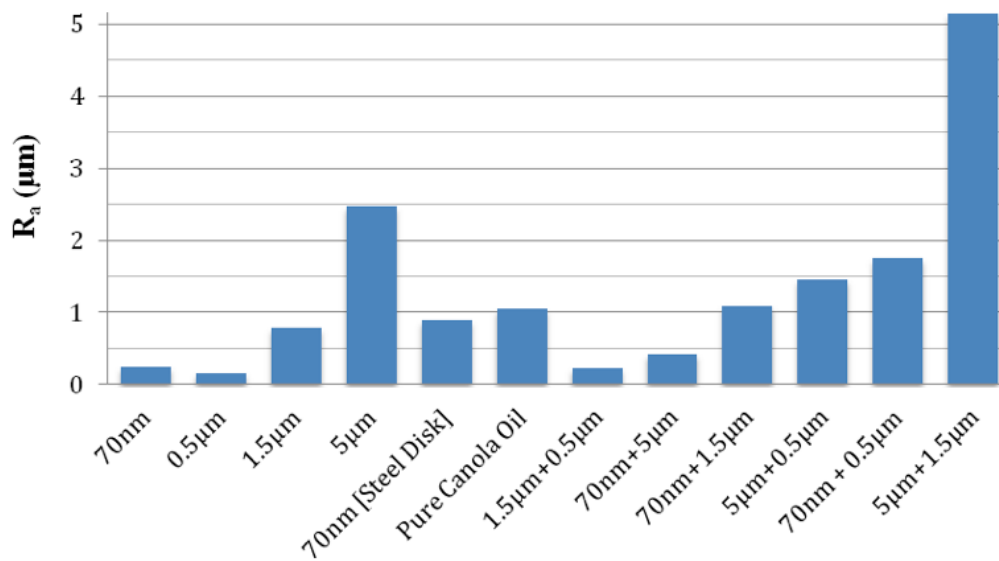
Figure 5.8: Variation of surface roughness with particulate mixture

To better quantify these relationships, two dimensionless hybrid roughness parameters are introduced, the particle size-to-surface roughness (PSR)-Index (Ψ_{SR}) and the particle-

to-particle (PP)-Index (Φ_{PP}). The Ψ_{SR} which defines the first relationship is described by Eq. (5.3):

$$\psi_{SR} = \frac{|R_a - n_p|}{R_a}$$

Eq. (5.3)

In Eq. (5.3), R_a is the arithmetic average of the disk surface before the test (with a value of 0.3 μm) and n_p is the average additive particle size in the individual particulate tests. The Φ_{PP} characterizes the second relationship by relating the PP size difference within each particulate mixture with multiple-sized particles and is defined in Eq. (5.4).

$$\phi_{PP} = \frac{|n_j - n_i|}{n_j}$$

Eq. (5.4)

In Eq. (5.4), n_j is the larger particle-size and n_i is the smaller particle-size within the mixture. Table 5.5 shows the Ψ_{SR} for various lubricant mixtures and Fig. 5.9 illustrates the actual and predicted Ψ_{SR} values and pin surface roughness values for varying particle sizes. Additionally, Fig. 5.9 shows the transitional boundaries for the particles geometrically transforming from spherical to plate-shaped. The transitional boundaries represent regions where various tribological mechanisms are occurring as a result of particle shape and size. Moreover, these boundaries are derived from the SEM micrographs in Fig. 5.2 and the schematic diagram in Fig. 5.4.

Table 5.5: Particle Size-to-Surface Index (Ψ_{SR})

Particle Size	R_a (µm) of initial disk surface	Ψ_{SR}	R_a (µm) of the pin
0.5µm	0.30	0.67	0.16
70nm	0.30	0.77	0.25
1.5µm	0.30	4.00	0.79
5.0µm	0.30	15.67	2.47
70nm (Steel)	0.30	0.77	0.89
Pure Canola Oil	0.30	1.00	1.05

Particle Size-to-Surface Index

$Ra = 0.0097n^3 - 0.0988n^2 + 0.2612n + 0.0779$
(where n is average particle size)
Correlation Coefficient - $R^2 = 1$

Region (A):
Spherical particles create thin monolayer protecting the surface

Region (B):
Semi-spherical particles create high stress concentrations and smooth surface

Region (C):
Semi-plate-shaped particles begin to roughen surface

Region (D):
Plate-shaped particles abrasively roll over surface

Average Particle Size (µm)

Ra (µm) of the pin

- - - - Predicted Particle-Size-to-Surface Index

● Particle-Size-to-Surface Index

Figure 5.9: Actual and predicted particle size-to-surface indices (Ψ_{SR}) and pin surface roughness (R_a) values for varying average particle size

For the 0.5 μm, 70 nm, 1.5 μm, and 5.0 μm particulate mixture tests the R_a value of the pin and the Ψ_{SR} value increase together as the particles deviate from the spherical geometry. This trend is important because it helps to validate the claim that the 0.5 μm hBN particles are of a similar magnitude to the surface roughness of the test disk, because they have the lowest Ψ_{SR}. This may suggest that the particles fill the inter-asperity valleys and create a smoother surface finish; however, they do act as an abrasive particle when traversing the surface, resulting in the higher friction. Figure 5.10, depicts the predicted Ψ_{SR} values for varying particle sizes and various initial disk surface roughness. From Fig. 5.10, it can be seen that Ψ_{SR} increases as the particle size increases for a constant surface roughness and that the Ψ_{SR} decreases with an increasing initial surface roughness, to an asymptotic value of 1 as shown in the line with an $R_a = 10$ μm. It should be noted that in Fig. 5.10, when the particle size approaches the size of the surface roughness, the predicted value is zero, rendering the prediction inaccurate at that *single* point. Despite this minute error, it does reveal that other physical mechanisms are contributing to the friction, wear, and surface roughness such as possible stress concentrations and particle shape geometry (i.e. spherical or plate-shaped).
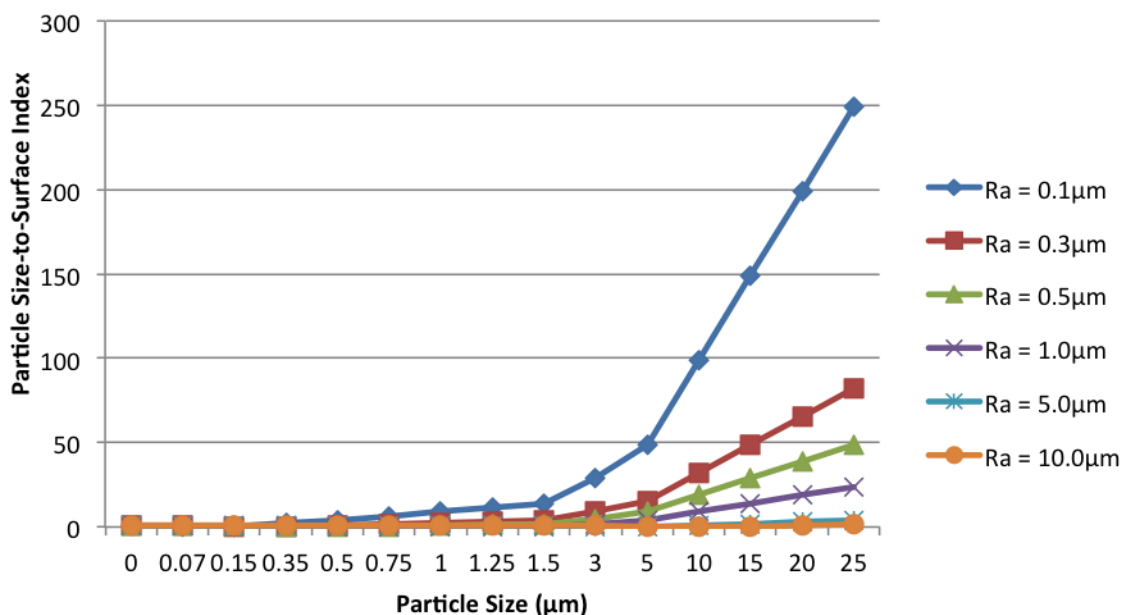
Figure 5.10: Predicted particle size-to-surface indices (Ψ_{SR}) for varying particle sizes and various initial disk surface roughnesses

It is speculated that particles having a size on the same order of magnitude as the initial surface roughness of the disk are the "problematic" size because they become entrapped in the asperity valleys. This is presumed to result in high-stress concentrations, which may become more pronounced the less spherical the particle is, thus facilitating the abrasive nature of the particles. For these reasons, it is hypothesized that these particles create a more disorderly and restrictive state that requires a higher degree of force to push the particles across the lubricating interface, thereby increasing friction and wear. The 70 nm hBN particulate mixture used in the steel disk test has a larger R_a value than the 70 nm particulate mixture used with the aluminum disk, because the steel disk permits the 70 nm hBN particles to flow out of the pin-disk interface. This results in a situation

where the pin-disk interface is primarily lubricated by the canola oil. The 70 nm steel disk test and the pure canola oil test have similar R_a values, which would support this claim. The pure canola oil test has no hBN particles in the lubricant mixture; therefore, it has a Ψ_{SR} value of 1.0 and minimal preventative wear mechanisms, and it remains a benchmark for comparative purposes.

The Φ_{PP} for various particulate mixtures is tabulated in Table 5.6 along with the corresponding R_a values. In this table, when Φ_{PP} equals 0.67, the corresponding particle sizes are 1.5 μm and 0.5 μm. Theoretically, the value of Φ_{PP} approaches zero when the particle sizes are similar. Also, it can be seen that the value of Φ_{PP} equals 0.99 when the 5.0 μm particles are combined with the 70 nm particles. Again, it can be inferred that as the value of Φ_{PP} approaches its upper limit of one, this represents a scenario where the smaller particle has become so small that its size is negligible or can be considered zero. In the combined particulate mixture tests, the worn pin surface roughness decreases inversely proportional to the Φ_{PP}, with the exception of the combination of the 1.5 μm and 0.5 μm particulate mixture test having a Φ_{PP} value of 0.67. This test (as shown in Table 5.6) has a small difference between the particle sizes, resulting in a smoother pin surface finish, having the lowest R_a value. A possible reason for this phenomenon is the competing nature of the boron nitride particles. In the cases where the Φ_{PP} is large (≥0.70), two substantial wear-reducing mechanisms are occurring. The first is by the smaller particles being able to fill the inter-asperity region and establish a thin powder transfer film protecting the surface; the second mechanism is caused by the larger

particles supporting the asperities contact loads, thereby potentially reducing the amount of asperities in contact.

Table 5.6: Particle-to-Particle Index (Φ_{PP})

Particle Size	Φ_{PP}	R_a (μm) of the pin
1.5μm+0.5μm	0.67	0.227
5.0μm+1.5μm	0.70	5.15
70nm + 0.5μm	0.86	1.75
5.0μm+0.5μm	0.90	1.46
70nm+1.5μm	0.95	1.09
70nm+5.0μm	0.99	0.423

As the Φ_{PP} decreases, the impact of the two wear-reducing mechanisms ends up competing as the particles struggle to fit into the same space, because they are relatively the same size and thereby increasing surface roughness. It should be noted that surface roughness is an independent parameter to the wear rate of the pin. The particle size dictates how much friction and wear takes place during a test, and the size effect of the particle with the initial surface roughness defines how rough the final worn surfaces will be. At the end of a test when profilometry measurements are conducted, hBN particles may remain impregnated on the surface of the pin, even after thorough washing. Nevertheless, the topographical measurements substantiate the theory that the larger particle sizes are more abrasive, as shown in Figs. 5.3, 5.5, and 5.7, and thus the presence

of the nano-sized particles to fill inter-asperity region is more important than the ability of the larger particles to support the asperity contact loads. In addition, the tribological performance of the particles is dependent upon their presence in the tribo-interface.

5.4.2 Avocado Oil Tests

In the current investigation, the author investigated the size effect of boron nitride and boric acid particulate additives mixed into canola oil for their effects on friction and wear [6, 93, 118, 320]. Canola oil was used as a carrier fluid to circulate the particulate additives during the pin-on-disk testing. Here, it is shown that the canola oil with the particulate additives demonstrated improved tribological performance. However, taking into consideration the presented fatty acid analysis from Chapter 4, canola oil was not the optimal natural oil lubricant for enhanced tribological performance. In fact, avocado oil has superior tribological properties that surpass those of canola oil in regards to friction, wear rate, and thermal-oxidative stability. Therefore, it can be speculated that using avocado oil with the particulate additives would lead to further improvements in the tribological properties of this class of biolubricants containing particulate additives for three reasons: (1) establishment of a superior fatty acid monolayer to lower the friction and wear, (2) enhancement of the thermal-oxidative stability, and (3) advancement of the particulate additives to further reduce friction and wear. In this section, current research progresses in this direction by studying the effect of varying sizes of hBN particulate additives on the tribological performance of avocado oil. In this investigation, the hBN particles were mixed into the avocado oil to form colloidal solutions in a similar process

to that of the canola oil with hBN particle additives. These tests were conducted using similar materials i.e. a copper pin sliding on an aluminum disk with comparable test parameters, a 10N normal load, 36mm/s sliding velocity, ambient conditions, and particles add at 5% by weight. The only difference this test was performed on a Ducom Instrument Material Characterization System tribometer. It should be noted that friction is a system dependent property that is dependent upon test environment, operating conditions, and surface geometrical configuration and therefore it is not so much the comparison on the lower friction between these tests but the impact of the particle additives to improve upon the avocado oil which is important.

5.4.2.1 Friction Results

Figure 5.11 shows the coefficient of friction results for avocado oil mixed with hBN particulate additives in a colloidal suspension after sliding contact. Figure 5(a) shows the variation of the COF with sliding distance and Fig. 5(b) shows the final COF results. It was revealed that the COF for the various lubricant mixtures decreases with sliding distance. Of the single particulate mixtures, the 70 nm hBN particles maintained the lowest COF followed by the 0.5 µm hBN, 1.5 µm hBN, and 5 µm hBN mixtures. Interestingly as the 70 nm particles are added to each of the other particulate tests, they witnessed a decrease in the COF. More still each of the avocado oil and hBN particulate mixtures maintained a lower COF value than the pure avocado oil. It can be inferred that the abrasive nature of the larger plate-shaped particles did not play as significant a roll in
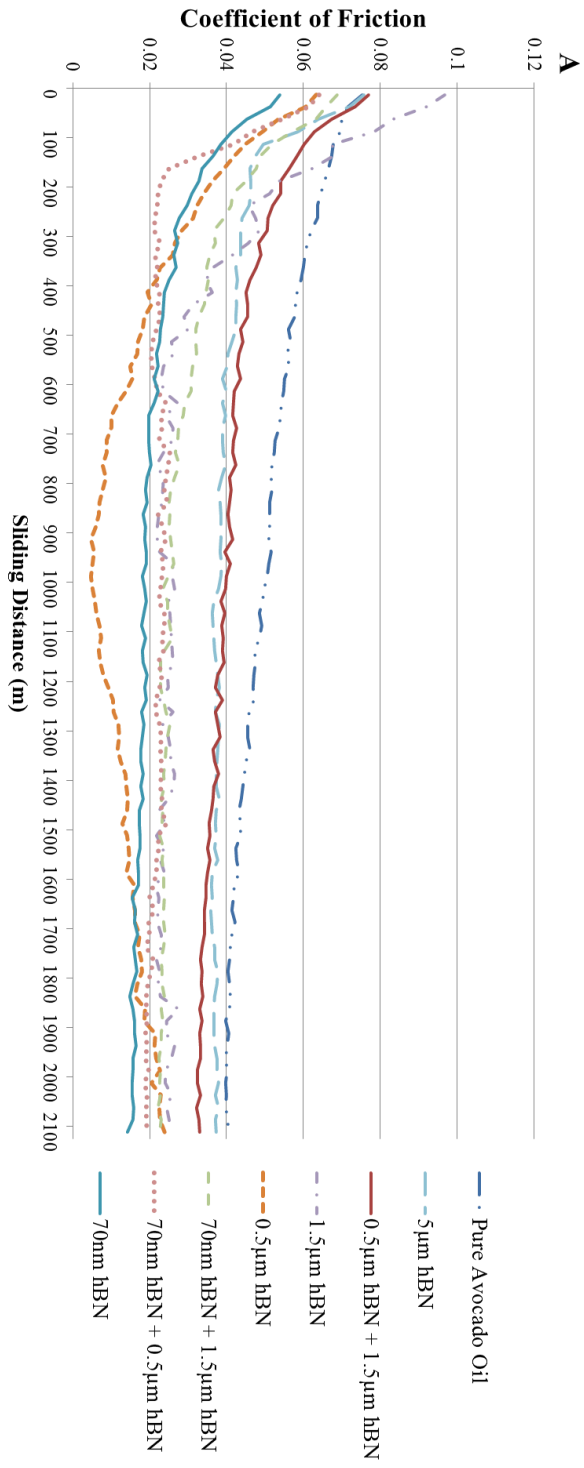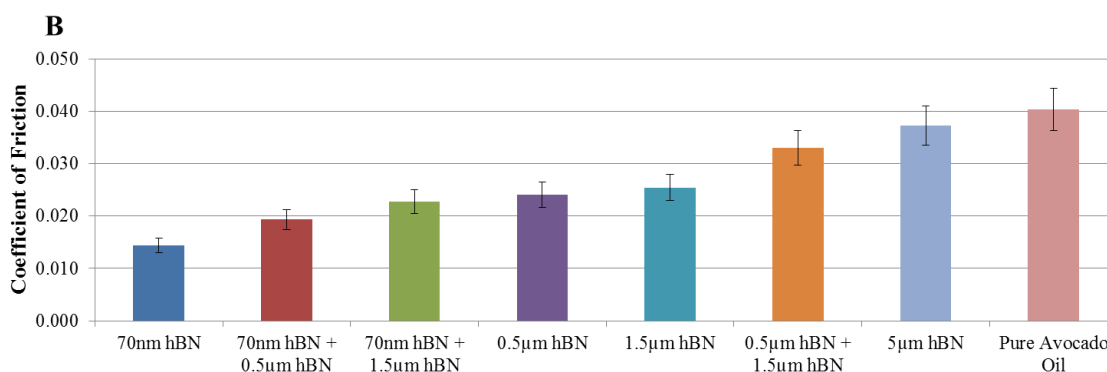
Figure 5.11: Coefficient of friction for boron nitride particles in avocado oil (a) variation of the COF with sliding distance and (b) variation of the COF at the end of the experiments

regards to influencing the friction coefficient. Table 5.7 shows the final COF values and the percent difference that particle had on the tribological performance of the avocado oil. In this table the individual particles were compared to the pure avocado oil in the percent different calculation and the combined particulate tests were compared to their larger particle size to gauge the improvement of the smaller particle being present in the combination mixture. It can be seen that the 70 nm hBN particles decreased the COF by 64% while the 5μm hBN particles only decreased the COF by 8%, when compared to the pure avocado oil. The influence of the 70 nm particles lowered the COF in the 0.5 μm and 1.5 μm hBN tests by 20% and 11% respectively. The combination of the 0.5 μm and 1.5 μm hBN as a particulate mixture resulted in an 30% increase in the COF when compared to the 1.5 μm hBN test.

Table 5.7: Influence of particle size on the coefficient of friction in avocado oil
particulate mixtures

Particle Combination	COF	Percent Difference (%)
70nm hBN	0.0144	-64[1]
70nm hBN + 0.5µm hBN	0.0193	-20[2]
70nm hBN + 1.5µm hBN	0.0227	-11[2]
0.5µm hBN	0.0240	-41[1]
1.5µm hBN	0.0255	-37[1]
0.5µm hBN + 1.5µm hBN	0.0330	30[2]
5µm hBN	0.0373	-8[1]
Pure Avocado Oil	0.0404	N/A

[1] Compared to pure avocado oil
[2] Compared to the larger of the two particle sizes

5.4.2.2 Wear Results

Figure 5.12 shows the wear volume results for the avocado oil particulate mixture tests. Figure 5.12(a) shows the variation of the wear volume with sliding distance. It can be seen in this figure that the wear volume increases with sliding distance. Figure 5.12(b), shows the wear volume at the completion of the tests and Table 5.8 shows the influence of the wear volume. It was revealed in the avocado particulate mixture tests that the 70 nm hBN tests have the lowest wear volume overall. Within the single particulate mixtures the 0.5 µm hBN, 1.5 µm hBN, and the 5 µm hBN particles showed a systematic increase in wear rate with particle size, which was in near perfect agreement with the friction results. It was shown that the 70 nm hBN particles decreased the amount of wear by over 70%, followed by a 63%, 50%, and 13% decrease in wear by the 0.5 µm hBN, 1.5 µm hBN, and the 5 µm hBN particles, respectively. When the 70 nm hBN particles were

added to the 0.5 µm hBN, 1.5 µm hBN mixtures they each saw a reduction in wear of 39% and 18% respectively. The combination of the 0.5 µm hBN, 1.5 µm hBN particles revealed a 26% increase in wear. The 70 nm hBN particles clearly dominated the performance of the particle additives revealing the importance of allowing smaller particles to coalesce in the asperity valleys and establish a thin smooth lubricious transfer film that can simultaneously lower the friction and minimize the wear rate.

A
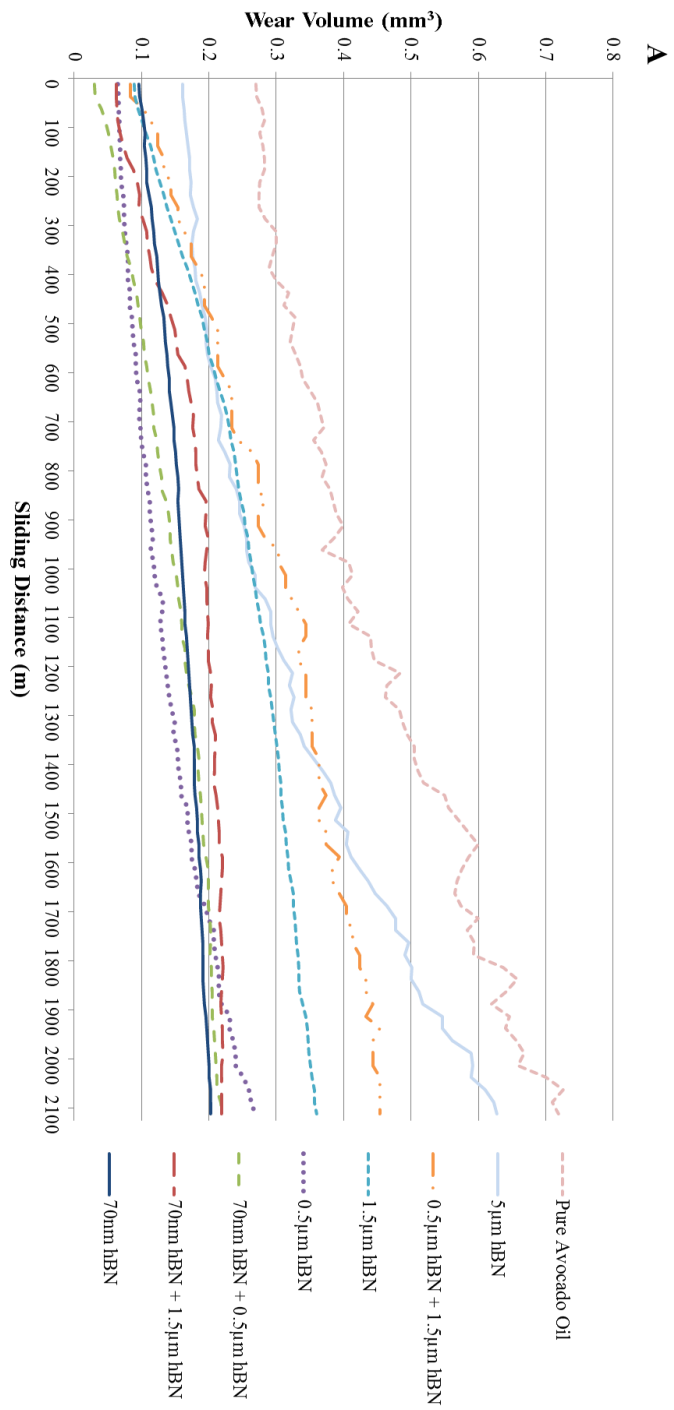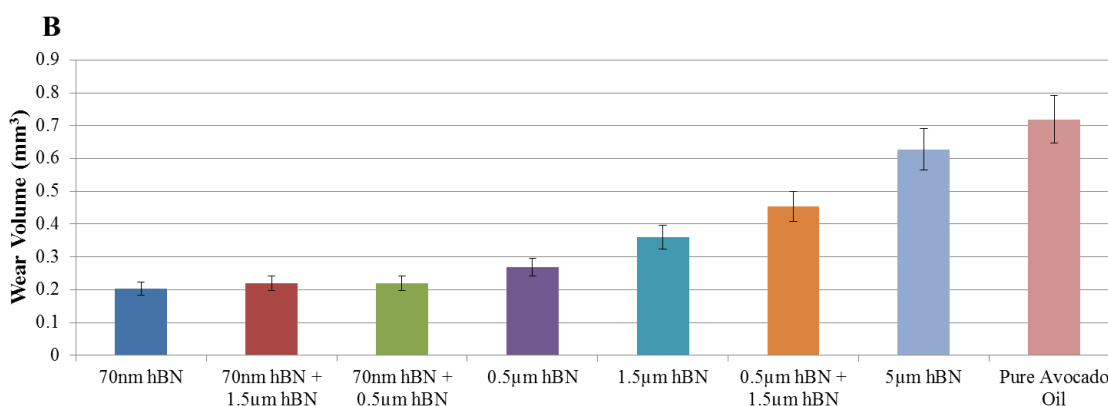
Figure 5.12: Wear volume for boron nitride particles in avocado oil (a) variation of the wear volume with sliding distance and (b) variation of the wear volume at the end of the experiments

Table 5.8: Influence of particle size on the wear volume in avocado oil particulate mixtures

Particle Combination	Wear Volume (mm^3)	Percent Difference (%)
70nm hBN	0.2028	-72[1]
70nm hBN + 1.5μm hBN	0.2190	-18[2]
70nm hBN + 0.5μm hBN	0.2202	-39[2]
0.5μm hBN	0.2683	-63[1]
1.5μm hBN	0.3600	-50[1]
0.5μm hBN + 1.5μm hBN	0.4537	26[2]
5μm hBN	0.6280	-13[1]
Pure Avocado Oil	0.7191	N/A

[1] Compared to pure avocado oil

[2] Compared to the larger of the two particle sizes

5.4.2.3 Surface Analysis

Figures 5.13 through 5.15 show the scanning electron micrographs for the various avocado particulate mixtures. It can be seen that the in Fig. 5.13, the worn surface of the pin all have a relatively similar and small worn surface, despite posttest effects of oxidation. These figures represent the worn surfaces of the 70nm hBN, 70nm and 1.5µm hBN combination, and 70nm and 0.5µm hBN combination mixtures. The diameter of the worn pin surfaces are in agreement to their corresponding wear volumes as they all wore approximately 0.21 ± 0.01 mm^3. Figure 5.14 shows the SEM images for the 0.5µm hBN, 1.5µm hBN, and 0.5µm and 1.5µm hBN combination mixtures. These images show a slight increase in surface roughness and wear track diameter amongst themselves and when compared to the images shown in Fig. 5.13. This is expected as the friction and wear rate increase for each of these lubricant mixtures. It is interesting to notice that in Fig. 5.14(b) the darker colors are not wear marks, but oxidation that developed on the surface during the posttest analysis. In Fig. 5.14(c), wear debris can be seen to have accumulated on the edge of the worn surface, whereas in Figs. 5.14(a) and 5.14(e) the wear debris has separated from the worn surface. Figure 5.15 reveals the worn surface for the 5µm hBN particles and the pure avocado oil tests. It is important to observe that the worn surface has noticeably increased in diameter indicative of increased wear. The presence of the larger 5µm hBN particle did result in any increased surface roughness of the worn surface as shown in Fig. 5.15(b). In fact, comparing the high magnification images of 5.15(b) to 5.15(d) showed minimal differences between having the larger particles and having no particles. The relatively smoother worn surfaces could be a result

of the more robust and highly effective monolayer that is able to minimize the asperity contact due to the increase percentage of the oleic acid (C18:1) in the avocado oil. More still the ability of the hBN particles to systematically increase the tribological properties of the avocado oil demonstrates that avocado oil when compared to canola oil does indeed act as a better carrier fluid due to its increased lubricity. Furthermore it can be speculated that under identical testing or operational conditions, the avocado oil would maintain a lower coefficient of friction thereby improving system efficiency as well as prevent surface damage by minimizing wear and surface roughness in the tribo-interface.

| 70nm hBN | 70nm + 1.5μm hBN | 70nm + 0.5μm hBN |
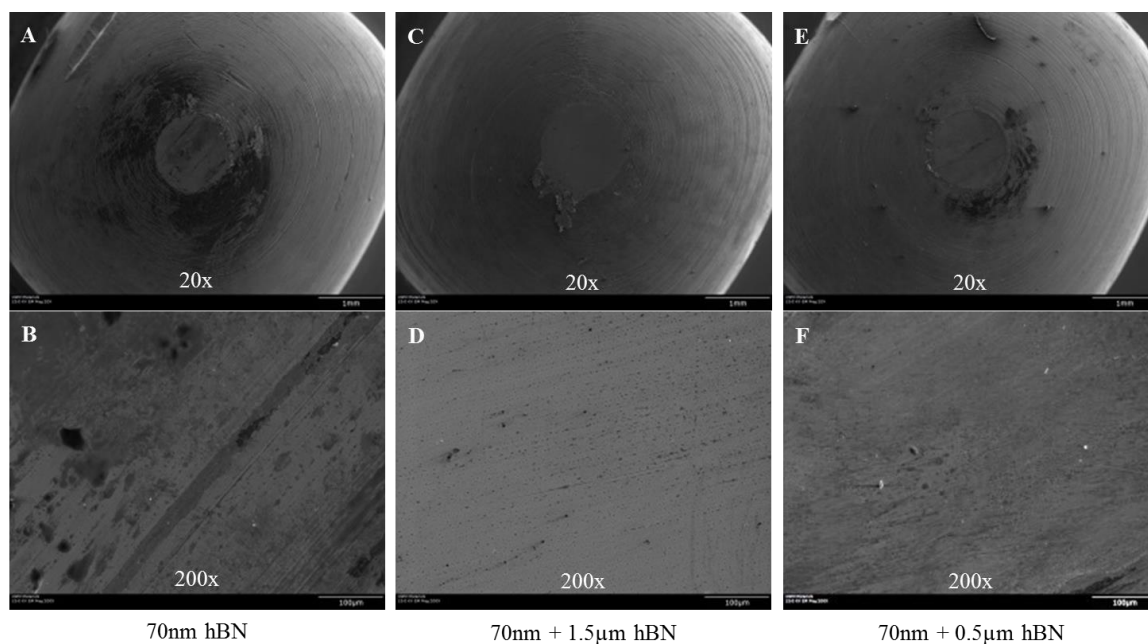
Figure 5.13: SEM images of pin worn surface for various particulate mixtures in avocado oil (a) and (b) 70nm hBN; (c) and (d) 70nm + 1.5μm hBN; and (e) and (f) 70nm + 0.5μm hBN

<table>
<tr><td>A
20x
1mm</td><td>C
20x
1mm</td><td>E
20x
1mm</td></tr>
<tr><td>B
200x
100µm</td><td>D
200x
100µm</td><td>F
200x
100µm</td></tr>
<tr><td>0.5µm hBN</td><td>1.5µm hBN</td><td>0.5µm hBN + 1.5µm hBN</td></tr>
</table>
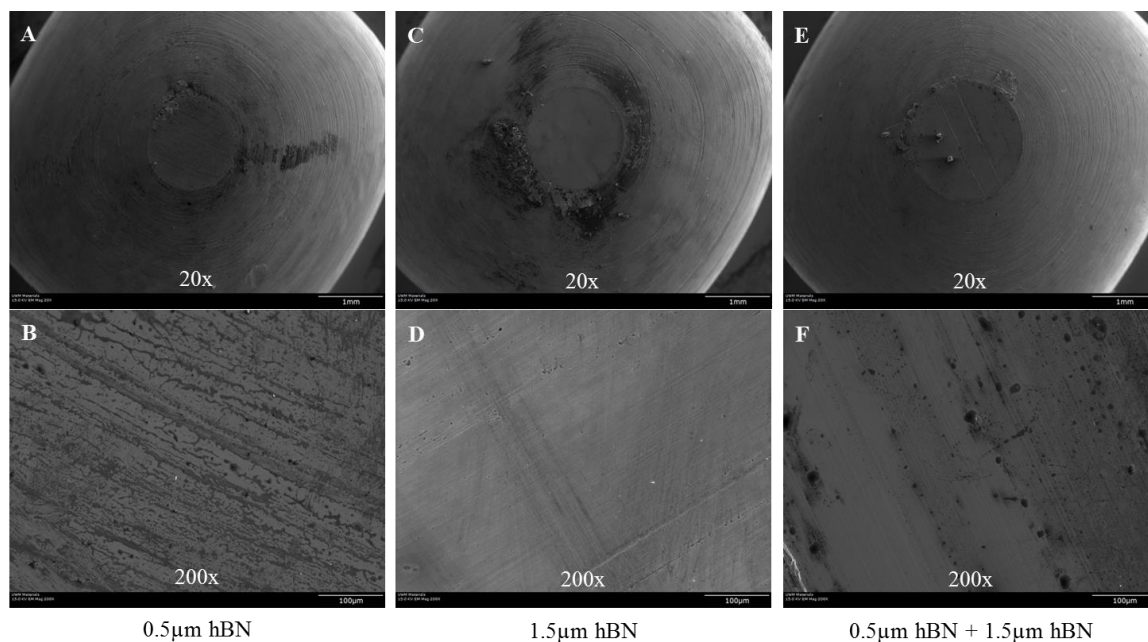
Figure 5.14: SEM images of pin worn surface for various particulate mixtures in avocado oil (a) and (b) 0.5µm hBN; (c) and (d) 1.5µm hBN; and (e) and (f) 0.5µm + 1.5µm hBN
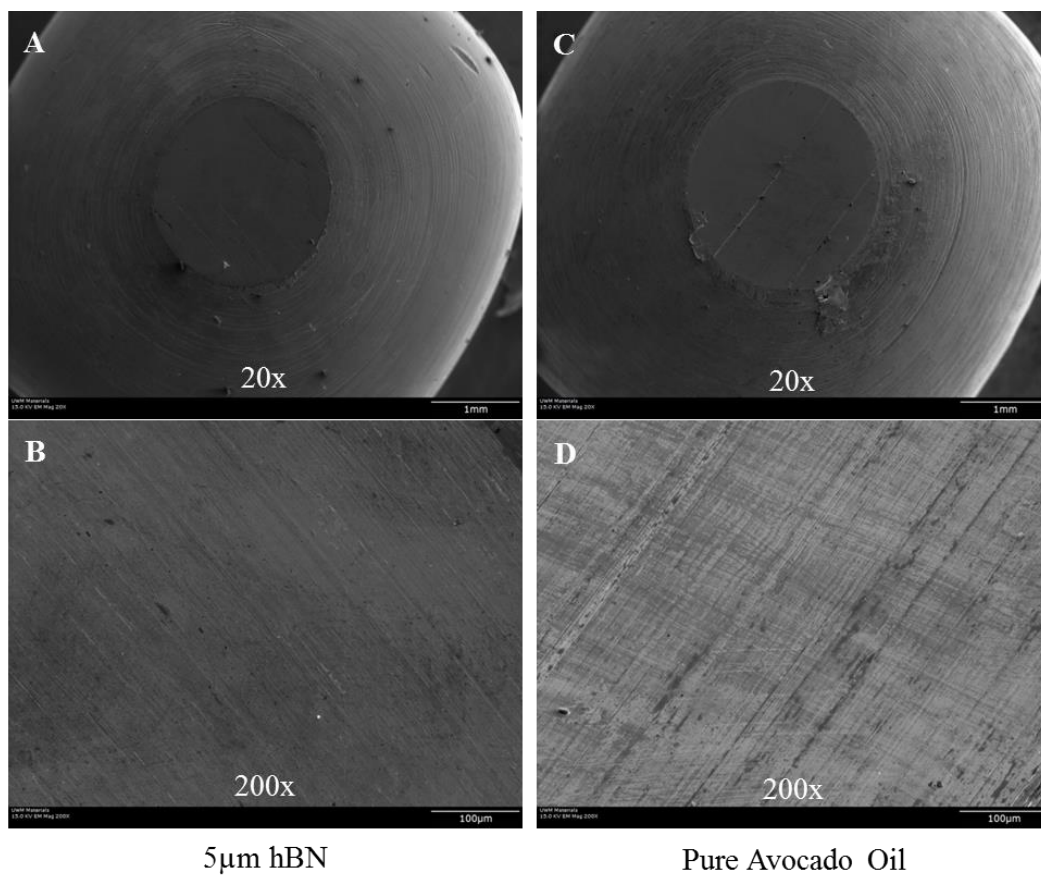
Figure 5.15: SEM images of pin worn surface for various particulate mixtures in avocado oil (a) and (b) 5µm hBN; and (c) and (d) pure avocado oil

5.5 Conclusions

The results of this study illustrate the importance of choosing the appropriately sized boron nitride particle to enhance the lubricity and minimize wear of the tribo-interface. By optimizing the particle size of the boron nitride and selecting a bio-based natural oil such as avocado oil to act as a carrier fluid, a colloidal solution can be established that does not degrade or separate. This in turn allows for a sustainable biolubricant to be developed that has properties that will lower friction and wear, thereby improving a systems energy economy by ultimately conserving more energy. The following conclusions can be drawn from the current research.

- Nano-sized particles were shown to offer the best tribological performance when compared to micron- and submicron-sized particles in canola and avocado oil. This is a result of the colloidal solution not degrading over time and therefore able to continuously maintain the hBN particulate additives in the lubricating interface.

- Particle additives that are larger than the asperities carry a portion of the load between the contacting asperities, resulting in a decrease of friction; however these larger particles are also more abrasive causing higher wear rates that have the potential to cause a rougher final surface finish.

- Nano-sized particles in natural oils coalesce in the asperities valleys creating a superior protective transfer film between the contacting surfaces that thwarts friction and wear. The nano-sized particles' ability to improve the tribological performance

remains to exist in mixtures containing submicron- and micron-sized boron nitride particles.

- A larger particle size to initial surface roughness difference results in a high surface roughness of the softer material after sliding contact and a larger particle-to-particle size difference decreases the surface roughness and the friction coefficient.

- Natural oils with higher levels of oleic acid such as avocado oil exhibit superior tribological properties (i.e. lower friction and wear) when compared to natural oils with lower amounts of oleic acid such as canola oil.

- Avocado oil exhibited less surface damage than canola oil with lower wear rates and a relatively smoother surface finish when using nanometer, submicron, and micron-sized hBN particulate additives.

Chapter 6 The Influence of Surface Roughness and Particle Size On the Tribological Performance of Environmentally Friendly Bio-based Lubricants with Boron Nitride Particulate Additives

6.1. Introduction

Bio-based lubricants derived from vegetable oils have been used as lubricants in lowering friction and preventing wear since antiquity [16, 24, 106, 107, 110, 111, 321]. At the start of the 20th century, investigations into the properties of bio-based lubricants have received much attention due to the fact that 50% of the utilized lubricants worldwide end up in the environment through usage, spill, volatility, or improper disposal [222, 286]. Among these lubricants, nearly 95% are composed of toxic petroleum-based oils that are harmful to environment. Bio-based oils have begun to witness acclaim due to increased environmental efforts to reduce the use of petroleum-based lubricants, depletion of oil reserves, increases in oil price, and higher lubricant disposal costs [6, 222, 286]. Moreover, the emphasis placed on bio-based lubricants is also a result of the increase in demand for ecologically safe lubricants that are environmentally benign, renewable, and provide feasible and economical alternatives to petroleum-based oils [6, 81, 322].

The interest in bio-based lubricants is due to their composition of triacylglycerol made up of esters derived from glycerol and long chains of polar fatty acids that are desirable in boundary lubrication for their ability to adhere to metallic surfaces, remain

closely packed, and create a monolayer that is effective at reducing friction and wear [24, 107, 321]. Recently, investigations involving bio-based lubricants derived from vegetable oils such as canola oil focused on understanding the influence of various fatty acids, their use as neat lubricants, additives in mineral oils, and as carrier fluids for lamellar particle additives in sliding contact [6, 90, 118, 196].

When compared to petroleum-based oils, bio-based lubricants composed of vegetable oils have a higher lubricity, lower volatility, higher shear stability, higher viscosity index, higher load carrying capacity, and superior detergency and dispersancy [56, 81, 90], making them a viable alternative to petroleum-based oils. Bio-based solid lubricants such as boric acid (H_3BO_3) and hexagonal boron nitride (hBN) are well-known solid lubricants for their low interlayer friction, ability to form a protective boundary layer, and accommodate relative surface velocities [6, 90, 92, 113, 194]. These properties of lamellar powder lubricants are a result of their crystal structure, in which atoms lying on the same layer are closely packed and strongly bonded together by covalent bonds, and the layers are relatively far apart due to the weak van der Waals force [9, 11, 195, 197], as illustrated for boron nitride in Fig. 1.12 [113]. These powders are effective in a broad range of applications to lower friction and minimize wear. Despite, their superior performance, lamellar powders can be forced out of the lubricating interface in sliding contact and thus must be replenished [16, 81, 113]. This is often accomplished by adding these powders to liquid lubricants to form colloidal solutions [6, 10, 118, 201-203]. Some lamellar powders such as boron nitride are environmentally-benign and inert to most

chemicals making them an attractive performance enhancing additive to vegetable oils [90, 198, 199].

6.2 Effect of granular particles on tribological performance

The influence of varying sized particulate additives such as graphite, MoS_2, hBN, and boric acid on the friction and wear properties has been well studied in the literature [10, 323-325]. Much of the research has indicated that submicron-sized particle additives improve the tribological properties of the base oil when compared to micron-sized particle additives because their size is on the same order of magnitude as the surface asperities [326-333]. As the particle sizes decrease, research have been able to show that nanometer-sized particles in combination with micron-sized particles used as an additive in a liquid paraffin colloidal mixture exhibited better wear resistance, friction-reducing performance, and extreme pressure properties [10]. In another investigation, the effects of lubricants having micron-sized particles and nanometer-sized particles and their combinations were studied for their effect on fuel efficiency. This study revealed that the combination of nanometer and micron-sized particles improved the friction, fuel efficiency (by 35%), and exhaust emissions (by 90%) [334]. Furthermore, in a study by Lovell et al., the influence of boric acid additives of varying sizes was investigated as an additive to a base lubricant [16]. Here, it was shown that the nanometer-sized particles had the most significant improvement on the tribological performance. The addition of nanometer-sized particles to submicron and micron-sized particles resulted in improvements on the performance of the submicron and micron-sized particles by

themselves, thus revealing that the benefit of nanometer-sized particles to coalesce and fill in the asperity valleys was more important than larger particles' ability to carry contact loads between the surfaces. Additionally, the larger particles may act abrasively since they were larger than the surface roughness [16]. It is well known that a tribo-system consisting of two surfaces separated by dry third-body particulates will exhibit multiple tribological regimes as a function of the particle size relative to the surface roughness [197, 335]. In an investigation by Menezes et al. [17] they attempted to characterize the domains in which the size of the particle influences the tribological regimes occurring in the interface. Here, if the particulate additives are smaller than a lower bound critical size, P_{lb}, the tribo-interface will experience adhesive wear. On the contrary, if the particulate additives are larger than an upper bound critical size, P_{ub}, the tribo-interface will experience abrasive wear. The speculation behind this theory is such that particles with sizes below the lower bound critical size coalesce in the asperity valleys forming solid rigid masses that promote adhesive wear. Particles above the upper bound critical size, can be greater than or equal to the surface roughness which leads to more abrasive wear. When the particle additives have a size that is between the lower and upper bounds, $P_{lb} < P < P_{ub}$, a tribological regime exists known as quasi-hydrodynamic powder lubrication [335]. In this regime, the particles undergo shearing to accommodate the relative surface velocities while behaving in a similar manner to hydrodynamic lubricants. It is therefore speculated that these effects of particle size to surface roughness govern the tribological performance of powder particle additives. The current research seeks to investigate this theory when the particles are dispersed within a colloidal mixture.

Other research has focused on the relationship between powder particle additive solid fraction and the influence it has on the COF. Experiments by Kabir, et al. have shown that there is a critical solid fraction, v_{cr} for solid particulate additive lubricant mixtures. Solid fraction values below the critical value, revealed that the COF decreased with increasing solid fraction; whereas above the critical value, the COF increased with increasing solid fraction [281]. This parameter provides yet another useful tool for determining the tribological regimes of a particulate lubricant mixture as a function of solid fraction.

Additionally, studying the effects of surface roughness, grind angle, and surface texture on the COF is an important preliminary step in understanding the many variables that influence the tribological regimes present in a tribo-interface. Menezes et al. have shown that the COF and the transfer layer formation are dependent on the direction of the grinding marks and surface texture of the harder surface in a tribo-contact, but remain to be independent of the surface roughness of the harder mating materials [280, 336]. Here, the grinding angle and surface texture effects were attributed to the variation of the plowing component of friction with grinding angle as well as the average slope of the surface profile.

6.3 Experimentation

Pin-on-disk tests at ambient conditions were conducted to characterize the tribological performance of bio-based lubricants composed of canola (rapeseed) oil and hexagonal boron nitride (hBN) particles during sliding contact. In the tests, four types of

hBN particles having sizes of 5 μm, 1.5 μm, 0.5 μm, and 70 nm were combined with the canola oil in a 5% by weight concentration forming a homogenous colloidal solution by mixing the contents in a vortex generator. The hBN particle sizes were verified through SEM [337] and determined to be in the appropriate range as the prescribed average particle size descriptions given by the manufacturer. It is important to note that in the micrographs it was also observed that the sphericity of the particles decreases as the average particle size increases. In the pin-on-disk tests, pins were made of copper (C101) and 440C stainless steel. The disks were made of both copper (C101) and aluminum alloy (Al-2024). Table 6.1 details the pin-on-disk material pairs that were used during the testing. The second material combination was studied for comparison.

Table 6.1: Pin-on-disk material pair for the tests

	Pin Material	Disk Material
Combination #1	440C Stainless Steel	C101 Copper
Combination #2	C101 Copper	2024 Aluminum Alloy

The disks were polished using one of three methods in order to vary the surface roughness with a random surface texture: (1) dry SiC emery paper with grit sizes of 80, 220, 320, 600, and 1200; (2) slurry SiC paste with a grit size of 1200; and (3) 1.0 μm aqueous diamond suspension. Chapter 3 details the surface preparation techniques and the initial surface roughness measurements. The pin-on-disk testing was performed under a 10 N load for a sliding distance of 100 m with a sliding velocity of 33 mm/s at ambient conditions.

6.4. Results and Discussion

6.4.1 Friction Results

Figure 6.1(a) shows the variation of the COF at the completion of the tests when steel pins are slid against copper disks of varying surface roughnesses in the presence of canola oil containing hBN additives of varying particle size. It is important to note that each of the four hBN particle sizes was used as a lubricant additive with each of the different polished disks. For disks with surface roughness (Ra) values of 0.09μm, 0.11μm, and 0.20μm, the COF decreased as the particle size decreased from 5.0μm to 0.07μm. However, for surfaces with R_a values of 0.49μm and 1.25μm, the COF increased as the particle size decreased in the lubricant from 5.0μm to 0.07μm. Note that in Fig. 6.1(a), the 0.07μm particle test conducted on the disk with the Ra value of 1.25μm seems to be an outlier to the witnessed trends. For comparison, similar tests were conducted with copper pins sliding against aluminum disk surfaces of different roughnesses in the presence of canola oil containing hBN additives. Figure 6.1(b) shows the variation of the COF at the completion of the tests. In this figure of a copper pin sliding on an aluminum disk similar trends prevail as observed for the steel pin sliding on a copper disk, where the COF decreases with a decrease in particle size for the surface with a Ra value of 0.22μm. The surface with a Ra value of 0.43μm showed that the COF increased as the particle size decreased. The surface with a roughness value of 0.27μm demonstrated a transformational surface roughness with COF values that did not vary much with surface roughness and contracted to the previous trends.
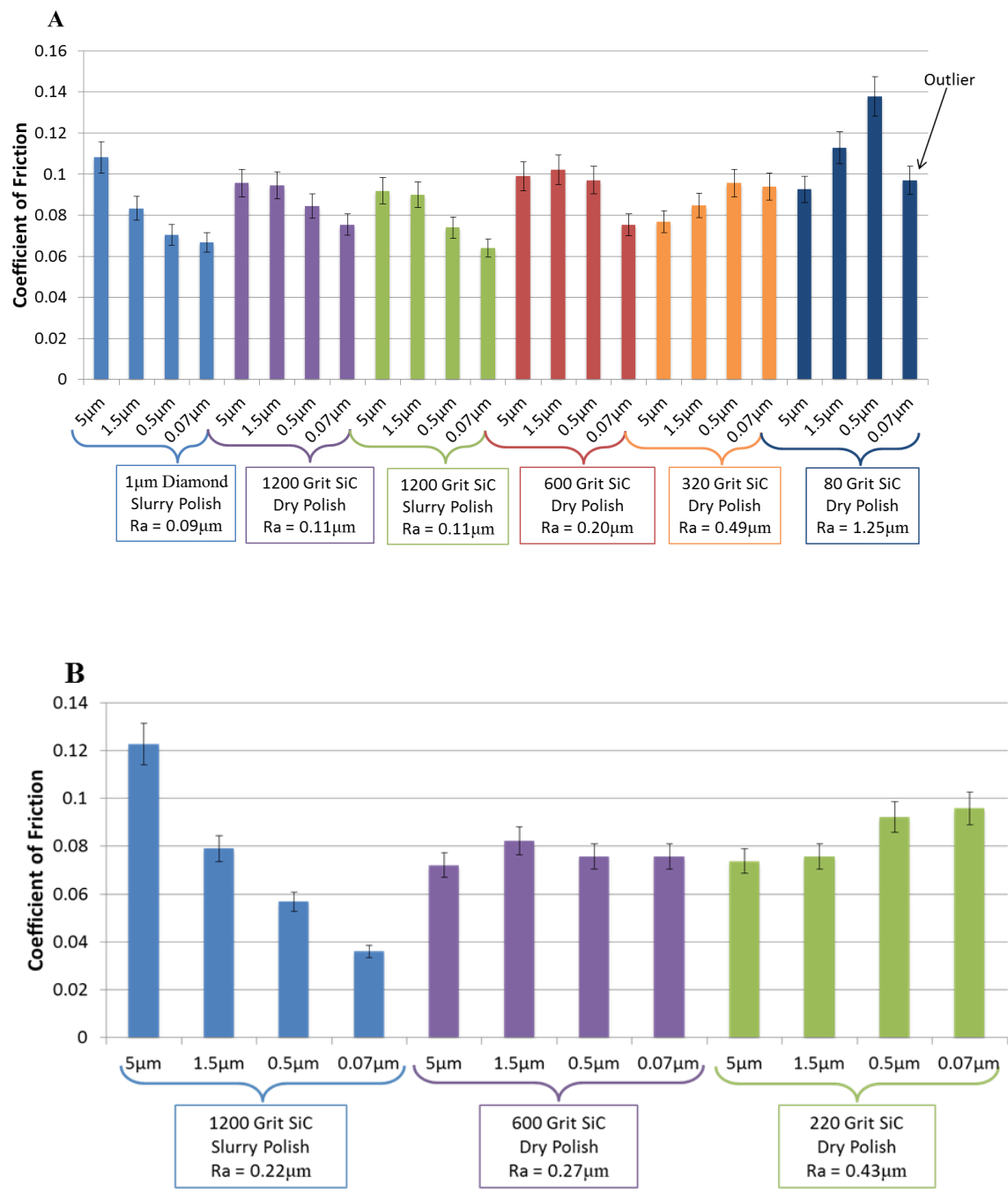
Figure 6.1: Coefficient of friction values at the completion of the tests for different sized hBN particulate mixtures and various disk surface roughnesses (a) steel pin sliding on a copper disk and (b) copper pin sliding on an aluminum disk

The experimental results indicate that the size and shape of the particles present in the canola oil as well as the surface roughness of the disk influence the tribological performance. Examining the average COF for each copper disk of variable surface roughness, it can be seen in Fig. 6.2(a) that as the surface roughness of the disk increases, the COF also increases with a 90% correlation coefficient (R-value) between surface roughness and friction. Similarly, for the aluminum disks, the COF increases with a 99% correlation coefficient between surface roughness and friction.
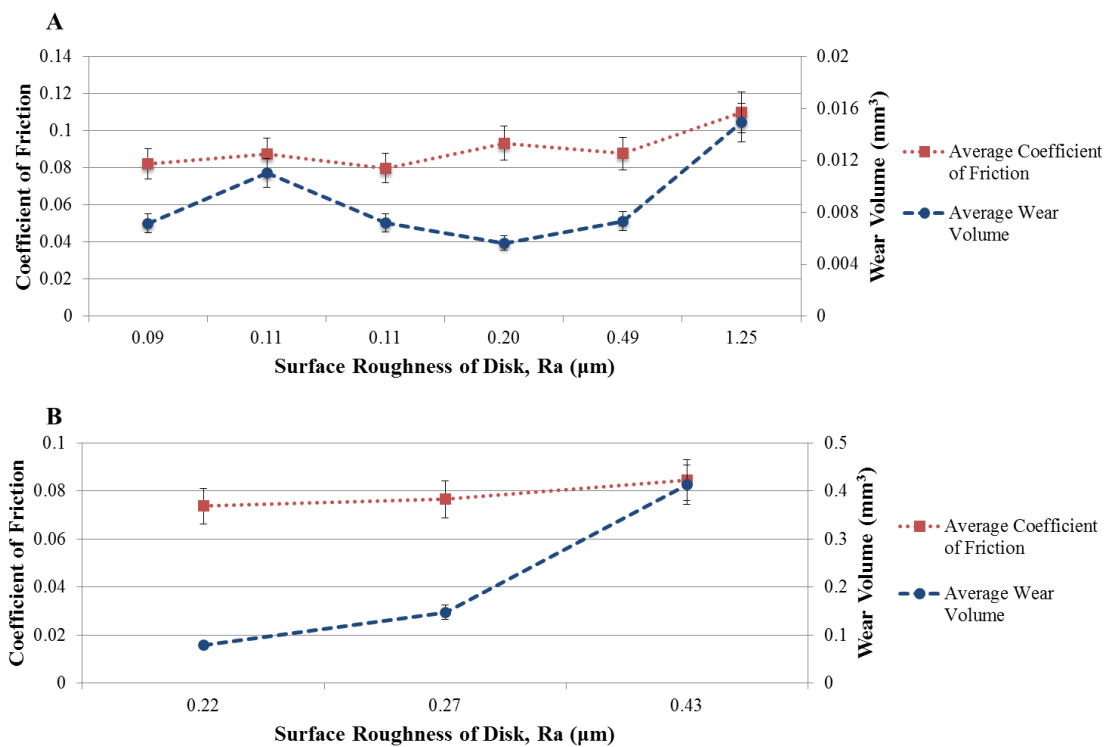
Figure 6.2: Average friction and wear volume values for each surface roughness (a) stainless steel pin sliding on copper disk and (b) copper pin sliding on aluminum alloy disk

The observed trends are in agreement with studies in the literature and fundamental laws of tribology for plastic contact situations that generally occur in metal to metal tribo-interfaces [7, 22, 25, 40, 338]. In a plastic contact, for a moderate range of roughness values, the COF is independent of roughness, where it tends to be high at very low roughness values because of the growth of the real are of contact, however the roughness also tends to be high at very high roughness values because of mechanical interlocking of the asperities. In either case, the effect of particulate additives is not included. Classical tribology in this situation describes the growth in the real area of contact as a result of plastic yielding of the contact zone. As surface roughness increases, there is an increase in the growth of the real area of contact which results in greater asperity contact that must be sheared by means of plastic deformation, this results in increased friction and potentially increased wear. Examining these trends based on particle size for each surface roughness reveals that the COF is indeed influenced by the third body hBN particulate additives present in the lubricant mixture. Table 6.2, shows the correlation coefficient for each roughness value between the COF values for each particle sizes and the particle size as well as showing the average COF calculated from all the particle size tests for individual R_a values.

Table 6.2: Correlation Coefficient, R-value between

hBN particle size and the coefficient of friction

Surface Roughness (µm)	Average COF	R-value	Disk Material
1.25	0.1100	-0.93[1]	C101 Copper Disk
0.49	0.0878	-0.94	
0.20	0.0933	0.51	
0.11	0.0799	0.79	
0.11	0.0875	0.76	
0.09	0.0822	0.99	
0.43	0.0844	-0.81	2024 Aluminum Disk
0.27	0.0765	0.99	
0.22	0.0737	0.97	

[1]Excludes the 0.07µm particle test

From Table 6.2, it is shown that the hBN particles having various sizes play an important role on tribological performance due to their interaction with the varying surface roughnesses. Investigating the relationship between surface roughness and coefficient of friction reveals a 98.4% negative correlation between particle size and the influence surface roughness has on friction. This relationship indicates that as the particle size decreases the influence that smoother surfaces have on friction becomes more dominant. This effect is depicted in Fig. 6.3, where the COF is plotted against each surface roughness for a given particle size. The 5.0µm hBN particles have the lowest R-value of -34% indicating that there is a low correlation between the surface roughness increasing and the coefficient of friction decreasing. The particles having sizes of 1.5µm, 0.5µm, and 0.07µm demonstrated higher correlation coefficients with values of 70%, 95% and

85%, respectively. These values indicate that there is a strong correlation between the surface roughness decreasing and the coefficient of friction increasing. Therefore it can be inferred that these particles behave as lubricious additives to be used in combination with smoother surfaces.

hBN Particle Size (μm)	5.0	1.5	0.5	0.07
Correlation Coefficient	-34%	70%	95%	85%
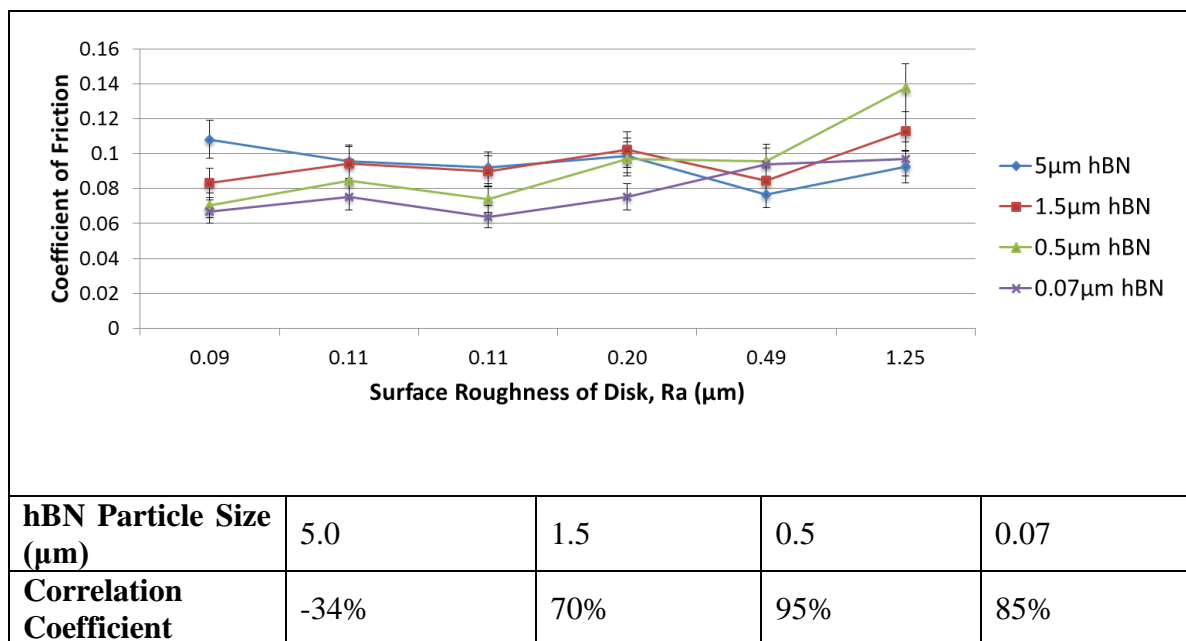
Figure 6.3: Correlation between particle size and the influence surface roughness has on friction; (a) plot of coefficient of friction vs. surface roughness of disk for individual particle sizes and (b) table of correlation percentages for individual particles.

6.4.2 Wear Results

The interaction between particle additives and a rough surface influences the wear rate that occurs in the tribo-interface. Figure 6.4(a) shows the variation of the wear volume at the completion of the tests when steel pins are slid against copper disks of different surface roughnesses. In this figure, it can be seen that for R_a values of 0.09μm,

0.11μm, and 0.20μm, the wear volume decreased as the particle size decreased from 5.0μm to 0.07μm. However for surface with R_a values of 0.49μm and 1.25μm, the wear volume increased as the particle size decreased in the lubricant. In context to the friction tests, the 0.07μm particle used in the lubricant with a surface roughness of 1.25μm where the steel pin slid against a copper disk is not regarded as an outlier, because its wear volume agrees with the current trend of the various particle tests used for this disk. Fig. 6.4(b) shows the variation of the wear volume at the completion of the tests when copper pins are slid against aluminum disk surfaces of different R_a values in the presence of canola oil containing hBN additives of varying particle size. In this figure the wear volume decreases with a decrease in particle size for R_a values of 0.22μm and 0.27μm. For R_a values of 0.43μm the wear volume increases with a decrease in hBN particle size. The resulting similarities in wear trends between the two material pairs shown in Fig. 6.4 demonstrate how the particle additives in combination with differing surface roughnesses influence the wear rate and this effect extends between the two material pairs.
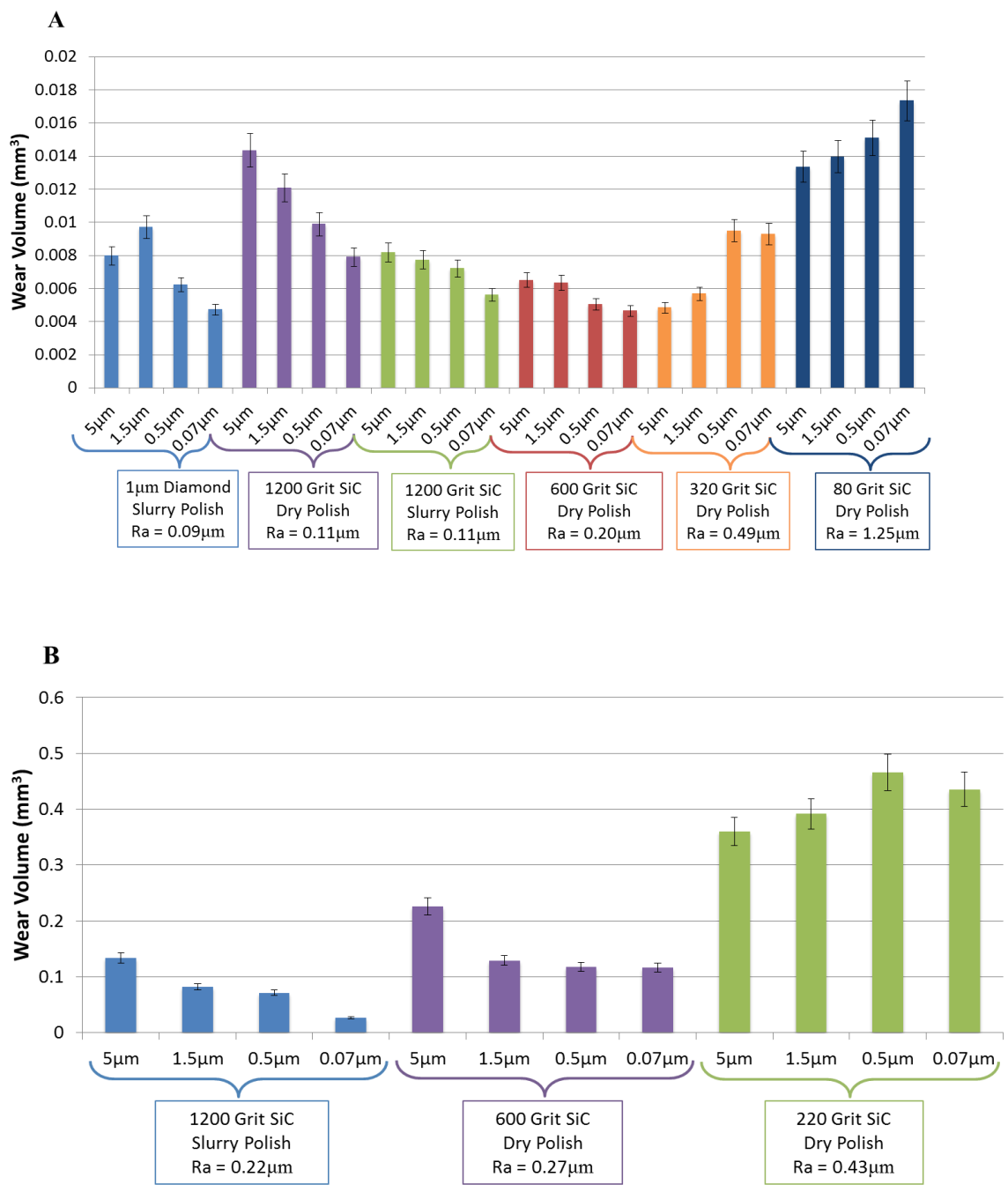
Figure 6.4: Wear volume values at the completion of the tests for different sized hBN particulate mixtures and various disk surface roughnesses (a) steel pin sliding on a copper disk and (b) copper pin sliding on an aluminum disk

The experimental results for wear volume remain in agreement with the friction results as they both indicate that the size and shape of the hBN particulate additives as well as the surface roughness of the counter material influence the tribological properties. Examining the average wear volume for each copper disk having a different surface roughness, it can be seen in Fig. 6.2(a) that as the surface roughness increases, the wear volume also increases with a 77% correlation coefficient (R-value) between surface roughness and the wear volume. Again, for comparative purposes, the aluminum disks were examined, see Fig. 6.2(b), and they revealed a 99% correlation between an increase in surface roughness and an increase in wear volume. These trends are expected in both material pairs because as an increase in surface roughness causes an increase in asperity contact by means of asperity interlocking. As the counter surfaces traverse past each other the increased asperity contacts require shearing in the form of plastic deformation and fracture to occur, which generally results in larger amounts of abrasive wear. Examining the wear volume trends based on particle size for each surface roughness reveals that the wear volume is indeed influenced by the third body hBN particulate additives present in the lubricant mixture. Table 6.3, shows the correlation coefficients between the average wear volume and the hBN particle sizes for a given surface roughness.

Table 6.3: Correlation Coefficient, R-value between

hBN particle size and the wear volume

Surface Roughness (µm)	Average Wear Volume (mm^3)	R-value	Disk Material
1.25	0.0149	-0.78	
0.49	0.0073	-0.85	
0.20	0.0056	0.81	C101 Copper Disk
0.11	0.0072	0.76	
0.11	0.0110	0.92	
0.09	0.0072	0.50	
0.43	0.4132	-0.86	
0.27	0.1475	0.99	2024 Aluminum Disk
0.22	0.0786	0.93	

In Table 6.3, the combined effects of boron nitride particles of differing sizes and various R_a values of surfaces can influence the wear mechanisms to different degrees as observed in the differing correlation coefficients (R-values). Here, surfaces that have a R_a value greater than 0.4µm demonstrate strong negative correlations between hBN particle size and wear volume indicating that as the particle size increases the wear volume decreases. This signifies that larger particles have a greater impact on the tribological performance. On the contrary, also from Table 6.3, surfaces with R_a values below 0.4µm show strong to moderate positive correlations between hBN particle size and wear volume indicating that as the particle size decreases the wear volume decreases. This suggests that with smoother surfaces, smaller particle have a better effect on the

tribological performance. Investigating the relationship between surface roughness and wear volume reveals a 90% negative correlation between particle size and the influence surface roughness has on wear and is depicted in Fig. 6.5(a) for the copper disk. Similarly, the correlation between surface roughness and wear volume was determined to be 99% for the aluminum disk. These correlations indicate that as the surface roughness decreases, the wear volume also tends to decrease, and the influence of smaller particle size becomes greater. In Fig 6.5(a) it can be easily observed that generally as the surface roughness increases the wear volume increases and the added effects of particle additives are inversely related. For example in the presence of rough surfaces, larger particles are optimal and in smoother surfaces smaller particles become desired. It can be seen in Fig. 5.2 that as the particle size decreases from 5.0 μm to 0.07μm, the particles undergo a transition from having a plate-shaped geometry to a more spherical-shaped geometry. It can be speculated that the particle size and shape influence the wear mechanisms where smaller particles have a greater impact. This is substantiated here in Fig. 6.5(b) by examining the correlation between surface roughness and wear for each individual particle. As the particle size decreases from 5.0μm to 0.07μm, the R-value (correlation percentage) increases from 33% to 96%, thus revealing the influence that smaller particulate additives have to improve the tribological performance of the lubricant.

hBN Particle Size (µm)	5.0	1.5	0.5	0.07
Correlation Coefficient	33%	50%	87%	96%
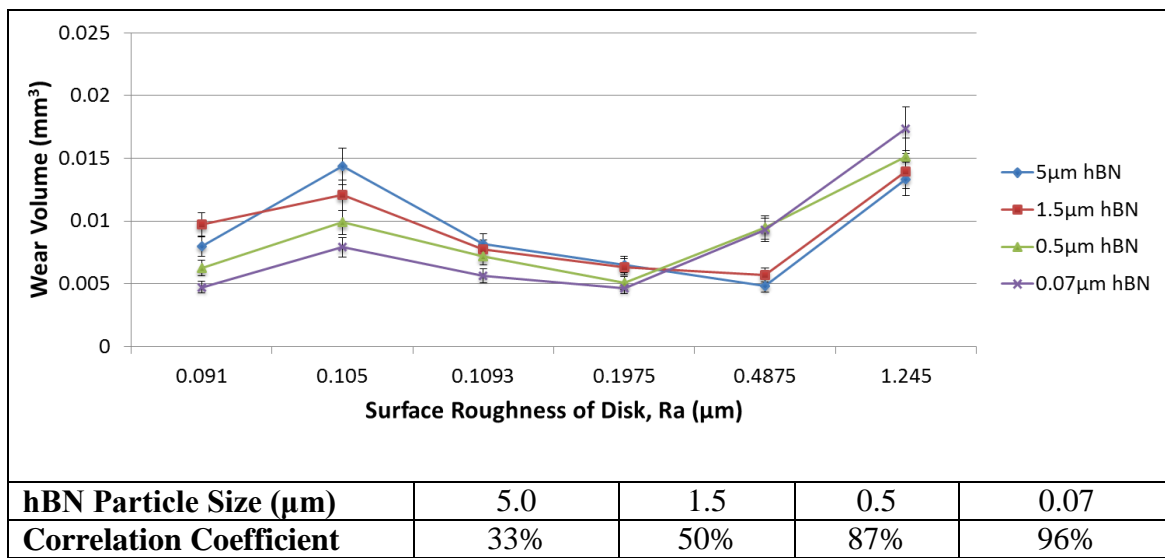
Figure 6.5: Correlation between particle size and the influence surface roughness has on wear volume; (a) plot of wear volume vs. surface roughness of disk for individual particle sizes and (b) table of correlation percentages for individual particles.

6.4.3 Surface Analysis

The effects of surface roughness and particle additive size on friction and wear are further examined through the use of scanning electron microscopy (SEM). The impacts can be visually observed through the micrographs shown in Figs. 6.6 and 6.7 for the copper disks with Ra values of 1.25µm and 0.11µm respectively. In Fig. 6.6, it can be seen that as the particle additives in the lubricant mixtures increase in size, two phenomena are observed: (1) the wear track is decreasing in width and (2) the wear track roughness is decreasing. These observations agree with the tribological results that both friction and wear generally increase with an increase in surface roughness. It can be speculated that in rough surfaces, the smaller particles' ability to coalesce in the asperity valleys and develop an effective transfer film to thwart friction and wear is reduced. As a

consequence to using the smaller particles as shown in Figs. 6.6(a) through (d), with relatively rougher surfaces, there is increased asperity contact resulting in more abrasive wear by plastic deformation. In this case, plowing occurs in the disk where material is removed and pushed to the sides creating grooves parallel to the direction of sliding. As larger particles are introduced into the tribo-interface, Figs. 6.6(e) through (h), the amount of plastic deformation occurring is reduced as the larger particles are able to support more of the asperity contact loads to reduce the friction and wear. Interestingly, Figs. 6.6(a) and (b) represent the wear track of the 0.07μm particulate additive slid again the disk with a Ra value of 1.25μm that was revealed to be an outlier to the witnessed trends of friction. It can be seen in Fig. 6.6(a) that the wear track shows signs of chattering, where the deformed material would actually build up on the pin before being pushed off to the sides of the wear track. This can be seen in the repetitious instances of material conglomeration where chattering took place causing the wear track to have discontinuous grooves as seen in higher magnification in Fig. 6.6(b). The chattering may have caused the test to have lower friction coefficients due to the skipping however it had a negligible impact on the wear rate.
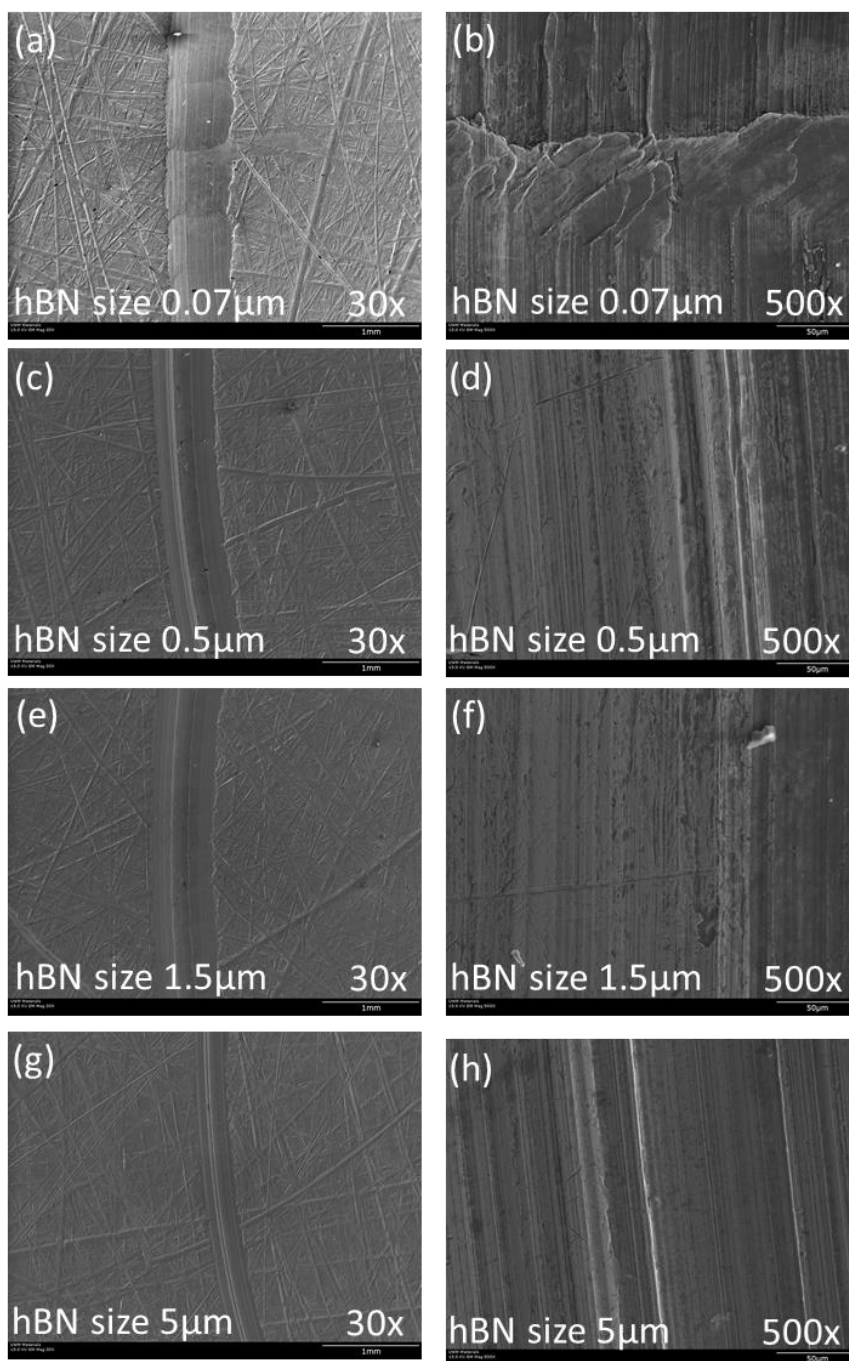
Figure 6.6: SEM micrographs of the wear tracks of the 80 grit SiC polished disk surface (Ra = 1.25μm) (a) & (b) hBN particle size 0.07μm, (c) & (d) hBN particle size 0.5μm, (e) & (f) hBN particle size 1.5μm, (g) & (h) hBN particle size 5μm

Figure 6.7 represent the surface of the wear track for a 1200 grit SiC polished disk surface with a Ra value of 0.11. The micrographs shown in the figure reveal contrasting trends where smaller particles dominate and large particles cause increased friction and wear. It can be seen that as the particle size increases the wear track width increases and the roughness of the wear track also increases. The observations are in agreement with the friction and wear results reported previously. It is inferred these observations are indicative of the smaller particles' ability to coalesce in the asperity valleys creating superior transfer films that lower friction and wear by minimizing the amount of asperity contact. In addition, the micrographs further substantiate through tribological theory that the larger particles behave as a third-body abrasive particle due to their size and plate-shaped geometry, despite their ability to support more of the contact load. When these larger particles having sizes of 1.5μm and 5.0μm traverse across the tribo-interface of a relatively smooth surface they abrade the surface resulting in significant plastic deformation that causes deep wear grooves to be formed as seen in Figs. 6.7(e) through (h).
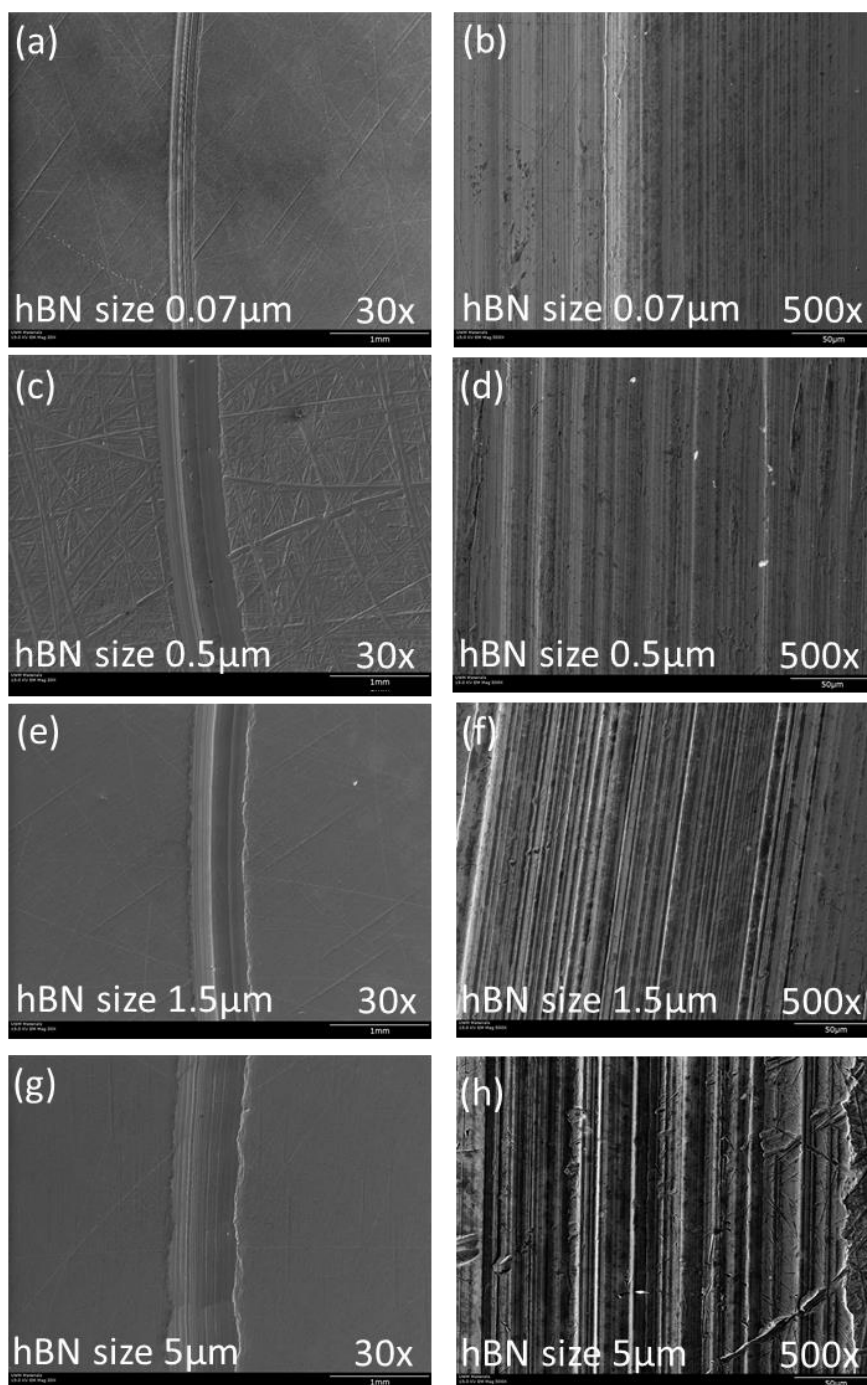
Figure 6.7: SEM micrographs of the wear tracks of the 1200 grit SiC polished disk surface (Ra = 0.11μm) (a) & (b) hBN particle size 0.07μm, (c) & (d) hBN particle size 0.5μm, (e) & (f) hBN particle size 1.5μm, (g) & (h) hBN particle size 5μm

6.4.4 Particle-Size Analysis

The overall influence that particulate additives have on the tribological properties requires investigating both the friction and wear volumes simultaneously. Quantifying the relationship between various tribological properties allows for a determination of an overall correlation coefficient of 0.60 between friction and wear. Table 6.4, shows the individual correlation percentages between friction and wear for each of the surface roughnesses studied.

Table 6.4: Individual correlation percentages between
friction and wear for each surface roughness investigated

Polishing Technique	1 μm Diamond Slurry Polish	1200 Grit SiC Dry Polish	1200 Grit Sic Slurry Polish	600 Grit Dry Polish	320 Grit Dry Polish	80 Grit SiC Dry Polish
Surface Roughness (μm)	0.09	0.11	0.11	0.20	0.49	1.25
R-value	0.60	0.95	0.95	0.78	0.97	0.99[1]

[1]Excludes the 0.07μm particle test

Studying the tribological properties reveals a parabolic trend between particle size and surface roughness that is evident in both the friction and wear values and it is illustrated in Fig. 6.8. Figure 6.8(a) depicts the coefficient of friction values for the copper disks and Fig. 6.8(b) depicts the wear volume for the corresponding copper disks with the parabolic trend lines.
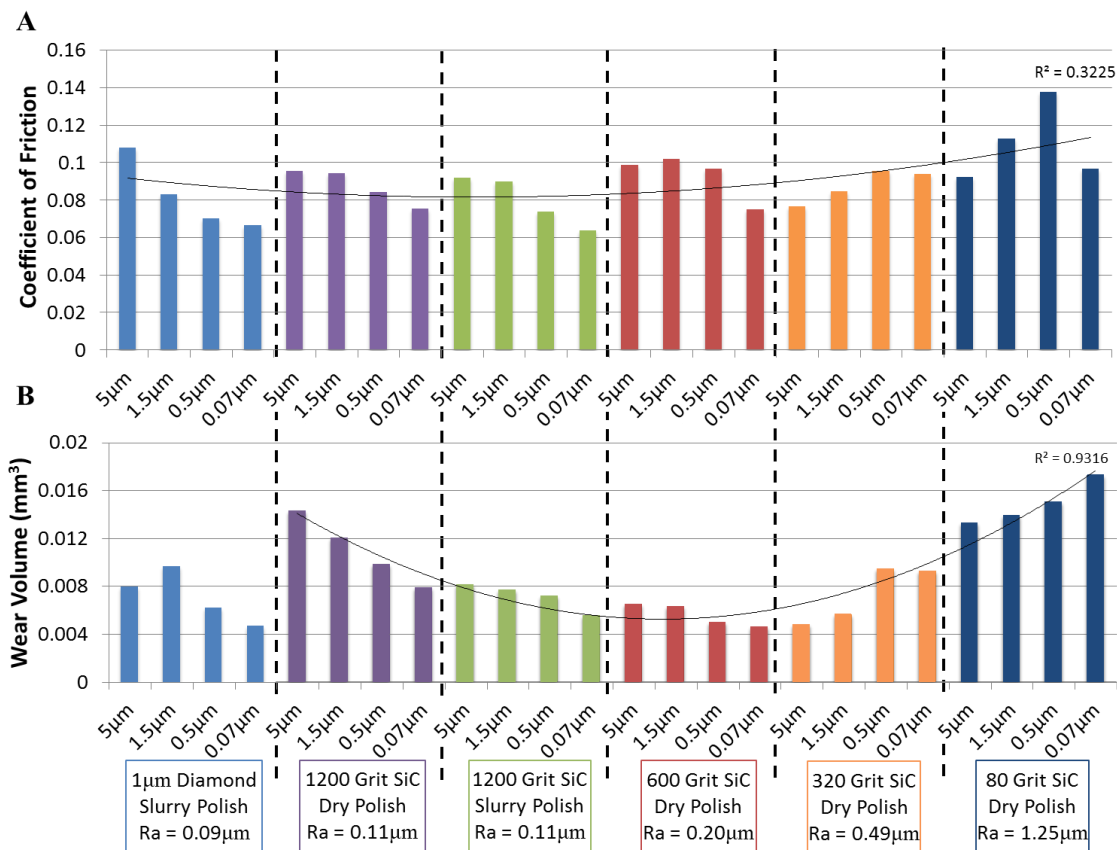
Figure 6.8: Friction and wear results at the competition of the tests for the copper disks (a) depicts the COF values and (b) depicts the wear volumes

From Fig. 6.8, it is speculated that two competing tribological phenomena are at work. On one end of the spectrum, there are smaller spherical-shaped particles particularly the 0.07μm hBN particles that have the ability to coalesce in the asperity valleys due to their small size and create thin lubricious transfer films to lower friction and wear. On the other end of the spectrum, there are the larger more plate-shaped particles that have the ability to support the contact load in the tribo-interface to minimize friction and wear.

Figure 6.9 illustrates the particle-to-surface interaction for the hBN particles and captures a scaled representation of the particle sizes for a given surface roughness.
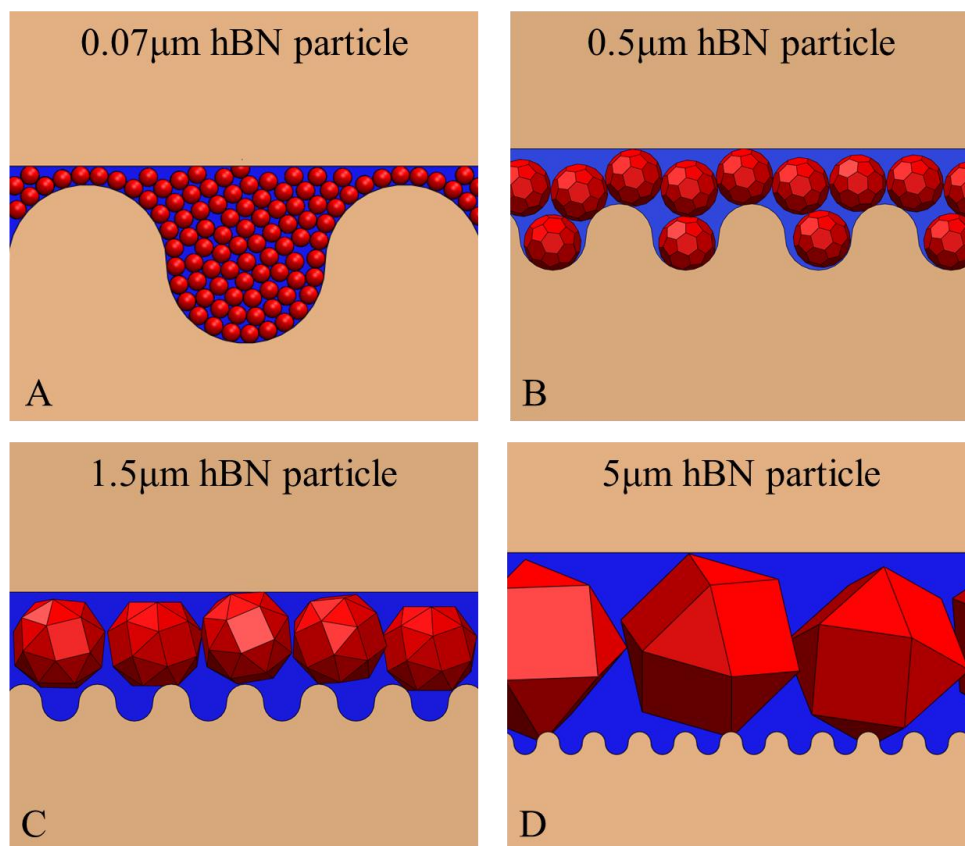
Figure 6.9: Schematic diagram of boron nitride and canola oil particulate mixtures with size (a) 70 nm, (b) 0.5 µm, (c) 1.5 µm, (d) 5.0 µm at the tribo-interface

The disks with Ra values of 0.09µm to 0.20µm show the friction and wear values are the lowest with the 0.07µm particles. This is considered to be a result of the smaller spherical-shaped particles being able to successfully establish an effective transfer film that can minimize friction and wear. The larger particles due to their significantly larger

size and plate-shaped geometry tend to behavior more abrasively thus increasing the friction and wear values as seen in previous work by the author [118]. As the parabolic trend line in Fig. 6.8 reaches its vertex at a Ra value of approximately 0.20μm, the competing tribological mechanisms begin to shift as the disk surface roughness increases. The disks with the surface roughness of 1.25μm and 0.49μm show that the larger particles act to lower the friction and wear, this is due to the competing tribological mechanisms where the larger particles' size and shape dominate. In this scenario, the effects of the larger particles are more beneficial because the surfaces are initially of a 'high' roughness where larger particles can physically move amongst the larger surface asperities to minimize further asperity contact in the tribo-interface by carrying a larger portion of the contact load. When the surface roughness is beyond the size of the smaller spherical particles such as the 0.07 μm hBN particles, the smaller particles ability to coalesce in the asperity valleys to lower friction and wear is minimized due to the overly rough surface where development of an effective transfer film is obstructed.

The trends demonstrated in Fig. 6.8 were for the first combination material pair between the 440C stainless steel pin sliding on the C101 copper disk. These trends are also evident in the second material pair where a C101 copper pin is sliding on a 2024 aluminum alloy disk illustrated in Fig. 6.10. Examining these results, shown in Figs. 6.1(b) and 6.4(b), demonstrate that the tribo-interactions between the hBN particles and the surface roughness are also affected by size and shape of the particles and surface roughness. The disks polished with the 220 grit emery paper had a surface roughness of 0.43μm. In this study, the COF and the wear rate decrease as the particle size increases

with an 81% and 86% correlation. This demonstrates that the presence of larger particles on a rough surface is more significant than the smaller particles despite the fact that the larger hBN particles have a more abrasive tendency as a result of their plate-shaped geometry as shown in Fig. 5.2. The disks polished with the 600 grit emery paper had a surface roughness of 0.27μm. These values revealed a transition in the tribological properties. As seen in Fig. 6.10, the COF and the wear rate steadily increase as the particle size increases with a 99% correlation. This demonstrates that as the surface roughness begins to decrease, the influence of the smaller particles begins to dominant and the larger plate-shaped particles begin to behave abrasively reducing the tribological performance. The disks polished with the 1200 grit emery paper had a surface roughness of 0.22μm. In this study, as the particle size increases, the COF and the wear rate increase sharply with a 97% and 93% correlation. These results illustrate that as the surface roughness continues to decrease, the influence of the smaller particles to lower friction and wear becomes paramount. Here, the smaller spherical-shaped particles are superior for their ability to coalesce in the asperity valleys establishing a thin, smooth, solid lamellar film between the contacting surfaces thus providing them the ability to decrease the friction coefficient and wear rate. Moreover, the abrasive nature of the larger plate-shaped particles increase the wear rate of smooth surfaces demonstrating their diminishing tribological advantage on a smooth surface as compared to a rough surface.

A

B
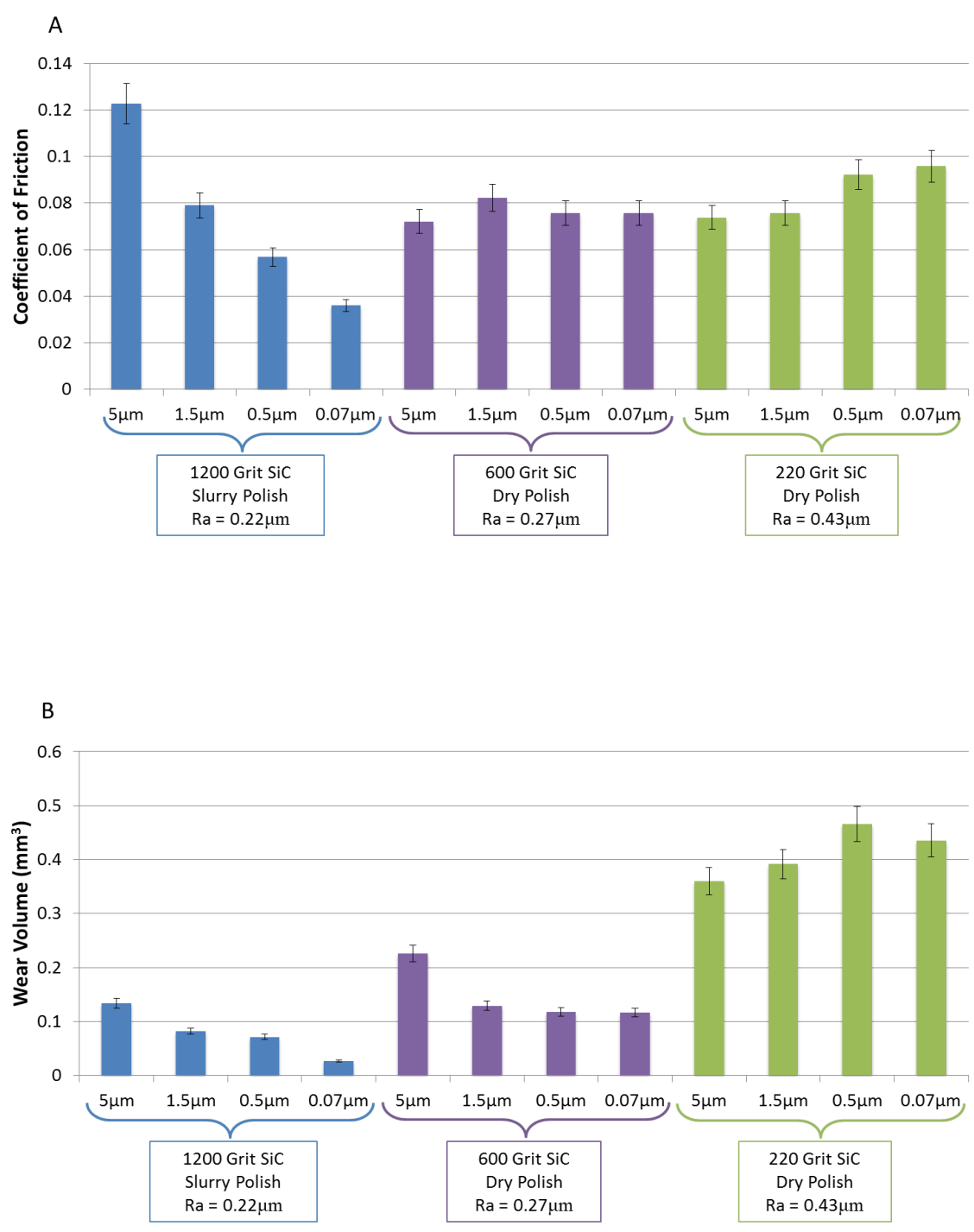
Figure 6.10: Friction and wear results at the competition of the tests for the aluminum disks (a) depicts the COF and (b) depicts the wear volume

6.4.5 Particle-Size to Surface Roughness Index

The use of particulate additives particularly lamellar particles in lubricants is widespread and ubiquitous in the lubrication industry, therefore the choice of the optimal solid particle additive is an important step to enhancing a lubricant. In an attempt to quantify the appropriate choice of a solid particle additive three variables should be considered as seen in this study: particle size, particle shape, and surface roughness. These three parameters establish causal relationships where they can beneficially or adversely affect the tribological performance of a lubricant. To define this relationship a two dimensional hybrid roughness parameter is introduced known as the particle size-to-surface roughness (PSR)-Index (Ψ_{SR}) [118]. The Ψ_{SR} is previously described in Chapter 5 by Eq. (5.3) and is illustrated below:

$$\Psi_{SR} = \frac{|R_a - n_p|}{R_a} \qquad \text{Eq. (5.3)}$$

In Eq. (5.3), R_a is the arithmetic average of the disk surfaces and n_p is the average additive particle size blended with the natural oil. Figure 6.11 depicts the particle size-to-surface index for each of the hBN additives used in this study over a range of surface roughness values.
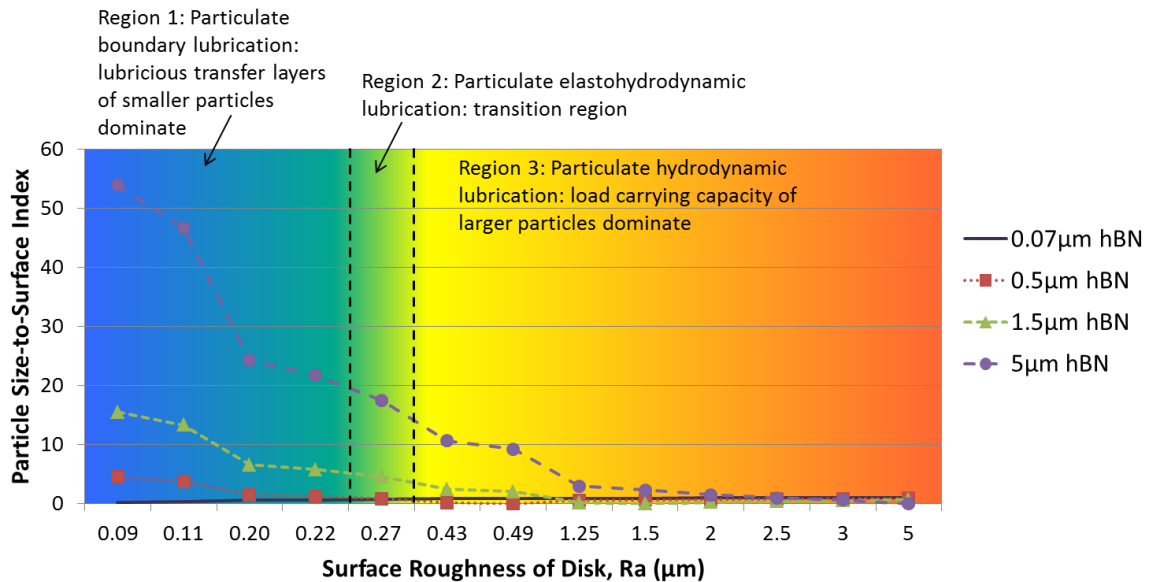
Figure 6.11: Predicted particle size-to-surface indices (Ψ_{SR}) for varying particle sizes and various initial disk surface roughnesses

Within Fig. 6.11, the plot is divided into three regions determined from the current experimental data, in actuality the transition between the regions would be better represented by the color gradient in the background. Here, the represents the first region on the left where thin film lubricious transfer films established by small spherical-shaped particles dominates as witnessed in the experimental results. In this region, the surface roughness is less than approximately 0.27μm (based of the current investigation) and is characterized by the large difference in particle size-to-surface index values. In this region, the smaller particles are able to successfully establish protective transfer films that lower friction and wear. It could be speculated that this region operates in a particulate boundary lubrication regime. On the contrary in region 1, the larger particles due to their plate-shaped geometry behave abrasively when traversing the surface thus

negatively influencing the tribological properties. The second region is a transitional region where the benefits of both the smaller and larger particles begin to converge and is depicted by a transition in colors in the background. In this region the size and shape properties of the particulate additives compete to improve or impair the tribological performance of the lubricant thus acting as a particulate elastohydrodynamic/mixed lubrication regime. The third region in Fig. 6.11 is where the particle size-to-surface index values have begun converging. This is indicative of the surface roughness increasing where larger asperities will begin to disrupt and retard the formation of transfer films formed by the smaller particles, making them unproductive. In this region, larger particles dominate where their plate-shaped geometry does not pose a threat to the friction and wear by causing unwanted abrasion. Instead the larger particles are able to successfully traverse the tribo-interface and support more load carrying capacity thus minimize the asperity contact therefore lowering the friction and wear. This regime could be redefined as the particulate hydrodynamic region.

6.5. Conclusions

The goal of this study was to evaluate the influence of particle size, particle shape, and surface roughness on the tribological properties of canola oil-based lubricants with hBN particulate additives. The results of this investigation illustrate the importance of choosing an appropriately sized boron nitride particle to enhance the lubricity and minimize wear in the tribo-interface. By choosing the appropriate particle size based on a pre-defined known surface roughness the combined effects of the particulate additive in

the lubricant can enhance the tribological properties. Furthermore, by selecting a particulate additive that is environmentally benign such as boron nitride and selecting a bio-base oil such as canola oil to act as a carrier fluid, a sustainable biolubricant can be developed that has properties that will lower friction and wear, thereby improving system efficiency and reliability. The following conclusions can be drawn from the current research.

- The ability of particulate additives to improve the tribological performance of bio-based lubricants is influenced by the surface roughness of the counter materials and the particle size and shape.

- Particle size and particle shape (i.e. change in sphericity) compete to improve or impair the tribological performance of the lubricant and can influence different particulate lubrication regimes.

- A new a 2D hybrid roughness parameter was introduced, the particle size-to-surface roughness, Ψ_{SR} and used to define the relationship between particle size, particle shape, and surface roughness.

- New particulate lubrication regimes were proposed and based off the Ψ_{SR} values to define the lubricating mechanisms: particulate boundary lubrication, particulate elastohydrodynamic lubrication, and particulate hydrodynamic lubrication.

- Rough surfaces benefit tribologically from particulate hydrodynamic lubrication due to larger particles, regardless of their shape, for their ability to carry a portion of the load between the contacting asperities resulting in lower friction and wear.

- Smoother surfaces benefit from particulate boundary lubrication where the smaller spherical particles coalesce in the asperity valleys and create lubricious transfer layers.

Chapter 7 The Tribological Performance of Imidazolium and Phosphonium Ionic Liquid Lubricants: An Advancement in Environmentally Friendly Biolubricants

7.1 Introduction

The use of biolubricants derived from plant oils and animal fats dates back to antiquity. Scientists have known for centuries that biolubricants provide favorable friction and wear properties. Since the beginning of the 20th century, investigations into the properties of bio-based oils have received significant attention due to the fact that 50% of all lubricants worldwide end up in the environment through usage, spill, volatility, or improper disposal [16, 107, 321]. Of these lubricants entering the environment, 95% are derived from petroleum-based oils and are detrimental to many biological ecosystems [152]. More still, within North America along, over 100 million gallons of toxic lubricants drip, spill, and leak into the environment annually. With the advent of petroleum-based oils in the mid-1800s, the use of bio-based oils as lubricants began to decline dramatically. Recently, there has been a reappearance of biolubricants due to increased environmental efforts to reduce the use of petroleum-based lubricants in addition to the depletion of oil reserves, increases in oil price, and rises in lubricant disposal costs [79, 80].

When compared to petroleum-based oils, biolubricants have a higher lubricity, lower volatility, higher shear stability, higher viscosity index, higher load carrying capacity, and superior detergency and dispersancy [6, 17, 96], therefore, they are excellent alternatives to petroleum-based oils. Biolubricants are typically derived from naturally occurring organic substances whose properties and utility vary based on biological factors such as nutrient availability, climate, light, temperature, and water [81, 92, 196]. Despite, these favorable attributes, the largest drawbacks to many bio-based oils are their poor thermal-oxidative stability, high pour points, and inconsistent chemical composition, which have led to the development of chemically modified synthetic biolubricants, the use of stabilizing additives, and ionic liquids [84].

7.2. Tribological Advancements

7.2.1 Conventional Biolubricants

The emphasis placed on biolubricants is a result of the increase in demand for environmentally-friendly lubricants that are less toxic to the environment, renewable, and provide feasible and economical alternatives to traditional lubricants. The interest surrounding liquid biolubricants derived from various bio-based vegetable oils is due to their composition of triacylglycerol molecules made up of esters derived from glycerol and long chains of polar fatty acids. The fatty acids are desirable in boundary lubrication for their ability to adhere to metallic surfaces due to their polar carboxyl group, remain closely packed, and create a monolayer film that is effective at reducing friction and wear by minimizing the asperity contact [106]. Much of the work with bio-based oils has

concentrated on understanding the fundamentals of saturated and unsaturated fatty acids with the bulk of the attention focusing on the use of natural oils as neat lubricants, fatty acids as additives in mineral oils, and bio-based feedstock for chemically-modified lubricants [16, 17, 24]. Recently, biolubricants are finding uses as carrier fluids for lamellar powder additives in sliding contact [6, 16, 98, 118].

Biolubricants composed of lamellar powders such as boric acid (H_3BO_3) and hexagonal boron nitride (hBN) are well-known solid lubricants for their low interlayer friction, ability to form a protective boundary layer, and accommodate relative surface velocities [17, 118]. As with many lamellar powders atoms on the same plane form layers through strong covalent bonds. The layers themselves are held together through the weak van der Waals force, providing the minimal shear resistance, and enabling the low interlayer friction. Lamellar powders are effective in a broad range of environments of extreme pressure and temperature as well as various applications from automotive to aerospace to lower friction and minimize wear [6, 81]. An important property of boron derived lamellar powders is that they are environmentally-benign and inert to most chemicals making them attractive performance enhancing additives to bio-based oils. Experiments have shown that these lamellar particles can be forced out of the contact zone in sliding contact and therefore adding them to natural oils such as canola oil create a superior bio-lubricant [16, 339]. This new class of biolubricant maintains the properties of the powder additives to coalesce and fill in the asperity valleys, thereby establishing a thin, smooth, solid lamellar film between the contacting surfaces, thus decreasing the friction coefficient, wear rate, and surface roughness[6]. In addition, these lubricants

maintain boundary lubrication characteristics by establishing the fatty acid adsorption film that thwarts metal-to-metal contact.

The use of biolubricants composed of natural plant oils or solid lubricants have their merits; however they do have their limitations, which have stifled their ability to be widely accepted within the lubrication industry. The drawbacks to these lubricants are summarized below. For natural oils, they suffer from thermal-oxidative instability, high pour points, inconsistent chemical composition, hydrolytic instability, and a sever susceptibility to biological deterioration. For lamellar powders, they suffer from concentration optimization (which affects their price making these lubricants expensive), unwanted abrasive behavior due to particle size and shape, particles can settle out of the colloidal suspension rendering them useless, large particles can block tubes and capillaries within critical engine parts, and they can clog oil filters in circulatory lubrication systems. These shortcomings of traditional biolubricants ultimately cause economic issues where the lubricants themselves can become very expensive in an effort to modify their properties for the many thousands of potential applications.

7.2.2 Ionic Lubricants

Ionic liquids were originally a novel class of solvents typically consisting of an organic cation in combination with any of a wide variety of organic or inorganic anions, exhibit a number of unique and useful characteristics, including high thermal stability, low melting point, a broad liquidus range, and negligible vapor pressure. The last of these properties, by minimizing solvent losses due to volatilization (*i.e.*, fugative

emissions), have led many to regard ionic liquids as "green solvents", and over the last decade, they have been evaluated in a wide range of applications, including the fabrication of dye-sensitized solar cells [340], the preparation of electrolytes for electrochemical storage devices [341] and batteries, the electrodeposition of metals [135], the recovery of metal ions from aqueous solutions *via* liquid-liquid extraction (LLE) [342, 343], and in the development of separation processes for various organic compounds [344]. Many of the same properties that make ILs useful in these applications also make them good candidates as high-performance lubricants [151].

The use of ionic liquids as lubricants was first reported in 1961, when fluoride-containing molten salts (*i.e.* LiF and BeF$_2$) were subjected to high-temperature (650-815°C) bearing tests [345]. Nearly four decades later, low-melting analogs of classical molten salts, room-temperature ionic liquids (RTILs), were first evaluated as synthetic lubricating fluids [346]. Since this time, considerable attention has been devoted to the utilization of ILs as lubricants. Three main applications have been most extensively explored: the use of ILs as base oils, as additives, and as thin films [136]. When employed as base oils, ILs have been reported to exhibit good tribological performance for steel/steel, steel/copper, steel/aluminum, ceramic/ceramic, and steel/ceramic sliding pairs [140, 347-359]. The negligible vapor pressure of ILs makes them good candidates for use under vacuum and in spacecraft applications [136]. ILs are also effective as additives to the main lubricant (*e.g.,* mineral oils), where because of their tendency to form strong boundary films, that enhance the tribological performance of the base lubricant [136, 360]. Thin-film lubrication employing ILs has been studied by many

researchers with the goal of replacing conventional perfluoropolyether (PFPE) lubricants [357, 358, 361-365].

Although the chemical structure of the cationic and anionic substituents of an IL can vary greatly, the most commonly studied ILs in tribological processes have been those containing a tetrafluoroborate (BF_4^-) or hexafluorophosphate (PF_6^-) anion [366, 367], the result of the superior tribological properties that boron- and/or phosphorus-containing compounds often exhibit under the high pressures and elevated temperatures that lubricants can encounter [368-371]. The frequent use of boron- and phosphorus-containing ILs as lubricants does not imply that either of them is optimum. Rather, ILs based on these anions are commonly studied because they are readily available and low cost [372]. In fact, BF_4^- and PF_6^- have been found to cause corrosion of steel under humid conditions. Moreover other hydrophobic anions, such as bis(trifluoromethanesulfonyl)amide (TFSA) and tris(tetrafluoroethyl)trifluorophosphate (FAP), actually exhibit better tribological properties for steel-steel contact [151, 372, 373]. In general, as the hydrophobicity of the anion increases, both the thermo-oxidative stability and the tribological properties improve [372].

Among the many possible IL cations, the imidazolium ion has probably been studied in the most detail, a result of the high thermal stability of imidazole-based rings [374]. Additionally, the chain length on the imidazolium cation can be readily altered. Increasing the chain length to make the IL more hydrophobic will decrease the friction coefficient in a manner similar to that observed when the anion is made more hydrophobic. In contrast to the improvement in thermo-oxidative stability observed with

hydrophobic anions, however, a decrease in stability is observed with more hydrophobic cations [372]. Nonetheless, ILs with longer alkyl chains and lower polarity have been reported to have excellent tribological properties from low to high temperature (-30°C to 200°C) [375]. Other ILs have been studied with the goal of improving their tribological properties include phosphonium [376-378] and ammonium [356, 357, 379-381].

7.3 Room Temperature Ionic Liquid Lubricants (RTILs)

As the industrial marketplace continues to become more ecologically focused with much of the attention centered on novel approaches to achieve efficient energy conservation and sustainability, new classes of green lubricants are being developed. Much of the development aims at creating environmentally friendly lubricants that contain many of the properties of the aforementioned biolubricants such as polar molecules (similar to the fatty acids), lamellar crystal structure (like the solid lubricants), derived from bio-based feedstock (natural plant-based oils), high thermal-oxidative stability, physicochemical consistency (which natural oils inherently lack), superior lubricity with minimal wear, and require minimal use of additives. Ionic liquids (ILs), particularly those that are fluid at room temperature, represent a promising new class of biolubricants that show potential to improve the limitations associated with petroleum-based oils, bio-based oils, and solid powder additives [132, 136, 140].

In this study, imidazolium and phosphonium ILs with carboylate anions are investigated for their ability to address the environmental, health, economic, and

performance challenges of modern lubricants. Room temperature ionic liquids are molten salts, which typically consist of combinations of a bulky, asymmetric organic cation and an appropriate organic anion with melting points below 100°C and a liquid range beyond 300°C [138, 382]. The atomic structure of an IL is shown in Fig. 2.1. This structure resembles a lamellar solid crystal structure, except with ILs the anions and the cations form ionic bonds to creating layers and these layers are help together with the weak van der Waals force [383]. This structure provides ILs with their liquid lamellar crystal structure [384]. ILs exhibit a number of unique and useful properties that make them well suited as the basis of a new family of lubricants and initial research has already begun investigating the properties of ILs [132, 137, 140, 151, 385, 386]. The appeal of ILs as lubricants becomes even more evident when one considers their many potential advantages over other lubricants including: (1) a broad liquid range (low melting and high boiling point); (2) negligible vapor pressure; (3) non-flammability and non-combustibility; (4) superior thermal stability; (5) high viscosity; (6) miscibility and solubility; (7) environmentally-benign (non-toxic); (8) lamellar-like liquid crystal structure; (9) long polar anion-cation molecular chains; and (10) economical costs [133, 135, 136, 151, 372, 387].

Additionally, ionic liquids have a consistent and easily tailorable chemical composition that affords them the ability to provide the level of thermal-oxidative stability and lubricity required for a variety of applications in the aerospace, automotive, manufacturing and magnetic storage industries [135, 347]. The consistent chemical composition allows ILs to have physicochemical properties that are readily reproducible.

Furthermore, they can be designed to be environmentally friendly by selecting both the cationic and anionic constituents to be non-toxic. In many instances, the ILs can be prepared from non-petroleum resources. Lastly, their capacity to overcome the variety of environmental, cost and performance challenges faced by conventional lubricants makes them a potentially attractive alternative lubricant [136, 138].

The possibility of preparing an ionic liquid capable of functioning as an efficient lubricant while exhibiting a variety of other useful properties is a result of the physicochemical characteristics, inherent tunability, and structural diversity of these novel compounds. Regarding the latter point, it has been estimated that as many as 10^{18} different combinations of anion and cation moieties are possible [134, 139]. Clearly, this vast assortment of possibilities can pose a significant challenge in ionic liquid design. As the number of desired properties increases, the number of possible candidate ILs declines dramatically. Here, for example, the desire for an environmentally friendly lubricant means that the use of highly fluorinated anions is unacceptable [388]. Instead, the use of carboxylic anions based on common food additives (e.g., benzoate$^-$ and salicylate$^-$, are well known preservatives) or artificial sweeteners (e.g., Saccharinate$^-$) are utilized. Similar considerations guide the choice of the cation and suggest that trihexyl(tetradecyl)phosphonium salts (i.e., $P_{666,14}^+$), some of which have been found to exhibit anti-microbial and biodegradable properties, can satisfy many of the desired criteria [148]. Along these same lines, the objective of employing renewable feedstocks for the preparation of the ILs suggests the use of certain 1,3-dialkylimidazolium cations, such as can be derived from fructose or other bio-based feedstock [144, 145, 389-392].

7.4. Experimentation

To access the potential of using ILs as base lubricants, two studies were conducted. In the first study, a series of experiments were performed with two conventional ionic liquids, a phosphonium-based ($P_{666,14}Tf_2N$) and an imidazolium-based ($C_{10}mimTf_2N$) ionic liquid that were both mixed with avocado oil in five different proportions as shown in Table 7.1 to investigate their use as an additive versus a base fluid. In the second study, another set of experiments were conducted by interchanging the cation-anion moieties of the phosphonium-based and imidazolium-based ionic liquids. Multiple IL lubricants having different ion pairs were then compared with various vegetable oils and commercial lubricants. In both studies, experiments were conducted using a Ducom Instruments pin-on-disk tribometer to characterize the tribological performance of the ionic liquids as possible biolubricants.

Table 7.1: Lubricant mixture composition of ionic liquids and avocado oil

Mixture Number	Ionic Liquid Percentage	Natural Oil Percentage	Notation
(1)	0%	100%	0% IL
(2)	25%	75%	25% IL
(3)	50%	50%	50% IL
(4)	75%	25%	75% IL
(5)	100%	0%	100% IL

7.5 Results and Discussions

7.5.1 Study 1: Ionic Liquids as Additives in Natural Oils

7.5.1.1 Friction Results

Figure 7.1, show the variation of the COF for different mixtures of phosphonium-based ILs and avocado oil. In Fig. 7.1(a) it can be seen that the lubricant mixtures generally decrease with sliding distance and eventually reach a steady state value at a sliding distance of approximately 1000m. Figure 7.1(b) shows the final COF values at the completion of the tests.
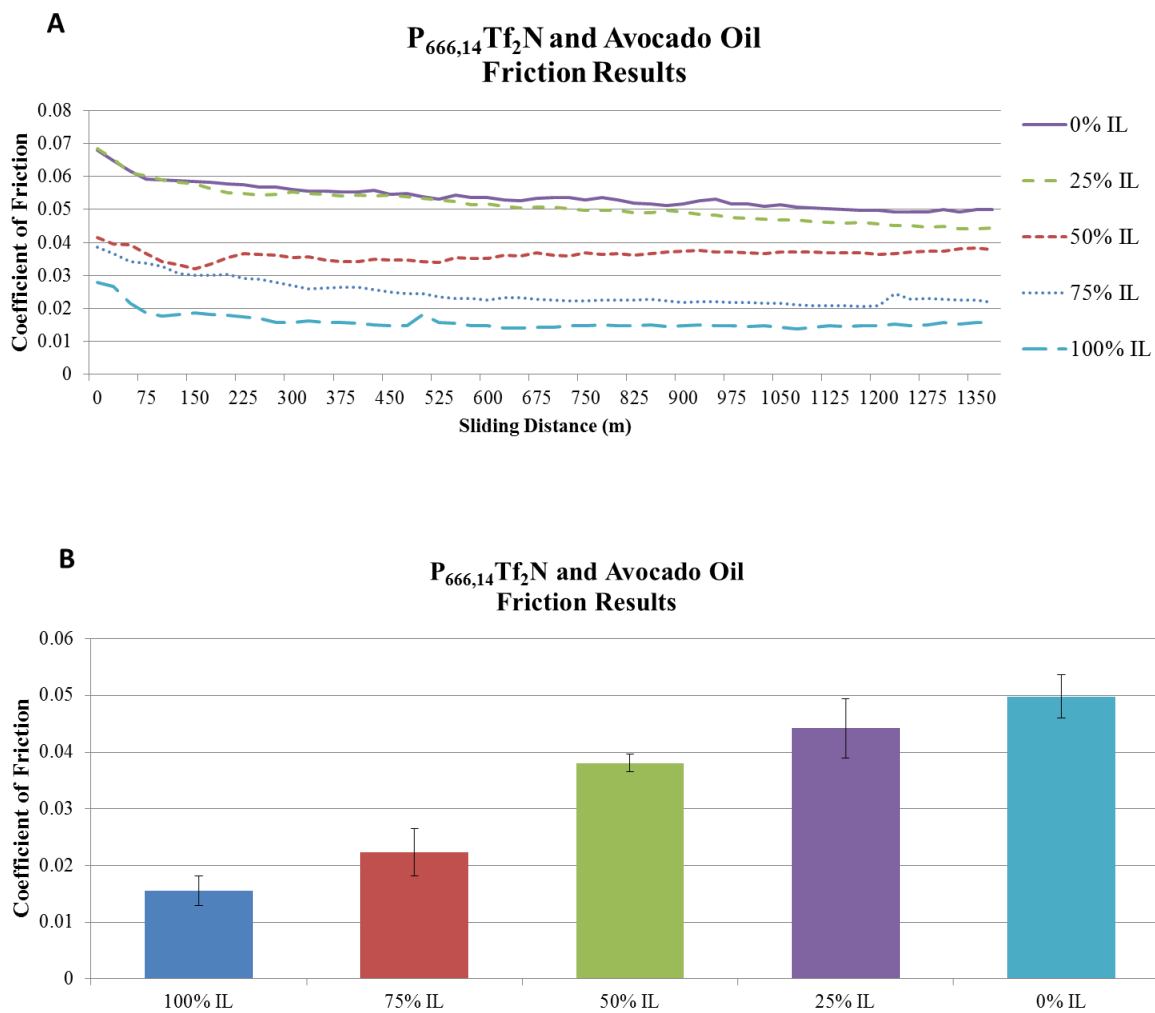
Figure 7.1: Variation of the coefficient of friction for different mixtures of phosphonium-based ionic liquid and avocado oil (a) lubricant mixtures with sliding distance and (b) lubricant mixtures at the completion of tests

It can be seen that as graph moves from left to right the amount of the IL sequentially decreases from 100% to 0%, in 25% decrements. This means that on the left, the 100% IL is a lubricant composed entirely of $P_{666,14}Tf_2N$ and on the right, the 0% IL is a lubricant composed entirely of avocado oil. The lubricant mixtures in the middle are composed of combinations of the two base fluids. Table 7.2 displays the friction results at the completion of the tests. The correlation between the friction results and the composition of the IL in the base fluid is strong with a negative correlation coefficient (R-value) of -0.982 as shown in Table 7.2. This indicates that as the percentage of the IL increases in the lubricant mixture the COF decreases.

Table 7.2: Friction and wear results of the $P_{666,14}Tf_2N$
and avocado oil lubricant mixtures at the completion of the tests

Mixture Number	Ionic Liquid Percentage	Natural Oil Percentage	Notation	COF	Wear (mm³)
(1)	0%	100%	0% IL	0.0155	0.0135
(2)	25%	75%	25% IL	0.0223	0.0185
(3)	50%	50%	50% IL	0.0381	0.0335
(4)	75%	25%	75% IL	0.0442	0.0401
(5)	100%	0%	100% IL	0.0498	0.0507
Correlation Coefficient, R-value				**-0.982**	**-0.991**

Having similar results to the phosphonium-based IL and avocado oil lubricant mixtures, Fig. 7.2, shows the variation of the COF for different mixtures of imidazolium-based IL and avocado oil lubricant mixtures. In Fig. 7.2(a) it can be seen that the

lubricant mixtures continue to decrease with sliding distance and eventually reach a steady state value at a sliding distance about of 1000m. Figure 7.2(b) shows the final COF values at the completion of the tests.

A

B
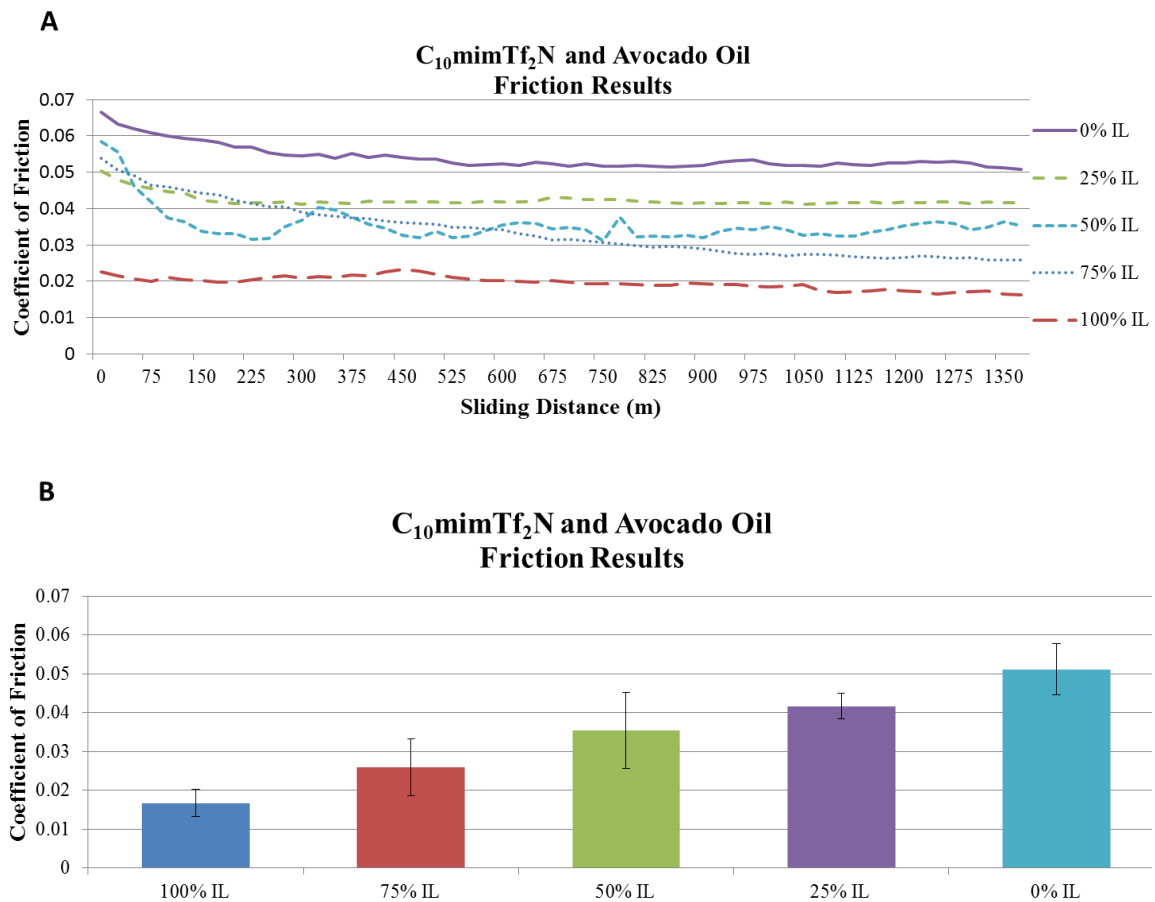
Figure 7.2: Variation of the coefficient of friction for different mixtures of imidazolium-based ionic liquid and avocado oil (a) lubricant mixtures with sliding distance and (b) lubricant mixtures at the completion of tests

Similarly, it can be seen that as graph moves from left to right the amount of the IL sequentially decreases from 100% to 0%. On the left the 100% IL is a lubricant

composed entirely of $C_{10}mimTf_2N$ and on the right, the 0% IL is a lubricant composed entirely of avocado oil. The lubricant mixtures in the middle are composed of combinations of the two base fluids. The correlation between the friction results and the composition of the IL in the base fluid is strong with a negative correlation coefficient (R-value) of -0.998, as shown in Table 7.3. This indicates that as the percentage of the IL increases in the lubricant mixtures the COF decreases.

Table 7.3: Friction and wear results for $C_{10}mimTf_2N$

and avocado oil lubricant mixture at the completion of the tests

Mixture Number	Ionic Liquid Percentage	Natural Oil Percentage	Notation	COF	Wear (mm^3)
(1)	0%	100%	0% IL	0.0168	0.0207
(2)	25%	75%	25% IL	0.0259	0.0267
(3)	50%	50%	50% IL	0.0355	0.0367
(4)	75%	25%	75% IL	0.0417	0.0411
(5)	100%	0%	100% IL	0.0512	0.0508
Correlation Coefficient, R-value				**-0.998**	**-0.994**

The friction results indicate that the presence of either the phosphonium-based or imidizolium-based IL as an additive improves the COF. As detailed in Tables 7.2 and 7.3, as the amount of the IL additive increases to the point where it becomes the majority fluid, effectively becoming the base-fluid, it continues to impart superior friction properties that outperform the avocado oil.

7.5.1.2 Wear Results

Figure 7.3, show the variation of the wear volume for different mixtures of phosphonium-based ILs and avocado oil. In Fig. 7.3(a) it can be seen that the lubricant mixtures generally increase with sliding distance and eventually reaches a steady wear rate at a sliding distance of approximately 1000m in agreement with the COF results shown in Fig. 7.1. Figure 7.3(b) shows the final wear volume at the completion of the tests. It can be seen that as the graph moves from left to right the amount of the IL sequentially decreases from 100% to 0% IL, in 25% decrements.
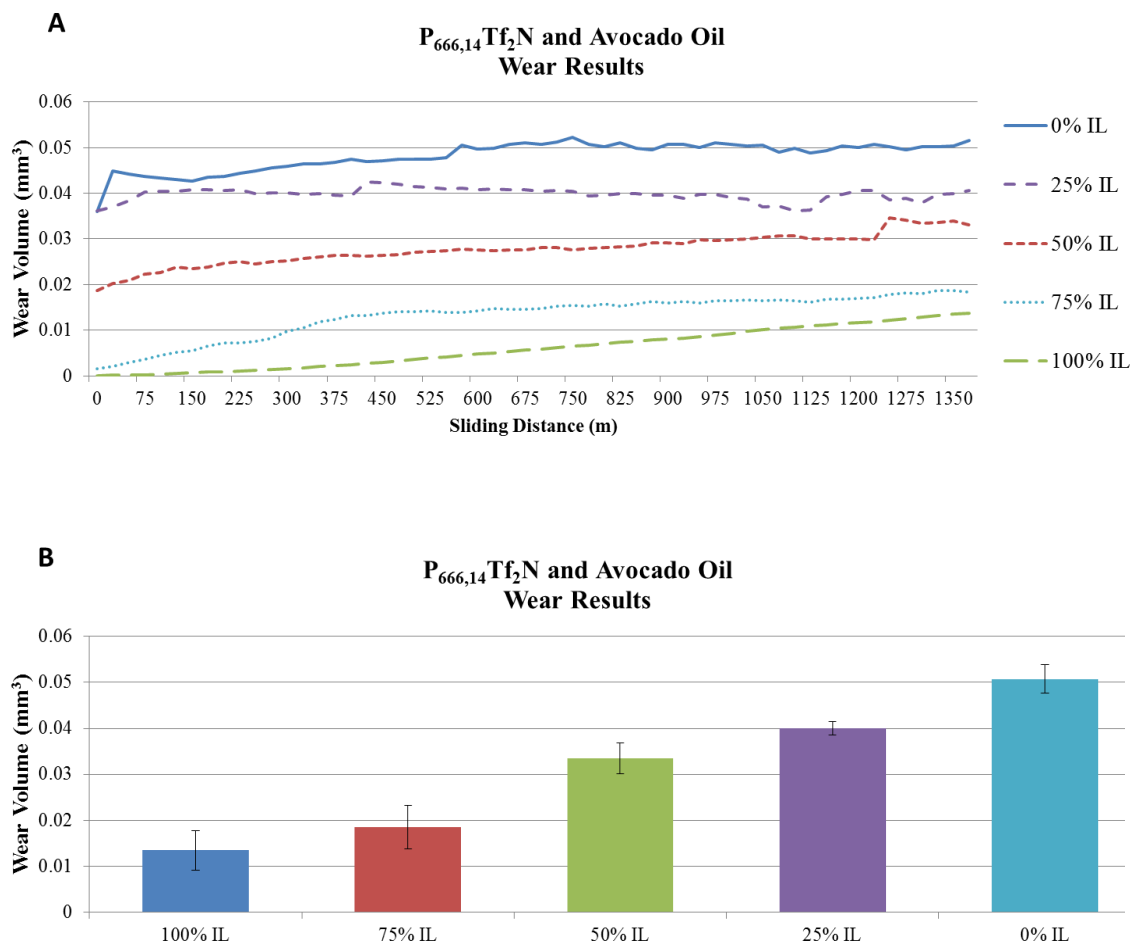
Figure 7.3: Variation of the wear volume for different mixtures of phosphonium-based ionic liquid and avocado oil (a) lubricant mixtures with sliding distance and (b) lubricant mixtures at the completion of tests

On the left the 100% IL is a lubricant composed entirely of $P_{666,14}Tf_2N$; on the right, the 0% IL is a lubricant composed entirely of avocado oil; and in the middle are lubricants composed of combinations of the two fluids. The correlation between the friction results and the composition of the IL in the base fluid is strong with a negative correlation

coefficient (R-value) of -0.998 as shown in Table 7.3. This indicates that as the percentage of the IL increases in the lubricant mixture the wear volume decreases. Figure 7.4, shows similar trends with the imidazolium-based ILs. Figure 7.4(a) shows the wear volume increasing with sliding distance and reaching a steady wear rate at about 1000m. Fig. 7.4(b) shows the final wear volume at the completion of the test.
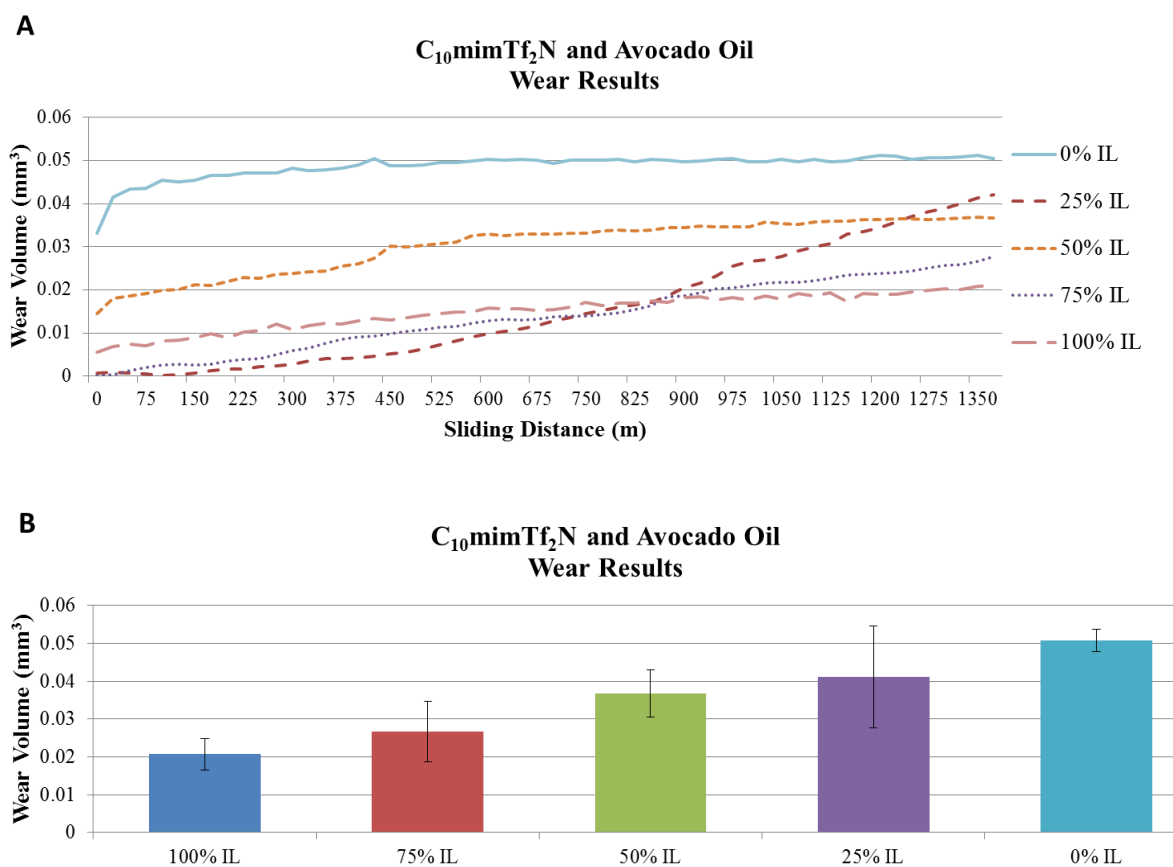
Figure 7.4: Variation of the wear volume for different mixtures of imidazolium-based ionic liquid and avocado oil (a) lubricant mixtures with sliding distance and (b) lubricant mixtures at the completion of tests

It can be seen in Table 7.3 that as the percentage of the IL declines, the wear volume increases with a strong negative correlation, having an R-value of -0.994.

7.5.1.3 Surface Analysis

Figure 7.5, shows the scanning electron micrographs of the worn pin surfaces lubricated with different lubricant mixtures of the phosphonium-based IL and avocado oil. It can be seen in Fig 7.5(a) that when 100% IL is used as the base fluid the worn surface has minimal wear scars and is relatively smooth. Fig. 7.5(b), shows a 50% IL mixture and the surface has become more rough and abrasive. Lastly, Fig. 7.5(c) shows the 0% IL mixture where the wear track is clearly noticeable, the surface is no longer smooth, and significant abrasion by means of plastic deformation caused by plowing has occurred.
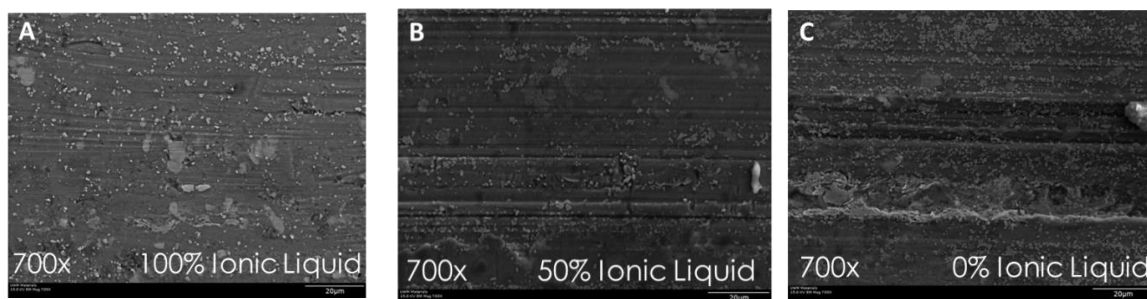
Figure 7.5: Scanning electron micrographs of a worn pin surface lubricated with different mixtures of phosphonium -based ionic liquid and avocado oil (a) 100% IL at 700x magnification; (b) 50% IL at 700x magnification; and (c) 0% IL at 700x magnification

The scanning electron micrographs reveal the positive effects of the ionic liquids present in the avocado oil lubricant mixtures. The friction and wear results indicate that the

presence of either the phosphonium-based or imidizolium-based IL as additives improve the tribological performance. As the amount of the IL additives increase to the point where they become the base-fluid (in the form of a neat lubricant), they continue to impart superior tribological properties that outperform any mixture containing avocado oil. The low friction properties of the ionic liquids are due to (1) their liquid crystal lamellar structure that affords them low internal resistance, (2) their anion-cation moiety that inherently adsorbs on to charged worn metal surfaces; and (3) their ability to establish monolayers that effectively minimize the amount of asperity contact [135, 136, 140].

This study demonstrates that ionic liquids can not only be considered as additives in lubricants, but they can also be considered as base fluids in the form of neat lubricants. In the following investigation, various ionic liquids having different anion-cation moieties will be examined for their friction and wear properties. The IL lubricants will be compared to other natural oils and well-known commercial lubricants from both petroleum-based and bio-base feedstock.

7.5.2 Study 2: Ionic Liquid Anion-Cation Moiety Manipulation

7.5.2.1 Friction Results

Figure 7.6, shows the variation of the coefficient of friction at the completion of the tests for different anion-cation moieties separated into two groups. The first group shown in Fig. 7.6(a), shows a cation study of different ionic liquids all with the same Tf_2N anion.
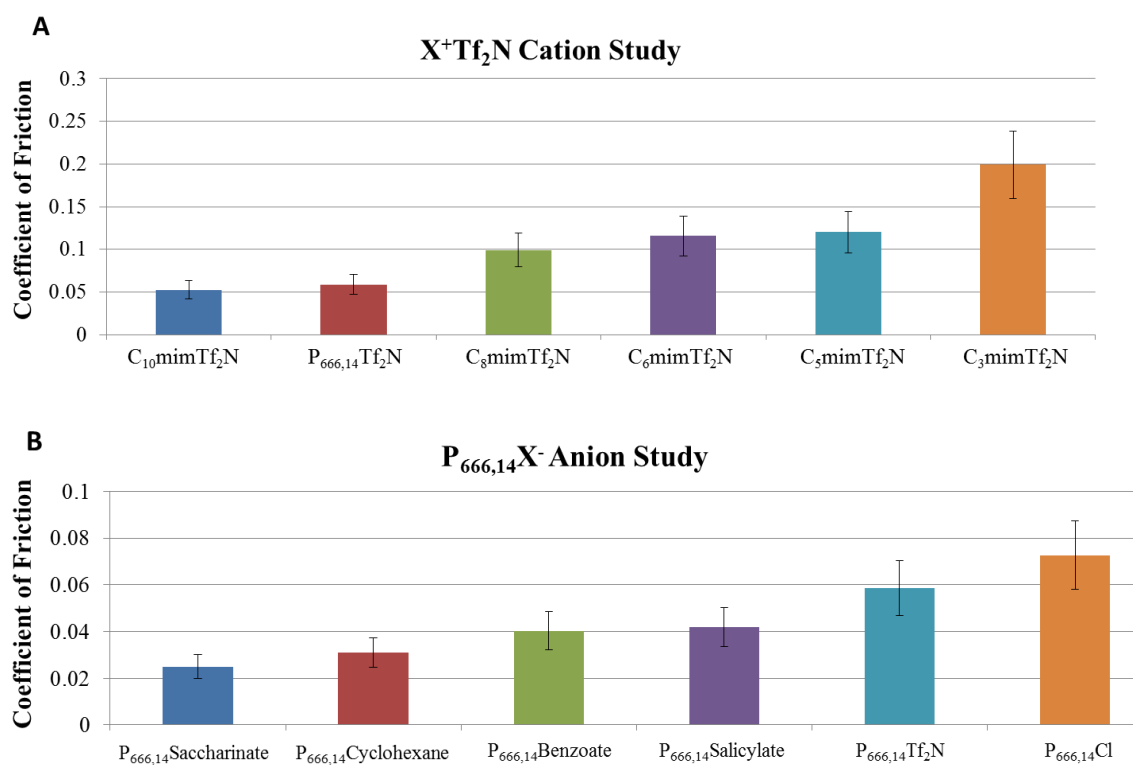
Figure 7.6: Variation of the coefficient of friction at the completion of the tests for different anion-cation moieties (a) X^+Tf_2N cation study and (b) $P_{666,14}X^-$ anion study

Here, an investigation into the influence of cation chain length was performed with the five imidazolium cations having chain lengths of 10, 8, 6, 5, and 3 carbons as well as the phosphonium cation, $P_{666,14}$ having a chain length of 14 carbon atoms. It can be seen in Fig. 7.6(a) and similarly in Table 7.4 that as the COF decreases, the cation chain length increases, with a strong negative correlation coefficient, R-value of -0.878.

Table 7.4: Friction and wear results for X^-Tf_2N cation chain length

Ionic Liquid	Cation	Anion	Chain Length	COF	Wear (mm^3)
$C_{10}mimTf_2N$	$C_{10}mim$	Tf_2N	10	0.0526	0.0342
$P_{666,14}Tf_2N$	$P_{666,14}$	Tf_2N	14	0.0586	0.0263
C_8mimTf_2N	C_8mim	Tf_2N	8	0.099	0.0487
C_6mimTf_2N	C_6mim	Tf_2N	6	0.116	0.0689
C_5mimTf_2N	C_5mim	Tf_2N	5	0.120	0.123
C_3mimTf_2N	C_3mim	Tf_2N	3	0.199	0.137
Correlation Coefficient, R-value				**-0.878**	**-0.894**

It can be seen that having 10 or 14 carbon atoms produces similar friction results with a 10% difference maintaining values of 0.0526 and 0.0586, respectively. The COF percent difference between 10 and 14 carbon atoms is approximately 10%, whereas the percent difference between 10 and 8 carbon atoms for two imidazolium-based cations is 47%. Furthermore, the COF percent difference between 8 and 3 carbon atoms is 50%. The

relative percent differences, indicate the importance of larger alkyl chains in the cation help to promote a thicker adsorbed monolayer film that is more effective at minimizing asperity contact. These results are in agreement with previous investigations of ionic liquids [136].

The second group shown in Fig. 7.6(b) reveals the anion study of different ionic liquids all with the same $P_{666,14}$ cation. This study examines the influence of anion ring size on the phosphonium-based ionic liquids. The anions invested are shown in Table 7.5 along with their corresponding ring size and final COF values.

Table 7.5: Friction and wear results for $P_{666,14}X^+$ anion ring size

Ionic Liquid	Cation	Anion	Ring Size	COF	Wear (mm^3)
$P_{666,14}$Saccharinate	$P_{666,14}$	Saccharinate	2	0.025	0.0139
$P_{666,14}$Cyclohexane	$P_{666,14}$	Cyclohexane	1	0.0309	0.0177
$P_{666,14}$Benzoate	$P_{666,14}$	Benzoate	1	0.0403	0.0460
$P_{666,14}$Salicylate	$P_{666,14}$	Salicylate	1	0.0419	0.0390
$P_{666,14}$Tf2N	$P_{666,14}$	Tf2N	0	0.0586	0.0263
$P_{666,14}$Cl	$P_{666,14}$	Cl	0	0.0727	0.0219
Correlation Coefficient, R-value				**-0.917**	**-0.881**

It can be seen in Fig. 7(b) and in Table 7.5 that as the COF decreases, the anion ring size increases, with a strong negative correlation coefficient, of -0.917. It can be seen that the saccharinate with 2 aromatic rings has the lowest COF value followed by cyclohexane

carboxylate. The cyclohexane has a 6-vertexed ring that does not conform to the shape of a perfect hexagon, thus its non-planar shape is often considered a 3D chair or boat conformation. The benzoate and the salicylate anions demonstrate similar properties as they have very similar aromatic molecular structures consisting of only one ring and a difference of one hydroxyl group as observed in Table 3.1. The Tf_2N and Cl anions have no ring shape and are included for comparative purposes. Interestingly, the ring shaped anions (saccharinate, cyclohexane, benzoate, and salicylate) maintain a significantly lower COF value than the C_{10}mim cation. The difference between the $P_{666,14}$Salicylate and the C_{10}mimTf_2N reveals a 20% difference in the friction values and this difference can only increase as the ring size increases. Therefore the influence of larger ring sized anions tends to improve upon the effect that longer alkyl chain length cations have on lowering friction.

7.5.2.2 Wear Results

The wear results at the completion of the tests for the two groups of anion-cation moieties are shown in Fig. 7.7. The first group shown in Fig. 7.7(a), depicts the cation study of different ionic liquids all with the same Tf_2N anion. Similar trends are observed with the wear volume results as witnessed with the COF results.
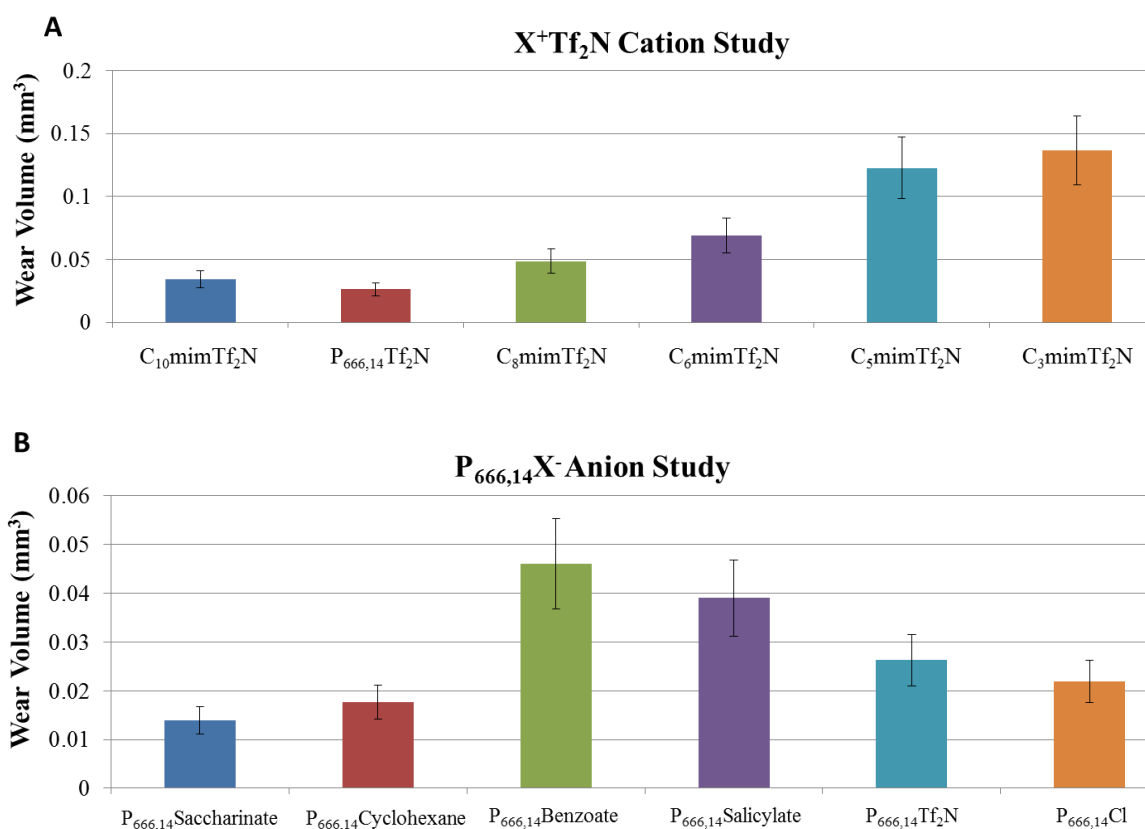
Figure 7.7: Variation of the wear volume at the completion of the tests for different anion-cation moieties (a) X^+Tf_2N cation study and (b) $P_{666,14}X^-$ anion study

The wear results and the R-value are shown in Table 7.4. As the wear volume decreases, the chain length increases with a strong negative correlation coefficient of -0.894. In this Fig. 7.7(a), the $P_{666,14}Tf_2N$ has the lowest COF followed by the $C_{10}mimTf_2N$ and the C_8mimTf_2N. The influence of the longer alkyl chains on the larger asymmetric cations positively influences the wear properties, by establishing an effective monolayer that continues to minimize asperity contact and reduce the wear rate.

Figure 7.7(b) reveals the wear volume at the completion of the tests for the anion study of different ionic liquids all with the same $P_{666,14}$ cation. In this study, the influence of larger anion ring size on the phosphonium-based ionic liquids continues to dominate, where the $P_{666,14}$Saccharinate and the $P_{666,14}$Cyclohexane have the lowest wear rates. The correlation between wear volume and anion ring size once again revealed a strong negative correlation coefficient with a R-value of -0.881 as denoted in Table 7.5. Despite this relatively strong correlation, Fig. 7.7(b) shows deviations in the wear volume trend, where benzoate and salicylate having similar aromatic structures had the highest wear rate. Table 7.5, shows the wear volume and the correlation coefficient for this study.

7.5.2.3 Surface Analysis

Examining the pin worn surfaces of the imizadolium-based and phosphonium-based ionic liquids from the anion and cation studies, revealed the influence of ion size on the tribological properties. Table 7.6 shows the friction and wear values aggregated for both the anion and cation study. Figure 7.8 depict the scanning electron micrographs for the pin worn surfaces for both studies as they increase in surface roughness. The visible increase in surface roughness of the pin worn surfaces is in agreement with the wear volume from Fig. 7.7 or as listed in Table 7.5. Examining the imidazolium-based ILs from the cation study in Fig. 7.8, shows that as the alkyl chain length decreases from C_{10}mimTf$_2$N to C_3mimTf$_2$N, the surfaces become increasingly more abraded by plastic deformation resulting in higher wear and thus increased friction as observed in Figs. 7.6(a) and 7.7(a).

Table 7.6: Friction and wear results for the

phosphonium and imidazolium ionic liquid lubricants

Lubricant	COF	Wear
$P_{666,14}$Saccharinate	0.025	0.014
$P_{666,14}$Cyclohexane	0.031	0.018
$P_{666,14}$Benzoate	0.040	0.046
$P_{666,14}$Salicylate	0.042	0.039
C_{10}mimTf$_2$N	0.053	0.034
$P_{666,14}$Tf$_2$N	0.059	0.026
$P_{666,14}$Cl	0.073	0.022
C_8mimTf$_2$N	0.099	0.049
C_6mimTf$_2$N	0.116	0.069
C_5mimTf$_2$N	0.120	0.123
C_3mimTf$_2$N	0.199	0.137
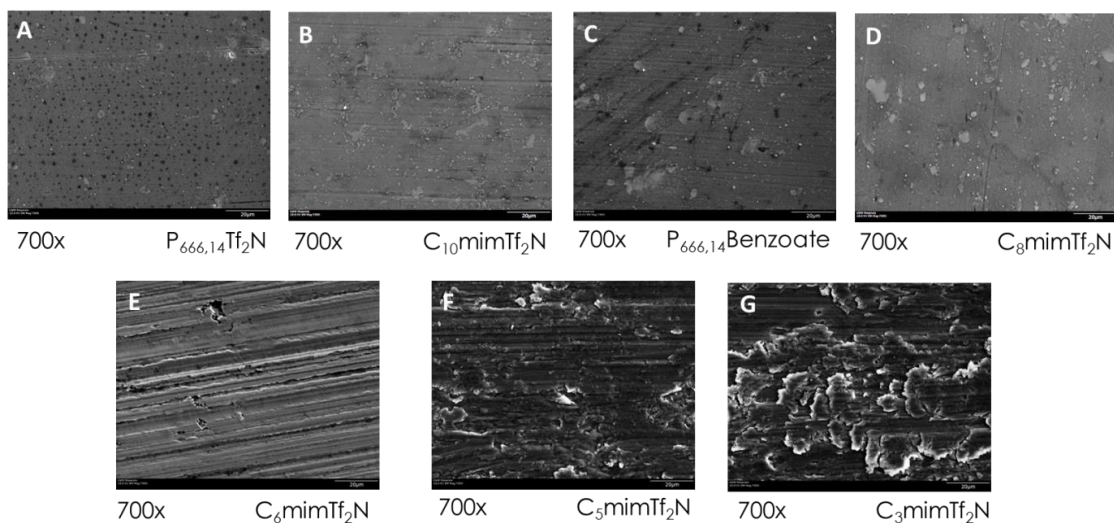
Figure 7.8: Scanning electron micrographs of a worn pin surface lubricated with different mixtures of imidazolium-based ionic liquid at 700x magnification (a) $P_{666,14}$Tf$_2$N; (b) C_{10}mimTf$_2$N; (c) $P_{666,14}$Benzoate; (d) C_8mimTf$_2$N; (e) C_6mimTf$_2$N; (f) C_5mimTf$_2$N; and (g) C_3mimTf$_2$N

The pin worn surfaces of the phosphonium-based ILs show a variety of surface effects. In Figure 7.8(a), the micrograph shows the $P_{666,14}Tf_2N$ worn pin surface as having a slightly smoother surface than Fig. 7.8(b), the $C_{10}mimTf_2N$. On the contrary, the $P_{666,14}Benzoate$ pin shown in Fig. 7.8(c) has a surface roughness that looks to be slightly more rough than the $C_{10}mimTf_2N$, Fig. 7.8(b). This comparison is validated when inspecting the wear volume in Table 7.6. Figure 7.9, shows the micrographs of the pin worn surfaces lubricated with the phosphonium-based ILs. Figures 7.9(a) through (c) show $P_{666,14}Saccharinate$, $P_{666,14}Cyclohexane$, and $P_{666,14}Cl$, respectively.
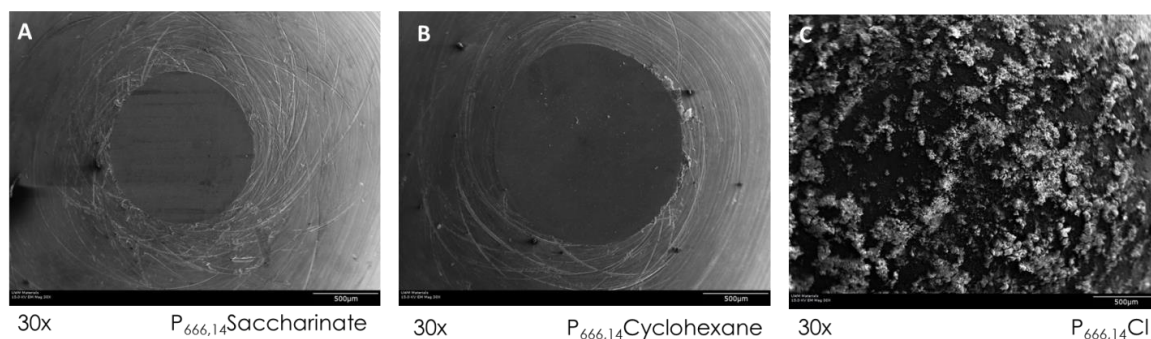
Figure 7.9: Scanning electron micrographs of a worn pin surface lubricated with different mixtures of phosphonium-based ionic liquid at 30x magnification (a) $P_{666,14}Saccharinate$; (b) $P_{666,14}Cylyclohexane$; and (c) $P_{666,14}Cl$

All of these lubricants maintain low wear, while only the $P_{666,14}Saccharinate$ and the $P_{666,14}Cyclohexane$ maintain low friction. Figures 7.9(a) and 7.9(b) show the relatively smooth surface finishes of these two lubricants and the small cross-sectional areas of the pin tips, indicating minimal wear and low friction. The pin lubricated with the $P_{666,14}Cl$, shown in Fig. 7.9(c), does not maintain low friction, in fact it has moderately high

friction as shown in Table 7.2 and Fig. 7.6(b). The micrograph in Fig. 7.9(c) shows a tribo-reaction on the surface of the pin tip. This is speculated to be the result of the IL lubricant causing a tribo-corrosion reaction at the sliding interface. It is well-known that the Cl is corrosive for some metallic pairs [393-397] and in this study it is speculated that the Cl anion contributed to the development of a tribo-chemical reaction that produced a thin reactionary film that resulted in minimized wear, but higher friction. An investigation into the tribo-reaction is beyond the scope of this study as this lubricant was used for comparative purposes only and is not considered environmentally friendly. Studies of the pin worn surfaces reaffirm that aromatic anions and long alkyl chain length cations are important for improved tribological properties. It can be inferred that this is due to density of the monolayer, to remain tightly packed on a surface thus covering more of the surface to prevent unwanted asperity contact and aiding to minimize wear.

7.5.6. Environmentally Friendly Ionic Liquid Lubricants

The anion-cation investigations thus far have shown that that different anionic and cationic constituents influence the performance of ionic liquids. Within the combinations of anion-cation moieties investigated, those ILs with superior tribological properties can server as practical lubricants. Further examination will compare the tribological properties of the ILs in particular, the ecofriendly ionic liquids to conventional ILs, bio-based (natural) oils, and petroleum-based oils. Table 7.7, classifies the lubricants into the four categories based on their source and Table 7.8 compiles all the friction and wear values for the lubricants tested.

Table 7.7: Classification of investigated lubricants based on source

Ecofriendly ILs	Conventional ILs	Bio-based Oils	Petroleum-based Oils
$P_{666,14}$Benzoate $P_{666,14}$Saccharinate $P_{666,14}$Salicylate	$P_{666,14}$Cyclohexane $P_{666,14}$Tf$_2$N $P_{666,14}$Cl C_{10}mimTf$_2$N C_8mimTf$_2$N C_6mimTf$_2$N C_5mimTf$_2$N C_3mimTf$_2$N	Peanut Avocado Canola (rapeseed) Vegetable (soybean) Commercial biolubricant	Synthetic Motor oil

Table 7.8: Classification of investigated lubricants

Lubricant	Classification	COF	Wear
$P_{666,14}$Saccharinate	Ecofriendly IL	0.025	0.014
$P_{666,14}$Cyclohexane	Conventional IL	0.031	0.018
$P_{666,14}$Benzoate	Ecofriendly IL	0.040	0.046
$P_{666,14}$Salicylate	Ecofriendly IL	0.042	0.039
C_{10}mimTf$_2$N	Conventional IL	0.053	0.034
$P_{666,14}$Tf$_2$N	Conventional IL	0.059	0.026
Vegetable (soybean) oil	Bio-based Oils	0.069	0.330
Peanut oil	Bio-based Oils	0.072	0.279
$P_{666,14}$Cl	Conventional IL	0.073	0.022
Avocado oil	Bio-based Oils	0.073	0.322
Canola (rapeseed) oil	Bio-based Oils	0.096	0.318
C_8mimTf$_2$N	Conventional IL	0.099	0.049
Commercial biolubricant	Bio-based Oils	0.106	0.327
C_6mimTf$_2$N	Conventional IL	0.116	0.069
C_5mimTf$_2$N	Conventional IL	0.120	0.123
Synthetic oil	Petroleum-based oil	0.173	0.463
C_3mimTf$_2$N	Conventional IL	0.199	0.137

7.5.3.1 Friction Results

Figure 7.10(a), depicts the final COF values at the completion of the tests for all of the lubricants studied in this investigation. The ionic liquid lubricants maintain superior tribological properties when compared to all other lubricants tested. More specifically, the environmentally friendly ILs ($P_{666,14}$Saccharinate, $P_{666,14}$Salicyate, and $P_{666,14}$Benzoate) exhibit lower coefficient of friction values better than all conventional ILs (except $P_{666,14}$Cyclohexane), bio-based oils, and petroleum-based oil.

Two trends emerge when analyzing the lubricant chemical composition and the friction values. As denoted previously in Fig. 7.6, the COF decreases as the alkyl chain length of the cation increases and as the aromatic ring size of the anion increases. These trends remain true with the ecofriendly ILs, as they consist of the largest cation with 14 carbon atoms in the alkyl chain and the largest anions with single or double aromatic rings that enables them to have low friction. Comparing the ecofriendly ILs to the bio-based natural oils, the ecofriendly ILs outperform the bio-based oils in all circumstances. This is speculated to be caused by the resilient monolayers composed of both anion and cation molecules. Here, the ionic liquids are able to maintain lower COF values due to their polar molecules that can adhere to the charged metallic surfaces, establish a monolayer, remain tightly packed, and minimize asperity contact as well as benefit from their lamellar-liquid crystal structure that affords the ILs the reduced internal resistance during shearing in the tribo-interface. On the contrary, the bio-based oils, maintain high lubricity due to their fatty acid composition consisting of over 70% of oleic acid (C18:1)

and linoleic acid (C18:2). These fatty acids having 18 carbon atoms and one or two double bonds can form a monolayer that promotes low friction, however their properties
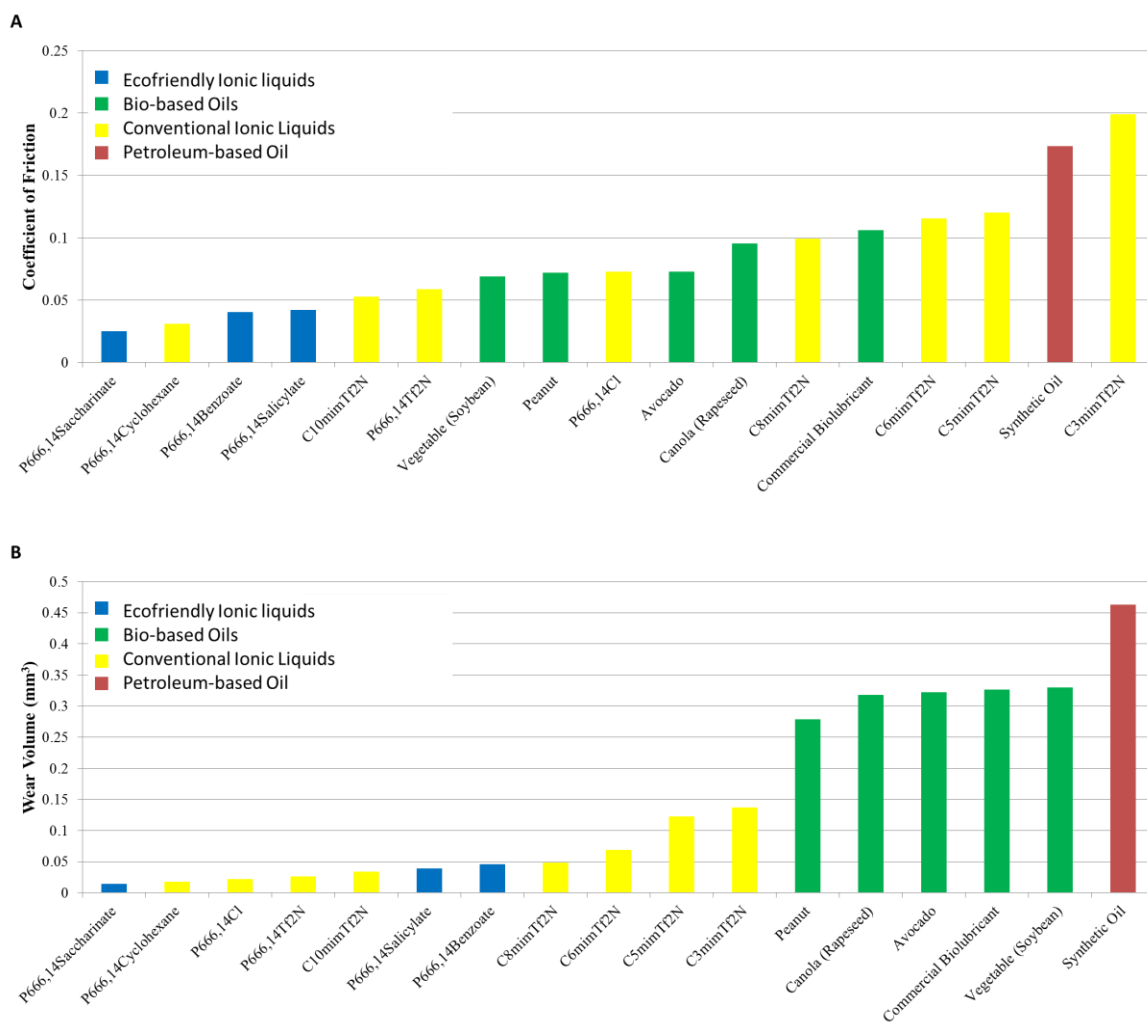
Figure 7.10: Variation of the tribological properties for different mixtures of ecofriendly ionic liquids, natural oils, conventional ionic liquids and commercial lubricants (a) coefficient of friction of the lubricant mixtures at the completion of tests and (b) wear volume of the lubricant mixtures at the completion of tests

are susceptible to rapid oxidation and chemical inconsistency which can impede their tribological performance. The synthetic motor oil tested exhibits the highest friction. The friction results are important because they directly reveal the advantages of ecofriendly ionic liquids that make them well suited as a new class of greener biolubricants.

7.5.3.2 Wear Results

Figure 7.10(b) reveals the final wear volume results at the completion of the test for each lubricant investigated. Here, the ecofriendly IL, $P_{666,14}$Saccharinate demonstrates superior wear resistance. The other two ecofriendly ILs, $P_{666,14}$Salicyate and $P_{666,14}$Benzoate demonstrated moderate wear rates when compared to other ionic liquids. Overall, the ILs as a whole demonstrate exceptionally low wear rates that were beyond those of the bio-based and petroleum-based oils. The synthetic motor oil tested for comparative purposes continues to have the highest wear rate. As revealed in Fig. 7.7, the ionic liquids exhibit trends within the wear volume. As the wear volume decreases the alkyl chain length of the cation increases and the ring size of the anion increases. When examining the trends in Fig. 7.10(b), it seems as if the anion and the cation size effects are competing to lower the wear rate when considering the relatively high wear volumes of the $P_{666,14}$Salicyate and $P_{666,14}$Benzoate ILs. Ultimately, when the largest anion and the largest cation are combined into the $P_{666,14}$Saccharinate, it reveals the lowest wear volume. Examining the bio-based and petroleum-based oils, they have a significantly higher wear rate than the IL lubricants, which again could be a result of the successful monolayer development being composed of anions and cations.

7.5.3.3 Surface Analysis

The tribological results for the ILs suggest that larger asymmetric cations and aromatic carboxylic anions improve friction and wear by providing a sufficiently resilient monolayer that adequately protects the surfaces of the pin-disk interface. These trends also suggest that for the ionic liquids, the combination of the aromatic carboxylic anion and the asymmetric cation both contribute to the wear rate minimization. Figure 7.11, displays micrographs of the disk surfaces after sliding contact. These micrographs further substantiate the effects of the monolayers.
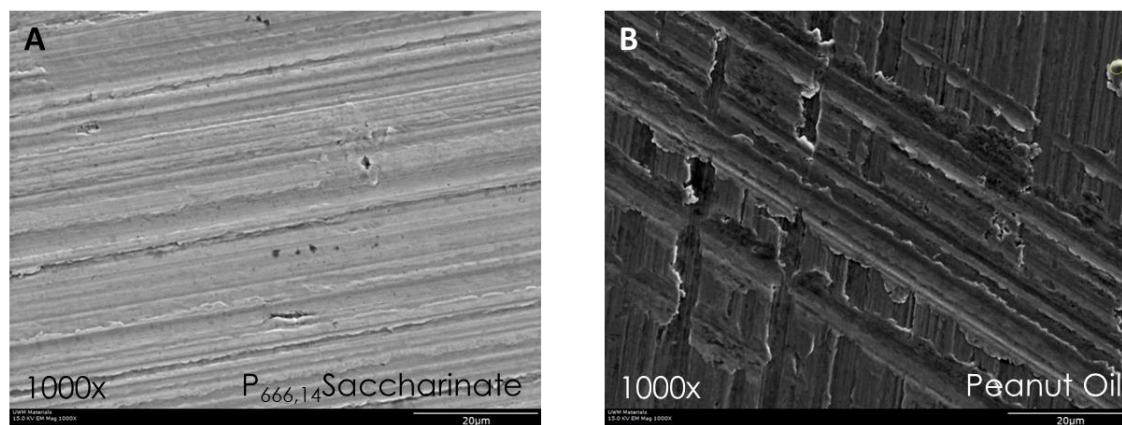
Figure 7.11: Scanning electron micrograph of the worn stainless steel disk lubricated with the (a) $P_{666,14}$Saccharinate and (B) peanut oil

Figure 7.11(a) is a micrograph of the $P_{666,14}$Saccharinate and Fig. 7.11(b) is a micrograph of the peanut oil. It can be seen that the $P_{666,14}$Saccharinate has a smoother surface finish after the test indicative of less wear occurrence. The peanut oil has a much rougher and

more abrasive looking surface suggesting higher levels of wear. In fact this is true, from Table 7.8, the $P_{666,14}$Saccharinate had 0.014 mm^3 of wear occur and the peanut oil had 0.279 mm^3 of wear occur. The peanut oil had about 95% more wear than the $P_{666,14}$Saccharinate. In both of these cases, EDS was performed on the surface and counter-surface of the worn specimen as shown in Fig. 7.12 with $P_{666,14}$Saccharinate in red and peanut oil in blue. The results revealed there was no evidence of a transfer layer or any physicochemical reactions to the materials, thus the only contributing factor to the difference in tribological performance are the lubricants themselves having different physiochemical compositions and structures.
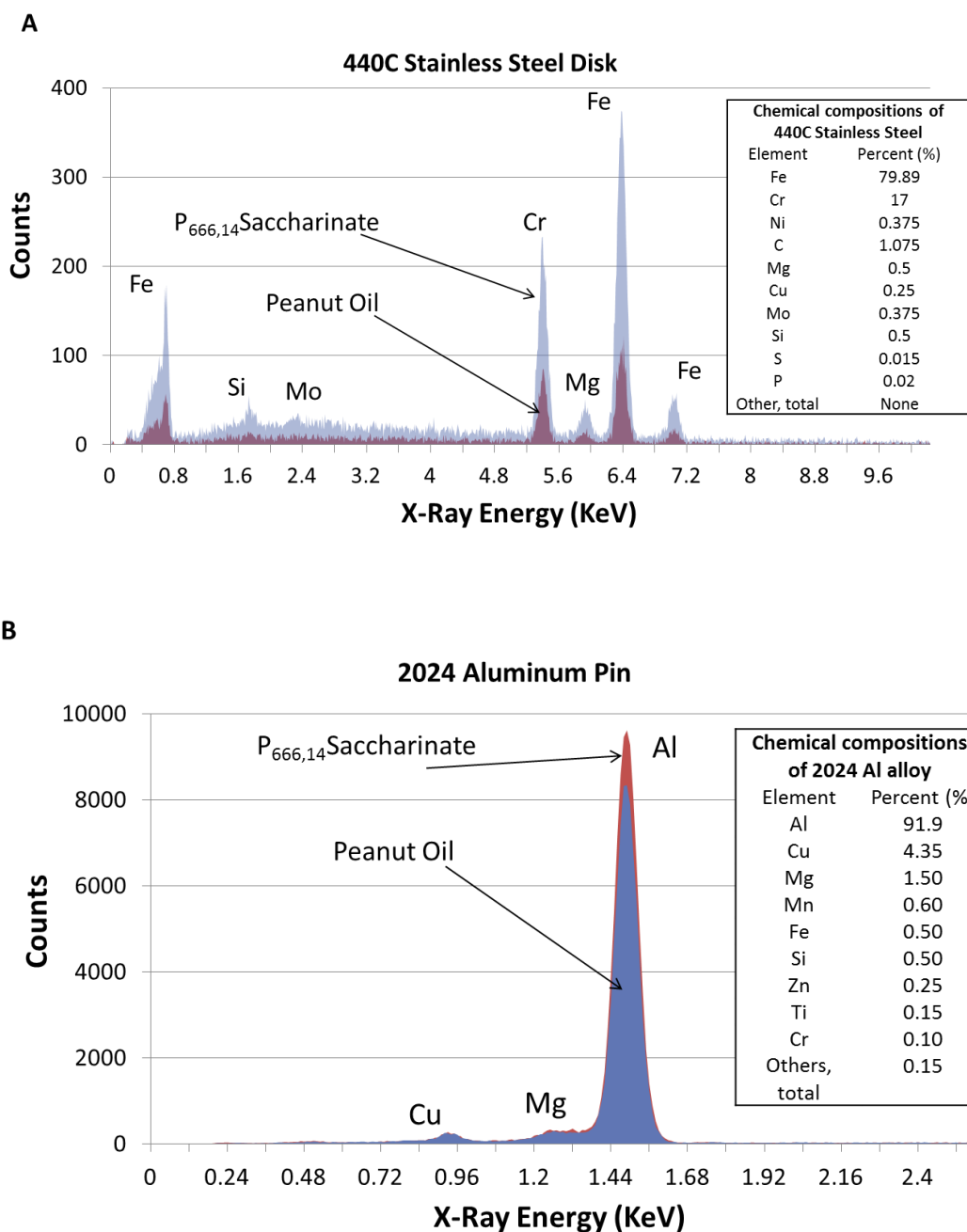
Figure 7.12: Energy-dispersive X-ray spectrograph of the (A) 440C stainless steel disk and (B) 2024 aluminum pin

The ILs have tribological properties better than the bio-based and the petroleum-based oils. When considered together with a variety of other physicochemical properties relevant to tribological behavior, these properties (e.g., their wide liquidus range, high viscosity, tunable miscibility, and lamellar-like liquid crystal structure) clearly indicate that ionic liquids, specifically the ecofriendly ILs, $P_{666,14}$Saccharinate, $P_{666,14}$Salicyate, and $P_{666,14}$Benzoate, offer tremendous potential as a new family of environmentally benign lubricants. Their superior protection in boundary lubrication is a result of the development of a physicochemical adsorption monolayer film caused by the negatively charged anion and positively charged cation adhering to the oppositely charged metal surface providing anti-wear properties and improved lubricity, making these ILs excellent lubricants and a next step in the advancement of biolubricants.

7.6. Conclusions

The results of this chapter shed light on a promising new class of environmentally friendly lubricants known as room temperature ionic liquid lubricants. It has been shown that their lamellar-like liquid crystal structure improves lubricity. The dipolar structure allows cations and anions to adsorb on charged worn metal surfaces facilitating self-assembling monolayers that create boundary films that minimize wear, reduce friction, and improve component operation. Environmentally friendly ILs were presented and demonstrated to be feasible in design and provide superior tribological properties.

The lubrication industry continues to make new strides towards sustainable biolubricants with properties that will lower friction and wear, thereby improving system

efficiency and ultimately conserving energy. Continuing this trend, future lubricants formulated from bio-based feedstock should offer the following advantages over petroleum-based oils: a higher lubricity lending to lower friction losses and improved efficiency, affording more power output and better economy. As oil prices rise, environmental awareness grows, and the demand for renewable and sustainable lubricants increases, biolubricants will begin to seek prominence. For this reason, fundamental research is an important step to the macroscale development, economical competence, and industrial use of biolubricants for energy conservation and sustainability. Room temperature ionic liquid lubricants represent a new class of novel "greener" lubricants that are non-toxic, obtainable from sustainable (non-petroleum) resources, and environmentally friendly. They have the ability to satisfy the combination of environmental, health, economic, and performance demands of modern lubricants. Their ability to be tunable establishes them as designer lubricants, where the optimization of cation-anion moiety facilitates energy conservation through superior tribological performance. The major findings of the current investigation of room temperature ionic liquid lubricants revealed the following conclusions

- Phosphonium and imidazolium ionic liquids can be utilized as additives for natural oils where the higher the IL concentration the better the tribological properties.

- Phosphonium and imidazolium ionic liquids with carboxylate anions outperform bio-based and petroleum-based oils due to their lamellar-like liquid crystal structure improving lubricity and wear resistance.

- Due to their unique dipolar structure, the charged anions and cations in the ionic liquids can potentially be adsorbed on to the oppositely charged worn metal surfaces therefore forming an effective boundary film that acts to minimize wear.

- Long bulky asymmetric organic cations ($\geq$10 atoms on the alkyl chain) and aromatic carboxylic organic anions (with 1 or 2 rings) effectively reduce friction and wear.

- $P_{666,14}$Saccharinate, $P_{666,14}$Salicyate, and $P_{666,14}$Benzoate ionic liquids maintain superior tribological properties and offer tremendous potential as a new family of environmentally benign lubricants.

Chapter 8 The Tribological Performance of Imidazolium and Phosphonium Ionic Liquids with Carboxylate Anions as Biolubricants for High Temperature Applications Involving Steel-Steel Contacts

8.1 Introduction

Room temperature ionic liquids (RTILs) are molten salts which represent a new class of designer lubricants that consist of an organic cation combined with an organic or inorganic anion and maintain melting points below 100°C and a liquid range beyond 300°C [138, 382]. As a result of the many properties associated with ionic liquids (ILs) they have found early success in a variety of applications, including solar cells, batteries, and thin films as well as many other applications [135, 340-344, 357, 358, 361-365]. The appeal of ILs as lubricants becomes even more evident when one considers their many potential advantages over other lubricants including: (1) a broad liquid range (low melting and high boiling point); (2) negligible vapor pressure; (3) non-flammability and non-combustibility; (4) superior thermal stability; (5) high viscosity; (6) miscibility and solubility; (8) lamellar-like liquid crystal structure; and (9) long polar anion-cation molecular chains [132, 133, 135-137, 140, 151, 372, 383-387]. Many of the these properties make ILs good candidates as high temperature lubricants [151].

The earliest reports of the use of ionic liquids as high temperature lubricants was in 1961, when fluoride-containing molten salts were subjected to high-temperature

bearing tests of 650 to 815°C [345]. Currently, ILs are beginning to gain relevance as synthetic lubricants with much of the attention concentrated on their utilization as base oils in steel/steel, steel/copper, steel/aluminum, ceramic/ceramic, and steel/ceramic tribo-interfaces [140, 346-359]. ILs are also effective as additives in mineral oils, because of their tendency to form strong boundary films, that enhance the tribological performance of the base oils [136, 360]. These properties along with their negligible vapor pressure make them alternative lubricants for use under vacuum for spacecraft applications and in the automotive, manufacturing and magnetic storage industries [135, 136, 347]. Although the chemical structure of the cationic and anionic constituents of an ILs can vary greatly, some of the more commonly studied ILs for high pressure and elevated temperature tribological processes are those containing tetrafluoroborate (BF_4^-), hexafluorophosphate (PF_6^-), bis(trifluoromethanesulfonyl)amide, and tris(tetrafluoroethyl)trifluorophosphate anions [151, 366-373]. In general, as the hydrophobicity of the anion increases, both the high thermo-oxidative stability and the tribological properties improve [372]. Investigations into the thermal properties of IL cations, include imidazolium ions due to their high thermal stability of imidazole-based rings [374]. In contrast, these cations exhibit a decrease in thermo-oxidative stability with an increase in hydrophobicity [372]. Nonetheless, ILs with longer alkyl chains and lower polarity have been reported to have excellent tribological properties from low to high temperatures (-30°C to 200°C) [375]. Other IL cations have been studied with the goal of improving their tribological properties include phosphonium [376-378] and ammonium [356, 357, 379-381] salts.

As the industrial marketplace continues to become more ecologically focused in an attempt to reduce the use of petroleum-based lubricants much of the attention has centered on novel approaches to achieve efficient energy conservation and sustainability [79, 80]. The development of creating environmentally friendly ILs that can function at both low and high temperature environments while providing effective lubrication with minimal wear, derived from bio-based feedstock, and maintain high thermal-oxidative stability can be challenging considering the are as many as 10^{18} different combinations of anion and cation moieties [134, 139]. The process of designing an IL to be environmentally friendly begins by selecting both the cationic and anionic constituents to be non-toxic i.e. prepared from non-petroleum resources. As the number of desired properties increases, the number of possible candidate ILs declines dramatically. Here, for example, the desire for an environmentally friendly lubricant means that the use of highly fluorinated anions is unacceptable [388]. Instead, the use of carboxylic anions based on common food additives (e.g., benzoate$^-$ and salicylate$^-$, well known preservatives) or artificial sweeteners (e.g., saccharinate$^-$) are utilized. Similar considerations guide the choice of the cation and suggest that trihexyl(tetradecyl)phosphonium salts (i.e., $P_{666,14}{}^+$), some of which have been found to exhibit anti-microbial and biodegradable properties [148]. Similarly, the objective of employing renewable feedstocks for the preparation of the ILs suggests the use of certain 1,3-dialkylimidazolium cations, such as can be derived from fructose or other bio-based feedstock [144, 145, 389-392]. Here, ecofriendly ILs are developed and tested in hopes that someday their wide scale utilization can overcome the variety of environmental, cost

and performance challenges faced by conventional lubricants therefore making them a potentially attractive alternative lubricant [136, 138]. RTILs represent a promising new class of biolubricants that show potential to improve the high temperature limitations associated with bio-based and petroleum-based oils due to their physicochemical characteristics, and thermal-oxidative instabilities [132, 136, 140].

8.2 Experimentation

In this investigation environmentally benign phosphonium-based and imidazolium-based ionic liquids undergoing cation-anion moiety manipulation were evaluated for their tribological and thermal properties under high temperature conditions by pin-on-disk testing and a thermogravimetric analysis. The IL lubricants having different ion pairs were then compared with bio-based and petroleum-based lubricants to investigate their tribological performance.

8.3 Results and Discussion

8.3.1 Friction Results

Figure 8.1 shows the coefficient of friction values for the various imidazolium-based ionic liquid lubricants. Figure 8.1(a) shows the variation of the COF for the imidazolium-based ILs with different anions over the sliding distance. It can be seen that generally as the sliding distance increases the COF decreases, reaching an approximate steady state at approximately 1200m. Figure 8.1(b) shows the final COF at the completion of the tests.

Figure 8.1: Variation of the coefficient of friction of different imidazolium-based ionic liquids (a) with sliding distance and (b) at the completion of the tests
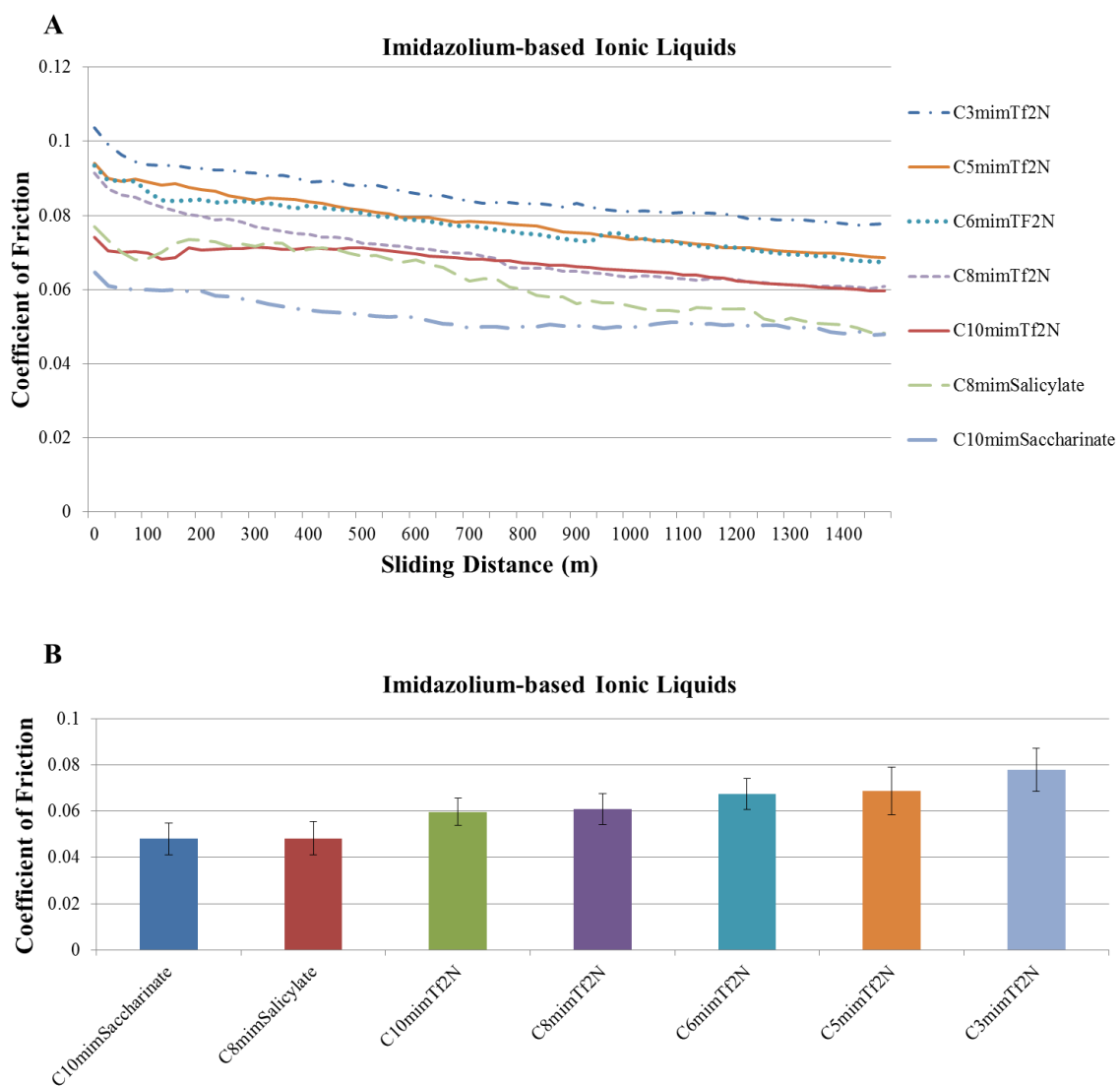
The effects of the various imidazolium alkyl chain length can be witnessed. As the COF decreases, the chain length increases from 3 carbon atoms to 10 carbon atoms for the $C_x mim Tf_2 N$ ionic liquids. When the $Tf_2 N$ anion is replaced with a carboxylic anion i.e. saccharinate or salicylate, the COF for the $C_{10} mim$ and $C_8 mim$ cations both decrease by approximately 20%. This demonstrates the effect that aromatic carboxylic anions have over the conventional non-aromatic anion such as the $Tf_2 N$. The correlation coefficient between the COF and the chain length illustrate a strong negative correlation with a R-value of -0.851 as shown in Table 8.1. When the $C_{10} mim Saccharinate$ and the $C_8 mim Salicylate$ ILs are omitted the correlation coefficient increases to -0.962 for the $C_x mim Tf_2 N$ ILs, revealing a stronger relationship between friction and alkyl chain length.

Table 8.1: Imidazolium-based ionic liquid lubricants – Cation investigation

Ionic Liquid	Cation	Anion	Cation Chain Length	COF	Wear (mm^3)
$C_{10} mim Saccharinate$	$C_{10} mim$	Saccharinate	10	0.0480	0.0192
$C_8 mim Salicylate$	$C_8 mim$	Salicylate	8	0.0483	0.0213
$C_{10} mim Tf_2 N$	$C_{10} mim$	$Tf_2 N$	10	0.0597	0.0246
$C_8 mim Tf_2 N$	$C_8 mim$	$Tf_2 N$	8	0.0609	0.0250
$C_6 mim Tf_2 N$	$C_6 mim$	$Tf_2 N$	6	0.0675	0.0291
$C_5 mim Tf_2 N$	$C_5 mim$	$Tf_2 N$	5	0.0687	0.0334
$C_3 mim Tf_2 N$	$C_3 mim$	$Tf_2 N$	3	0.0778	0.0416
Correlation Coefficient, R-value				**-0.851**	**-0.929**
Correlation Coefficient between COF and Wear, R-value				**0.955**	

Figure 8.2 shows the coefficient of friction values for the phosphonium-based ILs. Figure 8.2(a) shows the variation of the COF for the phosphonium-based ILs with different anions over sliding distance. In this figure, the COF decreases with sliding distance. Most of the ILs, reach a steady state COF by 1400m, except the $P_{666,14}$Salicylate, which tends to oscillate over the sliding distance. Figure 8.2(b) shows the COF value at the completion of the tests for the ILs. It can be seen that the $P_{666,14}$Cl has the highest COF value while the $P_{666,14}$Saccharinate maintains the lowest COF value.
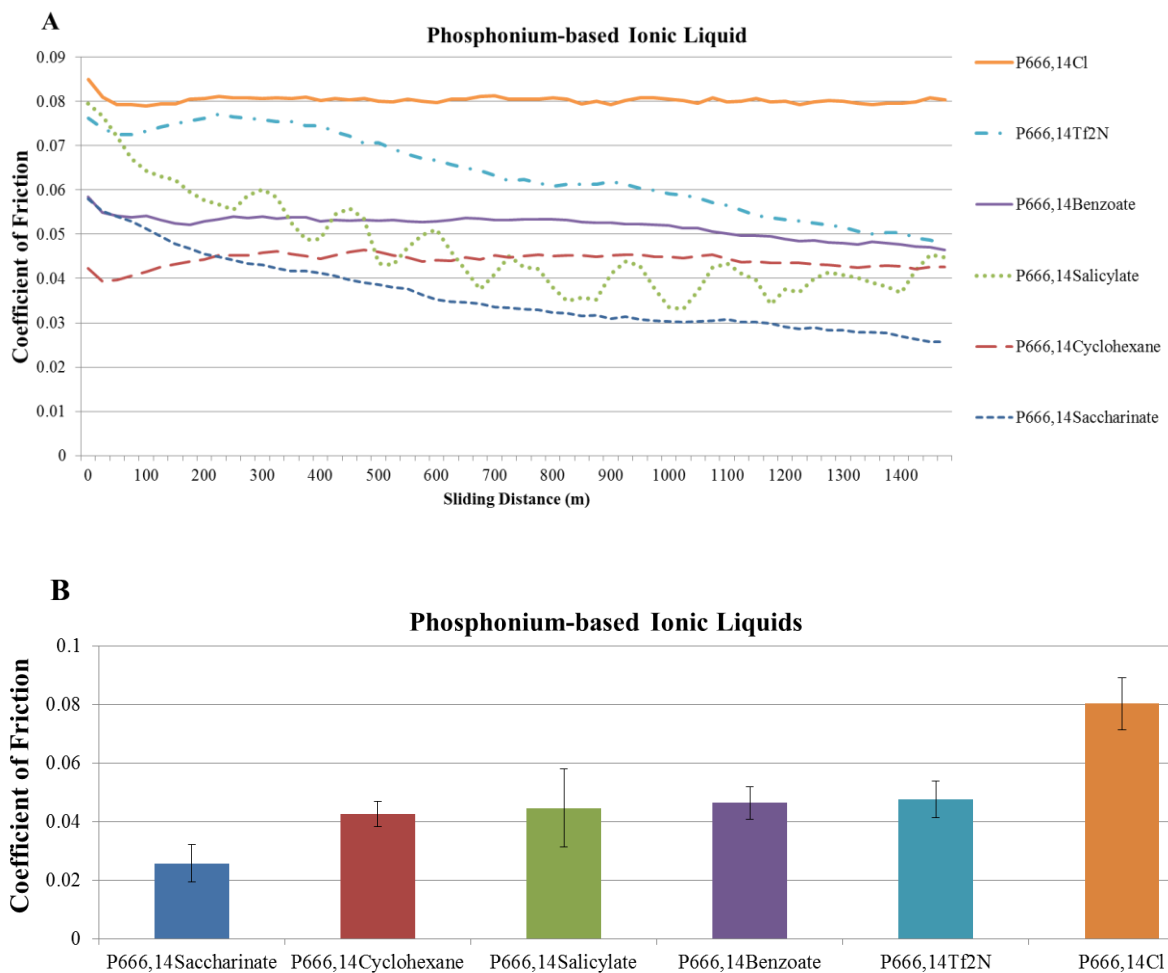
Figure 8.2: Variation of the coefficient of friction of different phosphonium-based ionic liquids (a) with sliding distance and (b) at the completion of the tests

As illustrated in Table 8.2, as the COF decreases, the anion ring size increases with a strong negative correlation coefficient of -0.813. Saccharinate having the most rings with two also has the lowest coefficient of friction followed by cyclohexane carboxylate. The cyclohexane carboxylate has a six-sided ring that does not conform to a hexagonal shape, instead it is non-planar and often considered a 3D chair or boat conformation. Here, benzoate and salicylate maintain similar COF values, despite the oscillations seen in the salicylate. The agreement between the two anions is not without surprise as they both are carboxylate anions with aromatic structures consisting of one ring. The difference between benzoate and salicylate is that salicylate has one addition hydroxyl group as shown in the structures of the molecules in Table 3.1.

Table 8.2: Phosphonium-based ionic liquid lubricants – Anion investigation

Ionic Liquid	Cation	Anion	Anion Ring Size	COF	Wear (mm^3)
$P_{666,14}$Saccharinate	$P_{666,14}$	Saccharinate	2	0.0257	0.0068
$P_{666,14}$Cyclohexane	$P_{666,14}$	Cyclohexane	1	0.0426	0.0091
$P_{666,14}$Salicylate	$P_{666,14}$	Salicylate	1	0.0447	0.0119
$P_{666,14}$Benzoate	$P_{666,14}$	Benzoate	1	0.0465	0.0142
$P_{666,14}$Tf2N	$P_{666,14}$	Tf2N	0	0.0477	0.0150
$P_{666,14}$Cl	$P_{666,14}$	Cl	0	0.0800	0.0686
Correlation Coefficient, R-value				**-0.813**	**-0.630**
Correlation Coefficient between COF and Wear, R-value				**0.934**	

8.3.2 Wear Results

Figure 8.3(a) shows the variation in the wear volume of the imidazolium-based ionic liquids with sliding distance. It can be seen that the ionic liquids generally increase in wear volume with sliding distance and at approximately 1000m begin to reach a steady state wear rate. This steady state is due to the tribo-surfaces conforming to each other by means of plastic deformation as the two surfaces remain in extended sliding contact. Figure 8.3(b) shows the final wear volume at the completion of the tests. The wear results are displayed in Table 8.1. These results are in agreement to their corresponding friction results as denoted by their high correlation coefficient between friction and wear having an R-value of 0.955. Similar trends present themselves in the wear results, where the wear volume decreases as the alkyl chain length increases in the $C_x$mim cation from 3 carbon atoms to 10 carbon atoms. The correlation coefficient between the cation chain length and the wear volume is -0.929, indicating a strong negative relationship as indicated in Table 8.1. Furthermore, it can be seen that as the carboxylate anions (i.e. saccharinate and salicylate) replace the Tf_2N anion, the wear volume for the C_{10}mim and C_8mim cation decrease by 22% and 15% respectively. This again shows how the aromatic carboxylate anions further reduce the wear rate for the ionic liquids.

Figure 8.4(a) shows the variation in the wear volume for selected phosphonium-based ionic liquids with sliding distance. It can be seen here that the ILs generally increase with sliding distance. Figure 8.4(b) shows the final wear volume for all of the phosphonium-based ILs and Table 8.2 shows the values of the wear volume.

A

B
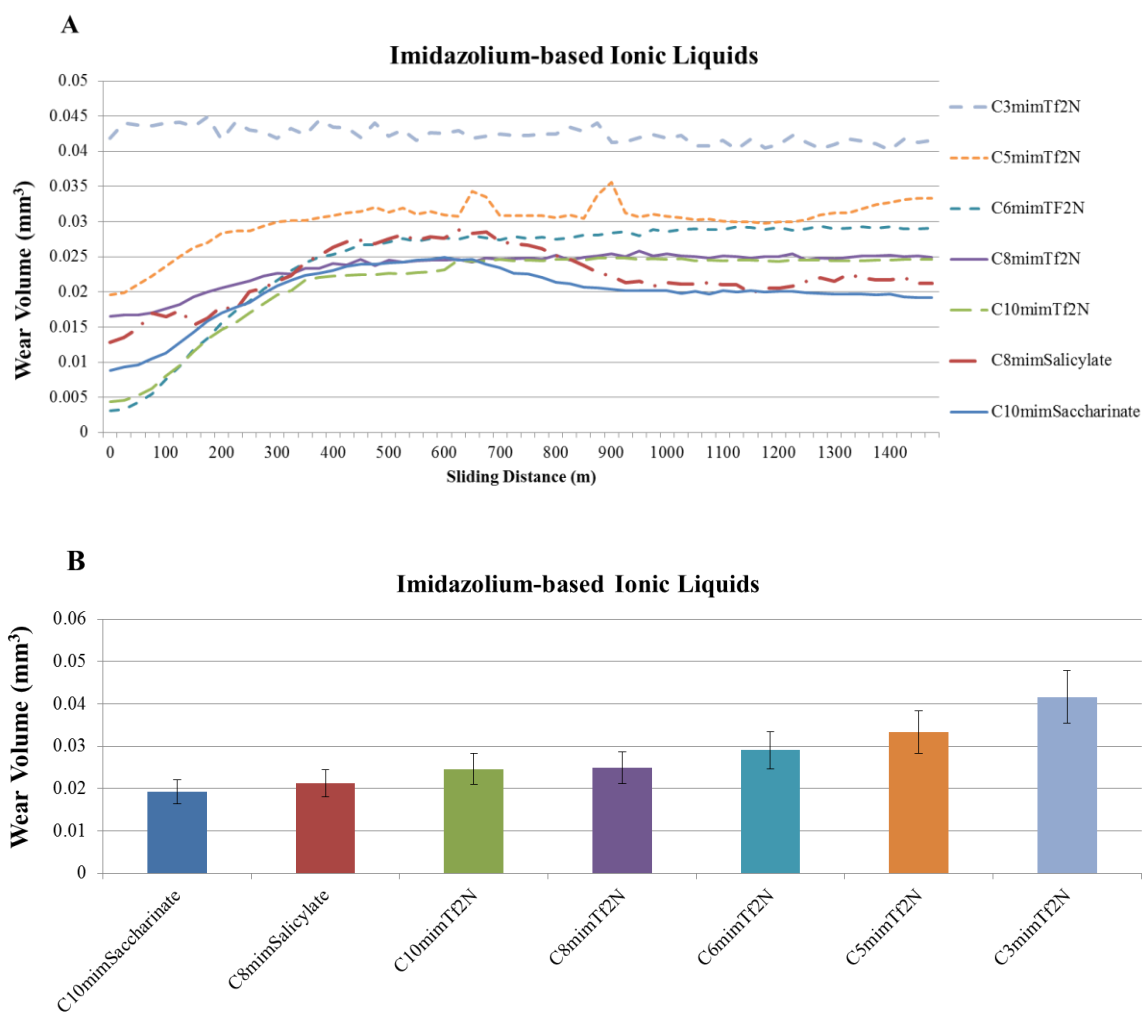
Figure 8.3: Variation of the wear volume of different imidazolium-based ionic liquids (a) with sliding distance and (b) at the completion of the tests

A

Phosphonium-based Ionic Liquids

Wear Volume (mm³) — Sliding Distance (m)

Legend:
- P666,14Cl
- P666,14Tf2N
- P666,14Benzoate
- P666,14Salicylate
- P666,14Cyclohexane
- P666,14Saccharinate
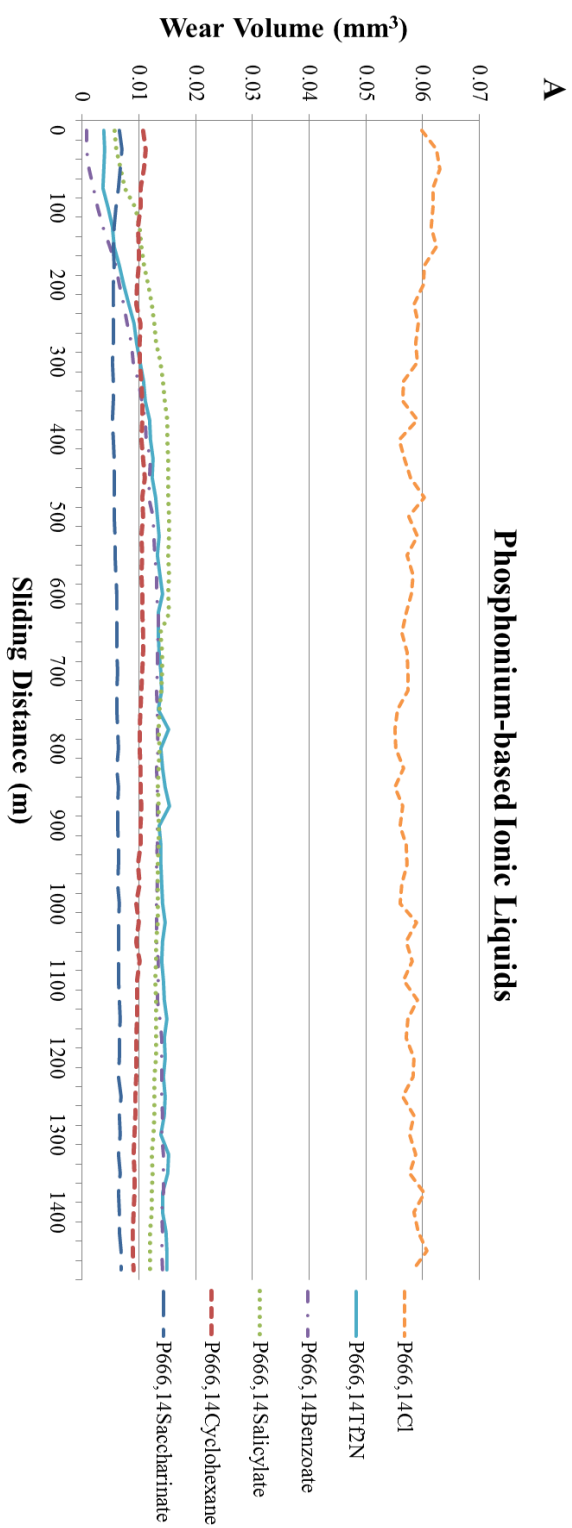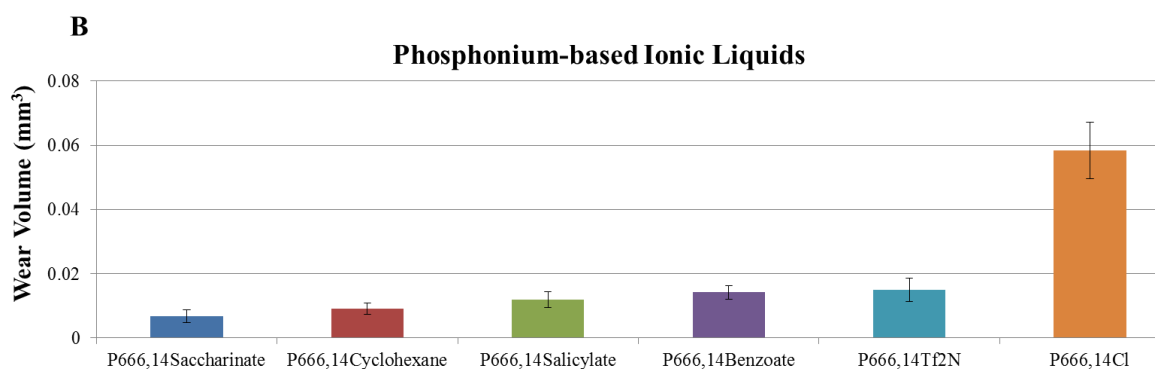
Figure 8.4: Variation of the wear volume of different phosphonium-based ionic liquids (a) with sliding distance and (b) at the completion of the tests

It can be seen that the $P_{666,14}$saccharinate has the lowest wear volume and $P_{666,14}$chloride has the highest wear. Similar to the friction results in Figure 8.2, the wear shows the trend of decreasing wear volume with an increasing ring size. The friction and wear results reveal a strong correlation coefficient for the phosphonium-based ionic liquids with an R-value of 0.934. Additionally from Table 8.2, the correlation coefficient, R-value of -0.630, indicates that there is a moderately negative correlation between an increase in the number of rings and a decrease in the wear volume.

8.3.3 Surface Analysis

Figure 8.5 shows the scanning electron micrographs for the worn pin surfaces of select imidazolium-based ionic liquids at two different magnifications 20x and 50x. From an EDS analysis there was no evidence of transfer layer formation or physicochemical reactions in the interface. From top to bottom in Fig. 8.5(a) and (b) are the C_{10}mimSaccharinate, (c) and (d) are the C_{10}mimTf$_2$N, (e) and (f) are the C_6mimTf$_2$N, (g)

and (h) are the C_5mimTf_2N, and (i) and (j) are the C_3mimTf_2N. In the micrographs the worn pin tips are in agreement with the tribological results where the ionic liquids with lower friction and wear rates have less of a wear scar. For example the $C_{10}mimSaccharinate$ in Fig 5(a) and (b) has a smaller wear scar diameter than the $C_{10}mimTf_2N$ shown in Fig. 5(c) and (d). As previously described, as the alkyl chain decreases, the wear rate increases as verified with the increasing wear scar with decreasing carbon atoms on the alkyl chains as well as the amount of wear debris on and around the worn surface. Interestingly, only minor abrasion marks were observable on the worn surfaces potentially indicating how the combined effects of sustained high temperatures with frictional heating may have slightly decreased the yield stress of the pin material while simultaneously allowing the strain rate to increase. These minute changes in mechanical properties could be enough to allow the material to undergo abrasive wear by plastic deformation where the damage to the surface roughness was minimal despite having wear occur. The phosphonium-based ionic liquids demonstrated similar results in their surface analysis where the larger ring sizes had minimal friction, lower wear, and smaller wear scars. The phosphonium-based ILs had very small wear tracks due to their already low wear rate. Ultimately, the surface analysis results indicate that the effect of increasing the alkyl chain length in the cation lowered the friction and wear rate as well as minimizing the wear scar. The effect of larger ring shaped anions additionally helped to benefit with further reductions of the friction, wear rate, and wear scar of the worn specimen.
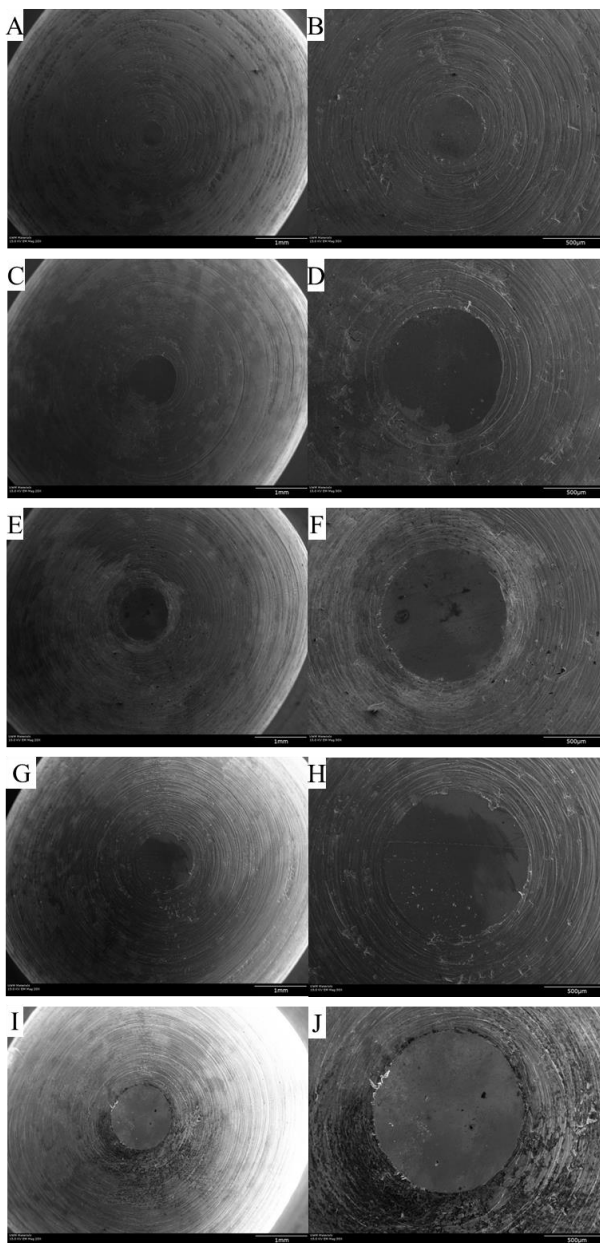
Figure 8.5: Scanning electron micrograph of the worn stainless steel disk lubricated with the Imidazolium-based ionic liquids (a) C_{10}mimSaccharinate at 20x, (b) C_{10}mimSaccharinate at 50x, (c) C_{10}mimTf$_2$N at 20x, (d) C_{10}mimTf$_2$N at 50x, (e) C_6mimTf$_2$N at 20x, (f) C_6mimTf$_2$N at 50x, (g) C_5mimTf$_2$N at 20x, (h) C_5mimTf$_2$N at 50x, (i) C_3mimTf$_2$N at 20x, and (j) C_3mimTf$_2$N at 50x

8.3.4. Ecofriendly Ionic Liquid Lubricants

The ionic liquids investigated demonstrate that specific combinations of the anions and cations perform better than others as potential high temperature lubricants in steel-steel tribo-contacts. Further examination will compare the tribological properties of imidazolium and phosphonium ILs incorporating environmentally friendly anions with various bio-based and petroleum-based lubricants. The classification of the investigated lubricants are shown in Table 8.3, where the ionic liquids are classified according to their source and type as ecofriendly ILs, toxic ILs, bio-based (natural) oils, and petroleum-based oils.

Table 8.3: Classification of investigated lubricants according to source and type

Ecofriendly ILs	Toxic ILs	Bio-based Oils	Petroleum-based Oils
$P_{666,14}$Benzoate	$P_{666,14}$Cyclohexane	Avocado	Synthetic Motor oil
$P_{666,14}$Saccharinate	$P_{666,14}$Tf$_2$N	Canola (rapeseed)	
$P_{666,14}$Salicylate	$P_{666,14}$Cl	Commercial	
		biolubricant	
C_{10}mimSaccharinate	C_{10}mimTf$_2$N		
C_8mimSalicylate	C_8mimTf$_2$N		
	C_6mimTf$_2$N		
	C_5mimTf$_2$N		
	C_3mimTf$_2$N		

Regarding the classification of an environmentally benign IL, due to the fact that both the imidazolium and phosphonium cations can be theoretically derived from bio-based

feedstock and produced in a manner that is ecofriendly, this investigation will only consider environmentally friendly ILs as those where the anion is non-toxic and ecofriendly. From Table 4 only the $P_{666,14}$Benzoate, $P_{666,14}$Saccharinate, $P_{666,14}$Salicylate, C_{10}mimSaccharinate, and C_8mimSalicylate ILs are considered ecofriendly.

Figure 8.6(a) shows the variation of the COF with sliding distance for all the lubricants tested. The general trend of the COF decreasing with sliding distance remains intact. Figure 8.6(b) shows the final COF at the completion of the tests for the lubricants and Table 8.4 shows the final COF values at the completion of the tests. It can be seen that overall, the ionic liquids maintain lower COF values than the bio-based and petroleum-based lubricants. Within the lubricants tested, the ecofriendly ILs maintain some of the lowest COF values, with $P_{666,14}$Saccharinate having the lowest COF. It can be seen here that the combination of longer alkyl chains on the cation and larger carboxylate aromatic anions provide the optimal lubricant with the lowest friction while remaining non-toxic and environmentally benign.

A

Coefficient of Friction

Sliding Distance (m)

Legend:
- SoyGold
- Motor Oil
- C3mimTf2N
- P666,14Cl
- Canola Oil
- C5mimTF2N
- C6mimTF2N
- Avocado Oil
- C10mimTf2N
- C8mimTf2N
- C10mimSaccharinate
- C8mimSalicylate
- P666,14Tf2N
- P666,14Benzoate
- P666,14Salicylate
- P666,14Cyclohexane
- P666,14Saccharinate
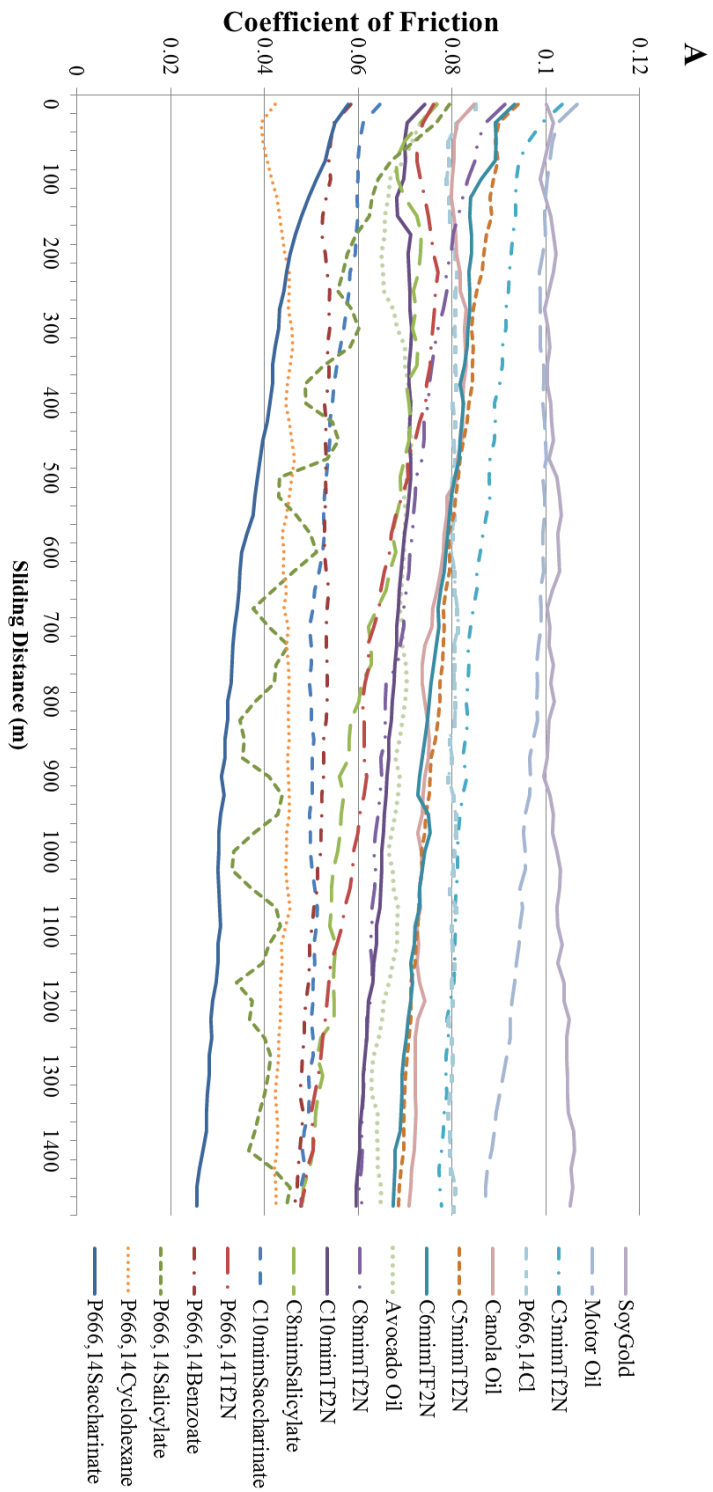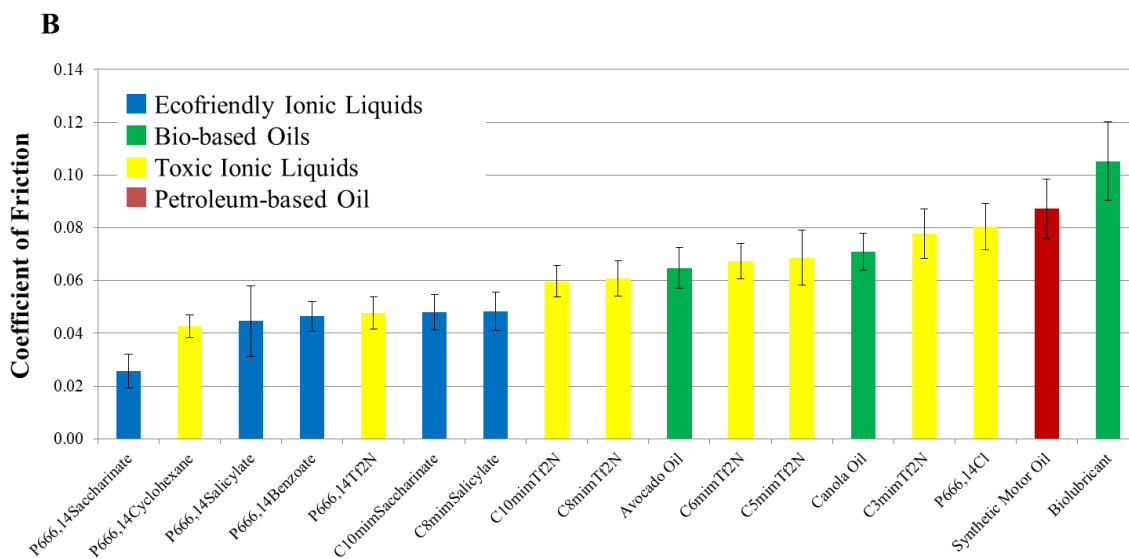
Figure 8.6: Variation of the coefficient of friction of different ecofriendly ionic liquids, natural oils, toxic ionic liquids, and petroleum-based oil (a) with sliding distance and (b) at the completion of tests

Table 8.4: Friction and wear results for the phosphonium-
based, imidazolium-based, bio-based , and petroleum-based
lubricants at 100°C

Lubricant	COF	Wear (mm^3)
$P_{666,14}$Saccharinate	0.0257	0.0068
$P_{666,14}$Cyclohexane	0.0426	0.0091
$P_{666,14}$Salicylate	0.0447	0.0119
$P_{666,14}$Benzoate	0.0465	0.0142
$P_{666,14}$Tf$_2$N	0.0477	0.0150
C_{10}mimSaccharinate	0.0480	0.0192
C_8mimSalicylate	0.0483	0.0213
C_{10}mimTf$_2$N	0.0597	0.0246
C_8mimTf$_2$N	0.0609	0.0250
Avocado Oil	0.0648	0.0304
C_6mimTf$_2$N	0.0675	0.0291
C_5mimTf$_2$N	0.0687	0.0334
Canola (rapeseed) Oil	0.0709	0.0440
$P_{666,14}$Cl	0.0800	0.0686
C_3mimTf$_2$N	0.0778	0.0416
Synthetic Motor Oil	0.0872	0.0505
Commercial Biolubricant	0.1053	0.0430

Figure 8.7(a) shows the variation of the wear volume with sliding distance for all the lubricants investigated. It can be seen that the wear rate generally increased with sliding distance. Figure 8.7(b) shows the wear volume at the completion of the tests for each of the lubricants tested. Table 8.4 shows the final wear volume values for each of the lubricants. Similar to the friction results, it can be seen in Fig. 8.7(b) that the ionic

liquids maintain lower wear rates than the bio-based and petroleum-based lubricants. The ecofriendly ionic liquids i.e. those ILs contains saccharinate, salicylate, or benzoate anions maintain some of the lowest wear rates with $P_{666,14}$,Saccharinate having the lowest.

A

Wear Volume (mm³)

Sliding Distance (m)

Legend:
- P666,14Cl
- Synthetic Oil
- Canola Oil
- SoyGold
- C3mimTf2N
- C5mimTf2N
- Avocado Oil
- C6mimTF2N
- C8mimTf2N
- C10mimTf2N
- C8mimSalicylate
- C10mimSaccharinate
- P666,14Tf2N
- P666,14Benzoate
- P666,14Salicylate
- P666,14Cyclohexane
- P666,14Saccharinate
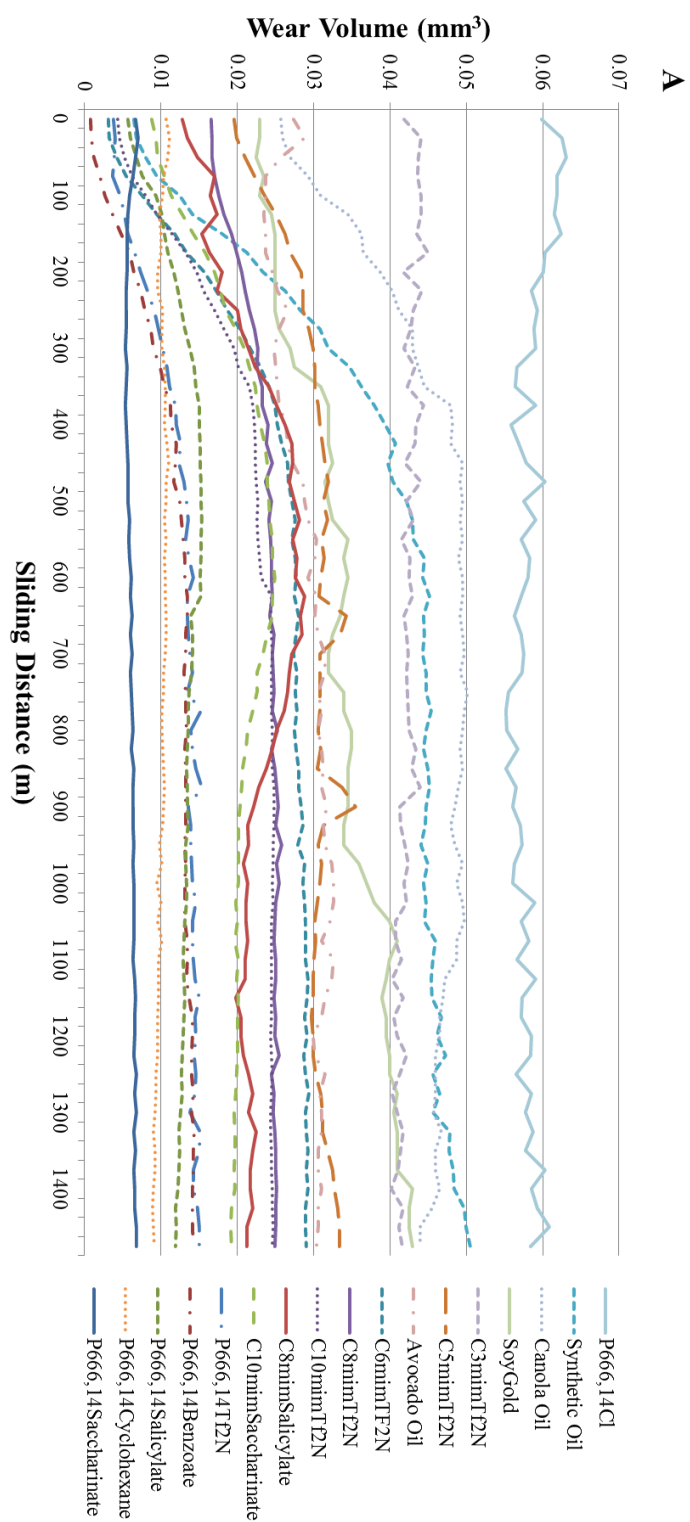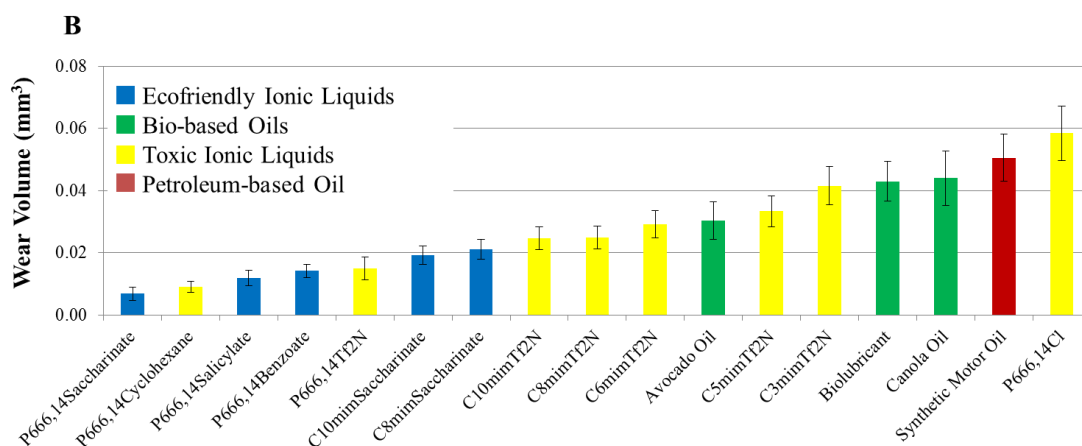
Figure 8.7: Variation of the wear volume of different ecofriendly ionic liquids, natural oils, toxic ionic liquids, and petroleum-based oil (a) with sliding distance and (b) at the completion of tests

Examining the friction and wear results indicate that ionic liquids as a whole have superior tribological properties i.e. higher lubricity and lower wear than bio-based and petroleum-based oils. It is not surprising that the bio-based oils outperform the petroleum-based oils as it is well known that natural oils maintain higher lubricity than many petroleum-based oils due to their high carboxylate acids amounts that exist in the form of fatty acids particularly oleic acid (C18:1) and linoleic acid (C18:2). These fatty acids are effective performance enhancing additives in oils for their ability to adsorb on to the charged metal surfaces due to their polar head. This allows the fatty acids to form monolayers that reduce the asperity contact and reduce the friction and wear. Ionic liquids maintain similar mechanisms for decreasing friction and wear. When considered together with a variety of other physicochemical properties relevant to tribological behavior, these properties (e.g., their wide liquidus range, high viscosity, tunable

miscibility, and lamellar-like liquid crystal structure) clearly indicate that ionic liquids, specifically the ecofriendly ILs, $P_{666,14}$Saccharinate, $P_{666,14}$Salicyate, $P_{666,14}$Benzoate, C_{10mim}Saccharinate, and C_8mimSalicylate offer tremendous potential as a new family of high temperature biolubricants. Their superior protection in boundary lubrication is a result of the development of (1) a physicochemical adsorption monolayer film caused by the negatively charged anion and positively charged cation adhering to the oppositely charged metal surface and (2) inherent liquid crystal lamellar structure that has low interlayer resistance due to the weak van der Waals' force providing anti-wear properties and improved lubricity which makes these ILs excellent biolubricants.

8.3.4 Thermogravimetic Analysis (TGA)

As previously mentioned, in many applications of steel-steel contacts it is important for lubricants such as motor oil, to be able to withstand elevated temperatures for extended period of time without significant decomposition. In fact in many applications, lubricants are used to not only provide lubrication but also dissipate heat from the tribo-interface. For these reasons the thermal stability of the ionic liquids and the bio-based oils were therefore investigated by thermogravimetric analysis. In this analysis, two different sets of decomposition experiments were carried out on the lubricants. First were dynamic decomposition measurements, in which the temperatures of the samples were increased at a constant rate to determine the temperature at which decomposition (as indicated by mass loss) begins and the temperature at which decomposition is complete. Once the temperature corresponding to the onset of

decomposition, $T_{d(onset)}$ was determined, the lubricants were then subjected to isothermal decomposition measurements, in which they were held at 100°C and 50°C below their $T_{d(onset)}$ for an eight hour period to determine stability over an extended period of time. Figures 8.8 and 8.9 show both the dynamic and isothermal decomposition graphs for selected ionic liquids and bio-based lubricants, respectively. In these figures the graphs on the left depict the dynamic decomposition tests and the graphs on the right depict the isothermal decomposition tests. In Fig. 8.8, the $P_{666,14}$Benzoate, $P_{666,14}$Salicyate, and $P_{666,14}$Saccharinate ionic liquid TGA results are shown. Similarly in Fig. 8.9 the TGA results for avocado, canola, vegetable and safflower oils are shown. Table 8.5 shows the combined TGA results for all the ionic ILs and the bio-based natural oils.
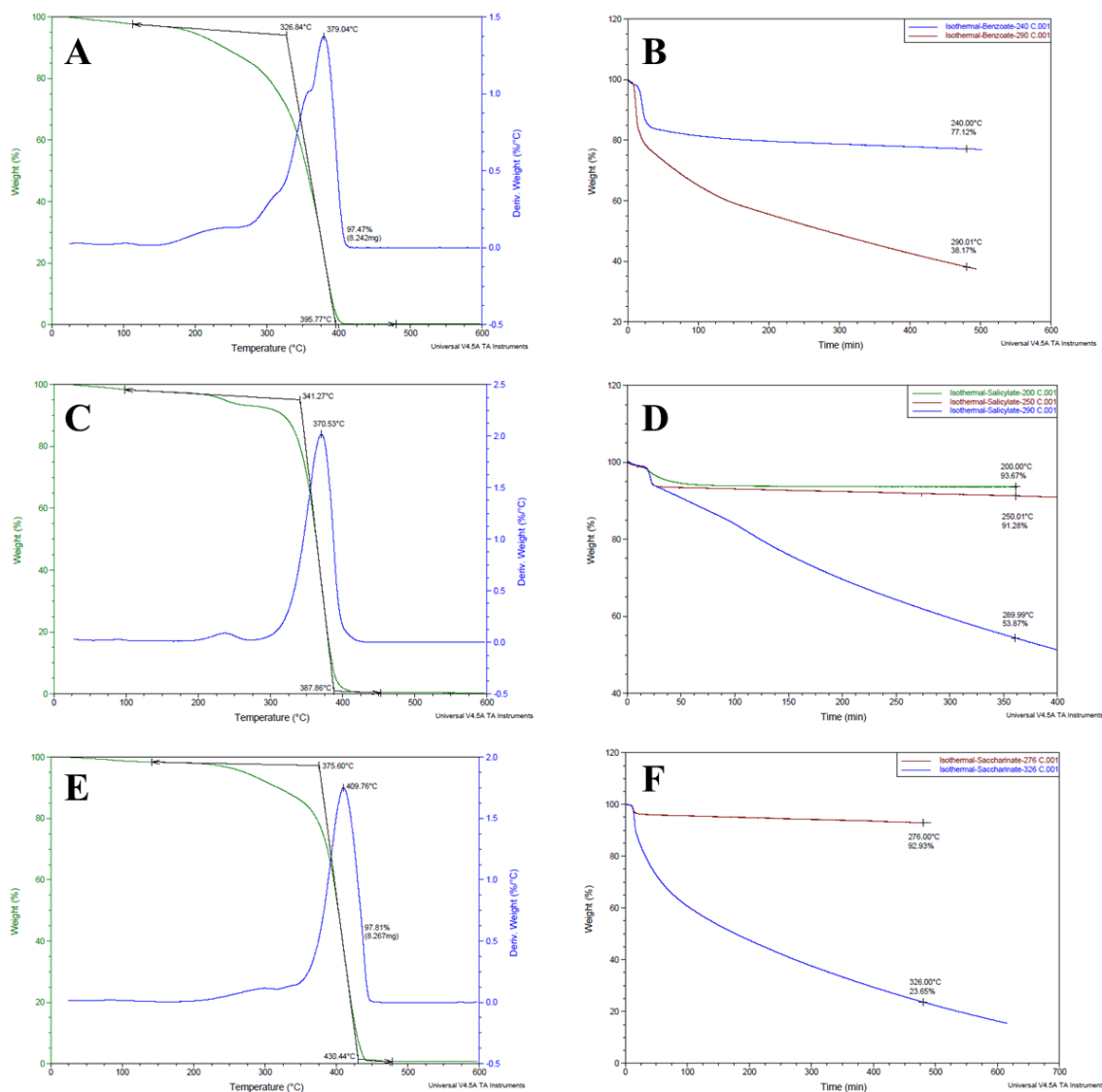
Figure 8.8: Decomposition data from a thermogravimetric analysis for various ecofriendly ionic liquids (a) dynamic decomposition graph of $P_{666,14}$Benzoate oil; (b) isothermal decomposition graph of $P_{666,14}$Benzoate oil; (c) dynamic decomposition graph of $P_{666,14}$Salicylate oil; (d) isothermal decomposition graph of $P_{666,14}$Salicylate oil; (e) dynamic decomposition graph of $P_{666,14}$Saccharinate oil; and (f) isothermal decomposition graph of $P_{666,14}$Saccharinate oil
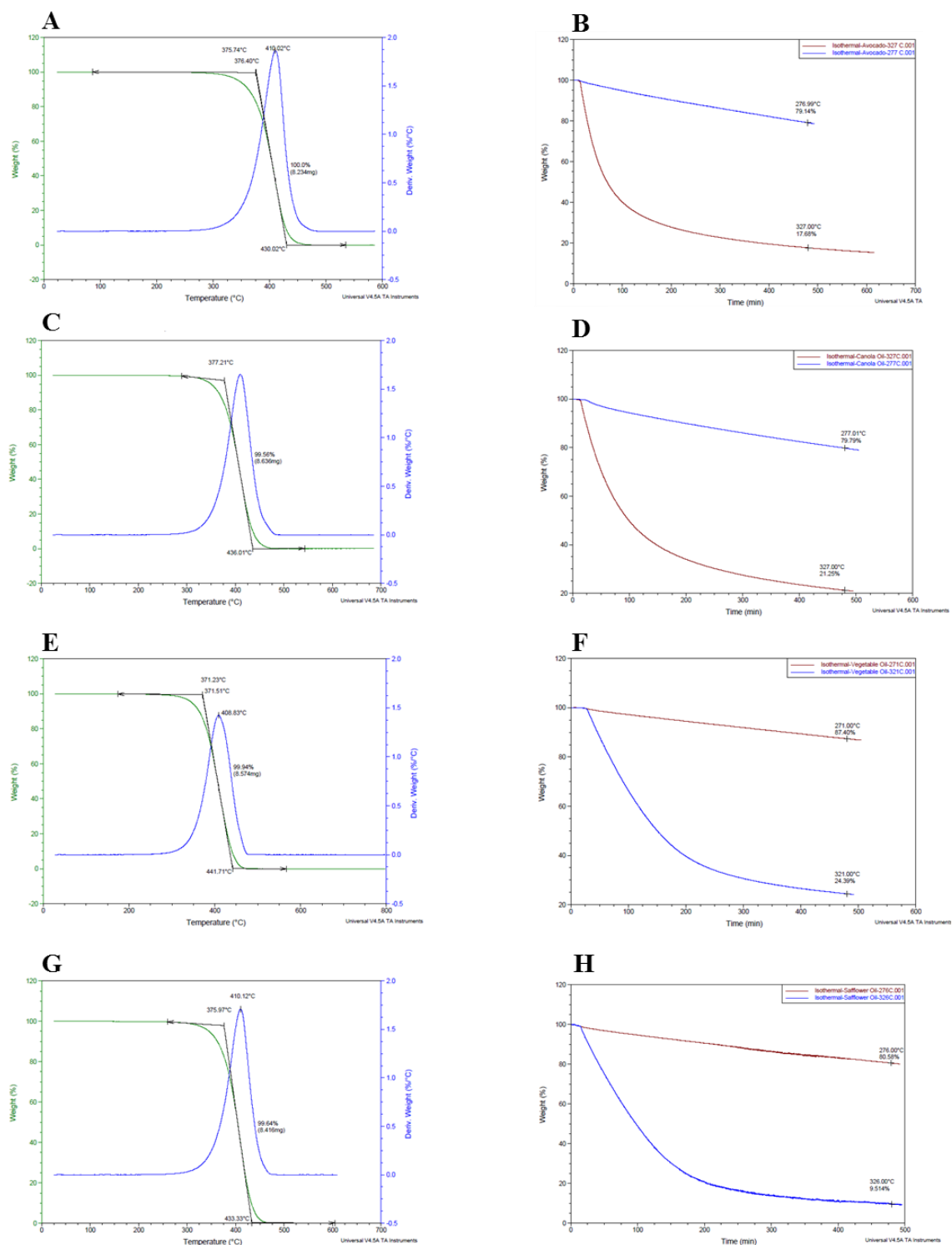
Figure 8.9: Decomposition data from a thermogravimetric analysis for various bio-based

oils (a) dynamic decomposition graph of avocado oil; (b) isothermal decomposition graph of avocado oil; (c) dynamic decomposition graph of canola (rapeseed) oil; (d) isothermal decomposition graph of canola (rapeseed) oil; (e) dynamic decomposition graph of vegetable (soybean) oil; (f) isothermal decomposition graph of vegetable (soybean) oil; (g) dynamic decomposition graph of safflower oil; and (h) isothermal decomposition graph of safflower oil

Table 8.5: Thermal degradation results for various natural oils,

ionic liquids, and petroleum-based oils

Oil/Ionic Liquid	$T_{d(onset)}$ (°C)	$T_{d(max)}$ (°C)	%decomposition ($T_{d(onset)}$-100°C)	%decomposition ($T_{d(onset)}$-50°C)	Smoke Point /Flash Point (°C)[a]
Avocado Oil	376	410	21	82	271
Canola Oil	377	410	20	79	226
Corn Oil	372	410	16	76	165
Olive Oil	377	411	27	86	160
Peanut Oil	378	411	18	92	107
Safflower Oil	376	410	19	91	160
Sesame Oil	370	407	32	72	177
Vegetable Oil	371	409	13	76	225[b]
C_5mimTf_2N	409	446	100	100	N/A
C_6mimTf_2N	409	448	100	100	N/A
C_8mimTf_2N	404	450	91	100	N/A
$C_{10}mimTf_2N$	409	451	87	100	N/A
$P_{666,14}Tf_2N$	406	408	43	100	N/A
$P_{666,14}Benzoate$	327	379	23	62	N/A
$P_{666,14}Salicylate$	341	371	10	55	N/A
$P_{666,14}Saccharinate$	376	410	7	76	N/A
Synthetic Motor Oil	-	-	-	-	232[*]

Reference [398]

Reference [399]

N/A ≡ Not Applicable

From Table 8.5 it can be seen that the imidazolium-based ionic liquid lubricants exhibit thermal decomposition temperatures approximately 40˚C higher than the bio-based oils. The phosphonium-based ILs demonstrate thermal decomposition temperatures that are comparable to or less than (by as much as 50˚C) the bio-based oils. When considering $T_{d(onset)}$ and $T_{d(max)}$ for the natural oils, it should be noted that the TGA was conducted in a nitrogen environment that reduces the effects of oil oxidation therefore the oils can sustain higher temperatures before significant thermal degradation is observed. In actuality, the bio-based oils would begin to breakdown as significantly lower temperatures, as can be seen in the table by their smoke temperatures range from 271˚C to 107˚C. At these temperatures in an oxygenated "open-air" environment the oils would have begun to breakdown and become inoperable lubricants. Even the synthetic motor oil would degrade around 232°C, much lower than the ILs. Ionic liquids on the other hand due not smoke and have no flash temperature because they are nonvolatile, noncombustible, and nonflammable as a result of their lack of vapor pressure. This feature alone, affords ILs the ability to operate in higher temperatures with increased thermal stability than bio-based and petroleum-based oils.

It has been suggested by some that decomposition temperature measurements in dynamic experiments provide inaccurate estimates of the thermal stability and only isothermal measurements appropriately characterize the thermal stability. For this reason, isothermal results are shown in Table 8.5 at temperatures 100˚C and 50˚C below the $T_{d(onset)}$. At 100˚C below the corresponding $T_{d(onset)}$, the bio-based natural oils show a moderate thermal stability with 32% or less of the bio-based lubricants decomposing. The

imidazolium-based ILs show a nearly complete thermal degradation at 100°C below the corresponding $T_{d(onset)}$ with 87% or more decomposition. It can be seen here, that the ILs with the Tf$_2$N anion show a decrease in the thermal degradation with an increase in the cation alkyl chain length. Exchanging the imidazolium cation for the phosphonium cation revealed much more stable ILs. The phosphonium-based ionic liquids exhibited the most thermal stability at 100°C below the corresponding $T_{d(onset)}$ and they revealed that an increase in aromaticity in the anion lower the amount of decomposition. At 50°C below the corresponding $T_{d(onset)}$, the bio-based oils and the imidazolium-based ILs were found to exhibit substantial and in many instance, nearly complete decomposition. The phosphonium-based ILs demonstrated high thermal decomposition as well, however with the aromatic anions the thermal stability witnessed minor improvements.

These results are encouraging for the potential use of the ecofriendly ILs as lubricants in high temperature environments. At higher temperatures they decomposed comparably or less than many of the other lubricants tests and at lower temperatures their thermal stability was far superior. Interestingly, the ecofriendly ILs were demonstrated to have lower onset of thermal degradation temperatures, yet they exhibited a significantly lower rate of thermal degradation when compared to the toxic ionic liquids, bio-based oils, and petroleum-based oil. This allows the ecofriendly ILs to be used for longer intervals and for longer heat exposures at slightly lower temperatures. The reasons for the thermal properties within the ILs has been considered to be in part caused by the electrostatic potential that exists between the cations and the anions quantitatively referred to as the lattice energy [400]. The combination of larger bulky asymmetric

cations and smaller aromatic anions, creates mismatches in the shape, size, and structure of the ion pairs. This in turn creates unbalanced anion-cation moieties which cause inefficient ion packing and effectively increase the interionic separation, thereby lowering the lattice energy and lowering the thermal stability [93]. Despite, the lower lattice energy, it is the global electrostatic potential that benefits the ionic liquids because with the cations and anions attracting each other, they collectively are responsible for the low melting points and non-measurable vapor pressure [93]. It is these properties that provide ionic liquids an advantage in high temperature applications because they are less sussceptible to flame, combustion, or otherwise dangerous reactions due to operation in high temperature conditions.

8.4 Conclusions

This chapter investigated the use of imidazolium- and phosphonium-based ionic liquids as a promising new class of environmentally friendly lubricants for high temperature applications involving steel-on-steel contacts. It has been shown that their lamellar-like liquid crystal structure, dipolar molecules, and electrostatic potential afford ionic liquids the ability to provide adequate lubrication with low friction, minimal wear, and high thermal stability while being feasible in design. These properties when considered together with a variety of other physicochemical properties (e.g., their wide liquidus range, high viscosity, tunable miscibility, nonvolatility, adsorption behavior, non-flammability, and non-combustibility) relevant to a new class of non-toxic, obtainable from sustainable (non-petroleum) resources, environmentally friendly IL

lubricants outperform bio-based and petroleum-based oils in high temperature applications. The ability of ILs to be tunable establishes them as designer lubricants, where the optimization of the cation-anion moiety facilitates energy conservation through superior tribological performance that can additionally help to satisfy the combination of environmental, health, economic, and performance demands of modern lubricants. As the lubrication industry continues striving for cleaner, safer, and less toxic lubricants, the demand for biolubricants will escalate, therefore fundamental research such as this, is an important step to the macroscale development, economical competence, and industrial use of biolubricants for energy conservation and sustainability. The major findings of this investigation of room temperature ionic liquid lubricants revealed the following conclusions:

- Longer alkyl chains on the bulky asymmetric organic imidazolium cations with bis(trifluoromethylsulfonyl)amide anions improve the tribological properties.

- Aromatic carboxylic organic anions have the greatest effect on the tribological performance of imidazolium and phosphonium ionic liquids to lower friction and wear.

- Phosphonium-based ionic liquids with carboxylate anions representing ecofriendly ionic liquids with potential environmentally friendly feed-stock derivation outperform bio-based and petroleum-based oils with lower friction and lower wear.

- Longer alkyl chains on the bulky asymmetric organic imidazolium cations with bis(trifluoromethylsulfonyl)amide anions enhance the thermal stability of the ionic liquids by lowering the thermal degradation.

- Natural oils have higher onsets of thermal degradation temperatures as well as higher rates of decomposition when compared to ionic liquids. This causes the natural oils to be more susceptible to thermal degradation and to succumb to it in a shorter time interval.

- Phosphonium-based ionic liquids incorporating carboxylate anions representing ecofriendly ionic liquids have lower onsets of thermal degradation temperatures and lower rates of thermal degradation than bio-based oils and imidazolium-based ionic liquids.

Chapter 9 The Effect of Particulate Additive Size on the Tribological Performance of Phosphonium Ionic Liquid Biolubricants Incorporating Carboxylate Anions

9.1. Introduction

In recent decades the lubrication industry has strived towards environmental responsibility and the development of environmentally friendly lubricants. Recent studies have focused on developing biolubricants by combining natural oils with solid particle additives in an attempt to provide a suitable alternative to petroleum-based lubricants. One reason for these compound biolubricants is due to the fact that solid particle lubricants such as boric acid and MoS_2 can be forced out of the contact zone during sliding contact resulting in an unlubricated dry scenario with high friction, high wear, and high potential to damage components [113]. In an attempt to remedy this problem, a carrier fluid is needed such as petroleum-based greases and oils or natural oils. The other reason is concerned with replacing the ubiquitous petroleum-based oils that are toxic to the environment with a more environmentally friendly lubricant such as canola oil or avocado oil [6, 81]. Natural oils such as canola oil are often chosen because they are readily available, inexpensive, and have a viscosity and surface tension similar to petroleum-based lubricants used in industrial applications for metal stamping and transmission fluids [81, 91, 92]. Studies have shown that molybdenum disulfide and boric acid with micron and nano-sized particle additives in canola oil establish a colloidal solution leading to improved friction and wear reduction in pin-on-disk tests [19, 81, 92,

196, 204-209]. Investigations have revealed that the carrier fluids allow the particle additives to remain in the contacting pin-disk interface without degrading over time. The presence of the nano-sized particulate mixtures by themselves or in combination with micron-sized particles has exhibited improvements in the tribological performance [113, 118, 196, 401]. Investigations have shown that ILs outperform natural oils, for this reason, to improve upon the current natural oil-based compound lubricants ionic liquids are used.

The particle additives used in these lubricants are often lamellar solids because they have a low interlayer friction such as graphite, molybdenum disulfide (MoS_2), tungsten disulfide (WS_2), boric acid (H_3BO_3), and hexagonal boron nitride (hBN) [9, 92, 197]. Lamellar powder lubricants are known for their crystal structure where atoms lying on the same layer are closely packed and strongly bonded together by covalent bonds and the layers are relatively far apart due to the weak van der Waals force [113, 401]. In some instances the particulate additives consist of multi-walled carbon nanotubes (MWNTs) instead of lamellar solid because they have atomically smooth surfaces and the concentric cylinders of graphene can rotate with minimal friction [402-406]. Carbon nanotubes (CNTs) are known for their high strength, hardness, and stiffness making them suitable for high contact pressure tribo-contacts [407-410]. Despite the type of additive whether a lamellar solid particle or carbon nanotube, these powder additives become entrained between the sliding surfaces and can adhere to the surface forming a protective boundary layer. This boundary layer prevents wear and acts as a lubricant in sliding contacts by accommodating the relative surface velocities. The lamellar solid particle lubricants accomplish this by aligning themselves parallel to the direction of motion and sliding

over one another with minimal friction while the CNTs displace the relative velocites by rotating amongst each other acting as a cylinderical bearing [403, 411]. Moreover, these powder additives can lubricate in extreme conditions such as high or low temperatures and pressures [11, 90-92, 113, 194, 195]. Within the particulate additives boron nitride is of specific interest because it is environmentally-friendly and inert to most chemicals furthermore it is highly refractory with physical and chemical properties similar to that of graphite [198]. In addition boron nitride has been demonstrated to show a change in shape with particle size where smaller nanometer sized particles maintain a lubricious spherical shaped geometry. As the particles increase in size to submicron and micron their particle shape also transitions to a less spherical geometry where they become abrasive and plate-shaped [6, 118].

Investigating the carrier fluids, as previously mentioned natural oils such as canola (rapeseed), vegetable (soybean), and avocado oil are being investigated as a renewable, biodegradable, and non-toxic alternatives to petroleum-based lubricants due to their triacylglycerol composition [24, 90, 106, 107, 110, 111, 117]. Within natural oils their long chains of polar fatty acids provide them with superior boundary lubricating properties allowing them to adhere to metallic surfaces, remain closely packed, and create a monolayer that is effective at reducing friction and wear [24, 106, 107, 117]. It is these properties that provide natural oils the ability to exhibit higher lubricity, lower volatility, higher shear stability, higher viscosity index, higher load carrying index, and superior detergency and dispersancy in comparisons with mineral and synthetic petroleum-based oils [24, 43, 81, 90]. Despite the environmental and tribological advantages to using

natural oils, they do suffer from poor thermal and oxidative stability, biological (bacterial) deterioration, hydrolytic instability, poor fluid flow behavior, solidification at low temperatures, inconsistent chemical composition, and on occasion high wear rates [109, 153-158].

As a means to progress beyond natural oils, environmentally friendly room temperature ionic liquid (RTIL) lubricants have been proposed as a next step in biolubrication for their similar properties to natural oils. Ionic liquids are composed of cations and anions that that can adsorb onto charged metallic surfaces forming monolayers that minimize the asperity contact thus reducing friction and wear [135, 136, 140]. Additionally, ILs have a lamellar liquid crystal structure that allows them low internal resistance and high lubricity [383, 384]. Other properties that make ILs attractive substitutes to both petroleum-based lubricants and natural oils are their broad liquid range; negligible vapor pressure; non-flammability and non-combustibility; high thermal-oxidative stability; high viscosity; miscibility and solubility; environmentally-benign (non-toxic) constituents; derivation from bio-based feedstock, and physicochemical consistency [132, 133, 135-137, 140, 151, 372, 383-387]. Ionic liquids are generally used as solvents in organic chemistry, recently they have found use as lubricants in steel/steel, steel/copper, steel/aluminum, ceramic/ceramic, and steel/ceramic tribo-contacts [140, 347-359] where they are used as base oils, additives, and thin films [136, 357, 358, 360-365].

9.2. Experimentation

In the present investigation, a phosphonium ionic liquid containing carboxylate anions was used as a carrier fluid with various particulate additives in a colloidal mixture and studied for its tribological effects as a two-phase compound biolubricant. The phosphonium-based IL lubricants were composed of trihexyl(tetradecyl)phosphonium ($P_{666,14}^+$) cations and salicylate anions (salicylate$^-$). This particular IL was chosen because in previous studies it was shown to be an effective lubricant and more specifically a potential biolubricant [132, 141, 142]. The IL, $P_{666,14}^+$Salicylate$^-$ (further referred to as $P_{666,14}$Salicylate) can be considered environmentally friendly because both the cation and the anion constituents are non-toxic and derived from bio-based feedstock. Investigations have shown that trihexyl(tetradecyl)phosphonium salts can exhibit anti-microbial and biodegradable properties [148]. Additionally, some carboxylate anions such as salicylate are derived from common food additives thus rendering them environmentally benign. The performance of this lubricant was studied by varying the size and type of the powder additives in the base oil. A pin-on-disk tribometer with a 440C stainless steel pin sliding against a 2024 aluminum disk was used to quantify the friction and wear properties of the lubricants. The steel used in these tests was selected for its high strength and the aluminum was selected for its high strength-to-weight ratio due to its varying elemental composition. The steel pin dimensions were 6.35 mm in diameter, 50 mm in length, and had a hemispherical tip. The aluminum disk dimensions were 70 mm in diameter, 6.35 mm in thickness, and were polished to a surface roughness having an arithmetic average, R_a, value of 0.2 ± 0.02 μm. During each test, 5 mL of $P_{666,14}$Salicylate oil were mixed

with 5% by weight of each particulate additive forming nine colloidal lubricant mixtures containing additives. Two additional tests were performed, the first with pure $P_{666,14}$Salicylate as a neat lubricant with no additive and the second a dry unlubricated test with neither IL lubricant nor particulate additives. The tests involving particulate additives are shown in Table 9.1.

Table 9.1: Lubricant Composition Mixtures involving

$P_{666,14}$Salicylate and Various Particle Additives

		Additive		
Test Name	**Additive Name**	**Composition**	**Size** (μm)	**Structure**
70nm hBN	Boron Nitride	h-BN	0.07	Lamellar
0.5μm hBN	Boron Nitride	h-BN	0.50	Lamellar
1.5μm hBN	Boron Nitride	h-BN	1.50	Lamellar
5μm hBN	Boron Nitride	h-BN	5.00	Lamellar
55nm WS_2	Tungsten Disulfide	WS_2	0.055	Lamellar
0.6μm WS_2	Tungsten Disulfide	WS_2	0.60	Lamellar
50nm Graphite	Graphite	C	0.05	Lamellar
2μm MoS_2	Molybdenum Disulfide	MoS_2	2.00	Lamellar
5μm MWNT	Multi-Walled Carbon Nanotube	C	O.D. x L 0.006-0.009 x 5.0	Cylindrical

O.D. = Outside Diameter

L = Length

The $P_{666,14}$Salicylate ionic liquid was combined with the particle additives by using a vortex generator to mix the lubricant until a homogenous mixture was present. Prior to each experiment test specimens were cleaned with soap, acetone, and hexane solutions in an ultrasonic cleaner. During each of the tests, the disk was completely covered by the lubricant mixture making the pin-disk interface continually lubricated throughout the test duration. Each test was repeated a minimum of three times to ensure repeatability and accuracy of the results.

9.3 Results and Discussions

9.3.1 Friction Results

Figure 9.1, shows the coefficient of friction (COF) for the various lubricant mixtures. It can be seen in Fig. 9.1(a) how the COF varies with sliding distance. The particulate additive mixtures reach steady state by the end of the tests with the exception of the dry test and the 5µm length multi-walled carbon nanotube (MWNT) test. When omitting these two trials, which had the highest and most volatile COF values, Fig. 9.1(b), shows the COF values with sliding distance for the particulate additive mixtures and the pure IL tests. It can be seen how stable the IL mixtures are and how they reach a steady-state COF by approximately 300m. Figure 9.1(c) shows the final COF values at the completion of the tests for each trial. The friction results reveal that in the IL, the smaller nanometer and submicron sized particles predominantly have lower COF values with the 70nm hBN particles having the lowest COF, preceded by the 55nm WS_2, 0.5µm hBN, and 0.6µm WS_2 particles. Here, the 70nm hBN particle demonstrates how an environmentally friendly particulate additive can maintain low friction in the presence of an ecofriendly ionic liquid such as $P_{666,14}$Salicylate. In the lubricant mixtures, larger particles of 1.5 or 2 microns exhibited lower COF values than that of the pure IL lubricant with no additives. This further revealed how smaller particles enhanced the tribological properties by establishing smooth protective transfer films. Interestingly, larger micron-sized particles such as the 5µm hBN particles and the 5µm MWNT exhibited higher friction coefficients beyond that of the pure IL. It is speculated that

A
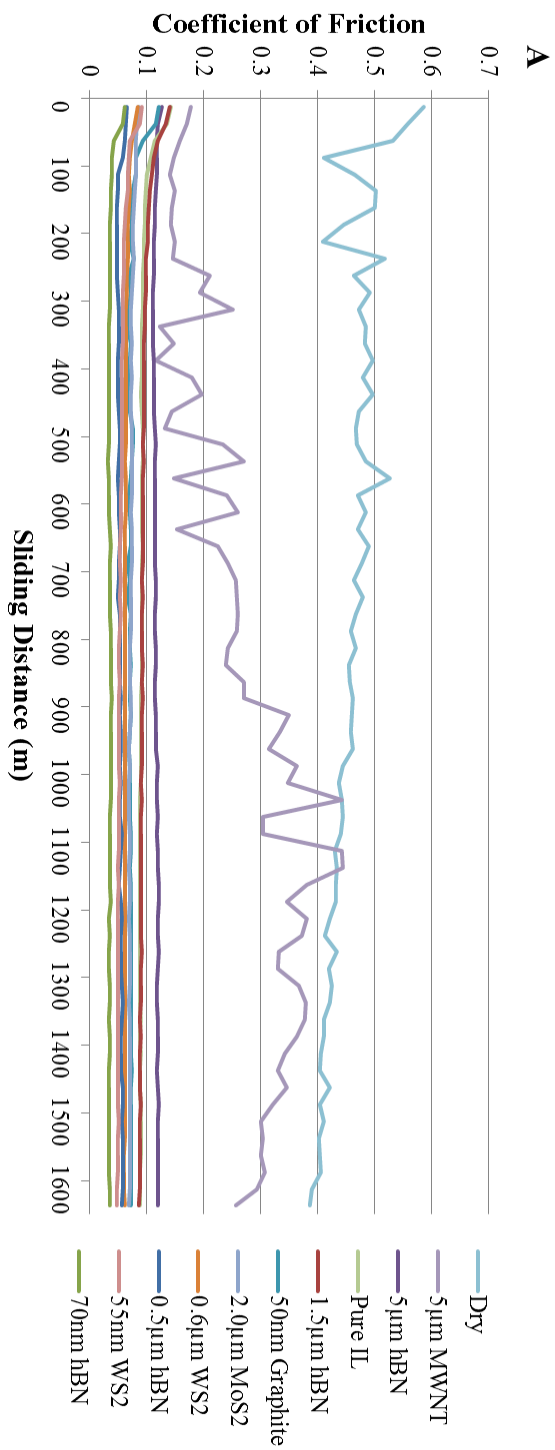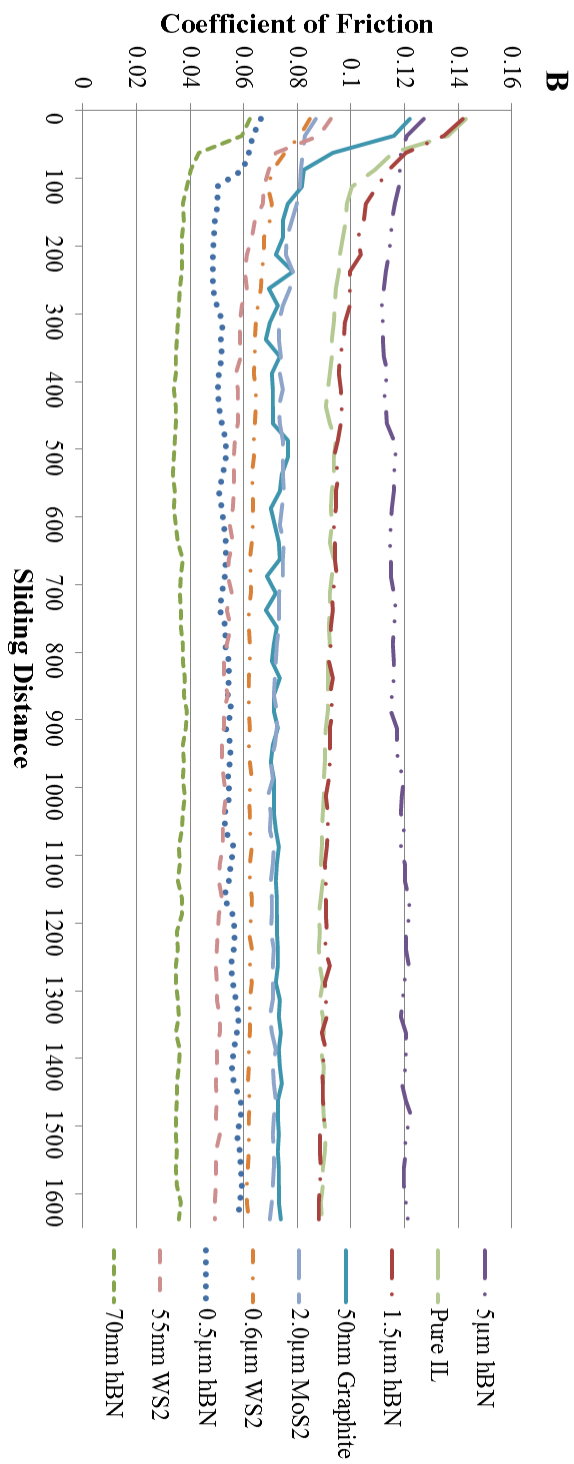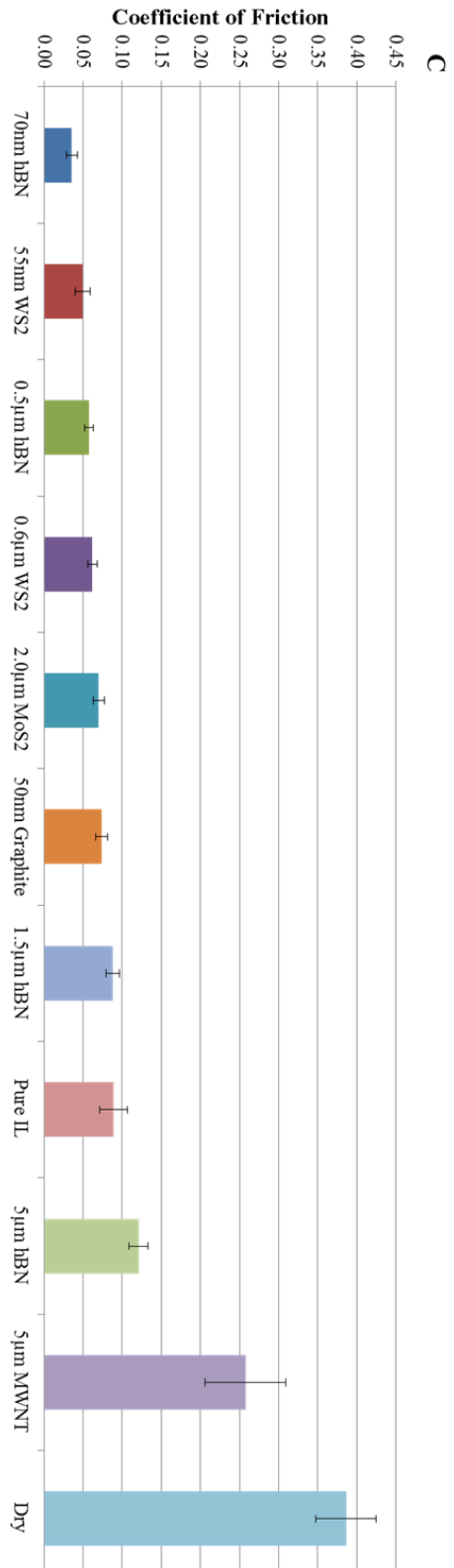
Figure 9.1: Variation of the coefficient of friction (a) for particulate mixtures with sliding distance; (b) for particulate mixtures with sliding distance, omitting the dry and MWNT tests, and (c) for particulate mixtures at completion of test

surface roughness could have potentially impacted the 5µm hBN particle performance because of the relatively low initial surface roughness the larger particles may not have had the ability to coalesce in the asperity values instead they had to traverse the asperity peaks and support the contact load [6, 118, 199, 337]. On the contrary, this is not the same for the carbon nanotubes. The MWNTs were tested for comparative reasons and they revealed interesting results. It was shown that during the tests the MWNTs exhibited low friction at the start of the tests as shown in Fig. 9.1(a), but slowly this fiction increased to a level similar to that of an unlubricated dry test, while simultaneously the available liquid in the lubricant mixture began drying up. The reason for this is due to capillaries effects caused by intermolecular forces i.e. surface tension and adhesion forces, whereby the lubricant is drawn into the carbon nanotubes [412, 413]. At the start of the test the lubricant mixture flows because there is a surplus of carrier fluid to circulate the MWNTs in the solution. It is as this instance where the MWNTs can act as small cylindrical bearings aligning themselves to the direction of motion in the tribo-interface thereby minimizing asperity contact and lowering friction [403]. Initially, the MWNTs provide low friction due to their telescoped cylindrical shells with atomically smooth surfaces enabling easy intershell sliding with rotational degrees of freedom, affording the MWNTs the ability to accommodate the relative surface velocities [402, 404-406, 414-416]. However, this is short lived in the experiment as the inherently polar ionic liquid begins interacting with the hydrophobic carbon surface causing the MWNT to wick the fluid inside it. At a molecular level, the energy involved in the capillary process is

proportional to the surface area through the surface tension. This energy is balanced by the bulk free energy which is proportional to the difference of the chemical potential of the ionic liquid [417]. As the IL is adsorbed into the MWNTs, this causes the nanotubes to no longer be circulated by the lubricant and thus it is forced out of the tribo-contact thereby entering a quasi-dry or unlubricated scenario where the COF increases to levels similar to the unlubricated test as observed in Fig. 9.1(a).

Figure 9.2 shows the influence of particle size with the COF as demonstrated with the boron nitride particle. Figure 9.2(a) shows the COF for boron nitride particulate mixtures with sliding distance and Fig. 9.2(b) shows the COF for hBN particles at the completion of the tests.
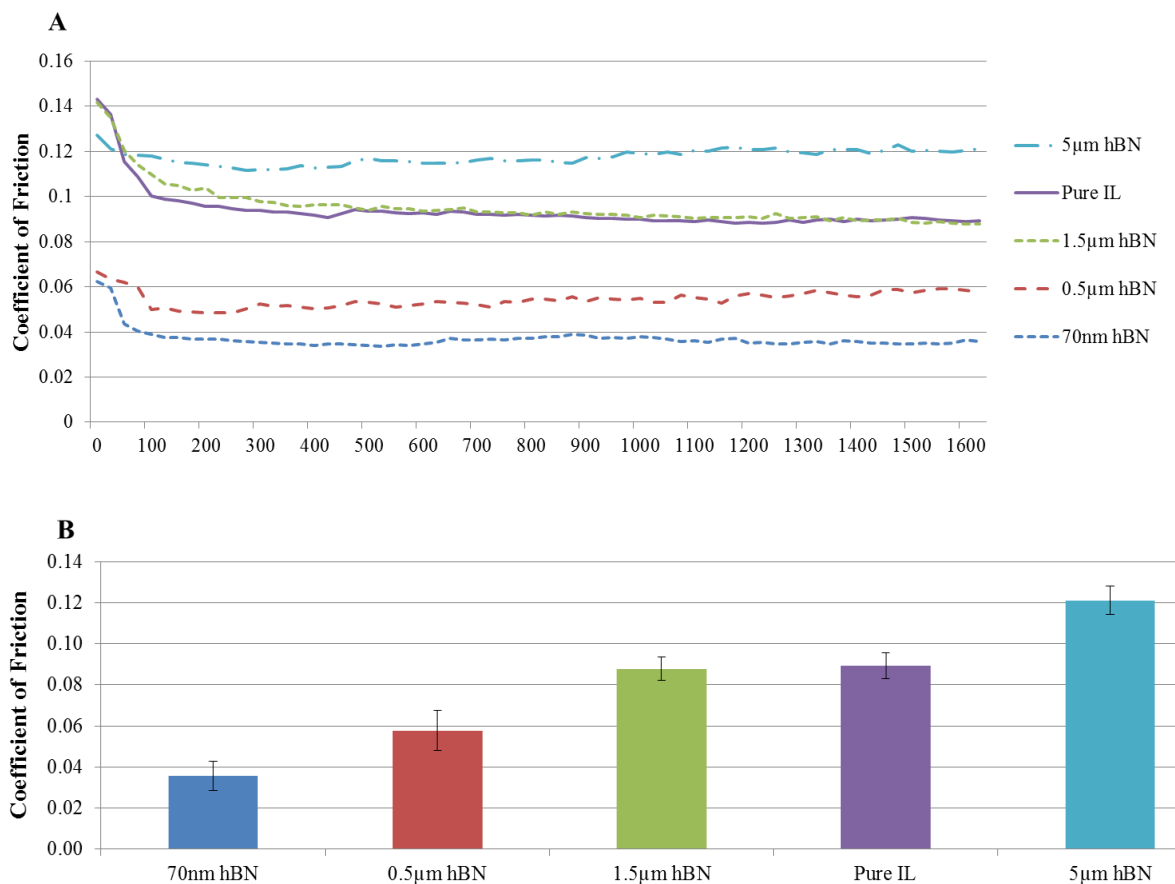
Figure 9.2: Variation of the coefficient of friction for hBN particulate additive mixtures (a) with sliding distance (b) at completion of test

The hBN particles are a clear example of the effect that particle size has on the friction properties. As in this figure, the smaller the particle size the lower the friction. This indicates that smaller more spherical shaped particulate additives in IL lubricants are more effective when they can coalesce in the asperity valleys, establish a thin smooth transfer film, accommodate the relative surface velocity, and provide minimal asperity contact in order to lower the friction coefficient [118]. On the contrary, larger more plate-

shaped particles such as the 5µm hBN are able to support more of the asperity contact load and minimize wear and friction. This function however does not seem effective which could be caused by the plate-shaped more abrasive tendencies of these larger particles. Large abrasive particles in the lubricant can damage the tribo-interface by acting as a third-body abrasive particle causing high friction [418, 419].

9.3.2 Wear Results

Figure 9.3, shows the wear volume for the various lubricant mixtures. It can be seen in Fig. 9.3(a) how the wear rate varies with sliding distance. In a similar manner to the COF results, the particulate containing lubricant mixtures show steady wear rates with the exception of the dry unlubricated and the MWNT tests, which show significant variation in their wear rates. Figure 9.3(b) shows the final wear volume values at the completion of the tests for each trial.
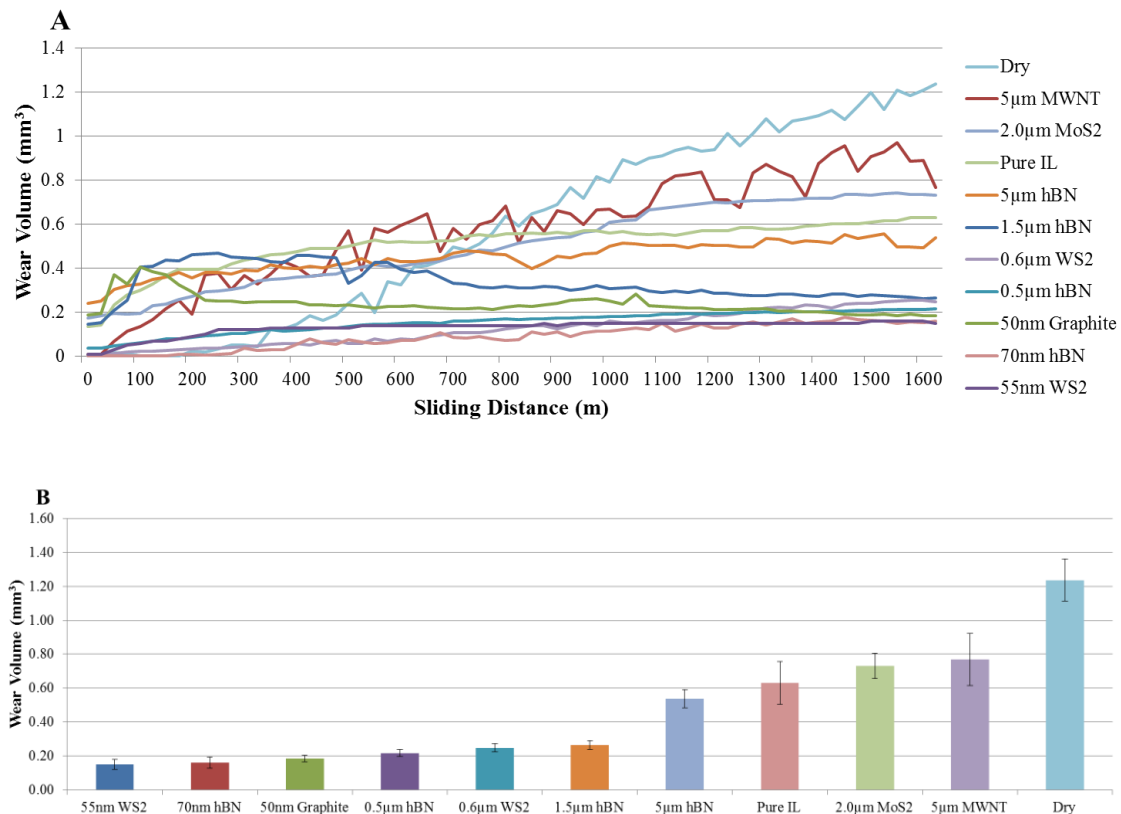
Figure 9.3: Variation of the wear volume (a) for particulate mixtures with sliding distance (b) for particulate mixtures at completion of test

The wear results reveal comparable trends to the friction results where smaller particles have lower wear volumes than larger particles. In the figure, there is a clear separation where the effects of the smaller particles dominate with the 55nm WS_2, 70nm hBN, and 50nm graphite particles having the lowest wear volumes, preceded by the 0.5µm hBN, 0.6µm WS_2, and 1.5µm hBN particles. Here, the environmentally benign particulate additives, hBN and graphite were shown to minimize the wear rate. It was

confirmed in the wear results that particulate lubricant mixtures containing particles with an approximate size of 1.5µm or smaller exhibit low wear rates that were lower than that of the pure lubricants with no additives. Examining the percent difference in wear rate between nanometer and micron-sized particles, it was calculated that a 43% percent difference occurred between the 55nm WS_2 and the 1.5µm hBN particles. The larger particles demonstrate a significant step up in wear rate, where the percent difference between the 1.5µm hBN and 5µm hBN particles is 51%. Again these results reveals how the smaller particles' ability to coalesce and establish a transfer layer to enhance the tribological properties is more significant than that of larger particles' ability to carry asperity contact loads. Interestingly, with regards to wear, larger particles such as the 5µm hBN, 2µm MoS_2, and the 5µm MWNT particles, were shown to have higher wear rates with only the latter two particles having wear rates greater than that of the pure lubricant with no additives. Although the 2µm MoS_2 has a smaller particle size than the 5µm hBN particles it has a higher wear rate. This could be due to the effects of moisture in the IL.

The MWNTs revealed a relatively volatile wear rate that fluctuated throughout the duration of the test as seen in Fig. 9.3(a). Again, the high wear volume in the MWNTs is caused by the continuously adsorbed $P_{666,14}$Salicylate oil. This resulted in the carbon nanotubes swelling up with fluid, creating a highly viscous two-phase mixture, and eventually being pushed out from the tribo-interface therefore starving the interacting surfaces with lubricant and creating the oscillatory behavior in wear volume as wear debris, saturated MWNTs, and lubricant agglomerated. Figure 9.4 shows the influence of

particle size with the wear volume as demonstrated with the boron nitride particle. Figure 9.4(a) shows the wear volume for boron nitride particulate mixtures with sliding distance and Fig. 9.4(b) shows the wear volume for hBN particulate mixtures at the completion of the tests. It can be seen in the figure that the effects of the smaller particles to improve upon the tribological properties i.e. wear volume, is significant.
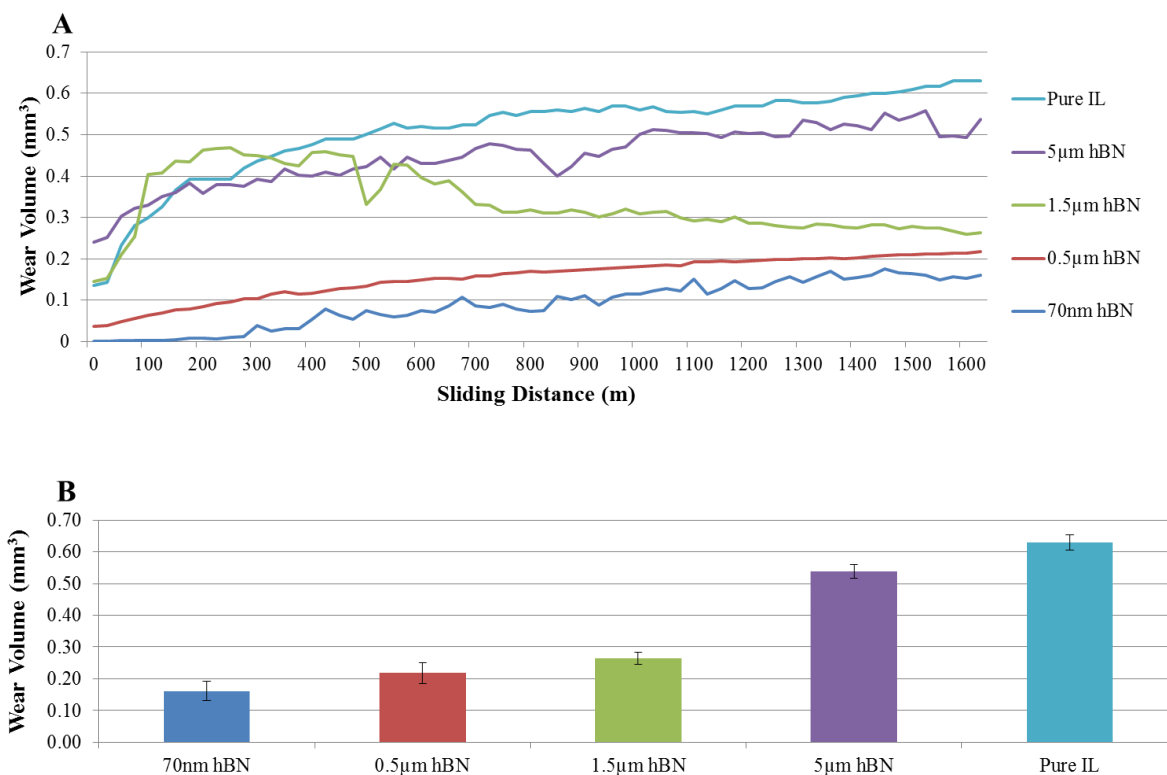
Figure 9.4: Variation of the wear volume for hBN particulate mixtures (a) with sliding distance (b) at completion of test

9.3.3 Surface Analysis

Figure 9.5 shows the scanning electron micrographs of the worn disk lubricated with the various mixtures under 200x magnification. Figures 9.5(a) through (c) are the SEM images for the 55nm WS_2, 70nm hBN, and 50nm graphite particles, respectively. These particles represent the smallest sized particles in this investigation having a size on the order of nanometers. Examining the SEM figures it can be seen that the wear tracks have the smallest diameter and they illustrate minimal abrasive wear due to plastic deformation caused by plowing from the harder pin thus corresponding to the low friction and low wear observed during the tribological testing. Figures 9.5(d) through (f) are the micrographs for the 0.5μm hBN, 0.6μm WS_2, and 1.5μm hBN particles, respectively. These particles represent the submicron and micron sized particles that revealed moderate friction and wear rates, which is demonstrated in the micrographs by the larger width in the wear track. The increased width in the wear track is representative of an increase in wear as more material is deformed and removed from the contacting interface. These particles along with the nanometer sized particles when used as an additive enhanced the tribological properties of base fluid for their ability to coalesce in the asperity valleys. Figures 9.5(g) through (i) represent the SEM images for the 5μm hBN, pure IL, and 2.0μm MoS_2 particle tests, respectively. These images reveal larger more abrasive wear tracks that are a result of the larger particulate additives having a plate-shaped geometry that abrades the lubricating surface as the particle traverses the surface. In Fig. 9.5(g) the 5μm hBN particles reveal a slightly narrower wear track than the pure IL test shown in Fig. 9.5(h), which corresponds to their lower wear rate than the pure IL test. Furthermore

the 2.0µm MoS$_2$ particles had a slightly higher wear rate than the pure IL test and this is confirmed by the wider more abrasive wear track shown in Fig. 9.5(i) that is beyond the frame of the image. The micrographs shown in Figs. 9.5(j) and (k) are for the 5µm MWNT particulate mixture and dry test respectively. As a result of the aforementioned phenomenon that occurred with the MWNT tests, it reasonable to observe a wear track that resembles the dry test. In the images, the wear tracks are extremely wide indicating the occurrence of significant wear as observed in the sliding tests. Furthermore, the high roughness of the surfaces as observed in the micrographs leads to the conclusion that as a result of the significant plastic deformation and material removal this could result in high friction as witnessed in these two tests. The micrographs shown in Fig. 9.5 do indicate that the effects of the particles due to their size, independent of the particle type does play an important role on the tribological performance of their use as additives in ionic liquid lubricants.
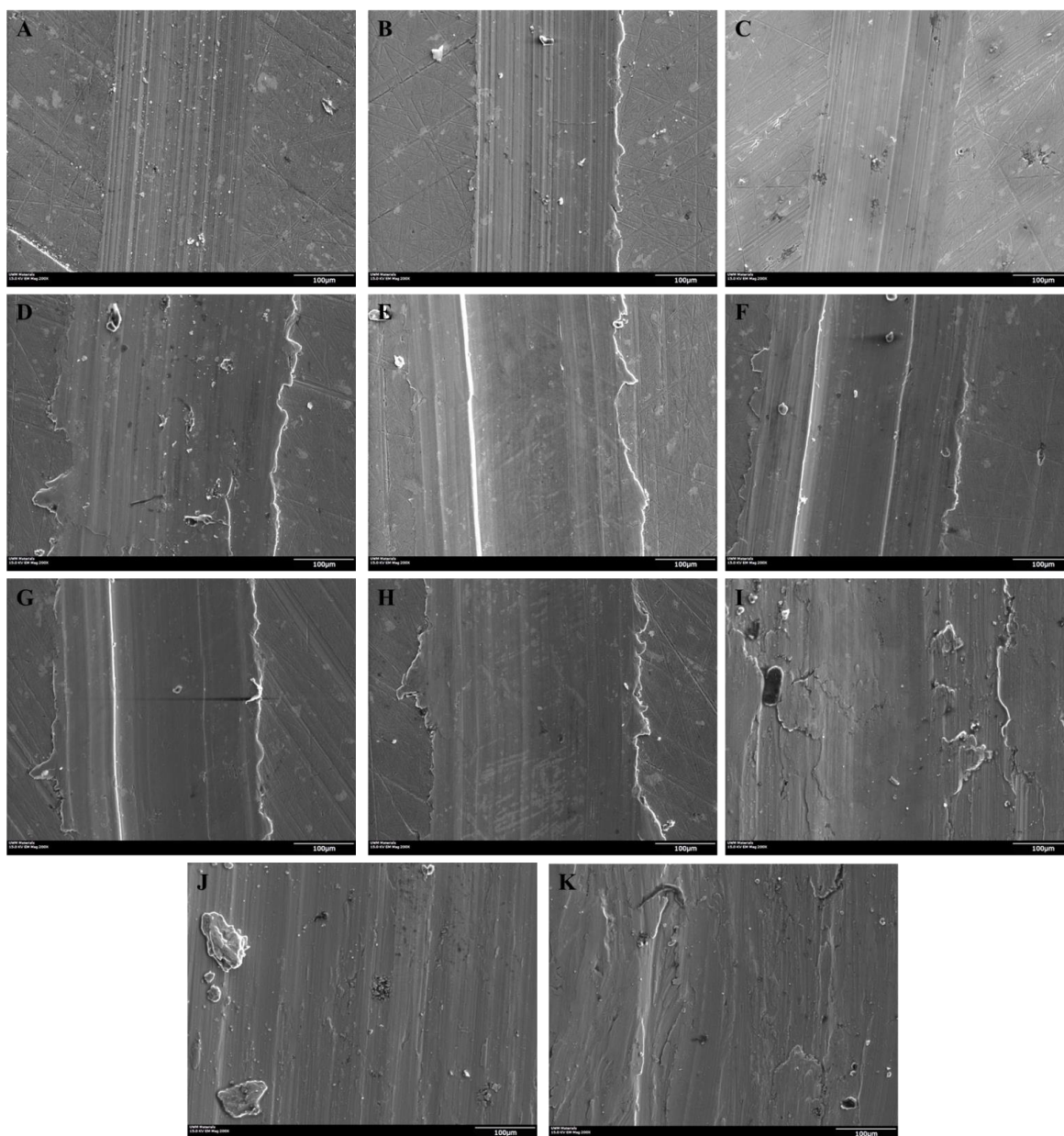
Figure 9.5: Scanning electron micrographs of the worn aluminum disk lubricated with the various particulate mixtures at 200x magnification (a) 55nm WS_2, (b) 70nm hBN, (c) 50nm Graphite, (d) 0.5μm hBN, (e) 0.6μm WS_2, (f) 1.5μm hBN, (g) 5μm hBN, (h) Pure IL, (i) 2.0μm MoS_2, (j) 5μm MWNT, and (k) Dry

9.4 Effect of Particulate Additives in Avocado Oil

As a basis for comparison, avocado oil was mixed with the same particulate additives as the $P_{666,14}$Salicylate to study the effect of these additives on the tribological performance. This investigation is a continuation of the experiments conducted in Chapter 5, section 5.4.2 – Avocado Oil Tests. Here, pin-on-disk tests were conducted using a C101 copper pin sliding on a 2024 aluminum disk with a 10N normal load, 36mm/s sliding velocity, at ambient conditions, and particles added at 5% by weight. Similar to the $P_{666,14}$Salicylate particulate additive testing, this study was performed using a Ducom Instrument Material Characterization System tribometer. It should be noted that friction is a system dependent property that is dependent upon test environment, operating conditions, and surface geometrical configuration. Therefore, friction is not a property to make direct comparisons in regards to coefficient of friction values. Nevertheless, these natural oil tests provide an important comparison to understand the impact of the particulate additives to improve upon the avocado oil.

9.4.1 Results and Discussion

9.4.2 Friction Results

Figure 9.6 shows the COF for all the particulate mixtures containing avocado oil. Figure 9.6(a) and (b) show the single- and multi-particle tests and the variation of the COF with sliding distance, respectively. Figure 9.6(c) shows the final COF values at the completion of the tests for all particulate mixtures. From these figures it can be seen that the COF generally decreases with sliding distance. It can be seen that the lower COF is

not necessarily dependent on the particle size, although smaller particles do lower friction, but it can be seen that hBN has the lowest friction and within the hBN particles the smaller sized particles maintain lower friction. This is what occurred in Chapter 5 with the avocado oil tests. Examining the types of particulate additives revealed that hBN outperforms, MoS_2, WS_2, graphite, and the MWNTs. The trends described in Chapter 5 for the hBN are present here for each type of particulate additive. These trends are more clearly observed in Figure 9.7 which depicted the final COF values for selected particulate mixtures. In Fig. 9.7(a), the trends of the individual particle mixtures can be seen. It was revealed that the particles align themselves according to their ability to lubricate within the avocado oil, but within each particular type of additive the were arranged based on particle size. This is different than the witnessed trends seen in the ionic liquid with particulate additives where size was the dominating characteristic. Figure 9.7(b), shows the effects of combining particles of different sizes for the boron nitride particles as explained in Chapter 5. The 70nm particles enhance the properties of the other lubricants be better filling the asperity valleys and better accommodating the relative surface velocities by establishing a lubricious transfer film. Interestingly, when the hBN particles are added to the MoS_2 particles as seen in Fig. 9.7(c), the trends of the hBN particles persist. Here, the hBN particles improving upon the friction properties of the MoS_2 and they remain in order of particle size despite having the MoS_2 present. In fact by adding the hBN particles to the MoS_2 the 70nm and 0.5μm particles lowered the COF of the MoS_2 by 33% and 14% respectively as shown in Table 9.2. The 1.5μm hBN particles had no effect on the COF and the 5.0μm hBN particles increased COF of the

MoS_2 by 45%. Of the four particles investigated only the hBN and MoS_2 particles improved the friction properties of the avocado oil. The WS_2 and graphite properties did not enhance the lubricity. The carbon nanotube particulate mixtures witnessed capillary effects as seen with the ionic liquids in the MWNTs that absorbed the lubricant, creating a highly viscous slurry, and rendering the particulate mixture useless as a lubricant.

A

Coefficient of Friction vs Sliding Distance (m)

Legend:
- 5μm MWNT
- 50nm Graphite
- 0.6μm WS2
- 55nm WS2
- Pure Oil
- 5μm hBN
- 1.5μm hBN
- 0.5μm hBN
- 70nm hBN
- 2μm MoS2

B

Coefficient of Friction

Sliding Distance (m)

- · 5μm hBN + 2μm MoS2
- · · · · 1.5μm hBN + 2μm MoS2
- – 0.5μm hBN + 1.5μm hBN
- · 0.5μm hBN + 2μm MoS2
- 70mm hBN + 2μm MoS2
- 70mm hBN + 1.5μm hBN
- · · · · 70mm hBN + 0.5μm hBN
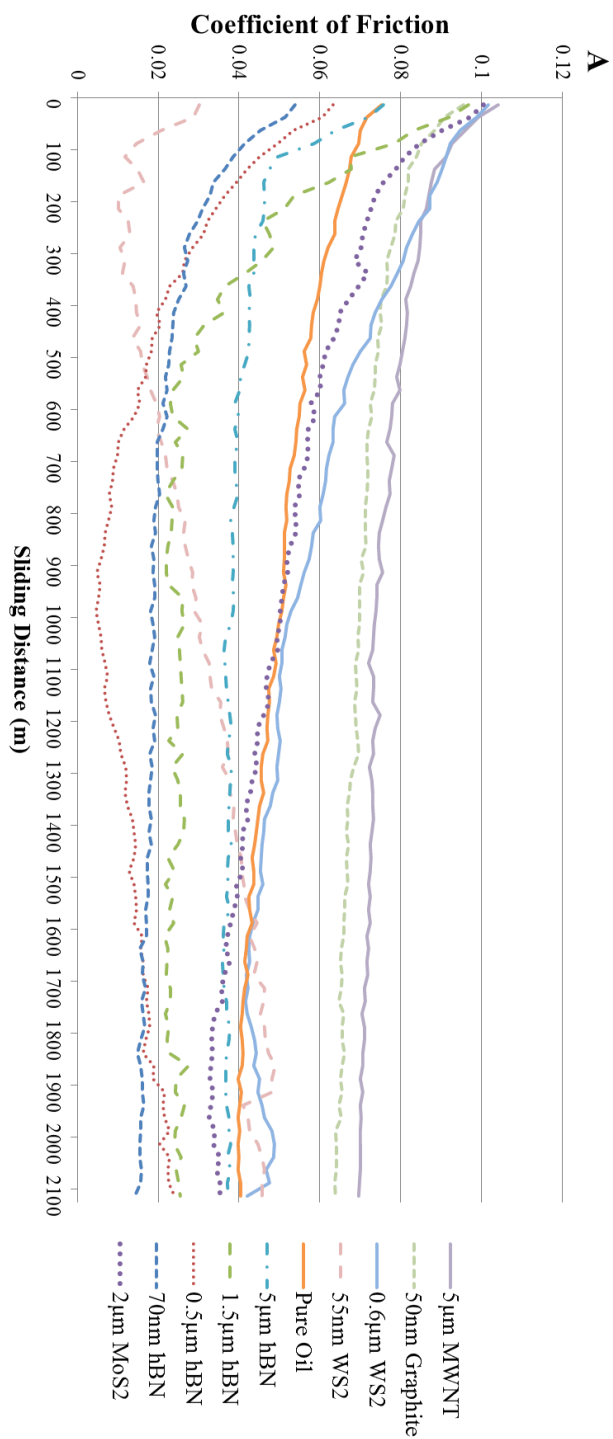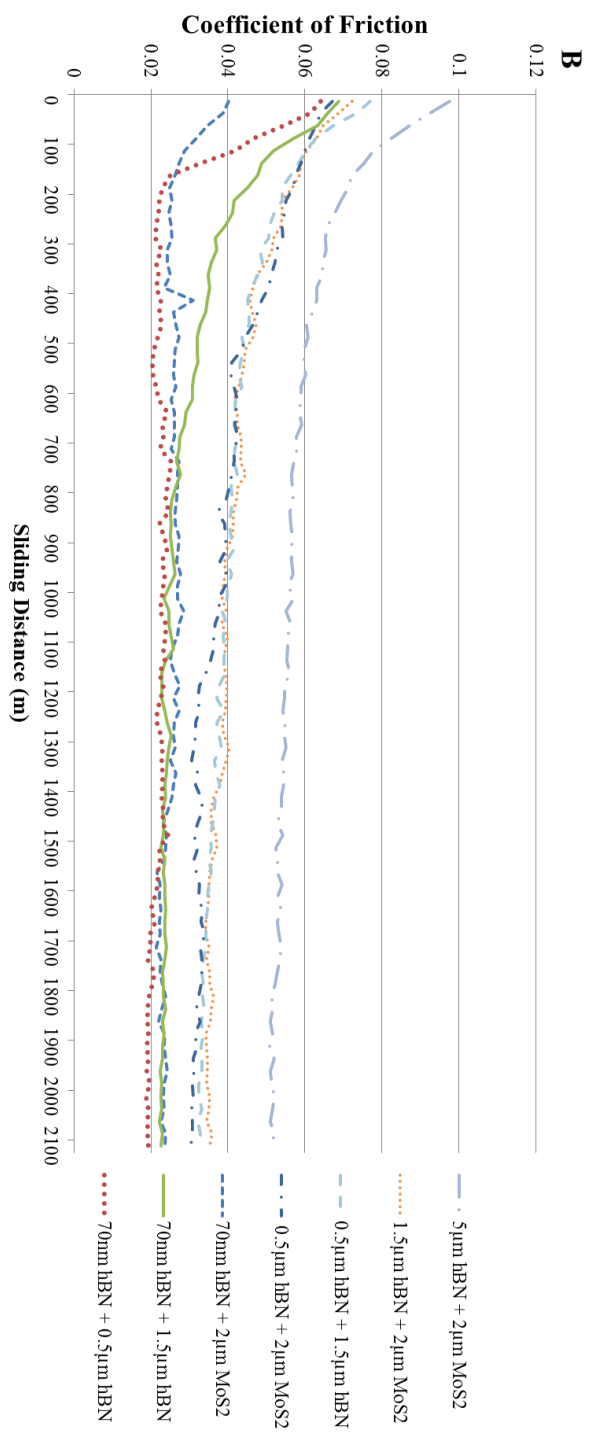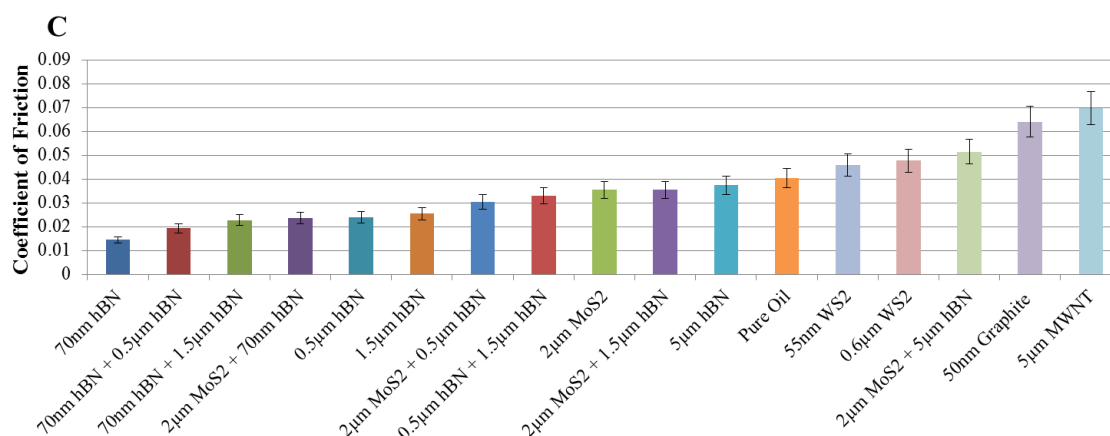
Figure 9.6: (a) Variation of the coefficient of friction with sliding distance for single particle mixtures; (b) variation of the coefficient of friction with sliding distance for multiple particle mixtures; and (c) final coefficient of friction for various single and multiple particle mixtures
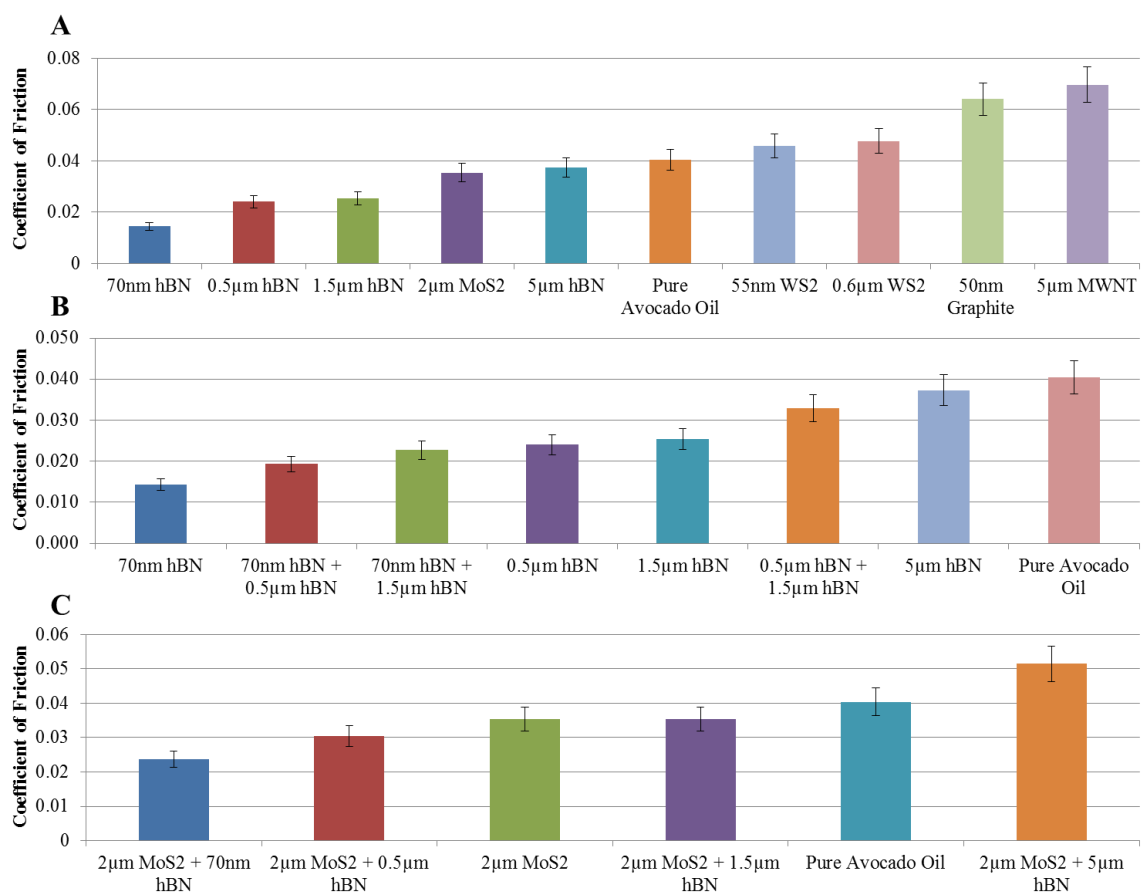
Figure 9.7: Final coefficient of friction for avocado oil and various particle additive mixtures, (a) for all single particle mixtures; (b) for all hBN particle mixtures; and (c) for all MoS_2 particle mixtures

Table 9.2 Percentage change due to the influence of hBN particles on the COF

Base Particle	Particle Additive			
	0.07μm hBN	0.5μm hBN	1.5μm hBN	5.0μm hBN
2μm MoS_2	-33%	-14%	-0.0%	45%

9.4.3 Wear Results

The wear results with sliding distance of the avocado particulate mixtures are shown in Figs. 9.8(a) and (b) for the single and multi-particle mixtures. As expected the wear volume increases with sliding distance. Figure 9.8(c) shows the final wear volume at the completion of the tests for the lubricant mixtures. The wear results reveal that the hBN particulate mixtures maintain the lowest wear values followed by the MoS_2, WS_2, graphite, and MWNT. Figure 9.9(a) shows the final wear volume at the completion of the tests for (a) the single particle mixtures, (b) hBN mixtures, and (c) the MoS_2 mixtures. From Fig. 9.9(a) the wear results reveal that for a single type of particle additive the smaller the particle size the lower the wear rate. These trends are in agreement with the friction results that smaller particles improve the friction properties. Examining Figs. 9.9(b) and (c) it is revealed that the addition of smaller hBN particles to a lubricant whether to boron nitride itself or MoS_2, the small size of the particle additive the lower the wear rate is. The analysis of Fig 9.9(b) was performed in Chapter 5, section 5.4.2 – Wear Volume Results, and it revealed that smaller hBN particles particularly the 70nm hBN particles greatly influences the effects of other particles because of its superior ability to coalesce in the asperity values and establish a transfer film that minimizes asperity contact and can accommodate the relative surface velocities therefore lowering the wear rate. The influence of the hBN particles on the MoS_2 revealed improvements where the 70nm, 0.5μm, and 1.5μm hBN particles lowered the wear volume of the MoS_2 by 48%, 21%, and 12%, respectively as shown in Table 9.3. The 5.0μm hBN particles increased the wear volume of the MoS_2 by 33%. Similar to the friction results only two

the five different particle additives were able to improve upon the wear volume, they were the hBN and the MoS_2 particles. The WS_2 and graphite particles exhibited higher wear volumes that slightly decreased for a particular particle type if the particle was smaller. For example 55nm WS_2 out performed 0.6μm WS_2, by having a smaller particle size despite WS_2 having some of the highest wear volumes in the investigation. The MWNT particles exhibited high wear due to the lubricant adsorption that rendered the lubricant mixture ineffective.

A

Legend:
- 5μm MWNT
- 50nm Graphite
- 0.6μm WS2
- 55nm WS2
- Pure Avocado Oil
- 5μm hBN
- 2μm MoS2
- 1.5μm hBN
- 0.5μm hBN
- 70nm hBN

X-axis: Sliding Distance (m)
Y-axis: Wear Volume (mm³)

B

Wear Volume (mm³) vs Sliding Distance (m)

Legend:
- .... 2μm MoS2 + 5μm hBN
- - - - 2μm MoS2 + 1.5μm hBN
- — ·· — 2μm MoS2 + 0.5μm hBN
- - - - 0.5μm hBN + 1.5μm hBN
- ········ 2μm MoS2 + 70nm hBN
- ——— 70nm hBN + 0.5μm hBN
- — · — 70nm hBN + 1.5μm hBN
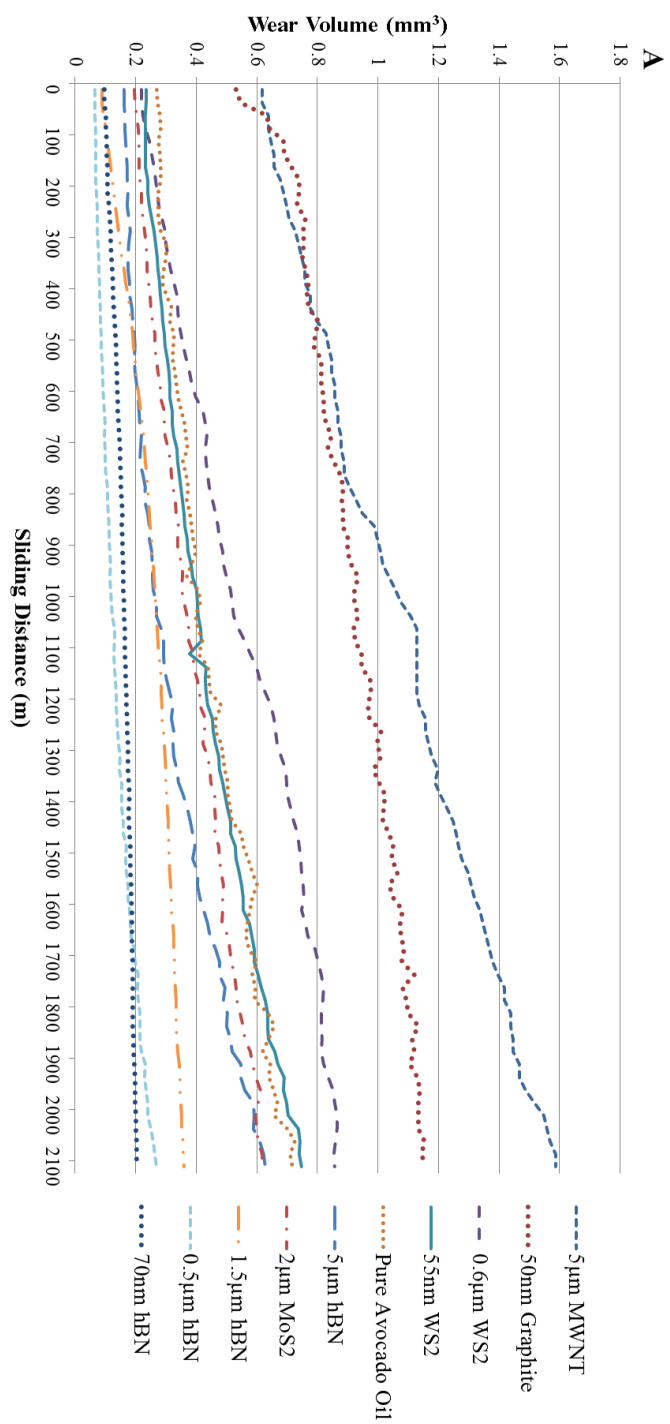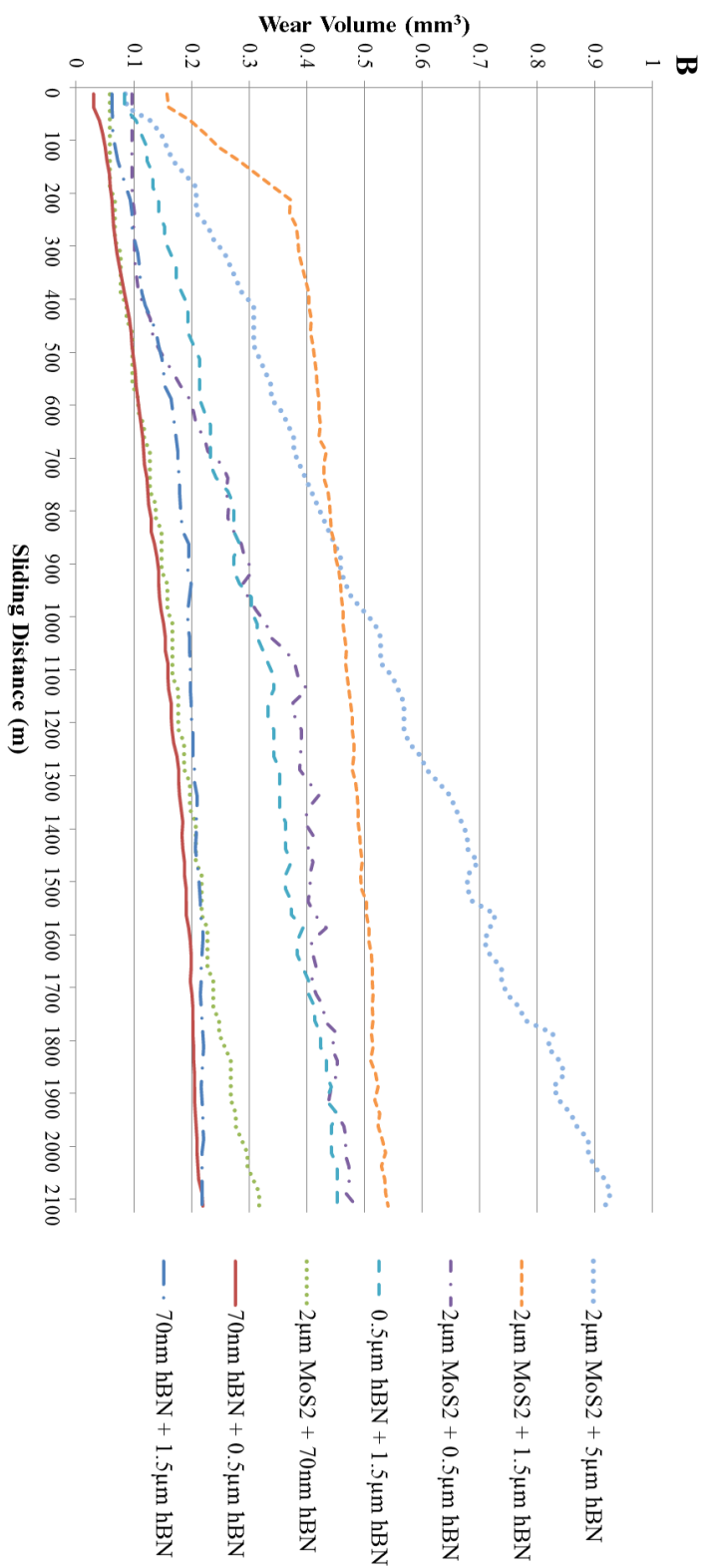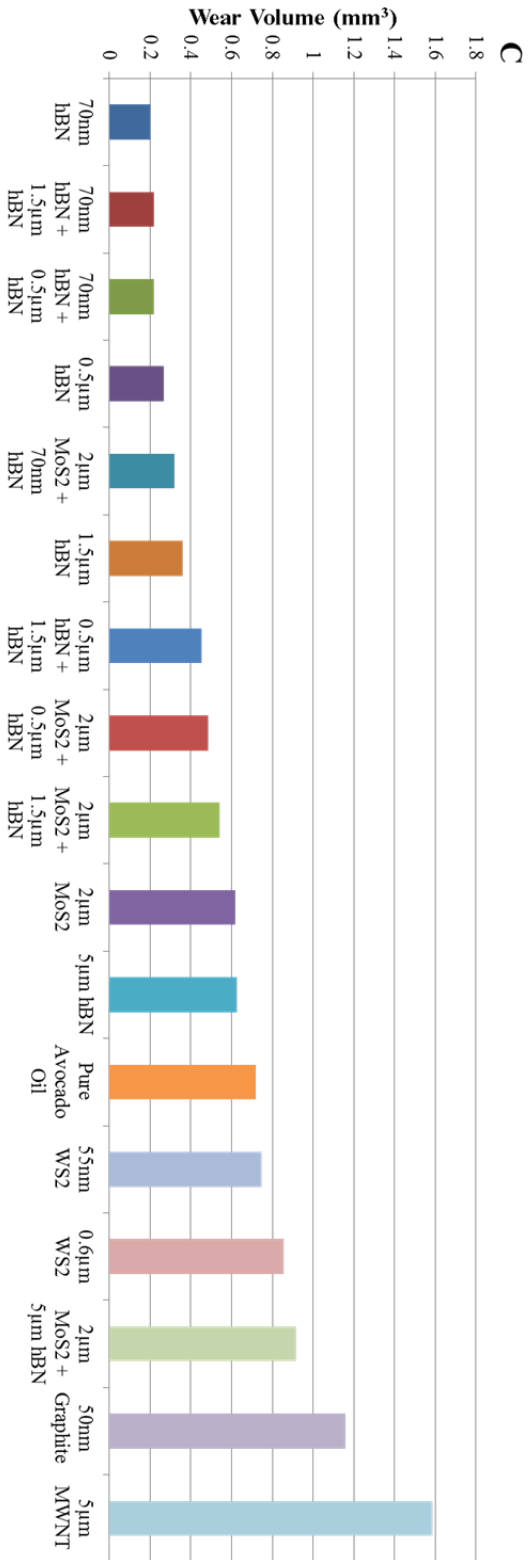
Figure 9.8: (a) Variation of the wear volume with sliding distance for single particle mixtures; (b) variation of the wear volume with sliding distance for multiple particle mixtures; and (c) final wear volume for various single and multiple particle mixtures
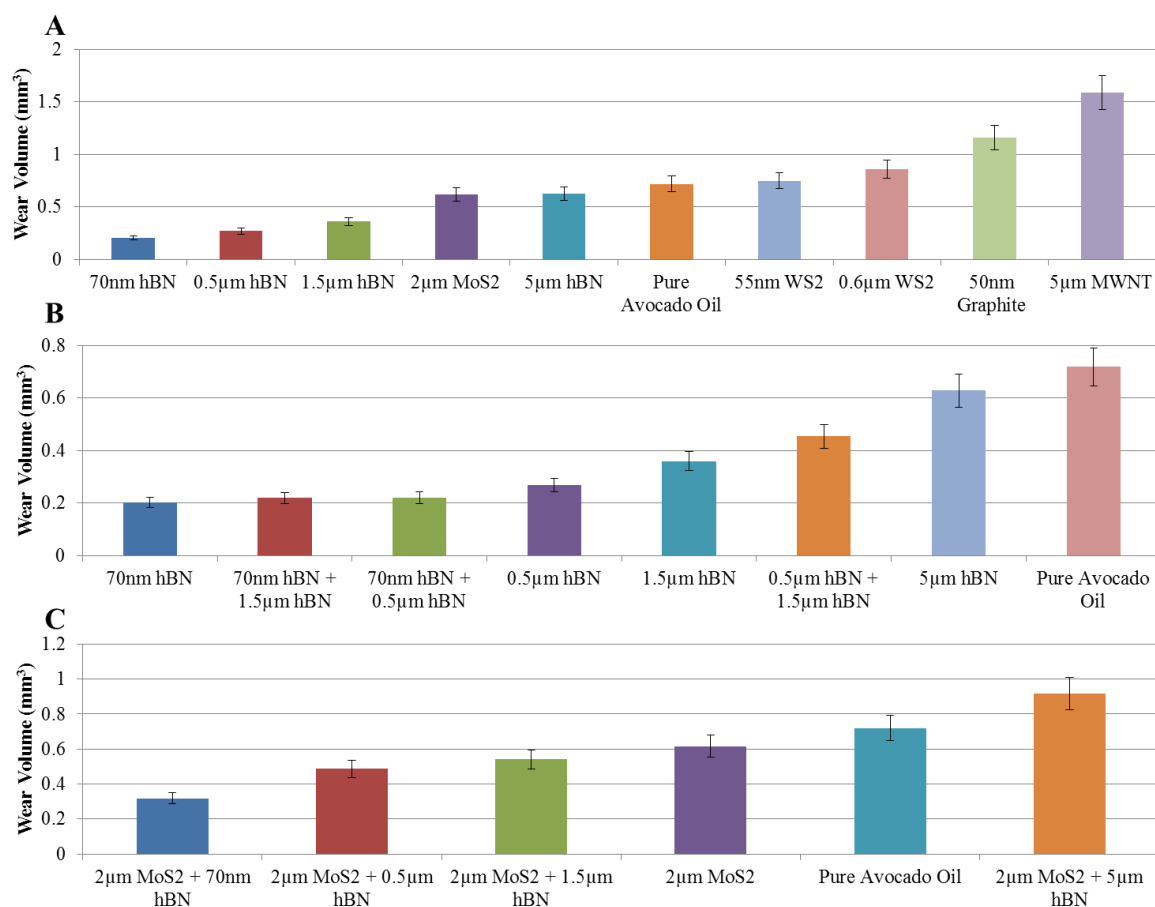
Figure 9.9: Final wear volume for avocado oil and various particle additive mixtures, (a) for all single particle mixtures; (b) for all hBN particle mixtures; and (c) for all MoS_2 particle mixtures

Table 9.3 Percentage change due to the influence of hBN particles on the wear volume

	Particle Additive			
Base Particle	0.07μm hBN	0.5μm hBN	1.5μm hBN	5.0μm hBN
2μm MoS_2	-48%	-21%	-12%	33%

The ability of the particulate additives to improve upon the tribological properties of the natural oils is drastically different than their method of improving the tribological properties of the ILs. In the natural oils, particle selection and then the choice of particle size, where the smaller size the better, are revealed as the selection criteria for using solid particle additives. In contrast, it was shown in the ionic liquid particulate mixtures that particle type was not as important as selecting the smallest particle to improve upon the tribological properties. These results indicate that intrinsic properties to the base fluids should be further instigated to understand why the particle additives perform differently within the two fluids. Nevertheless, the use of particle additive in natural oils or in ionic liquids does have the ability to enhance the tribological performance.

9.5 Fractal Analysis

Table 9.4, shows the final COF and wear volume results for the lubricant mixtures as well as the pure IL and unlubricated dry tests. As described previously, there is a clear divide in the ability of the particulate additives to positively influence the tribological properties. Lubricants that enhance the tribological performance of the $P_{666,14}$Salicylate depend primarily on particle size instead of the particle type. This is confirmed when examining the two correlation coefficients between particle size and COF and between particle size and wear volume shown in Table 9.4, where each has a strong positive correlation of 0.831 and 0.828, respectively. It can be generally inferred that as the particle size decreases the coefficient of friction and the wear volume decrease. Further examination into the particle types and sizes demonstrates that synthetic solid particle

additives i.e. hBN and WS_2, most strongly maintain these trends. For each of these additives, as the particle size decreases the COF values and the wear rate decrease with R-values greater than 0.94. This is speculated to be a result of these synthetic inorganic solid lubricants being highly refractory and thermo-chemically stable, thus allowing for sustained lubricity. Although MoS_2 and graphite are well known solid particulate additives, they exhibit minor enhancements to the base fluid with moderate friction values. Immediate speculation leads to the idea that hydrolytic instability caused by moisture in the form of water content in the lubricant due to hygroscopicity influenced these lubricant additives [420]. MoS_2 for example has been shown to have depleted performance in the presence of moisture, which has a detrimental effect on its lubricity [65, 66]. On the contrary, graphite is well known for exhibiting superior lubrication in moist air environments, while being a poor lubricant in dry or vacuum environments [421]. However, in these tests MoS_2 exhibited a high wear rate while graphite maintained a low wear rate which could be directly related to their large and small particle sizes, respectively. Most lamellar solids have good wetting capability and chemical affinity for ferrous surfaces thus adding to their lubricious behavior [64].

Table 9.4: Particle size-to surface roughness index, friction value,

and wear volume for various lubricant mixtures tested

Test Name	Particle Size	Particle size-to surface roughness index	Coefficient of Friction	Wear Volume (mm^3)
70nm hBN	0.070	0.650	0.0358	0.1613
55nm WS2	0.055	0.725	0.0493	0.1500
0.5μm hBN	0.500	1.50	0.0578	0.2177
0.6μm WS2	0.600	2.00	0.0620	0.2483
2.0μm MoS2	0.050	9.00	0.0699	0.7312
50nm Graphite	0.050	0.75	0.0737	0.1860
1.5μm hBN	1.500	6.50	0.0879	0.2641
Pure IL	0.000	N/A	0.0893	0.6300
5μm hBN	5.000	24.0	0.1212	0.5375
5μm MWNT	5.000	24.0	0.2576	0.7674
Dry	0.000	N/A	0.3862	1.2360
Correlation coefficients, R-value		**0.9976**	**0.8310**	**0.8277**
Correlation coefficient, between friction and wear			**0.8664**	

Previous research by the authors has shown that when a surface roughness becomes relatively smooth, the effects of smaller particulate additives in the lubricant to lower the friction and wear rate dominate. In this investigation the initial surface roughness, R_a value of 0.2 ± 0.02 μm, is within the region where smaller particles enhance the tribological properties. Furthermore investigation into the particle size-to-surface roughness (PSR)-Index (Ψ_{SR}) index reveals a threshold to which the effect of large particle sizes having adverse effects. In a previous investigation with boron nitride particles, when the Ψ_{SR} reached approximately 4.0, the larger sized particles began having detrimental effects on the tribological properties such as increases in friction, wear, and surface roughness [118]. In the current investigation, as the Ψ_{SR} approaches 6.50 this

becomes the upper limit where beyond this a transition occurs where larger particles become detrimental to the tribological performance.

An empirical model helps to illustrate the effects of the particle size on the tribological performance. As indicated in Table 9.4, the correlation coefficient between friction and wear is approximately 0.866. This indicates that there is a strong correlation between having high friction and high wear. Throughout this assessment and in the following calculations the friction model will be compared with the wear model. To describe the empirical model, it must start with the experimental data shown in Table 9.4 for both the friction and wear. Performing a 2nd order polynomial least squares regression on the friction and wear volume data allows two independent functions to be calculated with the following equations:

$$f(x) = 0.0026x^2 - 0.0147x + 0.0728 \qquad \text{Eq. (9.1a)}$$

$$w(x) = 0.0265x^2 - 0.386x + 0.7013 \qquad \text{Eq. (9.1b)}$$

In Eq. (9.1a), f(x) is the predicted coefficient of friction as a function of particle size, x. Similarly in Eq. (9.1b), w(x) is the predicted wear volume expressed as a function of particle size. These equations represent the basis for a set of macroscale fractal functions where the particle size represents the fractal dimension [422-424]. Here, x represents a wide variety of possible variables that could influence the performance of the particulate additive such as particle size, particle shape, interatomic layer distance, contacting materials, testing parameters, etc. In this analysis x will represent the particle size. Figure

9.11, illustrates the fractal function as a function of particle size based of the current experimental data for the friction and wear plots.
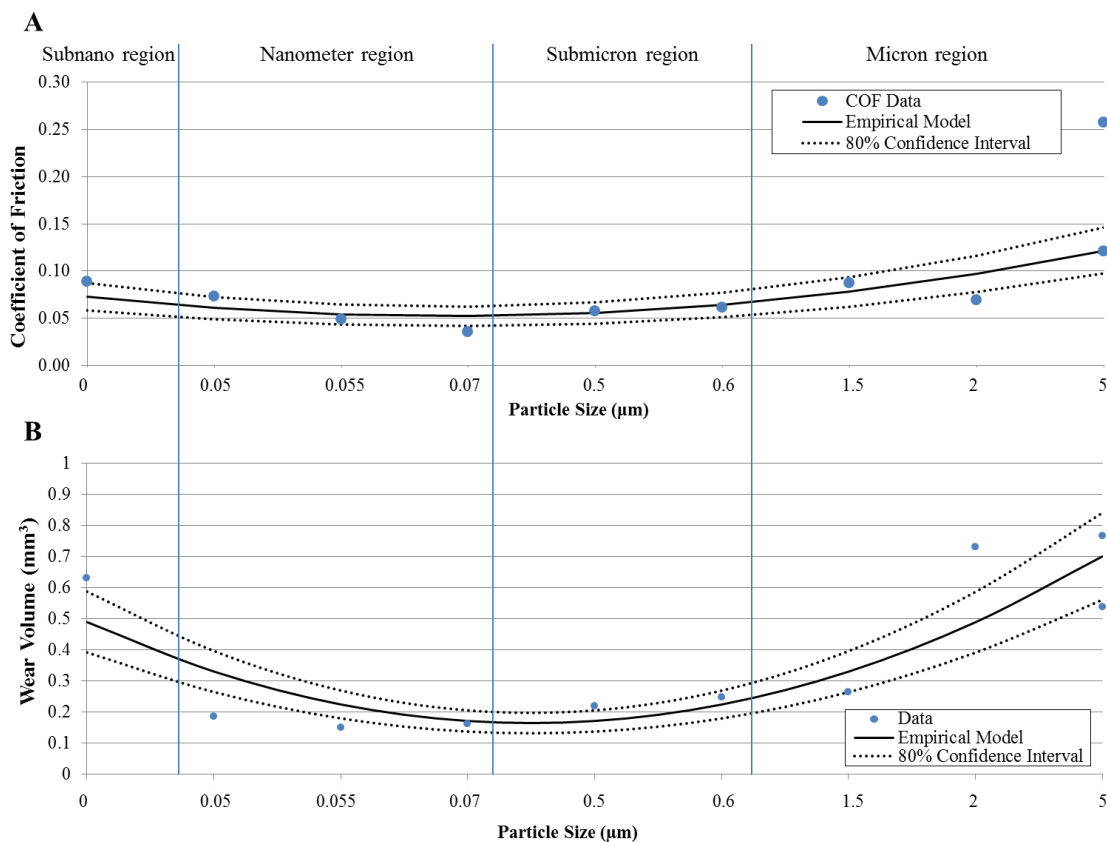
Figure 9.10: Empirical model derived from experimental data (a) friction and (b) wear volume

In Fig. 9.11, there are four regions that correspond to the respective particle sizes. It can be seen that the empirical model represents the trend line that corresponds to the data points with its corresponding confidence interval. The four regions denote areas where this function may behave as a fractal, on the basis that as the relative scale (in this instance, the size of the particles) could potentially change the complexity of the function

the complexity of the function could also change. Typically in tribology, a fractal analysis is reserved for surface roughness as a direct correspondence to Mandelbrot who developed fractal geometry to characterize the irregular and fragmented patterns within nature and to provide a means by which seemingly chaotic and random patterns could be quantified [425, 426]. When considering fractals, a rough or fragmented pattern will vary depending on the degree of roughness of the pattern. Further, the fractal dimension will also have a different value for each pattern type with the fractal dimension being specific for a particular pattern [427]. By utilizing a fractal analysis of the roughness and size distribution of granular materials by Hyslip et al. [428] and a simple fractal analysis method of surface roughness by Jahn et al. [429] a preliminary fractal analysis can be performed to determine if indeed the friction and wear behavior could be a fractal with particle size or surface roughness as the scale.

The fractal dimension of a particular pattern or function can change within consecutive regions especially when analyzed at different scales. This can create what is known as 'bi-fractality' or 'multi-fractality'. In the current empirical model the system is unscaled in Fig. 9.10. However, when analyzing the data in a scaled version as shown in Fig. 9.11 for both the COF and wear volume data the different regions can be postulated to undergo multi-fractality resulting in multiple fractal dimensions based on the scale of the particle size. It is these relative size scales ranging between subnano and micron that would be the basis for the fractal behavior. An inherent feature with the different scales is that different aspects of the pattern, characteristics of the particle, or influences of the tribo-interface can become apparent or become no longer noticeable. In the current

example, in the subnano region as the particles get infinitely small, the lubricant mixture will approach a consistency and physical behavior as if there were never particulate additives present and for this reason it becomes effectively a pure lubricant that has high friction and wear rate as seen in the experimental data, thus instantly moving from a subnano scale to a micron scale on the order of roughness. Within the nanometer range the particles may behave significantly differently or they may behave similarly as they did in the current investigation with consistently low friction values and low wear rates, however this could be a direct result of the surface roughness effects as denoted by the PSR-Index. Within the nanometer sized particles the PSR-Index varies by 15%, revealing how consistent the particles behave at the current surface roughness level. However like a fractal this could change significantly if the surface roughness was on the same order of magnitude as the nanometer sized particles. In the large scale regions, the submicron and micron sized particles could reveal an exponential progression that increases the wear rate tremendously as the particle size increases. Due to the significant range in particle size different regions of this empirical model could behave differently and is dependent on the fractal dimension resulting in incremental complexities to the functions derived in Eq. (9.1). The true scale shown in Fig. 9.11, reveals how a fractal line or fractal function could be used to represent the different regions as the scale increases or decreases revealing or concealing the complexities of the particulate additives that would affect friction and wear.
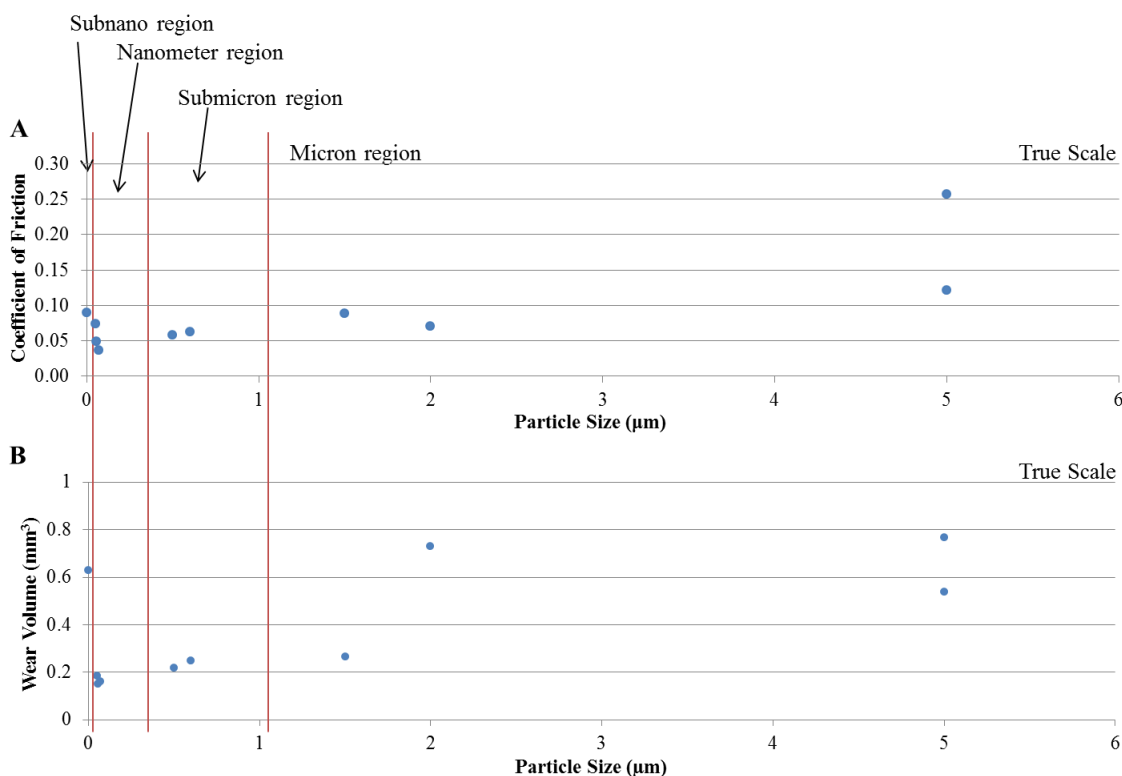
Figure 9.11: Friction and wear volume results on a true scale of particle size

Applying a modified version of Mandelbrot's definition of a fractal line derived from his theories of fractal power laws, $P(\lambda)$, to the 2nd order functions of friction and wear shown in Eq. (9.1), a fractal analysis can begin to take shape. The fractal line is defined as

$$P(\lambda) = n\lambda^{1-D_R}$$
Eq. (9.2)

where $P(\lambda)$ is the unit of measurement of length λ and is defined by Eq. (9.1) for friction and wear. In this case λ is the particle size and $P(\lambda)$ is the coefficient of friction and wear rate; n is the proportionality constant (equal to the actual and indeterminate size of the particle); D_R is the fractal dimension of the function which is a quantitative descriptor of "roughness" or in this case the relative scale between particle size and surface roughness.

Taking the logarithm of both sides of Eq. (9.2) yields the linear relationship between P(λ) and λ with D_R related to the linear slope coefficient, m by

$$D_R = 1 - m \qquad \text{Eq. (9.3)}$$

A plot of the fractal dimension versus the corresponding particle size, λ on a full logarithmic scale will result in a linear plot with the slope of the line through the individual data points related to the fractal dimension defined in Eq. (9.3) [428]. Here, a fractal line that increases in complexity with different scales should yield, $1 < D_R < 2$ [429]. If the fractal lines become geometrically smooth than $D_R = 1$ and if the fractal decreases in complexity then it is characterized by a $D_R < 1$. Figure 9.12 plots the two fractal dimensions for the COF and wear volume data based on the particle size as a function of the length scale, λ.
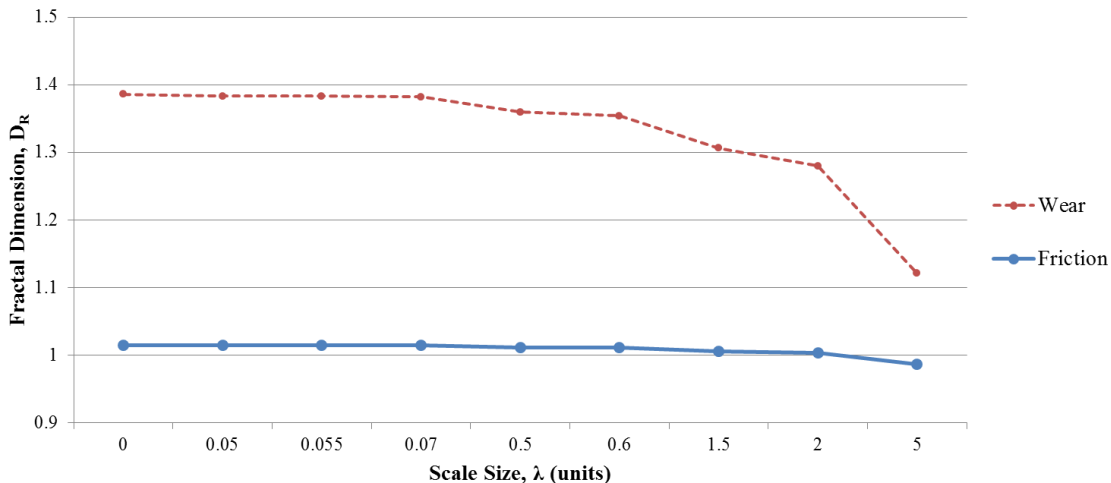
Figure 9.12: Fractal Dimension for the coefficient of friction and wear volume based off a modified Divider method.

It can be seen in Fig. 9.12 that for both the COF and wear volume, the fractal dimension decreases as the scale size (particle size) increases. The general trend and characteristics of Fig. 9.13 are in agreement with established techniques [428, 430]. The decrease in fractal dimension with an increase in scale size is expected because as particle size increases to microns the effects of surface roughness and other phenomena diminish resulting in a more simplified relationship that is less dependent on the scale size. In contrast, as the scale size decreases, the fractal dimension increases thus illustrating how the complexity of smaller particle sizes will influence friction and wear. This allows other phenomena such as inter-atomic layer distance, surface roughness, humidity, lubricant viscosity, etc. to become prevalent. The COF data reveals a relatively low fractal dimension, revealing minor complexities that would develop as the scale size decreased. These complexities would be affected the "texture" of the particles i.e. the macro-details such as major particle irregularities, surface roughness, lubricity, transfer films development, and aggregation properties of the particle additives. It can be seen that at a particle size of approximately 2μm, the fractal dimension crosses below unity revealing a more geometrical relationship between particle size and friction where the "structure" or larger macro scale physical properties such as particle size and shape dominate. Effectively, this would cause the topographical shape of the fractal function for friction to become over simplified. The fractal dimensions for wear are significantly greater than those for friction. Here, the complexities of the wear volume are significant and reveal strong textural influences. As the scale size decreases i.e. the particle size decreases, the fractal function for wear is expected to witness an increase in surface irregularities and

express a level of self-affinity [431]. This is to say that the wear rate due to the presence of smaller particles is likely to develop new levels of complexity from parts of the full fractal function at a lower scale. This level of speculation seems plausible because it is well known in tribology that roughness profiles are considered to be stochastic processes and therefore they are self-affine only in a stochastic sense. Here, the surface has similar features in all scales of view however not necessarily identical make it differentiable from self-similarity [429]. With regards to wear in a tribo-interface, there are many mechanisms contributing to the wear rate and thus a fractal function may reveal or conceal these mechanisms depending on the length scale.

This analysis is preliminary, however for the use of particulate additives in ionic liquids that were revealed to be independent of particle type and highly dependent on particle size, this fractal analysis was able to provide some insight. This relatively simple fractal model was able to reveal that the science in the current experimental investigations moves beyond the current length scale of surface roughness and into other regions where the particle size to surface roughness can and my exhibit scale-invariant properties. The current model does provide a macroscopic view of the influence of particle size on the friction and wear properties and provides a guideline to how other particulate additives of different sizes may behave. Furthermore it was shown that the current experimental data can be used to establish a fractal model that indicates the presence of fractal dimensions and scale-invariant behaviors.

9.6 Conclusions

The influence of particulate additives in a phosphonium-based environmentally friendly ionic liquid, $P_{666,14}$Salicylate was investigated and demonstrated to be a successful carrier fluid for circulating the particulate additives. It was shown that submicron or smaller particulate additives enhance the tribological performance. It was also revealed that an environmentally friendly two-phase lubricant consisting of ionic liquid and solid particles is possible. In the current investigation when the base fluid was combined with the 70nm hexagonal boron nitride (hBN) it was revealed to have among the lowest friction and wear rates of all the lubricant mixtures examined, thus illustrating the feasibility of an ecofriendly IL-based biolubricant. Below are the major conclusions from this experimental analysis.

- Particle size is independent of particle type as the dominating parameter that influences the effectiveness of solid particle additives in ionic liquids.

- Particle size is dependent on particle type as the dominating parameter that influences the effectiveness of solid particle additives in natural oils.

- Nanometer and submicron-sized particulate additives enhance the tribological properties of the ILs with smaller particles having the greatest effect.

- Larger micron-sized particles are detrimental to the tribological performance and increase the friction, wear, and surface roughness of the worn surface.

- Multi-walled carbon nanotubes initially act as a lubricant additive until capillary effects dominate rendering them inept.

- The influence of particulate additives can be empirically modeled by a single or piecewise composite function where the resolution is based on the particle size which is a fractal dimension. In the current model the fractal dimension was particle size.

- The major fractal dimensions were categorized into four regions, subnano, nanometer, submicron, and micron and are based in part on the physical particle size and the initial surface roughness of the tribo-interface.

- From the fractal analysis it is speculated that nanometer-sized particles approach an infinitely small size allowing the lubricant mixture to behave as if there are no particle present

- The fractal dimension increases with a decrease in scale length indicating the opportunity for the fractal model to significantly increase in complexity when investigating the effects at a micron, submicron, or nanometer scale.

- The fractal dimension decreases to a geometrical relationship of low complexity as the scale length increases to microns, indicating that macro scale effects such as surface roughness, shape, and particle size will dominate.

Chapter 10   Conclusions

10.1 Conclusions

The goal of this work was to investigate the feasibility of developing environmentally friendly lubricants. This endeavor began by investigating natural oils as biolubricants to gain an understanding of the effects that long chain fatty acids have on the tribological performance of natural oils. Although, previous research has explored the tribological performance of fatty acids, it was importat in this study to develop a basis of fundamental knowledge that revealed the lubricating mechanisms of multiple natural oils. The experimental investigations revealed that natural oils containing high amounts of stearic (C18:0), oleic (C18:1), and linoleic (C18:2) acids were best for enhancing the tribological performance of the natural oils. Within this subgroup of fatty acids, natural oils with low unsaturation numbers due to high concentrations of oleic acid demonstrated superior friction and wear properties as well as high thermal-oxidative stability. This result reaffirmed the results of many authors that oleic acid is a superior additive to lubricants because it is able to effectively adsorb to the metal surface, form a monolayer, and aid in minimizing the asperity contact in boundary lubrication all while exhibiting a low pour point and thermal-oxidative stability.

As a next step toward further improvements upon the natural oils, particulate additives were used. Extensive testing of multiple natural oils and various particulate additives composed of a variety of types, sizes, and shapes as well as surface roughnesses revealed that natural oils benefit tremendously from nanometer-sized spherical shaped

hexagonal boron nitride particles in smoother surface roughness applications, where the R_a value was lower. In situations where the R_a value was higher, larger particles were more effective at improving the tribological performance. This work provided new insight into the utilization of particulate additives in carrier fluids, especially the use of hBN particles which are considered environmentally benign and thus a two-phase compound biolubricant was developed. More still, a particle size-to surface index was developed to aid lubrication specialists in the choice of a particulate additive (shown in Fig. 6.11). Here, this choice of a particle additive is now dependent upon the surface roughness to allow for the greatest improvement of tribological performance and minimize the risk of unwanted abrasion or surface damage.

In an effort to further improve upon biolubricants composed of particulate additives in a natural oil suspension, room temperature ionic liquid lubricants were chosen because of their ability to lubricate in boundary lubrication due to their inherent polar molecules; their ability to be tuned for specific applications; and most notably their lack of vapor pressure provides numerous opportunities for liquid lubricants. For example, liquid lubricants were previously disregarded when considered for use in vacuum environments due to their volatility, however with ionic liquids and their lack of vapor pressure, now ionic liquid lubricants can be seriously considered for use in a vacuum environment. Investigations into the ionic liquid lubricants revealed that longer alkyl chains on the cations and larger aromatic carboxylate anions exhibited the most lubricity as a neat lubricant. Again, these lubricants were subjected to particulate additivation and it was revealed that smaller nanometer sized particles provided the greatest benefit to

lowering friction and minimizing wear. Interestingly, the ionic liquids demonstrated a high sensitivity to particle size independent of the particle type. The performance of the ionic liquids improved with the particulate additives and it was further verified through the literature that the phosphonium or imidazolium cations with food grade carboxylate anions such as saccharinate, salicylate, or benzoate could be considered as biolubricants and the current investigation demonstrated that they maintained superior tribological properties as well as high thermal-oxidative stability.

The results of this experimental investigation provide significant contribution to the lubrication industry because it has been demonstrated that room temperature ionic liquid lubricants do indeed represent a new class of novel "greener" lubricants that are non-toxic, sustainable, and environmentally benign. After a thorough examination of the ionic liquids' tribological performance, their tribological properties surpass currently used industry lubricants thus providing new opportunities for non-volatile liquid lubricants. Such new opportunities include the use of ionic liquids as lubricants in vacuum environments, as conventional biolubricants, as an anti-wear additive potentially to replace Zinc dialkyldithiophosphates (ZDDP); and as adsorption additives to replace fatty acids and esters. This investigation has illuminated the potential of bio-based ionic liquid lubricants to satisfy the growing environmental, health, economic, and performance concerns of modern lubricants. Although, ionic liquids as biolubricants may never fully replace petroleum-based lubricants due to their higher cost, they can act as a suitable replacement in applications with high vulnerability to environmental leakage thus minimizing the impact of toxic lubricants. This research brings attention to ionic

liquids and provides the fundamental basis for evaluating this new class of biolubricants, (which they were previously not considered as) in hopes that one day the macroscale development, economical competence, and industrial use will allow the lubrication industry to cleanly and safely move one step further to reaching its goals of energy conservation and sustainability.

The major conclusions based on the experimental studies are as follows:

1. Natural oils with high percentages of oleic acid maintain low COF values and low wear rates because the acid establishes a denser fatty acid monolayer that minimizes the asperity contact and protects the metallic surfaces.

2. Natural oils with low unsaturation numbers due to relatively high percentages of stearic and oleic acids are optimal to ensure superior thermal-oxidative stability in ambient and high temperature environments.

3. In an oxygen-free environment, the thermal stability of natural oils is dependent on individual fatty acid percentages and independent of the degree of unsaturation, while in an oxygen environment, the oxidative stability of natural oils is dependent on the unsaturation number which becomes coupled with thermal stability.

4. Phosphonium and imidazolium ionic liquids with carboxylate anions outperform bio-based and petroleum-based oils due to their lamellar-like liquid crystal structure and unique dipolar structure improving lubricity and wear resistance.

5. Long bulky asymmetric organic cations (≥10 atoms on the alkyl chain) and aromatic carboxylic organic anions (with 1 or 2 rings) effectively reduce friction and wear while enhancing the thermal stability by lowering the thermal degradation.

6. In a tribo-interface smooth surfaces benefit from the lubricity of smaller nano-sized particles for their ability to accommodate relative surface velocities by operating in the particulate boundary lubrication regime whereas rough surfaces benefit from improved load carrying capacities and particulate hydrodynamic lubrication due to micron-sized particles.

7. In ionic liquids, particle size is independent of particle type as the dominating parameter that influences the effectiveness of solid particle additives while in natural oils, particle size is dependent on particle type as the dominating parameter that influences the effectiveness of solid particle additives.

8. The effect of particulate additives in a lubricant is influenced by the surface roughness of the counter material, the particle size, and the particle shape, this behavior can be characterized as a fractal function with multiple variables as step lengths. Thus the selection of a particle additive to improve the tribological performance must be made in accordance with the initial surface roughness of the tribo-interface.

9. The fractal dimension increases with a decrease in step length indicating the opportunity for the fractal model to significantly increase in complexity when studying the effects of particulate additives or surface roughness at a micron, submicron, nanometer, or subnanometer scale.

10. $P_{666,14}$Saccharinate, $P_{666,14}$Salicyate, and $P_{666,14}$Benzoate ionic liquids maintain superior tribological properties and offer tremendous potential as a new family of environmentally benign biolubricants.

10.2 Future Work

Future work in the area of biolubricants and biolubrication technology is vast and ongoing as new industrial applications develop and environmental initiatives remain prevalent. In the current experimental investigation future work is encouraged to examine the following area:

- Perform a direct comparison of low, medium, and high temperature pin-on-disk testing of natural oils and ionic liquids in oxygenated and oxygen-free environments to understand the effects of thermal degradation in situ.

- Investigate the capillary effects of multi-walled carbon nanotubes when utilized as additives in a lubricant. This investigation would be to determine if non-lamellar particle additives can become a new class of solid particle lubricants.

- Explore the intrinsic properties of the various particulate additives to explain why particle size matters in ionic liquids but not to the same degree in natural oils.

- Develop a fractal model to characterize the influence of surface roughness and particle size at various step sizes from micron to nano-size in order to quantify and predict the tribological performance

- Investigate the influence of viscosity in both natural oils and ionic liquids as neat lubricants and as mixtures of particulate additives in order to understand the tribological regimes present in the tribo-interface.

- Perform a finite-element analysis of the pin-on-disk interface with the natural oils and ionic liquids as neat lubricants and as mixtures of particulate additives. In this

analysis the disk should capture the different surface roughness profiles and the particles should vary in size and sphericity.

- Perform a molecular dynamic simulation to understand more closely the boundary lubrication mechanisms that relate to the improved performance of the cationic-anionic adsorption monolayer and determine how it differs from the fatty acid adsorption monolayer.

- Perform a life cycle assessment (LCA) on the ionic liquids and determine if their synthesis, product use, and disposal processes are environment benign. This will help support their case as a truly viable lubricant for wide scale adoption.

10.3 References

[1] Bannister, K.E.: Lubrication for Industry. Industrial Press, New York, N.Y. (1996)

[2] Mang, T., Dresel, W.: Lubricants and lubrication. Wiley, Weinheim; Chichester (2006)

[3] United States. Central Intelligence, A.: The CIA world fact book. Central Intelligence Agency, (1997)

[4] Bartz, W.J.: Automotive and industrial lubrication 15th International Colloquium Tribology, January 2006. TAE, Ostfildern (2006)

[5] Lingg, G., Gosalia, A. The dynamics of the global lubricants industry - Markets, competitors & trends. Technische Akademie Esslingen International Tribology Colloquium Proceedings 16 (2008).

[6] Reeves, C.J., Menezes, P.L., Jen, T.-C., Lovell, M.R.: Evaluating the Tribological Performance of Green Liquid Lubricants and Powder Additive Based Green Liquid Lubricants STLE Annual Meeting & Exhibition. STLE (2012)

[7] Bhushan, B.: Modern tribology handbook. CRC Press, Boca Raton, FL (2001)

[8] Miyoshi, K.: Solid lubrication fundamentals and applications. Marcel Dekker, New York (2001)

[9] Winer, W. Molybdenum disulfide as a lubricant: A review of the fundamental knowledge. Wear 10:422-452 (1967).

[10] Hu, X. On the size effect of molybdenum disulfide particles on tribological performance. Industrial Lubrication and Tribology 57:255-259 (2005).

[11] Jamison, W.E. Structure and Bonding Effects on the Lubricating Properties of Crystalline Solids. ASLE Transactions 15:296-305 (1972).

[12] Petterson, M.B., Calabrese, S.J., Stupp, B., Wear Sciences Inc Arnold, M.D. Lubrication with Naturally Occurring Double Oxide Films. (1982).

[13] Argonne National, L. Wear-resisting oxide films for 900C . (1994).

[14] Scharf, T.W., Rajendran, a., Banerjee, R., Sequeda, F. Growth, structure and friction behavior of titanium doped tungsten disulphide (Ti-WS2) nanocomposite thin films. Thin Solid Films 517:5666-5675 (2009).

[15] Blanchet, T.A., Kennedy, F.E. Sliding wear mechanism of polytetrafluoroethylene (PTFE) and PTFE composites. Wear 153:229-243 (1992).

[16] Lovell, M.R., Menezes, P.L., Kabir, M.A., Higgs, C.F. Influence of boric acid additive size on green lubricant performance. Philos Trans R Soc A Math Phys Eng Sci 368:4851-4868 (2010).

[17] Menezes, P.L., Lovell, M.R., Kabir, M.A., Higgs III, C.F., Rohatgi, P.K.: Green Lubricants: Role of Additive Size. In: Nosonovsky M, Bhushan B (eds.) Green Tribology, pp. 265-286. Springer Berlin Heidelberg, (2012)

[18] Denton, R.M., Fang, Z.: Rock Bit Grease Composition. (1995)

[19] Erdemir, A., University of, C.: Lubrication from mixture of boric acid with oils and greases. United States (1995)

[20] Czichos, H.: Tribology a Systems Approach to the Science and Technology of Friction, Lubrication, and Wear. Elsevier,(1978)

[21] Czichos, H. Basic Tribological Parameters, Friction, Lubrication and Wear Technology. ASTM Handbook 18:474 (1992).

[22] Bhushan, B.: Introduction to tribology. John Wiley & Sons, New York (2002)

[23] Willing, A. Lubricants Based on Renewable Resources-An Environmentally Compatible Alternative to Mineral Oil Products. Chemosphere 43:89-98 (2001).

[24] Fox, N.J., Tyrer, B., Stachowiak, G.W. Boundary Lubrication Performance of Free Fatty Acids in Sunflower Oil. Tribology Letters 16:275-281 (2004).

[25] Bhushan, B.: Principles and Applications of Tribology. John Wiley, New York, NY [u.a.] (1999)

[26] Fischer, T.E., Bhattacharya, S., Salher, R., Lauer, J.L., Ahn, Y.J. Lubrication by a Smectic Liquid Crystal. Tribology Transactions 31:442-448 (1988).

[27] Hamrock, B.J., Dowson, D.: Minimum Film Thickness in Elliptical Contacts for Different Regimes of Fluid-film Lubrication. National Aeronautics and Space Administration, Springfield, Va. (1978)

[28] Hamrock, B.J., Dowson, D.: Ball bearing lubrication: the elastohydrodynamics of elliptical contacts. Wiley, New York (1981)

[29] Hamrock, B.J., Dowson, D.: Elastohydrodynamic lubrication of elliptical contracts for materials of low elastic modulus. National Aeronautics and Space Administration, Springfield, Va. (1978)

[30] Hamrock, B.J., Dowson, D.: Isothermal elastohydrodynamic lubrication of point contacts : IV, starvation results. National Aeronautics and Space Administration. Springfield, Va. (1976)

[31] Menezes, P.L., Kishore, Kailas, S.V. Effect of Roughness Parameter and Grinding Angle on Coefficient of Friction When Sliding of Al-Mg Alloy Over EN8 Steel. Journal of Tribology 128:697-704 (2006).

[32] Kumar, P.C., Menezes, P.L., Kailas, S.V. Role of Surface Texture on Friction under Boundary Lubricated Conditions. Online Tribology Online 3:12-18 (2008).

[33] Menezes P.L., Kishore, V., K.S. Study of friction and transfer layer formation in copper-steel tribo-system: Role of surface texture and roughness parameters. Tribology Transactions 52:611-622 (2009).

[34] Menezes P.L., Kishore, Kailas, S.V. Influence of roughness parameters and surface texture on friction during sliding of pure lead over 080 M40 steel. Journal of Advanced Manufacturing Technology 43:731-743 (2009).

[35] Menezes, P.L., Kishore, Kailas, S.V. On the effect of surface texture on friction and transfer layer formation-A study using Al and steel pair. Wear 265:1655-1669 (2008).

[36] Menezes, P.L., Kishore, Kailas, S.V., Lovell, M.R. Studies on Friction and Formation of Transfer Layer in HCP Metals. Journal of Tribology 131:031604 (2009).

[37] Menezes, P.L., Kishore, Kailas, S.V. Influence of surface texture and roughness parameters on friction and transfer layer formation during sliding of aluminium pin on steel plate. Wear 267:1534-1549 (2009).

[38] Menezes, P.L., Kishore, S.V., Lovell, M.R. Response of Materials During Sliding on Various Surface Textures. Journal of Materials Engineering and Performance 20:1438-1446 (2011).

[39] Moore, C.T, Menezes, P.L., Lovell, M.R., Beschorner, K.E. Analysis of shoe friction during sliding against floor material: Role of fluid contaminant. J Tribol Journal of Tribology 134 (2012).

[40] Stachowiak, G.W., Batchelor, A.W.: Engineering tribology. Elsevier Butterworth-Heinemann, Place Elsevier Butterworth-Heinemann (2005)

[41] Klaus, E.E., Ugwuzor, D.I., Naidu, S.K., Duda, J.L. Lubricant-Metal Interaction Under Conditions Simulating Automotive Bearing Lubrication. Proceeding of JSLE International Tribology Conference:859-864 (1985).

[42] Colclough, T. Role of additives and transition metals in lubricating oil oxidation. IIndustrial & Engineering Chemistry Research 26:1888-1895 (1987).

[43] Jayadas, N.H., Nair, K.P., Ajithkumar, G.: Vegetable oils as base oil for industrial lubricants-evaluation oxidative and low temperature properties using TGA, DTA and DSC. World Tribology Congress, pp. 539-540. American Society of Mechanical Engineers, (2005)

[44] Birova, A., Pavlovicov, A., Cvenros, J. Lubricating oils based on chemically modified vegetable oils. Journal of Synthetic Lubrication 18:291-299 (2002).

[45] Meier, M.A.R., Metzger, J.O., Schubert, U.S. Plant oil renewable resources as green alternatives in polymer science. Chemical Society Reviews 36:1788-1802 (2007).

[46] King, J.W., Holliday, R.L., List, G.R., Snyder, J.M. Hydrogenation of vegetable oils using mixtures of supercritical carbon dioxide and hydrogen. Journal of the American Oil Chemists' Society 78:107-113 (2001).

[47] Erhan, S.Z., Adhvaryu, A., Sharma, B.K. Chemically Functionalized Vegetable Oils. Chemical industries 111:361-388 (2006).

[48] Doll, K.M., Sharma, B.K., Erhan, S.Z. Synthesis of Branched Methyl Hydroxy Stearates Including an Ester from Bio-Based Levulinic Acid. Industrial and Engineering Chemistry Research 46:3513-3519 (2007).

[49] Yunus, R., Fakhru l-Razi, A., Ooi, T.L., Iyuke, S.E., Perez, J.M. Lubrication properties of trimethylolpropane esters based on palm oil and palm kernel oils. European Journal of Lipid Science and Technology 106:52-60 (2004).

[50] Hwang, H.-S., Adhvaryu, A., Erhan, S.Z. Preparation and properties of lubricant basestocks from epoxidized soybean oil and 2-ethylhexanol. Journal of the American Oil Chemists' Society 80:811-815 (2003).

[51] Verkuijlen, E., Kapteijn, F., Mol, J.C., Boelhouwer, C. Heterogeneous metathesis of unsaturated fatty acid esters. Journal of the Chemical Society (1977).

[52] Schmidt, M.A., Dietrich, C.R., Cahoon, E.B. Biotechnological Enhancement of Soybean Oil for Lubricant Applications. Chemical industries 111:389-398 (2006).

[53] Holser, R., Doll, K., Erhan, S. Metathesis of methyl soyate with ruthenium catalysts. Fuel 85:393-395 (2006).

[54] Erhan, S.Z., Bagby, M.O., Nelsen, T.C. Drying Properties of Metathesized Soybean Oil. Journal of American Oil Chemists Society 74:703-706 (1997).

[55] Salih, N., Salimon, J., Yousif, E. The physicochemical and tribological properties of oleic acid based triester biolubricants. Industrial Crops & Products 34:1089-1096 (2011).

[56] Jayadas, N.H., Nair, K.P. Coconut oil as base oil for industrial lubricants-evaluation and modification of thermal, oxidative and low temperature properties. Tribology International 39:873-878 (2006).

[57] Papay, A.G. Antiwear and extreme-pressure additives in lubricants. Lubrication Science 10:209-224 (1998).

[58] Campbell, M.E., Loser, J.B., Sneegas, E., Midwest Research, I.: Solid lubricants. National Aeronautics and Space Administration; Washington (1966)

[59] Booser, E.R.: CRC handbook of lubrication. Theory and practice of tribology: Volume II: Theory and design. CRC Press Inc.,Boca Raton, FL, United States (1984)

[60] Lince, J.R., Fleischauer, P.D., Aerospace Corp El Segundo Ca Technology, O. Solid Lubrication for Spacecraft Mechanisms.   (1997).

[61] Lockheed, M., Space, C., Goetzel, C.G., Rittenhouse, J.B., Singletary, J.B.: Space materials handbook. Addison-Wesley Pub. Co., Reading, Mass. (1965)

[62] Donnet, C., Erdemir, a. Solid Lubricant Coatings: Recent Developments and Future Trends. Tribology Letters 17:389-397 (2004).

[63] Bhattacharyya, S., Schwartzbart, H., Iit Research Inst, C. Wear And Friction Of Fiber-Metal Molybdenum Bodies Impregnated With Molybdenum Disulfide. American Society of Metals, Trans Quart, 62: 318-23 (1969).

[64] Bhushan, B.: Modern tribology handbook. CRC Press, Place CRC Press (2001)

[65] Peterson, M.B., Johnson, R.L., United States. National Advisory Committee for, A.: Friction and wear investigation of molybdenum disulfide. 1 - Effect of moisture. National Advisory Committee for Aeronautics, Washington, D.C. (1953)

[66] Fusaro, R.L., United States. National, A., Space Administration, S., Technical Information, O.: Lubrication and failure mechanisms of molybdenum disulfide films. National Aeronautics and Space Administration, Scientific and Technical Information Office; Springfield, Va. (1978)

[67] Rohatgi, P.K., Ray, S., Liu, Y. Tribological properties of metal matrix-graphite particle composites. International Materials Reviews 37:129-149 (1992).

[68] Prasad, S.V., McConnell, B.D.: Tribology of aluminum metal-matrix composites. Lubrication by graphite. International Conference on Wear of Materials, April 7, 1991 - April 11, 1991, pp. 149-157. Publ by ASME, (1991)

[69] Gangopadhyay, A., Jahanmir, S. Friction and wear characteristics of silicon nitride-graphite and alumina-graphite composites. Tribology Transactions 34:257-265 (1991).

[70] Rabinowicz, E., Imai, M. Frictional properties of pyrolitic boron nitride and graphite. Wear 7:298-300 (1964).

[71] Kimura, Y., Wakabayashi, T., Okada, K., Wada, T., Nishikawa, H. Boron nitride as a lubricant additive. Wear 232:199-206 (1999).

[72] Funatani, K., Kurosawa, K. Composite coatings improve engines. Advanced Materials and Processes 146:6:27-34 (1994).

[73] Westergard, R., Ahlin, A., Axen, N., Hogmark, S. Sliding wear and friction of Si 3N 4SiC-based ceramic composites containing hexagonal boron nitride. Journal of Engineering Tribology 212:381-387 (1998).

[74] Naegely, P.C.: Environmentally Acceptable Lubricants, in Seed Oils for the Future. AOCS Press, Champaign, IL (1993)

[75] Schneider, M.P. Plant-oil-based lubricants and hydraulic fluids. J Sci Food Agr 86:1769-1780 (2006).

[76] IENICA: Biolubricants: Market Data Sheet. IENICA, Place IENICA (2004)

[77] Salimon, J., Salih, N., Yousif, E. Biolubricants: Raw materials, chemical modifications and environmental benefits. European Journal of Lipid Science and Technology 112:519-530 (2010).

[78] Aluyor, E.O., Obahiagbon, K.O., Ori-jesu, M. Biodegradation of vegetable oils: A review. Sci Res Essays 4:543-548 (2009).

[79] Deffeyes, K.S.: Hubbert's peak. Princeton University Press, Princeton (N.J.); Oxford (2009)

[80] Goodstein, D.L.: Out of gas : the end of the age of oil. Norton, New York (2005)

[81] Lovell, M., Higgs, C.F., Deshmukh, P., Mobley, A. Increasing Formability in Sheet Metal Stamping Operations Using Environmentally Friendly Lubricants. Journal of materials processing technology 177:87 (2006).

[82] Li, W., Kong, X.H., Ruan, M., Ma, F.M., Jiang, Y.F., Liu, M.Z., et al. Green waxes, adhesives and lubricants. Philosophical Transactions of the Royal Society A: Mathematical, Physical and Engineering Sciences 368:4869-4890 (2010).

[83] Backé, W. The present and Future of Fluid Power. Proceedings of the Institution of Mechanical Engineers, Part I: Journal of Systems and Control Engineering 207:193-212 (1993).

[84] Kumar, A., Sharma, S. An evaluation of multipurpose oil seed crop for industrial uses (Jatropha curcas L.): A review. Industrial Crops and Products 28:1-10 (2008).

[85] Feldmann, D.G., Remmelmann, A. Biologisch schnell abbaubare Hydraulikfluessigkeiten - Ergebnisse von Pruefstandstests und Folgerungen fuer die Anwendung. Aachener Fluidtechnisches Kolloquium 12:59-80 (1996).

[86] Feldmann, D.G., Kessler, M. Fluid qualification tests - evaluation of the lubricating properties of biodegradable fluids. Industrial Lubrication and Tribology 54:117-129 (2002).

[87] Feldmann, D.G., Hinrichs, J. Evaluation of the Lubrication Properties of Biodegradable Fluids and Their Potential to Replace Mineral Oil in Heavily Loaded Hydrostatic Transmissions. ASTM special technical publication 1310:220 (1997).

[88] Fessenbecker, A., Korff, J. Additives for Environmentally More Friendly Lubricant. Journal of Japanese Society of Tribologists 40:306 (1995).

[89] Korff, J., Fessenbecker, A. Additives for Biodegradable Lubricants. NLGI spokesman 57:19 (1993).

[90] Lovell, M.R., Menezes, P.L., Kabir, M.A., Higgs III, C.F. Influence of boric acid additive size on green lubricant performance. Philosophical Transactions of the Royal Society A: Mathematical, Physical and Engineering Sciences 368:4851-4868 (2010).

[91] Duzcukoglu, H., Sahin, O.S. Investigation of wear performance of canola oil containing boric acid under boundary friction condition. Tribology Transactions 54:57-61 (2011).

[92] Erdemir, A., Argonne National Lab, I.L., Conference: 45. annual meeting of the Society of, T., Lubrication Engineers, D.C.O.M.: Tribological properties of boric acid and boric acid forming surfaces: Part 1, Crystal chemistry and self-lubricating mechanism of boric acid. United States (1990)

[93] Reeves, C.J., Menezes, P. L., Jen, T.C., and Lovell, M. R.: Evaluating the tribological performance of green liquid lubricants and powder additive based green liquid lubricants 2012 STLE Annual Meeting & Exhibition. STLE, (2012)

[94] Werman, M.J., Neeman, I. Avocado oil production and chemical characteristics. Journal of the American Oil Chemists Society 64:229-232 (1987).

[95] Nosonovsky, M., Bhushan, B.: Green tribology biomimetics, energy conservation and sustainability. Springer, Place Springer (2012)

[96] Bennion, M., Scheule, B.: Introductory foods. Prentice Hall, Upper Saddle River, N.J. (2010)

[97] Biermann, U., Metzger, J.O. Synthesis of alkyl-branched fatty acids. European Journal of Lipid Science and Technology 110:805-811 (2008).

[98] Grushcow, J., Smith, M.A. Next Generation Feedstocks From New Frontiers in Oilseed Engineering. ASME Conference Proceedings 2005:487-488 (2005).

[99] Randles, S.J.: Formulation of Environmentally Acceptable Lubricants. 49th STLE Annual Meeting. Place (1994)

[100] Smith, S.A., King, R.E., Min, D.B. Oxidative and thermal stabilities of genetically modified high oleic sunflower oil. Food Chemistry 102:1208-1213 (2007).

[101] Marmesat, S., Morales, A., Velasco, J., Carmen, D.M. Influence of fatty acid composition on chemical changes in blends of sunflower oils during thermoxidation and frying. Food Chemistry 135:2333-2339 (2012).

[102] Fox, N.J., Stachowiak, G.W. Vegetable oil-based lubricants A review of oxidation. JTRI Tribology International 40:1035-1046 (2007).

[103] Jayadas, N.H., Nair, K.P. Coconut oil as base oil for industrial lubricants-evaluation and modification of thermal, oxidative and low temperature properties. Tribology International 39:873-878 (2006).

[104] Zeman, A., Sprengel, A., Niedermeier, D., Späth, M. Biodegradable lubricantsstudies on thermo-oxidation of metal-working and hydraulic fluids by differential scanning calorimetry (DSC). Thermochimica Acta 268:9-15 (1995).

[105] Mendoza, G., Igartua, A., Fernandez-Diaz, B., Urquiola, F., Vivanco, S., Arguizoniz, R. Vegetable oils as hydraulic fluids for agricultural applications. Grasas Aceites 62:29-38 (2011).

[106] Grushcow, J.: High oleic plant oils with hydroxy fatty acids for emission reduction. 2005 World Tribology Congress III, pp. 485-486. American Society of Mechanical Engineers, (2005)

[107] Lundgren, S.M., Ruths, M., Danerlov, K., Persson, K. Effects of unsaturation on film structure and friction of fatty acids in a model base oil. Journal of Colloid And Interface Science 326:530-536 (2008).

[108] Hu, Z.-S., Hsu, S.M., Wang, P.S. Tribochemical Reaction of Stearic Acid on Copper Surface Studied by Surface Enhanced Raman Spectroscopy. Tribology Transactions 35:417-422 (1992).

[109] Erhan, S.Z., Sharma, B.K., Perez, J.M. Oxidation and low temperature stability of vegetable oil-based lubricants. Industrial Crops and Products 24:292-299 (2006).

[110] Koshima, H., Kamano, H., Hisaeda, Y., Liu, H., Ye, S. Analyses of the Adsorption Structures of Friction Modifiers by Means of Quantitative Structure-Property Relationship Method and Sum Frequency Generation Spectroscopy. Tribology Online 5:165-172 (2010).

[111] Bowden, F.P., Leben, L., Tabor, D. The influence of temperature on the stability of a mineral oil. Transactions of the Faraday Society 35 (1939).

[112] Bauccio, M., American Society for, M.: ASM metals reference book. ASM International, Materials Park, Ohio (1993)

[113] Deshmukh, P., Lovell, M., Sawyer, W.G., Mobley, A. On the friction and wear performance of boric acid lubricant combinations in extended duration operations. Wear 260:1295-1304 (2006).

[114] Lovell, M.R., Menezes, P.L., Kabir, M.A., Higgs III, C.F. Influence of Boric Acid Additive Size on Green Lubricant Performance. Philosophical Transactions of the Royal Society A: Mathematical, Physical and Engineering Sciences 368:4851-4868 (2010).

[115] Havet, L. Blouet, J., Robbe, V.F., Brasseur, E., Slomka, D. Tribological characteristics of some environmentally friendly lubricants. Wear 248:140-146 (2001).

[116] Santos, O.D.H., Morais, J.M., Andrade, F.F., Aguiar, T.A., Rocha, F.P.A. Development of Vegetable Oil Emulsions with Lamellar Liquid-Crystalline Structures. Journal of Dispersion Science and Technology 32:433-438 (2011).

[117] Lundgren, S.M., Persson, K., Mueller, G., Kronberg, B., Clarke, J., Chtaib, M., et al. Unsaturated fatty acids in alkane solution: adsorption to steel surfaces. Langmuir : the ACS journal of surfaces and colloids 23:10598-10602 (2007).

[118] Reeves, C., Menezes, P., Lovell, M., Jen, T.-C. The Size Effect of Boron Nitride Particles on the Tribological Performance of Biolubricants for Energy Conservation and Sustainability. Tribology Letters 51:437-452 (2013).

[119] Shubkin, R.L.: Synthetic lubricants and high-performance functional fluids. Dekker, New York,N.Y. (1993)

[120] Uosukainen, E., Linko, Y.Y., Lamsa, M., Tervakangas, T., Linko, P. Transesterification of trimethylolpropane and rapeseed oil methyl ester to environmentally acceptable lubricants. J Am Oil Chem Soc 75:1557-1563 (1998).

[121] Kodali, D.R. Biobased lubricants-Chemical modification of vegetable oils. Inform Champaign 14:121-143 (2003).

[122] Wagner, H., Luther, R., Mang, T. Lubricant base fluids based on renewable raw materials - Their catalytic manufacture and modification. Applied catalysis A, 221:429 (2002).

[123] Andersen, M.P.S., Hurley, M.D., Wallington, T.J., Blandini, F., Jensen, N.R., Librando, V., Hjorth J., Marchionni, G., Avataneo, M., Visca, M. Atmospheric Chemistry of CH3~O(CF2~CF2~O)n~CH3~ (n = 1-3): Kinetics and Mechanism of Oxidation Initiated by Cl Atoms and OH Radicals, IR Spectra, and Global Warming Potentials. Journal of Physical Chemistry A 108:1964-1972 (2004).

[124] United States National Oceanic Atmospheric Administration, NASA: Scientific assessment of ozone depletion, 2002. United Nations Environment Programme; World Meteorological Organization; European Commission, Washington, DC; Nairobi, Kenya; Geneva, Switzerland; Brussels, Belgium (2003)

[125] Wallington, T.J., Schneider, W.F., Sehested, J., Bilde, M., Platz, J., Nielsen, O.J., Christensen, L.K., Molina, M.J., Molina, L.T., Wooldridge, P.W. Atmospheric Chemistry of HFE-7100 (C4F9OCH3): Reaction with OH Radicals, UV Spectra and Kinetic Data for C4F9OCH2· and C4F9OCH2O2· Radicals, and the Atmospheric Fate of C4F9OCH2O· Radicals. Journal of Physical Chemistry A 101:8264-8274 (1997).

[126] Marchionni, G., Avataneo, M., De Patto, U., Maccone, P., Pezzin, G. Physical properties of four a, -dimethoxyfluoropolyethers. FLUOR Journal of Fluorine Chemistry 126:463-471 (2005).

[127] Marco A., Patto, U.D., Giuseppe, M.: Liquid-liquid extraction of polar organic substances from their aqueous solutions with fluorinated extracting liquids. European Patent Application, EP20030004057 (2003)

[128] Giuseppe, M., Mario, V.: Perfluoropolyethers (PFPEs) having at least an alkylether end group and respective preparation process. European Patent Application, EP20020013790. (2003)

[129] Marchionni, G., Petricci, S., Guarda, P.A., Spataro, G., Pezzin, G. The comparison of thermal stability of some hydrofluoroethers and hydrofluoropolyethers. Journal of Fluorine Chemistry 125:1081-1086 (2004).

[130] Marchionni, G., Maccone, P., Pezzin, G. Thermodynamic and other physical properties of several hydrofluoro-compounds. Journal of Fluorine Chemistry 118:149-155 (2002).

[131] Asadauskas, S., Erhan, S. Depression of pour points of vegetable oils by blending with diluents used for biodegradable lubricants. Journal of the American Oil Chemists' Society 76:313-316 (1999).

[132] Reeves, C.J., Garvey, S. L., Menezes, P. L., Dietz, M. L., Jen, T. C., and Lovell, M. R.: Tribological Performance of Environmentally Friendly Ionic Liquid Lubricants. ASME/STLE 2012 International Joint Tribology Conference. STLE, Place STLE (2012)

[133] Bermúdez, M.D., JimÈnez, A.E., Sanes, J., Carriun, F.J. Ionic Liquids as Advanced Lubricant Fluids. Molecules (Basel, Switzerland) 14:2888-2908 (2009).

[134] Canter, N. Evaluating Ionic Liquids as Potential Lubricants. Tribology and Lubrication Technology 61:15-17 (2005).

[135] Liu, W., Ye, C., Gong, Q., Wang, H., Wang, P. Tribological Performance of Room-Temperature Ionic Liquids as Lubricant. Tribology Letters 13:81-85 (2002).

[136] Zhou, F., Liang, Y., Liu, W. Ionic liquid lubricants: designed chemistry for engineering applications. Chemical Society Reviews 38:2590-2599 (2009).

[137] Conference, A.S.T., American Society of Mechanical Engineers. Tribology, D., Society of, T., Lubrication, E.: Lubrication of DLC and Tin Coatings with Two Ionic Liquids used as Neat Lubricant and Oil Additives. Proceedings of the STLE/ASME International Joint Tribology Conference--2011. American Society of Mechanical Engineers, (2011)

[138] Freemantle, M.: An Introduction to ionic liquids. RSC Pub., Cambridge, UK (2010)

[139] Sheldon, R.A., Arends, I., Hanefeld, U.: Green chemistry and catalysis Wiley, Weinheim (2007)

[140] Yao, M., Liang, Y., Xia, Y., Zhou, F. Bisimidazolium ionic liquids as the high-performance antiwear additives in poly(ethylene glycol) for steel-steel contacts. ACS Applied Materials and Interfaces 1:467-471 (2009).

[141] Reeves, C.J., Menezes, P.L., Garvey, S., Jen, T.C., Dietz, M., Lovell, M.R.: The effect of anion-cation moiety manipulation to characterize the tribological performance of

environmentally benign room temperature ionic liquid lubricants. 2013 STLE Annual Meeting & Exhibition (STLE2013) Society of Tribologists & Lubrication Engineers, (2013)

[142] Reeves, C.J., Menezes, P.L., Lovell, M.R., Jen, T.C., Garvey, S., Dietz, M.: The tribological performance of bio-based room temperature ionic liquid lubricants: A possible next step in biolubricant technology. World Tribology Congress - 5th. Society of Tribologists & Lubrication Engineers, (2013)

[143] Quijano, G., Couvert, A., Amrane, A., Darracq, G., Couriol, C., Le Cloirec, P., Paquin, L., Carrie, D. Toxicity and biodegradability of ionic liquids: New perspectives towards whole-cell biotechnological applications. Chem Eng J 174:27-32 (2011).

[144] Gathergood, N., Scammells, P.J., Garcia, M.T. Biodegradable ionic liquids Part III. The first readily biodegradable ionic liquids. Green Chemistry 8:156-160 (2006).

[145] Gathergood, N., Scammells, P.J., Garcia, M.T. Biodegradable ionic liquids Part II. The first readily biodegradable ionic liquids. Green Chemistry 8:156-160 (2006).

[146] Wu, M., Navarrini, W., Spataro, G., Venturini, F., Sansotera, M. An Environmentally Friendly Class of Fluoropolyether: Alpha-Omega-Dialkoxyfluoropolyethers. Applied Sciences 2:351-367 (2012).

[147] Somers, A.E., Howlett, P.C., MacFarlane, D.R. Transition in Wear Performance for Ionic Liquid Lubricants under Increasing Load. Tribology Letters 40:279-284 (2010).

[148] Atefi, F., Garcia, M.T., Singer, R.D., Scammells, P.J. Phosphonium ionic liquids: design, synthesis and evaluation of biodegradability. Green Chemistry 11:1595-1604 (2009).

[149] Phillips, B.S., Zabinski, J.S. Ionic Liquid Lubrication Effects on Ceramics in a Water Environment. Tribology Letters 17:533-541 (2004).

[150] Freire, M., Carvalho, P.J., Gardas, R.L., Marrucho, I.M., Santos, L.M., Coutinho, J. A. Mutual solubilities of water and the $[C(n)mim][Tf(2)N]$ hydrophobic ionic liquids. The Journal of Physical Chemistry B 112:1604-1610 (2008).

[151] Liu, X., Zhou, F., Liang, Y., Liu, W. Tribological Performance of Phosphonium Based Ionic Liquids For an Aluminum-On-Steel System And Opinions on Lubrication Mechanism. Wear 261:1174-1179 (2006).

[152] Schneider, M.P. Plant-oil-based lubricants and hydraulic fluids. Journal of the science of food and agriculture 86:1769-1780 (2006).

[153] Sharma, B.K., Liu, Z., Adhvaryu, A., Erhan, S.Z. One-pot synthesis of chemically modified vegetable oils. Journal of Agricultural and Food Chemistry 56:3049-3056 (2008).

[154] Hwang, H.S., Erhan, S.Z. Modification of Epoxidized Soybean Oil for Lubricant Formulations with Improved Oxidative Stability and Low Pour Point. Journal of the American Oil Chemists' Society 78:1179-1184 (2001).

[155] Li, S., Blackmon, J., Demange, A., Jao, T.C. Linear sulphonate detergents as pour point depressants. Lubrication Science 16:127-137 (2004).

[156] Adamczewska, J.Z., Wilson, D. Development of ecologically responsive lubricants. Journal of Synthetic Lubrication 14:129-142 (1997).

[157] Coscione, A.R., Artz, W.E. Vegetable oil stability at elevated temperatures in the presence of ferric stearate and ferrous octanoate. Journal of agricultural and food chemistry 53:2088-2094 (2005).

[158] Dunn, R.O. Effect of antioxidants on the oxidative stability of methyl soyate (biodiesel). Fuel Processing Technology 86:1071-1085 (2005).

[159] Adhvaryu, A., Sharma, B.K., Hwang, H.S., Erhan, S.Z., Perez, J.M. Development of biobased synthetic fluids: Application of molecular modeling to structure-physical property relationship. Ind Eng Chem Res 45:928-933 (2006).

[160] Asadauskas, S., Perez, J.M., Duda, J.L. Oxidative Stability and Antiwear Properties of High Oleic Vegetable Oils. Lubrication Engineering - Illinois 52:877-882 (1996).

[161] Honary, L.A.T. An investigation of the use of soybean oil in hydraulic systems. Bioresource Technology 56:41-47 (1996).

[162] Lal, K., Carrick, V. Performance Testing of Lubricants based on High Oleic Vegetable Oils. Journal of synthetic lubrication 11:189 (1994).

[163] Ullmann, F.G.W.: Ullmann's encyclopedia of industrial chemistry. VCH., (1988)

[164] Totten, G.E., Westbrook, S.R., Shah, R.J.: Fuels and lubricants handbook technology, properties, performance, and testing. ASTM International, West Conshohocken, PA (2003)

[165] Quinchia, L.A., Delgado, M.A., Franco, J.M., Spikes, H.A., Gallegos, C. Low-temperature flow behaviour of vegetable oil-based lubricants. Industrial Crops and Products 37:383-388 (2012).

[166] Salimon, J., Salih, N. Oleic acid diesters: Synthesis, characterization and low temperature properties. European Journal of Scientific Research 32:216-222 (2009).

[167] Hart, H., Schuetz, R.D.: Organic chemistry: a short course. Houghton Mifflin, Boston (1978)

[168] Fessenbecker, A.K.J. Additive fuer oekologisch unbedenklichere Schmierstoffe. Tribologie Und Schmierungstechnik 42:26 (1995).

[169] Roehrs, I., Fessenbecker, A. A new additive for the hydrolytic and oxidative stabilization of ester based lubricants and greases. NLGI spokesman 61:10-17 (1997).

[170] Boyde, S. Hydrolytic stability of synthetic ester lubricants. Journal of synthetic lubrication 16:297-312 (2000).

[171] Adhvaryu, A., Biresaw, G., Sharma, B.K., Erhan, S.Z. Friction Behavior of Some Seed Oils: Biobased Lubricant Applications. Industrial and Engineering Chemistry Research 45:3735-3740 (2006).

[172] Adhvaryu, A., Erhan, S. Z., Liu, Z.S., Perez, J.M. Oxidation kinetic studies of oils derived from unmodified and genetically modified vegetables using pressurized differential scanning calorimetry and nuclear magnetic resonance spectroscopy. Thermochimica Acta 364:87-97 (2000).

[173] Adhvaryu, A., Erhan, S. Z., Liu, Z.S., Perez, J.M. Tribological studies of thermally and chemically modified vegetable oils for use as environmentally friendly lubricants. Wear Wear 257:359-367 (2004).

[174] Jahanmir, S., Beltzer, M. An Adsorption Model for Friction in Boundary Lubrication. A S L E Transactions A S L E Transactions 29:423-430 (1986).

[175] Jahanmir, S., Beltzer, M. Effect of Additive Molecular Structure on Friction Coefficient and Adsorption. J Tribol Journal of Tribology 108:109 (1986).

[176] Jahanmir, S. Chain length effects in boundary lubrication. Wear 102:331-349 (1985).

[177] Beltzer, M., Jahanmir, S. Role of Dispersion Interactions Between Hydrocarbon Chains in Boundary Lubrication. ASLE Transactions 30:47-54 (1987).

[178] Beltzer, M., Jahanmir, S. Effect of additive molecular structure on friction. Lubrication Science 1:3-26 (1988).

[179] Schey, J.A.: Tribology in metalworking : friction, lubrication, and wear. American Society for Metals, Metals Park, Ohio (1983)

[180] Rudnick, L.R., Shubkin, R.L.: Synthetic lubricants and high-performance functional fluids. Marcel Dekker, Place Marcel Dekker (1999)

[181] Eisentraeger, A., Schmidt, M., Murrenhoff, H., Dott, W., Hahn, S. Biodegradability testing of synthetic ester lubricants-effects of additives and usage. Chemosphere 48:89-96 (2002).

[182] Verkuijlen, E., Kapteijn, F., Mol, J.C., Boelhouwer, C. Heterogeneous metathesis of unsaturated fatty acid esters. Journal of the Chemical Society, Chemical Communications (1977).

[183] Saad, B., Wai, W.T., Lim, B.P. Comparative Study on Oxidative Decomposition Behavior of Vegetable Oils and Its Correlation with Iodine Value Using Thermogravimetric Analysis. Journal of Oleo Science 57:257-261 (2008).

[184] Yanishlieva, N.V., Marinova, E.M. Stabilisation of Edible Oils with Natural Antioxidants. European Journal of Lipid Science and Technology 103:752-767 (2001).

[185] Kapilan, N., Reddy, R.P., Ashok Babu, T.P. Technical aspects of biodiesel and its oxidation stability. International Journal of ChemTech Research 1:278-282 (2009).

[186] Domingos, A.K., Saad, E.B., Vechiatto, W.W.D., Wilhelm, H.M., Ramos, L.P. The Influence of BHA, BHT and TBHQ on the Oxidation Stability of Soybean Oil Ethyl Esters (Biodiesel). Journal- Brazilian Chemical Society 18:416-423 (2007).

[187] International Organization for, S.: Animal and vegetable fats and oils : determination of oxidative stability (accelerated oxidation test). International Organization for Standardization, Geneva (2006)

[188] Gertz, C., Klostermann, S., Kochhar, S.P. Testing and comparing oxidative stability of vegetable oils and fats at frying temperature. European Journal of Lipid Science and Technology 102:543-551 (2000).

[189] Brimberg, U.I., Kamal-Eldin, A. On the kinetics of the autoxidation of fats: influence of pro-oxidants, antioxidants and synergists. European Journal of Lipid Science and Technology 105:83-91 (2003).

[190] Gordon, M.H., Kourimska, L. The Effects of Antioxidants on Changes in Oils during Heating and Deep Frying. J Sci Food Agr 68:347-353 (1995).

[191] Schober, S., Mittellbach, M. The impact of antioxidants on biodiesel oxidation stability. European Journal of Lipid Science and Technology 106:382-389 (2004).

[192] Ruger, C.W., Klinker, E.J., Hammond, E.G. Abilities of some antioxidants to stabilize soybean oil in industrial use conditions. J Am Oil Chem Soc 79:733-736 (2002).

[193] Farrington, A.M., Slater, J.M. Monitoring of Engine Oil Degradation by Voltammetric Methods Utilizing Disposable Solid Wire Microelectrodes. The Analyst 122:593 (1997).

[194] Clauss, F.J.: Solid lubricants and self-lubricating solids. Academic Press, New York (1972)

[195] Kanakia, M.D., Peterson, M.B., Southwest Research Inst San Antonio Tx Belvoir, F., Lubricants Research, F.: Literature Review of Solid Lubrication Mechanisms. Defense Technical Information Center, Ft. Belvoir (1987)

[196] Duzcukoglu, H., Sahin, O. Investigation of Wear Performance of Canola Oil Containing Boric Acid under Boundary Friction Condition. Tribology Transactions 54:57-61 (2011).

[197] Wornyoh, E.Y.A., Jasti, V.K., Higgs III, C.F. A Review of Dry Particulate Lubrication: Powder and Granular Materials. Journal of Tribology 129:438-449 (2007).

[198] Peng, Q., Ji, W., De, S. Mechanical properties of the hexagonal boron nitride monolayer: Ab initio study. Computational Materials Science 56:11-17 (2012).

[199] Lelonis, D.A., Tereshko, J.W., Andersen, C.M.: Boron Nitride Powder A High-Performance Alternative for Solid Lubrication. Copyright 2006-2007 Momentive Performance Materials Inc. All rights reserved. (2007)

[200] Clayton, G.D., Clayton, F.E., Allan, R.E., Patty, F.A.: Patty's industrial hygiene and toxicology. Wiley, New York (1991)

[201] Huang, H.D., Tu, J.P., Gan, L.P., Li, C.Z. An investigation on tribological properties of graphite nanosheets as oil additive. Wear 261:140-144 (2006).

[202] Sunqing, Q., Junxiu, D., Guoxu, C. A review of ultrafine particles as antiwear additives and friction modifiers in lubricating oils. Lubrication Science 11:217-226 (1999).

[203] Xiaodong, Z., Xun, F., Huaqiang, S., Zhengshui, H. Lubricating properties of Cyanex 302-modified MoS2 microspheres in base oil 500SN. Lubrication Science Lubrication Science 19:71-79 (2007).

[204] Duzcuko, x11f, lu, H., Acaro, lu, M. Lubrication Properties of Vegetable Oils Combined with Boric Acid and Determination of Their Effects on Wear. Energy Sources, Part A: Recovery, Utilization, and Environmental Effects 32:275-285 (2010).

[205] Erdemir, A., Bindal, C. Formation and self-lubricating mechanisms of boric acid on borided steel surfaces. Surface & coatings technology 76-77:443 (1996).

[206] Erdemir, A., Bindal, C., Fenske, G.R., Argonne National Laboratory, A.I.L. Formation of ultralow friction surface films on boron carbide. Applied Physics Letters 68:1637-1639 (1996).

[207] Erdemir, A. Preparation of ultralow-friction surface films on vanadium diboride. Wear 205:236-239 (1997).

[208] Erdemir, A., Eryilmaz, O.L., Fenske, G.R. Self-replenishing solid lubricant films on boron carbide. Surface Engineering 15:291-295 (1999).

[209] Erdemir, A., Fenske, G.R., Nichols, F.A., Erck, R.A., Busch, D.E., Argonne National Lab, I.L., et al.: Self-lubricating boric acid films for tribological applications. United States (1990)

[210] Streitwieser, A., Heathcock, C.H., Kosower, E.M.: Introduction to organic chemistry. Prentice Hall, Upper Saddle River, N.J. (1992)

[211] Kodali, D.R. Biobased lubricants-Chemical modification of vegetable oils. Inform-Champaign 14:121-143 (2003).

[212] Canter, N. It Isn't Easy Being Green-The Promise, Perils, and Progress of Environmentally Friendly Lubricants. Lubricants World 9:16-21 (2001).

[213] Salimon, J., Salih, N., Yousif, E. Improvement of pour point and oxidative stability of synthetic ester basestocks for biolubricant applications. Arabian Journal of Chemistry 5:193-200 (2012).

[214] Sharma, B.K., Stipanovic, A.J. Development of a new oxidation stability test method for lubricating oils using high-pressure differential scanning calorimetry. Thermochimica Acta 402:1-18 (2003).

[215] Gapinski, R.E., Joseph, I.E., Layzell, B.D., Society of Automotive, E.: A vegetable oil based tractor lubricant. Society of Automotive Engineers, Warrendale, Pa. (1994)

[216] Becker, R., Knorr, A. An evaluation of antioxidants for vegetable oils at elevated temperatures. Lubrication Science 8:95-117 (1996).

[217] Ohkawa, S., Konishi, A., Hatano, H., Ishihama, K. Oxidation and Corrosion Characteristics of Vegetable-Base Biodegradable Hydraulic Oils. SAE Transactions 104:737 (1996).

[218] Jayadas, N.H., Nair, K.P. Coconut oil as base oil for industrial lubricantsevaluation and modification of thermal, oxidative and low temperature properties. Tribology International 39:873-878 (2006).

[219] Salimon, J., Salih, N., Yousif, E. Improvement of pour point and oxidative stability of synthetic ester basestocks for biolubricant applications. Arabian Journal of Chemistry 5:193-200 (2012).

[220] Salimon, J., Salih, N., Yousif, E. Chemically modified biolubricant basestocks from epoxidized oleic acid: Improved low temperature properties and oxidative stability. J Saudi Chem Soc 15:195-201 (2011).

[221] Crivello, J.V., Fan, M.X. Catalysis of Ring-Opening and Vinyl Polymerizations by Dicobaltoctacarbonyl. J Polym Sci Pol Chem 30:31-39 (1992).

[222] Findley, T.W., Swern, D., Scanlan, J.T. Journal of the American Chemical Society 67:412-414 (1945).

[223] Rangarajan, B., Havey, A., Grulke, E.A., Dean Culnan, P. Kinetic Parameters of a Two-Phase Model for in situ Epoxidation of Soybean Oil. Journal American Oil Chemists Society 72:1161 (1995).

[224] Sonnet, P.E., Foglia, T.A. Epoxidation of Natural Triglycerides with Ethylmethyldioxirane. Journal American Oil Chemists Society 73:461-464 (1996).

[225] Debal, A., Rafaralahitsimba, G., Ucciani, E. Epoxidation of Fatty Acid Methyl Esters with Organic Hydroperoxides and Molybdenum Oxide. Fat Science Technology 95:236 (1993).

[226] Ucciani, E., Bonfand, A., Rafaralahitsimba, G., Cecchi, G. Epoxidation of monoenic fatty esters with cumilhydroperoxide and hexacarbonyl-molybdenum. Revue Francaise Des Corps Gras 39:279 (1992).

[227] Debal, A., Rafaralahitsimba, G., Bonfand, A., Ucciani, E. Catalytic Epoxidation of Methyl Linoleate - Cyclisation Products of the Epoxyacid Esters. Fat Science Technology 97:269 (1995).

[228] Semel, J., Steiner, R. Renewable raw materials in the chemical industry. Nachr Chem, Tech Lab 31:8:632-635 (1983).

[229] Rusch gen Klaas, M., Warwel, S. Chemoenzymatic Epoxidation of Unsaturated Fatty Acid Esters and Plant Oils. The journal of the American Oil Chemists' Society 73:1453 (1996).

[230] Kende, A.S., Mckusick, B.C. Performic Acid Epoxidation. Chem Eng News 65:3-3 (1987).

[231] Rusch gen. Klaas, M., Warwel, S. Complete and partial epoxidation of plant oils by lipase-catalyzed perhydrolysis. Industrial Crops and Products 9:125-132 (1999).

[232] Chou, T.C., Lee, S.V. Epoxidation of Oleic Acid in the Presence of Benzaldehyde Using Cobalt(II) Tetraphenylporphyrin as Catalyst. Industrial and engineering chemistry research 36:1485-1490 (1997).

[233] Salimon, J., Salih, N. Preparation and characteristic of 9, 10-epoxyoleic acid-hydroxy ester derivatives as biolubricant base oil. European Journal of Scientific Research 31:265-272 (2009).

[234] Salimon, J., Salih, N. Improved low temperature properties of 2-ethylhexyl 9(10)-hydroxy-10(9)-acyloxystearate derivatives. European Journal of Scientific Research 31:583-591 (2009).

[235] Salimon, J., Salih, N. Substituted esters of octadecanoic acid as potential biolubricants. European Journal of Scientific Research 31:273-279 (2009).

[236] Biermann, U., Friedt, W., Lang, S., Lühs, W., Machmüller, G., Metzger, U.O., et al.: New Syntheses with Oils and Fats as Renewable Raw Materials for the Chemical Industry. Biorefineries-Industrial Processes and Products, pp. 253-289. Wiley-VCH Verlag GmbH, (2008)

[237] Biermann, U., Metzger, J.O. Friedel-Crafts Alkylation of Alkenes: Ethylaluminum Sesquichloride Induced Alkylations with Alkyl Chloroformates. Angewandte Chemie - International Edition In English- 38:3675-3677 (1999).

[238] Metzger, J.O., Riedner, U.: Free radical additions to unsaturated fatty acids. (1989)

[239] Metzger, J.O., Linker, U. New Results of Free Radical Additions to Unsaturated Fatty Compounds. Lipid / Fett 93:244-249 (1991).

[240] Metzger, J.O., Biermann, U. Alkylaluminium Dichloride Induced Friedel-Crafts Acylation of Unsaturated Carboxylic Acids and Alcohols. Liebigs Annalen der Chemie 1993:645-650 (1993).

[241] Biermann, U., Metzger, J.O. Lewis Acid Catalyzed Additions to Unsaturated Fatty Compounds. II: Alkylaluminium Halide Catalyzed Ene Reactions of Unsaturated Fatty Compounds and Formaldehyde. Lipid Fett 93:282-284 (1991).

[242] Pryde, E.H. Hydroformylation of unsaturated fatty acids. Journal of the American Oil Chemists Society 61:419-425 (1984).

[243] Frankel, E., Pryde, E. Catalytic hydroformylation and hydrocarboxylation of unsaturated fatty compounds. Journal of the American Oil Chemists' Society 54:A873-A881 (1977).

[244] Xia, Z., Kloeckner, U., Fell, B. Hydroformylation of Mono and Multiple Unsaturated. Fatty Substances with Heterogenized Cobalt Carbonyl and Rhodiumcarbonyl catalysts Fett Lipid 98:313-321 (1996).

[245] Behr, A., Laufenberg, A. Synthesis of new branched fatty acids by rhodium catalyzed homogeneous oligomerization. Fat Science Technology 93:20-24 (1991).

[246] Henkel, K., Olefinic unsaturated adducts of ethylene in polyunsaturated fatty acids and fettsaeureester, process for their production and their use. Dusseldorf, Germany. European Patent Application, DE 4002012 A1 (1991)

[247] Keller, U., Fischer, J., Hoelderich, W., F. New lubricants from renewable resources: ecotoxicites and oxidative characteristics. Oelhydraulik und Pneumatik 4:240-245 (2000).

[248] Isbell, T.A. Chemistry and physical properties of estolides. Grasas Aceites Grasas y Aceites 62:8-20 (2011).

[249] Cermak, S.C., Isbell, T.A. Improved oxidative stability of estolide esters. Industrial Crops and Products 18:223-230 (2003).

[250] Cermak, S.C., Isbell, T.A. Synthesis and physical properties of mono-estolides with varying chain lengths. Industrial Crops and Products 29:205-213 (2009).

[251] Johansson, L.E.: Copper catalysts in the selective hydrogenation of soybean and rapeseed oils. S.l (1979)

[252] Behr, A., Doring, N., Durowitz-Heil, S., Lohr, C., Schmidtke, H. Selective Hydrogenation of Multi-Unsaturated Fatty-Acids in the Liquid-Phase. Fat Science Technology 95:2-11 (1993).

[253] Behr, A. Homogeneous transition-metal catalysis in oleochemistry. Fat Science Technology 92:375-388 (1990).

[254] Fell, B., Schafer, W. Selective hydrogenation of fats and derivatives using Ziegler-Type organometallic catalysts. 1. Selectivehydrogenation of methyllinoleat and other dienic compounds with isolated double-bonds. Fat Science Technology 92:264-272 (1990).

[255] Haase, K., D., Heynen, A., J., Laane, N., L., M. composition and application of isostearic acid. Fat Science Technology 91:350-353 (1989).

[256] Link, W., Spitellar, G. Products of the dimerization of unsaturated fatty acids. I: The fraction of monomers obtained by dimerization of pure oleic acid. Fat Science Technology 92:19-25 (1990).

[257] Sheldon, R.A., Arends, I., Hanefeld, U.: Green chemistry and catalysis. Wiley; John Wiley distributor, Weinheim Chichester (2007)

[258] Perin, G., Alvaro, G., Westphal, E., Jacob, R.G., Lenardao, E.J., Viana, L.H., et al. Transesterification of castor oil assisted by microwave irradiation. Fuel Fuel 87:2838-2841 (2008).

[259] Battersby, N.S., Morgan, P. A note on the use of the CEC L-33-A-93 test to predict the potential biodegradation of mineral oil based lubricants in soil. Chemosphere 35:1773-1779 (1997).

[260] Tocci, L. What does biodegradable really mean? Lubes 'n' Greases 10:40-43 (2004).

[261] Organisation for Economic, C.-o., Development: Guidance Document for the Development of OECD Guidelines for Testing of Chemicals. OECD Publishing, (2002)

[262] Pagga, U. Testing biodegradability with standardized methods. Chemosphere 35:2953-2972 (1997).

[263] Willing, A. Oleochemical esters - environmentally compatible raw materials for oils and lubricants from renewable resources. Lipid -Weinheim 101:192-198 (1999).

[264] Remmele, E., Widmann, B.: Hydraulic fluids based on rapeseed oil in agricultural machinery-sustainability and environmetalimpact during use, in. In: Bartz W, J. (ed.) 11th International Colloquium. Industrial and Automotive Lubrication, (1998)

[265] Battersby, N. A correlation between the biodegradability of oil products in the CEC L-33-T-82 and modified Sturm tests. Chemosphere 24:1989-2000 (1992).

[266] Benchaita, M.T., Lockwood, F.E. Reliable model of lubricant-related friction in internal combustion engines. Lubrication Science 5:259-281 (1993).

[267] Miller, S., Scharf, C., Miller., M.: Utilizing new crops to grow the biobased market. ASHS Press, Alexandria, VA (2002)

[268] Torbacke, T.N., Kopp, M. Environmentally adapted lubricants in the Nordic marketplace - recent developments. Industrial Lubrication and Tribology 54:109-116 (2002).

[269] USDA: BioPreferred Program. USDA, (2013)

[270] Bonhote, P., Dias, A.P., Papageorgiou, N., Kalyanasundaram, K., Graetzel M. Hydrophobic, Highly Conductive Ambient-Temperature Molten Salts. Inorganic chemistry 35:1168-1178 (1996).

[271] Deetlefs, M.S., Kenneth, R. Improved preparations of ionic liquids using microwave irradiation. Green Chemistry 5:181-186 (2003).

[272] Egorov, V.M., Djigailo, D.I., Momotenko, D.S., Chernyshov, D.V., Torocheshnikova, I.I., Smirnova, S.V., Pletnev, I.V. Task-specific ionic liquid trioctylmethylammonium salicylate as extraction solvent for transition metal ions. Talanta 80:1177-1182 (2010).

[273] Branneen, W.T., Burt G.D., DcDonald, R.A.: Phosphite amine lubrciant for metal working and machining. In: No UP (ed.). Place (1990)

[274] Barton, T. In Situ Lubrication with Boric Acid: Powder Delivery of an Environmentally Benign Solid Lubricant. Tribology Transactions 49:284-290 (2006).

[275] Liang, H., Jahanmir, S. Boric Acid as an Additive for Core-Drilling of Alumina. Journal of Tribology 117:65 (1995).

[276] Rao, K.P., Wei, J.J. Performance of a new dry lubricant in the forming of aluminum alloy sheets. Wear-Lausanne- 249:85-92 (2001).

[277] Rao, K.P., Xie, C.L. A comparative study on the performance of boric acid with several conventional lubricants in metal forming processes. Tribology International 39:663-668 (2006).

[278] Harris, J., Stocker, H.: Handbook of mathematics and computational science. Springer, New York (1998)

[279] Hamrock, B.J., Dowson, D.: Ball bearing lubrication: the elastohydrodynamics of elliptical contacts. Wiley, New York (1981)

[280] Menezes, P.L., Kailas, S.V., Kishore. Effect of Roughness Parameter and Grinding Angle on Coefficient of Friction When Sliding of Al–Mg Alloy Over EN8 Steel. Journal of Tribology 128:697-704 (2006).

[281] Kabir, M.A., Higgs III, C.F., Lovell, M.R. A Pin-on-Disk Experimental Study on a Green Particulate-Fluid Lubricant. Journal of Tribology 130:041801 (2008).

[282] Lovell, M.R., Deng, Z. Experimental investigation of sliding friction between hard and deformable surfaces with application to manufacturing processes. Wear 236:117-127 (1999).

[283] Stojanovic, A., Kogelnig, D., Galanski, M., Krachler, R., Keppler, B.K., Fischer, L., Hann, S., Groessl, M. Phosphonium and ammonium ionic liquids with aromatic anions: Synthesis, properties, and platinum extraction. Australian Journal of Chemistry 63:511-524 (2010).

[284] Fraser, K.J., Izgorodina, E.I., Forsyth, M., Scott, J.L., MacFarlane, D.R. Liquids intermediate between "molecular" and "ionic" liquids: Liquid Ion Pairs? Chemical Communications:3817-3819 (2007).

[285] Fraser K.J, MacFarlane, D.R. Phosphonium-based ionic liquids: An overview. Australian Journal of Chemistry 62:309-321 (2009).

[286] Sharma, B.K., Liu, Z., Adhvaryu, A., Erhan, S.Z. Lubricant base stock potential of chemically modified vegetable oils. Journal of Agricultural and Food Chemistry 56:8919-8925 (2008).

[287] Hwang, H.-S., Adhvaryu, A., Erhan, S.Z. Preparation and properties of lubricant basestocks from epoxidized soybean oil and 2-ethylhexanol. Journal of the American Oil Chemists' Society 80:811-815 (2003).

[288] Obi, A.I., Oyinlola, A.K. Frictional characteristics of fatty-based oils in wire drawing. Wear 194:30-37 (1996).

[289] Erhan, S.Z., Perez, J.M.: Biobased industrial fluids and lubricants. AOCS Press, Champaign (2002)

[290] Ataei, S., Yahya, R., Gan, S.N., Hassan, A. Study of Thermal Decomposition Kinetics of Palm Oleic Acid-Based Alkyds and Effect of Oil Length on Thermal Stability. Journal of Polymers and the Environment 20:507-513 (2012).

[291] Institute for Occupational Safety and Health of the German Social Accident Insurance: Databases on hazardous substances (GESTIS). German Institut für Arbeitsschutz, IFA, (2012)

[292] Badertscher, M., Bischofberger, K., Munk, M.E., Pretsch, E. A novel formalism to characterize the degree of unsaturation of organic molecules. Journal of chemical information and computer sciences 41 (2001).

[293] Lambert, J.B.: Organic structural spectroscopy. Pearson Prentice Hall, Upper Saddle River, N.J. (2011)

[294] Lal, K., Carrick, V. Performance testing of lubricants based on high oleic vegetable oils. Journal of synthetic lubrication 11:189-206 (1994).

[295] Asadauskas, S., Perez, J.M., Duda, J.L. Oxidative Stability and Antiwear Properties of High Oleic Vegetable Oils. Lubrication Engineering -Illinois- 52:877-882 (1996).

[296] Honary, L.A.T. An investigation of the use of soybean oil in hydraulic systems. Bioresource Technology 56:41-47 (1996).

[297] Arnsek, A., Vizintin, J. Scuffing Load Capacity of Rapeseed-Based Oils. Lubrication Engineering 55:11-18 (1999).

[298] Arnsek, A., Vizintin, J. Lubricating properties of rapeseed-based oils. Journal of synthetic lubrication 16:281-296 (2000).

[299] BÌrov·, A., Pavlovicov·, A., Cvenros, J. Lubricating oils based on chemically modified vegetable oils. Journal of Synthetic Lubrication 18:291-299 (2002).

[300] Aleinikov, F.K. Determination of the principal characteristics of the grinding process by the mutual-grinding method. Glass and Ceramics 14:271-276 (1957).

[301] Richardson, R.C.D. The wear of metals by relatively soft abrasives. Wear 11:245-275 (1968).

[302] Rabinowicz, E., Doherty, P., Boyd, D.M. Measurement of the abrasive wear resistance of hard coatings. Thin Solid Films 53:301-302 (1978).

[303] Rabinowicz, E., Mutis, A. Effect of abrasive particle size on wear. Wear 8:381-390 (1965).

[304] Rabinowicz, E., Dunn, L.A., Russell, P.G. The Abrasive wear resistance of some bearing steels: Lubrication Eng., 17 (1961) 587-593; Wear 5:252-253 (1962).

[305] Xie, Y., Bharat, B. Effects of particle size, polishing pad and contact pressure in free abrasive polishing. Wear 200:281-295 (1996).

[306] Menezes, P.L, Kishore, Kailas, S.V., Lovell, M.R. Factors influencing stick-slip motion: Effect of hardness, crystal structure and surface texture. American Society of Mechanical Engineers, Tribology Division, TRIB:71-73 (2011).

[307] Menezes, P.L., Kishore, Kailas, S.V., Lovell, M.R. Tribological response of materials during sliding against various surface textures.207-242 (2012).

[308] Menezes, P.L, Kishore, Lovell, M.R., Kailas, S.V. The role of strain rate response on tribological behavior of metals. Journal of Tribology 135 (2013).

[309] Menezes, P.L., Kishore, Kailas, S.V., Lovell, M.R. Tribological response of soft materials sliding against hard surface textures at various numbers of cycles. Lubrication Science 25:79-99 (2013).

[310] Menezes, P.L, Kishore, Kailas, S.V., Lovell, M.R. Response of materials as a function of grinding angle on friction and transfer layer formation. Journal of Advanced Manufacturing Technology 49:485-495 (2010).

[311] Menezes, P.L, Kishore, Kailas, S.V. Study of friction and transfer layer formation in copper-steel tribo-system: Role of surface texture and roughness parameters. Tribology Transactions 52:611-622 (2009).

[312] Menezes, P.L, Kishore, Kailas, S.V. Role of surface texture of harder surface on subsurface deformation. Wear 266:103-109 (2009).

[313] Menezes, P.L, Kishore, Kailas, S.V. Subsurface deformation and the role of surface texture--A study with Cu pins and steel plates. Sadhana 33:191-201 (2008).

[314] Menezes, P.L, Kishore, Kailas, S.V. Studies on friction in an iron-steel tribo-system under dry and lubricated conditions. Materials and Manufacturing Processes 23:698-707 (2008).

[315] Menezes, P.L, Kishore, Kailas, S.V. Effect of Surface Topography on Friction and Transfer Layer during Sliding. Tribology Online 3:25-30 (2008).

[316] Menezes, P.L, Kishore, Kailas, S.V., Lovell, M.R. Role of Surface Texture, Roughness, and Hardness on Friction During Unidirectional Sliding. Tribology Letters 41:1-15 (2011).

[317] Dieter, G.E.: Mechanical metallurgy. McGraw-Hill, New York (1976)

[318] Nayar, A.: The metals databook. McGraw-Hill, New York (1997)

[319] Bauccio, M.A.S.f.M.: ASM metals reference book. ASM International, Materials Park, Ohio (1993)

[320] Menezes, P.L., Lovell, M.R., Kabir, M.A., Higgs, C.F., Rohatgi, P.K.: Green Lubricants: Role of Additive Size. In: Nosonovsky M, Bhushan B (eds.) Green Tribology, pp. 265-286. Springer Berlin Heidelberg, (2012)

[321] Lundgren, S.M., Persson, K., Mueller, G., Kronberg, B., Clarke, J., Chtaib, M., et al. Unsaturated Fatty Acids in Alkane Solution: Adsorption to Steel Surfaces. Langmuir: The ACS Journal of Surfaces and Colloids 23:10598-10602 (2007).

[322] Li, W., Kong, X.H., Ruan, M., Ma, F.M., Jiang, Y.F., Liu, M.Z., et al. Green waxes, adhesives and lubricants. Philos Trans R Soc A Math Phys Eng Sci 368:4869-4890 (2010).

[323] Hu, X.G., Hu, S.L., Zhao, Y.S. Synthesis of nanometric molybdenum disulphide particles and evaluation of friction and wear properties. Lubrication Science 17:295-308 (2005).

[324] Ilie F, Tita, C. Tribological properties of solid lubricant nanocomposite coatings on base of tungsten disulphide nanoparticles. Tribologia Tribologia 27:5-11 (2008).

[325] Shao, X.L., Weimin, X.Q. The tribological behavior of micrometer and nanometer TiO2 particle-filled poly(phthalazine ether sulfone ketone) composites. Journal of applied polymer science 92:906 (2004).

[326] Huang, H.D., Tu, J.P., Gan, L.P., Li, C.Z. An investigation on tribological properties of graphite nanosheets as oil additive. Wear 261:140-144 (2006).

[327] Sunqing, Q., Junxiu, D., Guoxu, C. A review of ultrafine particles as antiwear additives and friction modifiers in lubricating oils. Lubrication Science 11:217-226 (1999).

[328] Xiaodong, Z., Xun, F., Huaqiang, S., Zhengshui, H. Lubricating properties of Cyanex 302-modified MoS_2 microspheres in base oil 500SN. Lubrication Science 19:71-79 (2007).

[329] Cizaire, L., Vacher B., Le Mogne, T., Martin, J.M., Rapoport, L., Margolin, A., Tenne, R. Mechanisms of ultra-low friction by hollow inorganic fullerene-like MoS2 nanoparticles. Surface & Coatings Technology 160:282 (2002).

[330] Leshchinsky, V., Alyoshina, E., Lvovsky, M., Volovik, Y., Lapsker, I., Tenne, R., Rapoport, L. Research & Development - Inorganic Nanoparticle Impregnation of Self Lubricated Materials. International Journal of Powder Metallurgy 38:50 (2002).

[331] Leshchinsky, V., Alyoshina, E., Lvovsky, M., Volovik, Y., Lapsker, I., Tenne, R., Rapoport, L. Behavior of solid lubricant nanoparticles under compression. Journal of Materials Science 39:4119-4129 (2004).

[332] Rapoport, L., Fleischer, N., Tenne, R. Fullerene-like WS2 Nanoparticles: Superior Lubricants for Harsh Conditions. ADMA Advanced Materials 15:651-655 (2003).

[333] Rapoport, L., Leshchinsky, V., Lvovsky, M., Lapsker, I., Volovik, Y., Feldman Y., Popovitz-Biro, R., Tenne, R. Superior tribological properties of powder materials with solid lubricant nanoparticles. Wear 255:794-800 (2003).

[334] Narayan, J.: Lubricant having nanoparticles and microparticles to enhance fuel efficiency, and a laser synthesis method to create dispersed nanoparticles. In: USPTO (ed.). Jagdish Narayan, Place Jagdish Narayan (2011)

[335] Heshmat, H. The Rheology and Hydrodynamics of Dry Powder Lubrication. Tribology Transactions 34:433-439 (1991).

[336] Menezes, P.L., Kishore, Kailas, S.V. Effect of surface roughness parameters and surface texture on friction and transfer layer formation in tin-steel tribo-system. Journal of Materials Processing Tech 208:372-382 (2008).

[337] Reeves, C.J., Menezes, P.L., Jen, T.-C., Lovell, M.R.: The effect of surface roughness on the tribological performance of environmentally friendly bio-based lubricants with varying particle size. 2013 STLE Annual Meeting & Exhibition. STLE, Place STLE (2013)

[338] Williams, J.A.: Engineering tribology. Oxford University Press, Oxford ; New York (1994)

[339] Liang, H., Jahanmir, S. Boric Acid as an Additive for Core-Drilling of Alumina. Journal of Tribology 117 (1995).

[340] Li, Y., Pang, A., Wang, C., Wei, M. Metalorganic frameworks: promising materials for improving the open circuit voltage of dye-sensitized solar cells. Journal of Materials Chemistry 21:17259-17264 (2011).

[341] Passerini, S., Alessandrini, F., Appetecchi, G.B., Conte, M. Ionic Liquid Based Electrolytes for High Energy Electrochemical Storage Devices. ECS Transactions 1:67-71 (2006).

[342] Garvey, S.L., Hawkins, C.A., Dietz, M.L. Effect of aqueous phase anion on the mode of facilitated ion transfer into room-temperature ionic liquids. Talanta 95:25-30 (2012).

[343] Hawkins, C.A., Garvey, S.L., Dietz, M.L. Structural variations in room-temperature ionic liquids: Influence on metal ion partitioning modes and extraction selectivity. Separation and Purification Technology 89:31-38 (2012).

[344] Zaijun, L., Jie, C., Haixia, S., Jiaomai, P. Advance of Room Temperature Ionic Liquid as Solvent for Extraction and Separation. Reviews in Analytical Chemistry 26:109-153 (2007).

[345] Smith, P.G. High-Temperature Molten-Salt Lubricated Hydrodynamic Journal Bearings. ASLE Transactions 4:263-274 (1961).

[346] Ye, C., Liu, W., Chen, Y., Yu, L. Room-temperature ionic liquids: a novel versatile lubricant. Chemical communications (Cambridge, England) 2001:2244-2245 (2001).

[347] Phillips, B.S., Zabinski, J.S. Ionic Liquid Lubrication Effects on Ceramics in a Water Environment. Tribology Letters 17:533-541 (2004).

[348] Wang, H., Lu, Q., Ye, C., Liu, W., Cui, Z. Friction and wear behaviors of ionic liquid of alkylimidazolium hexafluorophosphates as lubricants for steel/steel contact. Wear 256:44-48 (2004).

[349] Liu, W., Ye, C., Chen, Y., Ou, Z., Sun, D.C. Tribological behavior of sialon ceramics sliding against steel lubricated by fluorine-containing oils. Tribology International 35:503-509 (2002).

[350] Mu, Z., Liu, W., Zhang, S., Zhou, F. Functional Room-temperature Ionic Liquids as Lubricants for an Aluminum-on-Steel System. Chemistry Letters 33:524-525 (2004).

[351] Lu, Q., Wang, H., Ye, C., Liu, W., Xue, Q. Room temperature ionic liquid 1-ethyl-3-hexylimidazolium-bis(trifluoromethylsulfonyl)-imide as lubricant for steelsteel contact. Tribology International 37:547-552 (2004).

[352] Reich, R.A., Stewart, P.A., Bohaychick, J., Urbanski, J.A. Base Oil Properties of Ionic Liquids. Lubrication Engineering 59:16-21 (2003).

[353] Mu, Z., Zhou, F., Zhang, S., Liang, Y., Liu, W. Effect of the functional groups in ionic liquid molecules on the friction and wear behavior of aluminum alloy in lubricated aluminum-on-steel contact. Tribology International 38:725-731 (2005).

[354] Jimenez, A.E., Bermudez, M.D., Iglesias, P., Carrion, F.J., Martinez-Nicolas, G. 1-N-alkyl -3-methylimidazolium ionic liquids as neat lubricants and lubricant additives in steel-aluminium contacts. Wear 260:766-782 (2006).

[355] Jimenez, A.E., Bermudez, M.D., Iglesias, P., Carrion, F.J., Martinez-Nicolas, G. Room temperature ionic liquids as lubricant additives in steel-aluminium contacts: Influence of sliding velocity, normal load and temperature. Wear 261:347-359 (2006).

[356] Omotowa, B., Phillips, B.S., Zabinski, J.S., Shreeve, J.M. Phosphazene-based ionic liquids: synthesis, temperature-dependent viscosity, and effect as additives in water lubrication of silicon nitride ceramics. Inorganic chemistry 43:5466-5471 (2004).

[357] Yu, G., Zhou, F., Liu, W., Liang, Y., Yan, S. Preparation of functional ionic liquids and tribological investigation of their ultra-thin films. Wear 260:1076-1080 (2006).

[358] Yu, B., Zhou, F., Mu, Z., Liang, Y., Liu, W. Tribological properties of ultra-thin ionic liquid films on single-crystal silicon wafers with functionalized surfaces. Tribology International 39:879-887 (2006).

[359] Xia, Y., Wang, S., Zhou, F., Wang, H., Lin, Y., Xu, T. Tribological properties of plasma nitrided stainless steel against SAE52100 steel under ionic liquid lubrication condition. Tribology International 39:635-640 (2006).

[360] Qu, J., Bansal, D.G., Yu, B., Howe, J.Y., Luo, H., Dai, S., Li, H., Blau, P.J., Bunting, B.G., Mordukhovich, G., Smolenski, D.J., Antiwear performance and mechanism of an oil-miscible ionic liquid as a lubricant additive. ACS Applied Materials & Interfaces 4:997-1002 (2012).

[361] Mo, Yufei, Zhao, W., Zhu, M., Bai, M. Nano/Microtribological Properties of Ultrathin Functionalized Imidazolium Wear-Resistant Ionic Liquid Films on Single Crystal Silicon. Tribology Letters 32:143-151 (2008).

[362] Zhu, M., Yan, J., Mo, Y., Bai, M. Effect of the anion on the tribological properties of ionic liquid nano-films on surface-modified silicon wafers. Tribology Letters 29:177-183 (2008).

[363] Palacio, M., Bhushan, B. Ultrathin Wear-Resistant Ionic Liquid Films for Novel MEMS/NEMS Applications. Advanced Materials 20:1194-1198 (2008).

[364] Bhushan, B., Palacio, M., Kinzig, B. AFM-based nanotribological and electrical characterization of ultrathin wear-resistant ionic liquid films. Journal of Colloid and Interface Science 317:275-287 (2008).

[365] Palacio M, Bhushan, B. Nanotribological and nanomechanical properties of lubricated PZT thin films for ferroelectric data storage applications. Journal of Vacuum Science and Technology A: Vacuum, Surfaces and Films 26:768-776 (2008).

[366] Minami, I., Inada, T., Sasaki, R., Nanao, H. Tribo-Chemistry of Phosphonium-Derived Ionic Liquids. Tribology Letters 40:225-235 (2010).

[367] Zeng, Z., Shreeve, J.M., Phillips, B.S., Xiao, J.C. Polyfluoroalkyl, polyethylene glycol, 1,4-bismethylenebenzene, or 1,4-bismethylene-2,3,5,6-tetrafluorobenzene bridged functionalized dicationic ionic liquids: Synthesis and properties as high temperature lubricants. Chemistry of Materials 20:2719-2726 (2008).

[368] Shah, F., Glavatskih, S., Antzutkin, O.N. Synthesis, physicochemical, and tribological characterization of S-Di-n-octoxyboron-O,O'-di-n-octyldithiophosphate. ACS Applied Materials & Interfaces 1:2835-2842 (2009).

[369] Mosey, N.J. Molecular Mechanisms for the Functionality of Lubricant Additives. Science Science 307:1612-1615 (2005).

[370] Mangolini, F., Rossi, A., Spencer, N.D. Chemical reactivity of triphenyl phosphorothionate (TPPT) with Iron: An ATR/FT-IR and XPS investigation. Journal of Physical Chemistry C 115:1339-1354 (2011).

[371] Shah, F., Glavatskih, S., Höglund, E., Lindberg, M., Antzutkin, O.N. Interfacial antiwear and physicochemical properties of alkylborate-dithiophosphates. ACS applied materials & interfaces 3:956-968 (2011).

[372] Minami, I. Ionic liquids in tribology. Molecules (Basel, Switzerland) 14:2286-2305 (2009).

[373] Itoh, T., Ishioka, A., Hayase, S., Kawatsura, M., Watanabe, N., Inada, K. Design of alkyl sulfate ionic liquids for lubricants. Chemistry Letters 38:64-65 (2009).

[374] Ohtani, H., Ishimura, S., Kumai, M. Thermal decomposition behaviors of imidazolium-type ionic liquids studied by pyrolysis-gas chromatography. Analytical sciences: The International Journal of the Japan Society for Analytical Chemistry 24:1335-1340 (2008).

[375] Jimâenez, Ana-Eva, Bermâudez, M. Ionic liquids as lubricants for steel-aluminum contacts at low and elevated temperatures. Tribology Letters 26:53-60 (2007).

[376] Shah, F., Ullah, G., Sergei, M., MacFarlane, D.R., Somers, A., Forsyth, M., Antzutkin O.N. Novel halogen-free chelated orthoborate-phosphonium ionic liquids: synthesis and tribophysical properties. Physical Chemistry Chemical Physics (Incorporating Faraday Transactions) 13:12865-12873 (2011).

[377] Sun, J., Howlett, P.C., MacFarlane, D.R., Lin, J., Forsyth, M. Synthesis and physical property characterisation of phosphonium ionic liquids based on P(O)2(OR)2 and P(O)2(R)2 anions with potential application for corrosion mitigation of magnesium alloys. Electrochimica Acta 54:254-260 (2008).

[378] Weng, L., Jun, L., Xu, Q., Liang, Y., Min, X., Qun, J. Effect of tetraalkylphosphonium based ionic liquids as lubricants on the tribological performance of a steel-on-steel system. Tribology Letters 26:11-17 (2007).

[379] Minami, I, Kamimura, H., Mori, S. Thermo-oxidative stability of ionic liquids as lubricating fluids. Journal of Synthetic Lubrication 24:135-147 (2007).

[380] Kamimura, H., Kubo, T., Minami, I., Mori, S. Nordtrib. Effect and mechanism of additives for ionic liquids as new lubricants. Tribology International 40:620-625 (2007).

[381] Zhao, W., Mo, Y., Pu, J., Bai, M. Effect of cation on micro/nano-tribological properties of ultra-thin ionic liquid films. Tribology International 42:828-835 (2009).

[382] Matlack, A.: Introduction to Green Chemistry. Taylor & Francis Group, (2010)

[383] Manahan, S.E.: Environmental chemistry. Lewis, Boca Raton (1994)

[384] Suisse, J., Bellemin-Laponnaz, S., Douce, L., Maisse-François, A., Welter, R. A new liquid crystal compound based on an ionic imidazolium salt. Tetrahedron Letters 46:4303-4305 (2005).

[385] Yao, Y., Wang, X., Guo, J., Yang, X., Xu, B. Tribological property of onion-like fullerenes as lubricant additive. Materials Letters 62:2524-2527 (2008).

[386] Xia, Y., Sasaki, S., Murakami, T., Nakano, M., Shi, L., Wang, H. Ionic liquid lubrication of electrodeposited nickel-Si3N4 composite coatings. Wear 262:765 (2007).

[387] Xue, H., Tong, Z.F., Wei, F.Y., Qing, S.G. Crystal structure of room-temperature ionic liquid 1-butyl-isoquinolinium gallium tetrachloride [(BIQL)GaCl4]. Comptes Rendus Chimie 11:90-94 (2008).

[388] Wang, H., Malhotra, S.V., Francis, A.J. Toxicity of various anions associated with methoxyethyl methyl imidazolium-based ionic liquids on Clostridium sp. CHEM Chemosphere 82:1597-1603 (2011).

[389] Handy, S.T. Greener Solvents: Room Temperature Ionic Liquids from Biorenewable Sources. CHEM Chemistry - A European Journal 9:2938-2944 (2003).

[390] Gathergood, N., García Ramón, M.T., Scammells, P.J. Biodegradable ionic liquids: Part I. Concept, preliminary targets and evaluation. Green Chemistry 6:166-175 (2004).

[391] Corma, A., Iborra, S., Velty, A. Chemical Routes for the Transformation of Biomass into Chemicals. CHIN ChemInform 38:no (2007).

[392] Zhang, Z.C. Catalytic transformation of carbohydrates and lignin in ionic liquids. WENE Wiley Interdisciplinary Reviews: Energy and Environment:n/a (2013).

[393] Chang, J.-K., Chen, S.-Y., Tsai, W.-T., Deng, M.-J., Sun, I.W. Electrodeposition of aluminum on magnesium alloy in aluminum chloride (AlCl3)–1-ethyl-3-methylimidazolium chloride (EMIC) ionic liquid and its corrosion behavior. Electrochemistry Communications 9:1602-1606 (2007).

[394] Weng, L., Liu, X., Liang, Y., Xue, Q. Effect of tetraalkylphosphonium based ionic liquids as lubricants on the tribological performance of a steel-on-steel system. Tribology Letters 26:11-17 (2007).

[395] Milosev, I.M.-H.M. Effect of chloride concentration range on the corrosion resistance of Cu-xNi alloys. Journal of Applied Electrochemistry 29:393-402 (1999).

[396] Warraky, A., El Shayeb, H.A., El Sherif, E.M. Pitting corrosion of copper in chloride solutions. Anti-Corrosion Methods and Materials 51:52-61 (2004).

[397] Barril, S., Mischler, S., Landolt, D. Electrochemical effects on the fretting corrosion behaviour of Ti6Al4V in 0.9% sodium chloride solution. Wear 259:282-291 (2005).

[398] Morgan, D.A. Smoke, fire, and flash points of cottonseed, peanut, and other vegetable oils. Oil Soap Oil & Soap 19:193-198 (1942).

[399] Koh, S.P., Arifin, N., Lai, O.M., Yusoff, M.S.A., Long, K., Tan, C.P. Oxidative stability of palm- and soybean-based medium- and long-chain triacylglycerol (MLCT) oil blends. Journal of the Science of Food and Agriculture 89:455-462 (2009).

[400] Appetecchi, G.B., Montanino, M., Carewska, M., Moreno, M., Alessandrini, F., Passerini, S. Chemical–physical properties of bis(perfluoroalkylsulfonyl)imide-based ionic liquids. Electrochimica Acta 56:1300-1307 (2011).

[401] Bartz, W.J. Some Investigations on the Influence of Particle Size on the Lubricating Effectiveness of Molybdenum Disulfide. ASLE Transactions 15:207-215 (1972).

[402] Bourlon, B., Glattli, D.C., Miko, C., Forro, L., Bachtold, A. Carbon Nanotube Based Bearing for Rotational Motions. Nano Letters 4:709-712 (2004).

[403] Cumings, J., Zettl, A. Low-Friction Nanoscale Linear Bearing Realized from Multiwall Carbon Nanotubes. Science 289:602-604 (2000).

[404] Kolmogorov, A.N., Crespi, V.H. Smoothest Bearings: Interlayer Sliding in Multiwalled Carbon Nanotubes. Physical Review Letters 85:4727-4730 (2000).

[405] Legoas S., Coluci, V.R., Braga, S.F., Coura, P.Z., Dantas, S.O., Galvão, D.S. Molecular-dynamics simulations of carbon nanotubes as gigahertz oscillators. Physical Review Letters 90 (2003).

[406] Zhao, Y., Ma, C.C., Chen, G., Jiang, Q. Energy dissipation mechanisms in carbon nanotube oscillators. Physical Review Letters 91 (2003).

[407] Yu, M. Strength and Breaking Mechanism of Multiwalled Carbon Nanotubes Under Tensile Load. Science 287:637-640 (2000).

[408] Hong, C., Han, J., Zhang, X., Meng, S. Multiwalled Carbon Nanotubes-TiB2-Ni Composite: Microstructure and Mechanical Properties. International Journal of Applied Ceramic Technology 6:525-530 (2009).

[409] Popov, M., Kyotani, M., Nemanich, R.J., Koga, Y. Superhard phase composed of single-wall carbon nanotubes. Physical Review -Series B- 65:033408 (2002).

[410] Ruoff, R.S., Lorents, D.C. Mechanical and thermal properties of carbon nanotubes. Carbon 33:925-930 (1995).

[411] Vander Wal, R.L., Miyoshi, K., Street, K.W., Tomasek, A.J., Peng, H., Liu, Y., et al. Friction properties of surface-fluorinated carbon nanotubes. Wear 259:738-743 (2005).

[412] Vigolo, B. Macroscopic Fibers and Ribbons of Oriented Carbon Nanotubes. Science 290:1331-1334 (2000).

[413] Mattia, D., Gogotsi, Y. Review: static and dynamic behavior of liquids inside carbon nanotubes. Microfluidics and Nanofluidics 5:289-305 (2008).

[414] Charlier, J.C., Michenaud, J.P. Energetics of multilayered carbon tubules. Physical Review Letters 70:1858-1861 (1993).

[415] Saito, R., Matsuo, R., Kimura, T., Dresselhaus, G., Dresselhaus, M.S. Anomalous potential barrier of double-wall carbon nanotube. Chemical Physics Letters 348:187-193 (2001).

[416] Servantie J, Gaspard, P. Methods of calculation of a friction coefficient: application to nanotubes. Physical Review Letters 91 (2003).

[417] Lum, K., Chandler, D., Weeks, J.D. Hydrophobicity at Small and Large Length Scales. Journal Of Physical Chemistry B 103:4570-4577 (1999).

[418] Rabinowicz, E.: Friction and wear of materials. Wiley, New York (1965)

[419] Rabinowicz, E., Dunn, L.A., Russell, P.G. A study of abrasive wear under three-body conditions. Wear 4:345-355 (1961).

[420] Tariq, M., Forte, P.A.S., Gomes, M.F.C., Lopes, J.N.C., Rebelo, L.P.N. Densities and refractive indices of imidazolium- and phosphonium-based ionic liquids: Effect of temperature, alkyl chain length, and anion. The Journal of Chemical Thermodynamics 41:790-798 (2009).

[421] Ingole, S., Nosonovsky, Michael, Kailas, Satish Vasu, Lovell, Michael R., and Menezes, Pradeep L.: Tribology for Scientists and Engineers. Springer, (2012)

[422] Barnsley, M.F. Fractal functions and interpolation. Constructive Approximation 2:303-329 (1986).

[423] Barnsley, M.F.: Hidden variable fractal interpolation functions. School of Mathematics, Georgia Institute of Technology, Atlanta (1986)

[424] Barnsley, M.F., Rising, H.: Fractals everywhere. Academic Press Professional, Boston (1993)

[425] Mandelbrot, B.B.: The fractal geometry of nature. W.H. Freeman, New York (1983)

[426] Mandelbrot, B.B.: Fractals : form, chance, and dimension. W.H. Freeman, San Francisco (1977)

[427] Kaye, B.H.: A random walk through fractal dimensions. VCH Publishers, New York, NY, USA (1989)

[428] Hyslip, J.P., Vallejo, L.E. Fractal analysis of the roughness and size distribution of granular materials. Engineering geology 48:231 (1998).

[429] Jahn, R., Truckenbrodt, H. A simple fractal analysis method of the surface roughness. Journal of Materials Processing Technology 145:40-45 (2004).

[430] Gagnepain, J.J., Roques-Carmes, C. Fractal approach to two-dimensional and three-dimensional surface roughness. Wear 109:119-126 (1986).

[431] Russ, J.C.: Fractal surfaces. Plenum Press, New York (1994)

Appendix: Sample Calculation of the Pearson product-moment correlation coefficient

Using Eq. 3.2 shown below can be rewritten in an alternative form, Eq. (A1) for computing the sample correlation coefficient.

$$r = \frac{\sum_{i=1}^{n}(X_i-\bar{X})(Y_i-\bar{Y})}{\sqrt{\sum_{i=1}^{n}(X_i-\bar{X})^2 \sum_{i=1}^{n}(Y_i-\bar{Y})^2}} \qquad \text{Eq. (3.2)}$$

$$r = \frac{\sum_{i=1}^{n}X_iY_i-(\sum_{i=1}^{n}X_i)(\sum_{i=1}^{n}Y_i)/n}{\sqrt{\sum_{i=1}^{n}X_i^2-(\sum_{i=1}^{n}X_i)^2/n}\sqrt{\sum_{i=1}^{n}Y_i^2-(\sum_{i=1}^{n}Y_i)^2/n}} \qquad \text{Eq. (A1)}$$

Consider the following data:

X	18	1	24	5	7	8	19	16	2
Y	117	3	170	22	34	41	126	101	7

The sample correlation coefficient, r for the data above may be obtained by first constructing the Table A1, then by using Eq. (A1) with n = 9.

Table A1: Numerical Calculations

	X_i	Y_i	X_i^2	Y_i^2	X_iY_i
	18	117	324	13738.54	2109.81
	1	3	1	7.49	2.74
	24	170	576	29025.61	4088.86
	5	22	25	491.53	110.85
	7	34	49	1178.93	240.35
	8	41	64	1668.27	326.76
	19	126	361	15812.17	2389.18
	16	101	256	10114.49	1609.13
Sum	100	620.72	1660.00	72082.43	10891.15

Resulting in

$$r = \frac{(10891.15) - (100)(620.72)/9}{\sqrt{1660 - (100)^2/9}\sqrt{72082.43 - (620.72)^2/9}} \approx -0.9965$$

Here, r is close to -1, indicating a strong negative linear relationship between x and y.

CURRICULUM VITAE

Carlton J Reeves

Graduate Research Assistant
Department of Mechanical Engineering
College of Engineering and Applied Science
University of Wisconsin-Milwaukee

EMS Bldg. Room 1210
3200 N. Cramer St., Milwaukee, WI, 53211
email: reevescj@uwm.edu
office: (414) 229-6895

EDUCATION

University of Wisconsin-Milwaukee   Milwaukee, WI
Doctor of Philosophy in Mechanical Engineering,   May 2013
  Dissertation: "*An Experimental Investigation Characterizing the Tribological Performance of Natural and Synthetic Biolubricants Composed of Carboxylates for Energy Conservation and Sustainability*",
Advisors: Tien-Chien Jen, Ph.D. and Michael R. Lovell, Ph.D.
Minor in Mathematics

Carnegie Mellon University   Pittsburgh, PA
Master of Science in Mechanical Engineering,   December 2009
Bachelor of Science in Mechanical Engineering, May 2009
Minor in Business Administration

RESEARCH EXPERIENCE

Green Lubrication & Tribology Laboratory University of Wisconsin-Milwaukee
June 2013 –Current

• Studied new advancements in green lubrication technologies with natural and synthetic esters and the influence of nanometer and micron-sized particulate additivation

Thermal Machining Laboratory   University of Wisconsin-Milwaukee
January 2012 – June 2013

• Developed, tested, and modeled environmentally friendly bio-based lubricants for energy conservation and sustainability

Tribology & Energy Diagnostics Lab   University of Wisconsin-Milwaukee
January 2010 – January 2012

• Studied tribological properties and applications involving nano-powder dry lubricants and green lubrication technology

Particle Flow & Tribology Lab   Carnegie Mellon University
April 2009 – December 2009

- Studied the tribological properties of filter cake accumulation in a slurry mixture in a simulated deep oil drilling filtration rig

WORK EXPERIENCE

Reeves Technologies, LLC |Tali Payments   Milwaukee, WI
Founder & President,   October 2012 to current

- An electronic payment services company that provides mobile point-of-sales software for the restaurant industry

Sporkwise, LLC   Milwaukee, WI
Co-founder & Developer,   January 2012 to current

- A software-as-a-service business that makes personalized recommendations to help people explore their culinary world based on their unique set of metric

Cybex International Incorporated   Medway, MA
Associate Mechanical Engineering Intern,
Cybex World Headquarters,   Summer 2007 & Summer 2008

- Worked in a research and development lab redesigning audio/video systems on new products entering the market

Reeves Company Incorporated   Attleboro, MA
Engineering Intern,   January 2000-2009

- Used SolidWorks to aid in the design and build of a Staubli 6-Axis Robotic automation system for production

TEACHING EXPERIENCE

Graduate Teaching Assistant   Milwaukee, WI
Mechanical Engineering Department   Spring, 2010

- Taught undergraduates two lab sections in Design of Machine Elements, while creating and grading homeworks and quizzes

PUBLICATIONS

Book Chapters

1. "Macroscale Applications in Tribology," **Carlton J. Reeves**, Pradeep L. Menezes, Michael R. Lovell, and Tien-Chien Jen. Tribologists for Scientists and Engineers, p. 881-919, Springer, 2013

2. "Microscale Applications in Tribology," **Carlton J. Reeves**, Pradeep L. Menezes, Michael R. Lovell, and Tien-Chien Jen. Tribologists for Scientists and Engineers, p. 921-948, Springer, 2013

3. "Fundamentals of Lubrication," Pradeep L. Menezes, **Carlton J. Reeves**, and Michael R. Lovell. <u>Tribology for Scientists and Engineers</u>, p. 295-340, Springer, 2013

4. "Self-lubricating behavior of graphite-reinforced composites," Pradeep L. Menezes, **Carlton J. Reeves**, Pradeep K. Rohatgi and Michael R. Lovell. <u>Tribology for Scientists and Engineers</u>, p. 341-389, Springer, 2013

5. "Tribology of Solid Lubricants," **Carlton J. Reeves**, Pradeep L. Menezes, Michael R. Lovell, and Tien-Chien Jen. <u>Tribology for Scientists and Engineers</u>, p.447-494, Springer, 2013

6. "Tribology in Metal Forming," Pradeep L. Menezes, **Carlton J. Reeves**, Satish V. Kailas, and Michael R. Lovell. <u>Tribology for Scientists and Engineers</u>, p. 783-818, Springer, 2013

<u>Journal & Conference Papers</u>
1. "The Influence of Surface Roughness and Particulate size on the Tribological Performance of Environmentally Friendly Bio-based Lubricants with Particle Additives," **Carlton J Reeves**, Pradeep L. Menezes, Michael R. Lovell, and Tien-Chien Jen. Lubricants, 2014 (In Preparation)

2. "The Influence of Fatty Acids on Tribological and Thermal Properties of Natural Oils as Sustainable Biolubricants," **Carlton J Reeves**, Pradeep L. Menezes, Michael R. Lovell, and Tien-Chien Jen. Journal of Physics D: Applied Physics, 2014 (In Preparation)

3. "The Tribological Performance of Bio-Based Room Temperature Ionic Liquid Lubricants: A Possible Next Step in Biolubricant Technology," **Carlton J. Reeves**, Pradeep L. Menezes, Michael R. Lovell, Tien-Chien Jen, Sarah Garvey, and Mark Dietz. World Tribology Congress – 5, Torino, Italy, 2013 (in CD)

4. "The Size Effect of Boron Nitride Particles on the Tribological Performance of Biolubricants for Energy Conservation and Sustainability," **Carlton J. Reeves**, Pradeep L. Menezes, Michael R. Lovell and Tien-Chien Jen. Tribology Letters, 51(3), 2013, 437-452.

5. "The Effect of Surface Roughness on the Tribological Performance of Environmentally Friendly Bio-Based Lubricants with Varying Particle Size," **Carlton J. Reeves**, Pradeep L. Menezes, Tien-Chien Jen, and Michael R. Lovell. 2013 STLE Annual Meeting & Exhibition (STLE2013), Detroit, USA, 2013 (in CD)

6. "The Effect of Anion-Cation Moiety Manipulation to Characterize the Tribological Performance of Environmentally Benign Room Temperature Ionic Liquid Lubricants," **Carlton J. Reeves**, Pradeep L. Menezes, Sarah Garvey, Tien-Chien Jen, Mark Dietz, and Michael R. Lovell. 2013 STLE Annual Meeting & Exhibition (STLE2013), Detroit, USA, 2013 (in CD)

7. "Evaluating the Tribological Performance of Green Liquid Lubricants and Powder Additives Based Green Liquid Lubricants," **Carlton J. Reeves**, Pradeep L. Menezes, Tien-Chien Jen, and Michael R. Lovell. 2012 STLE Annual Meeting & Exhibition (STLE2012), St. Louis, USA, 2012 (in CD)

8. "Tribological Performance of Environmentally-Friendly Ionic Liquid Lubricants," **Carlton J. Reeves**, Sarah Garvey, Pradeep L. Menezes, Mark Dietz, Tien-Chien Jen, and Michael R. Lovell. ASME/STLE International Joint Tribology Conference (IJTC2012), Denver, USA, 2012, (in CD)

INVENTION DISCLOSURE

"Environmentally-Friendly Biodegradable Ionic Liquid Lubricants," Carlton J Reeves, Mark L. Dietz, Sarah Garvey, Tien-Chien Jen, Pradeep L. Menezes, and Michael R. Lovell. March 2012.

HONORS & AWARDS

- 1st Place Student Poster Symposium, ASME/STLE International Joint Tribology Conference 2012 (IJTC 2012), Denver, CO, "Tribological Performance of Environmentally Friendly Ionic Liquid Lubricants for Energy Conservation and Sustainability"

- 3rd Place in Top 40 National Science Foundation, 2012 ASME-International Mechanical Engineering Congress and Exposition Student Poster Symposium, "Bio-Based Room Temperature Ionic Liquid Lubricants for Energy Conservation and Sustainability"

- 1st Place, UWM – College of Engineering and Applied Science, Graduate Research Poster Competition, 2012, "Natural Oil and Ionic Liquid Lubricants for Energy Conservation and Sustainability"

- 2nd Place, UWM – College of Engineering and Applied Science, Undergraduate Research Poster Competition, 2012, "Room Temperature Ionic Liquid as Environmentally Friendly Lubricants: The Next Step in Green Tribology"

- Chancellor's Award, University of Wisconsin-Milwaukee, 2010 –2013

- Top 10 National Finalists, MillerCoors Urban Entrepreneurs Series Business Plan Competition, 2013

- 1st Place Finalist, Scheinfeld Entrepreneurial Award Fund, 2013

- 1st Place Finalist, Scheinfeld Entrepreneurial Award Fund, 2012

- 2nd Place, BizStarts Milwaukee – Collegiate Business Plan Competition, 2012

- 2nd Place, UWM – Lubar School of Business – New Venture Business Plan Competition, 2012

PRESENTATIONS
Oral Presentations

1. "The Tribological Performance of Bio-Based Room Temperature Ionic Liquid Lubricants: A Possible Next Step in Biolubricant Technology," **Carlton J. Reeves**, Pradeep L. Menezes, Michael R. Lovell, Tien-Chien Jen, Sarah Garvey, and Mark Dietz. World Tribology Congress – 5, Torino, Italy, 2013

2. "The Effect of Surface Roughness on the Tribological Performance of Environmentally Friendly Bio-Based Lubricants with Varying Particle Size," **Carlton J. Reeves**, Pradeep L. Menezes, Tien-Chien Jen, and Michael R. Lovell. 2013 STLE Annual Meeting & Exhibition (STLE2013), Detroit, USA, 2013

3. "The Effect of Anion-Cation Moiety Manipulation to Characterize the Tribological Performance of Environmentally Benign Room Temperature Ionic Liquid Lubricants," **Carlton J. Reeves**, Pradeep L. Menezes, Sarah Garvey, Tien-Chien Jen, Mark Dietz, and Michael R. Lovell. 2013 STLE Annual Meeting & Exhibition (STLE2013), Detroit, USA, 2013

4. "Tribological Performance of Environmentally-Friendly Ionic Liquid Lubricants," **Carlton J. Reeves**, Sarah Garvey, Pradeep L. Menezes, Mark Dietz, Tien-Chien Jen, and Michael R. Lovell. ASME/STLE International Joint Tribology Conference (IJTC2012), Denver, USA, 2012

5. "Evaluating the Tribological Performance of Green Liquid Lubricants and Powder Additives Based Green Liquid Lubricants," **Carlton J. Reeves**, Pradeep

L. Menezes, Tien-Chien Jen, and Michael R. Lovell. 2012 STLE Annual Meeting & Exhibition (STLE2012), St. Louis, USA, 2012

Poster Presentations

6. "Multi-Functional 'Designer' Bio-Fluids for Controlled Environments in Terrestrial and Extraterrestrial Applications," **Carlton J. Reeves**, Pradeep L. Menezes, Tien-Chien Jen, Michael R. Lovell, Sarah Garvey, and Mark Dietz. 2013 STLE Annual Meeting & Exhibition (STLE2013), Detroit, USA, 2013

7. "Multi-Functional 'Designer' Bio-Fluids for Controlled Environments in Terrestrial and Extraterrestrial Applications," **Carlton J. Reeves**, Pradeep L. Menezes, Tien-Chien Jen, Michael R. Lovell, Sarah Garvey, and Mark Dietz. College of Engineering and Applied Science, University of Wisconsin-Milwaukee, Graduate Research Poster Competition, Spring 2013

8. "Bio-Based Room Temperature Ionic Liquid Lubricants for Energy Conservation and Sustainability," **Carlton J. Reeves**, Pradeep L. Menezes, Tien-Chien Jen, Michael R. Lovell, Sarah Garvey, and Mark Dietz. 2012 ASME-International Mechanical Engineering Congress and Exposition (IMECE2012), Houston, TX, USA, 2012. Top 40 National Science Foundation Student Poster Symposium.

9. "Tribological Performance of Environmentally-Friendly Ionic Liquid Lubricants for Energy Conservation and Sustainability," **Carlton J. Reeves**, Sarah Garvey, Pradeep L. Menezes, Mark Dietz, Tien-Chien Jen, and Michael R. Lovell. ASME/STLE International Joint Tribology Conference (IJTC2012), Denver, USA, 2012

10. "Natural Oil and Novel Ionic Liquid Lubricants for Energy Conservation and Sustainability," **Carlton J. Reeves**, Sarah Garvey, Pradeep L. Menezes, Mark Dietz, Tien-Chien Jen, and Michael R. Lovell. College of Engineering and Applied Science, University of Wisconsin-Milwaukee, Graduate Research Poster Competition, Spring 2012

GUEST LECTURER

1. **Professional Seminar**, EAS-200   December 2013
    University of Wisconsin-Milwaukee
    "My Journey through Academia, Research, Entrepreneurship, & Innovation"

2. **Transitioning Your Leadership…Series**   November, 2013
    University of Wisconsin-Milwaukee
    "A Didactic Journey in the Making"

3. **Friction and Wear**, ME-465   September, 2013

University of Wisconsin-Milwaukee

4. **Milwaukee Tribology Consortium**   February, 2012
   University of Wisconsin-Milwaukee
   "*An Investigation in Green Tribology: On the Size Effect of Boron Nitride Particles and the Tribological Performance of Canola Oil*"

5. **Milwaukee Tribology Consortium**   September, 2012
   University of Wisconsin-Milwaukee
   "*Tribology of Green Ionic Liquid Lubricants*"

PROJECTS

Biologically Inspired Micro/Nano Robotics Project, Fall 2009
- Designed a robot that mimics the jumping characteristics of insects to jump into the air using shape memory alloys

Mechanical Engineering Senior Capstone Design Project, Spring 2009
- Designed and prototyped a home-use callisthenic exercise machine to offer a full body workout to the user

Decision Tools in Mechanical Engineer & Entrepreneurship Project, Spring 2009
- Created a business model for the production of Nanofiber Bio-scaffolding used in liver transplants

Google Lunar X-Prize, Astrobotics, Fall 2008
- Assisted in engineering and enterprise work to send a robot designed by students faculty to the moon to video record the Apollo landing sites

VOLUNTEER EXPERIENCE
- Alternative Break: Peru Service Learning Trip   March 2009
  Led trip to improve impoverished community's wellbeing
- Alternative Break: Ecuador Trip   March 2008
  Led trip to biomarine reserve to assist in rainforest ecosystem preservation
- Hurricane Katrina Relief Trip   March 2007
  Led a group of students to New Orleans to help rebuild homes and communities
- Dominican Republic Trip   March 2005
  Setup clinics in impoverished villages and provided personnel healthcare
- East Africa Trip   June - August 2004
  Computer education teacher at Kilimani Primary School in Arusha, Tanzania

LEADERSHIP EXPERIENCE
- Entrepreneurship Advisory Committee, December 2012 – Current
  Milwaukee Area Technical College,
- College of Engineering and Applied Sciences Graduate Student Senator
  University of Wisconsin Milwaukee, 2011- 2012

Student Leadership Award, Carnegie Mellon University, 2009
- Alternative Break Community Service Organization, 2007-2009
  Carnegie Mellon University
  President, 2008-2009; and Head Spring Trip Leader, 2006-2008
- Judicial Board Member, Carnegie Mellon University, 2007-2009

SKILLS & SOFTWARE

Operating Systems: Windows, MacOS, Linux
Software: SolidWorks, MATLAB, Mathematica, ANSYS, Fluent, ADAMS, ProEngineer, PeopleSoft, LabVIEW, LS-DYNA
Laboratory Equipment: SEM with EDX/EDS, AFM, 2D & 3D Optical Profilometer, Tribometers of various configurations

ACTIVITIES & HONORS

- Private Pilot's License, Allegheny Airport, PA, 2009
- University Athletic Association Champions, Men's Track and Field
  NCAA Division III, 2007